

**On-line and Off-line Enrichment Techniques  
Combined with Capillary Electromigration Separation  
Methods in the Analysis of Highly Hydrophilic  
Analytes in Biological and Environmental Samples**

**Kumulative Dissertation**

zur

Erlangung des Doktorgrades

der Naturwissenschaften

(Dr. rer. nat.)

dem

Fachbereich Chemie der Philipps-Universität Marburg

vorgelegt von

**M.Sc. Azza Hesham Mansour Mahmoud Rageh**

aus

Ägypten

Marburg an der Lahn 2015



Die vorliegende Dissertation entstand in der Zeit von Juli 2011 bis Mai 2015 unter der Leitung von Prof. Dr. Ute Pyell am Fachbereich Chemie der Philipps-Universität Marburg

Vom Fachbereich Chemie der Philipps-Universität Marburg als Dissertation am 28-5-2015 angenommen.

Erstgutachter: Prof. Dr. Ute Pyell

Zweitgutachter: Prof. Dr. Hermann Wätzig (Technische Universität Braunschweig)

Tag der mündlichen Prüfung: 29-5-2015

Hochschulkennziffer: 1180

"Gerdruckt mit Unterstützung des Deutschen Akademischen Austauschdienstes"



## **Erklärung**

Ich erkläre, dass eine Promotion noch an keiner anderen Hochschule als der Philipps-Universität Marburg, Fachbereich Chemie, versucht wurde.

Ich versichere, dass ich meine vorgelegte Dissertation

*“On-line and off-line enrichment techniques combined with capillary electromigration separation methods in the analysis of highly hydrophilic analytes in biological and environmental samples”*

selbst und ohne fremde Hilfe verfasst, nicht andere als die in ihr angegebenen Quellen oder Hilfsmittel benutzt, alle vollständig oder sinngemäß übernommenen Zitate als solche gekennzeichnet sowie die Dissertation in der vorliegenden oder einer ähnlichen Form noch bei keiner anderen in- oder ausländischen Hochschule anlässlich eines Promotionsgesuchs oder zu anderen Prüfungszwecken eingereicht habe.

Marburg, April 2015

Unterschrift

(Azza H. Rageh)



## *Dedication*

*This thesis is dedicated to my beloved husband **Mohamed** and my beautiful children, **Salma** and **Tarek**, for their love, endless support, and understanding; to **my parents**, who have been giving me so much that I can never pay back; and to my sisters **Nahed** and **Ola** and my brother **Abdullah** for their unconditional love and continuous encouragement*





# Acknowledgement

First and above all, praise be to **Allah** for guidance and inspiration throughout this work.

Uppermost credit is due to my supervisor, **Professor Dr. Ute Pyell**. Her broad support, permanent motivation and continuous encouragement stimulated the implementation of a fruitful project. I sincerely and heartily appreciate her patience and commitment as well as the numerous valuable discussions. Profuse thanks to her for giving me the opportunity to work on such an interesting project and for providing me the facilities to complete it.

I wish to express my sincere thanks and deepest gratitude to **Professor Dr. Hnin Pwint Aung** for her valuable instructions regarding the solid phase extraction experiments. Thanks to **Professor Dr. Mohamed Marahiel** for providing the lyophilizer. Thanks to **M.Sc. Mohamed Abdelmegeed** and **M.Sc. Achim Kaltz** for their assistance in the first publication of this dissertation.

My sincere appreciation to **Professor Dr. Karl-Friedrich Klein** for providing the laser head and the laser head controller. My thanks are extended to **Kathrin Geiger** and **Wolf Fronius** for their help in the fifth publication of the dissertation. Special thanks to **M.Sc. Julia Rybka** for the translation of the summary part of the thesis into German.

Thanks to the Egyptian ministry of higher education and the ministry of state for scientific research and the Deutscher Akademischer Austauschdienst (**DAAD**) for funding my PhD scholarship through German Egyptian Research Long-Term Scholarship program (**GERLS**). I would like to thank the Marburg University Research Academy (**MARA**) for the financial support.

My doctoral studies were so pleasant because of the good relationships and cheerful atmosphere within the working group. I would like to express my thanks to my colleagues in the research group of Prof. Pyell. Special thanks to **Dr. Mohamed El-Awady** for the fruitful discussion and the sincere help. I wish to thank my colleagues in Marburg University for their cooperation and nice company.

To my big family (**my mother, my father, my sisters and my brother**), my small family (**my husband and my beloved children**) and to all who have contributed to the creation of this work, I feel heavily indebted.

*Azza H. Rageh*



## Table of Contents

<b>Preface</b> .....	i
<b>List of abbreviations and symbols</b> .....	iii
<b>1. Introduction</b> .....	1
<b>1.1. Principles of capillary electromigration separation techniques</b> .....	3
1.1.1. Historical background, current status and application.....	3
1.1.2. Instrumentation.....	4
1.1.3. Basic concepts.....	5
1.1.3.1. Electrophoresis.....	5
1.1.3.2. Electroosmotic flow (EOF) and regulation of EOF.....	6
<b>1.2. CE modes</b> .....	10
1.2.1. Capillary zone electrophoresis (CZE).....	10
1.2.2. Micellar electrokinetic chromatography.....	11
1.2.2.1. Separation principle.....	11
1.2.2.2. Mechanism of interaction between the micelles and analyte.....	13
1.2.2.3. Retention factor in MEKC.....	14
1.2.2.4. Classes of surfactants.....	15
<b>1.3. Detection techniques</b> .....	19
<b>1.4. Improvement of the detection sensitivity</b> .....	21
1.4.1. Off-line enrichment techniques.....	22
1.4.2. On-line enrichment techniques.....	23
1.4.2.1. Stacking.....	23
1.4.2.1.1. Field-amplified sample stacking and field-amplified sample injection.....	24
1.4.2.1.2. Large volume sample stacking .....	25
1.4.2.2. Dynamic pH junction.....	26
1.4.2.3. Sweeping.....	27
<b>1.5. Biological and environmental applications of capillary electromigration techniques</b> .....	29
<b>1.6. References</b> .....	31
<b>2. Motivations and Objectives</b> .....	37
<b>3. Summary</b> .....	39
<b>4. Zusammenfassung</b> .....	41
<b>5. Cumulative part (publications)</b> .....	43
<b>5.1. Publication I</b> .....	45
5.1.1. Summary and discussion.....	47

5.1.2. Author contribution.....	49
5.1.3. Main article.....	51
5.1.4. Supplementary data.....	63
5.1.5. Copyright license agreement.....	87
<b>5.2. Publication II.....</b>	<b>89</b>
5.2.1. Summary and discussion.....	91
5.2.2. Author contribution.....	93
5.2.3. Main article.....	95
5.2.4. Electronic Supplementary Material.....	115
5.2.5. Copyright license agreement.....	127
<b>5.3. Publication III.....</b>	<b>129</b>
5.3.1. Summary and discussion.....	131
5.3.2. Author contribution.....	133
5.3.3. Main article.....	135
5.3.4. Supporting information.....	147
5.3.5. Copyright license agreement.....	161
<b>5.4. Publication IV.....</b>	<b>163</b>
5.4.1. Summary and discussion.....	165
5.4.2. Author contribution.....	167
5.4.3. Main manuscript.....	169
5.4.4. Supplementary data.....	203
<b>5.5. Publication V.....</b>	<b>209</b>
5.5.1. Summary and discussion.....	211
5.5.2. Author contribution.....	213
5.5.3. Main manuscript.....	215
5.5.4. Supplementary data.....	257
<b>6. Curriculum Vitae.....</b>	<b>265</b>

# Preface

This cumulative dissertation is concerned with the investigation of on-line and off-line enrichment techniques combined with capillary electromigration separation methods in the analysis of highly hydrophilic analytes in biological and environmental samples. The dissertation is based on the following five **publications**, which are referred to within the text by the Roman numerals I-V. The publications are reproduced with kind permission from the publishers:

- **Publication I: Imidazolium-based ionic liquid-type surfactant as pseudostationary phase in micellar electrokinetic chromatography of highly hydrophilic urinary nucleosides.**  
Azza H. Rageh, Ute Pyell,  
Journal of Chromatography A, 1316 (2013) 135-146 [doi: 10.1016/j.chroma.2012.09.044].
- **Publication II: Determination of urinary nucleosides via borate complexation capillary electrophoresis combined with dynamic pH junction-sweeping-large volume sample stacking as three sequential steps for their on-line enrichment.**  
Azza H. Rageh, Achim Kaltz, Ute Pyell,  
Analytical and Bioanalytical Chemistry, 406 (2014) 5877-5895 [doi: 10.1016/j.chroma.2013.04.069].
- **Publication III: Boronate affinity-assisted MEKC separation of highly hydrophilic urinary nucleosides using imidazolium-based ionic liquid-type surfactant as pseudostationary phase.**  
Azza H. Rageh, Ute Pyell,  
Electrophoresis, 36 (2015) 784-795 [doi: 10.1002/elps.201400357].
- **Publication IV: "Pseudostationary ion-exchanger" sweeping/dynamic pH junction/FASS on-line enrichment for the determination of nucleosides in urine via micellar electrokinetic chromatography after solid phase extraction with phenylboronate affinity gel.**  
Azza H. Rageh, Ute Pyell,  
Submitted to: Journal of Chromatography A.
- **Publication V: Off-line and on-line enrichment of  $\alpha$ -aminocephalosporins for their analysis in surface water samples using CZE coupled to LIF.**  
Azza H. Rageh, Karl-Friedrich Klein, Ute Pyell,  
Submitted to: Talanta.

In addition, the results of this work were presented as **oral** and **poster presentations** in the following seminars and scientific conferences:

#### **Oral presentations:**

- “New strategy for MEKC analysis of highly hydrophilic urinary nucleosides using imidazolium-based IL-type surfactant” **weekly seminar** of the research groups of analytical chemistry in the Department of Chemistry, University of Marburg, Marburg, Germany.
- “Imidazolium-based ionic liquid-type surfactant as pseudostationary phase in micellar electrokinetic chromatography of highly hydrophilic urinary nucleosides” in **24. Doktorandenseminar** des Arbeitskreises Separation Science der GDCh-Fachgruppe Analytische Chemie 2014 in Hohenroda, Germany.
- “Off-line and on-line enrichment of  $\alpha$ -aminocephalosporins for their analysis in surface water samples using CZE coupled to LIF”, **CE Forum 2014** - Capillary Electromigration Separation Techniques, Marburg, Germany.

#### **Poster presentations:**

- “New strategy for MEKC analysis of highly hydrophilic urinary nucleosides using imidazolium-based IL-type surfactant”, **CE Forum 2012** - Capillary Electromigration Separation Techniques, Aalen, Germany.
- “Sweeping-large volume sample stacking (LVSS) as two sequential steps for online enrichment of some cancer biomarkers”, **HPLC 2013**, 39th International Symposium on High Performance Liquid Phase Separations and Related Techniques, Amsterdam, the Netherlands.
- “Determination of urinary nucleosides by dynamic pH junction-sweeping-LVSS-capillary electrophoresis”, **CE Forum 2013** - Capillary Electromigration Separation Techniques, Jena, Germany.
- “Boronate affinity-assisted MEKC separation of highly hydrophilic urinary nucleosides using imidazolium-based ionic liquid-type surfactant as pseudostationary phase”, **CE Forum 2014** - Capillary Electromigration Separation Techniques, Marburg, Germany.

## List of abbreviations and symbols

### Abbreviations

Ado	Adenosine
$\alpha$ -CD	$\alpha$ -Cyclodextrin
BBA	1-Butylboronic acid
$\beta$ -CD	$\beta$ -Cyclodextrin hydrate
BGE	Background electrolyte
CAE	Capillary affinity electrophoresis
CD	Cyclodextrin
CE	Capillary electrophoresis
CEC	Capillary electrochromatography
Cefd	Cefadroxil
Cefx	Cefalexin
CGE	Capillary gel electrophoresis
CIEF	Capillary isoelectric focusing
CITP	Capillary isotachopheresis
CMC	Critical micelle concentration
C <sub>14</sub> MImBr	1-Tetradecyl-3-methylimidazolium bromide
C <sub>16</sub> MImBr	1-Hexadecyl-3-methylimidazolium bromide
CSE	Capillary sieving electrophoresis
Cyd	Cytidine
CTAB	Cetyltrimethylammonium bromide
CZE	Capillary zone electrophoresis
DC-CE	Dynamic compelexation-capillary electrophoresis
DBA	1-Dodecylboronic acid
DDAB	Didodecyldimethylammonium bromide
EF	Enrichment factor
EKC	Electrokinetic chromatography
EOF	Electroosmotic flow
FASS	Field-amplified sample stacking
Guo	Guanosine
HILIC	Hydrophilic interaction liquid chromatography
HBA	1-Hexylboronic acid

HLB	Hydrophilic lipophilic balance
HPLC	High performance liquid chromatography
2-HP- $\beta$ -CD	2-Hydroxypropyl- $\beta$ -cyclodextrin
2-HP- $\gamma$ -CD	2-Hydroxypropyl- $\gamma$ -cyclodextrin
I.D.	Inner diameter
ICH	International conference on harmonisation
IHP	Inner Helmholtz plane
IL	Ionic liquid
Ino	Inosine
ITP	Isotachopheresis
IUPAC	International union of pure and applied chemistry
LIF	Laser-induced fluorescence
LOD	Limit of detection
LOQ	Limit of quantitation
LVSS	Large volume sample stacking
MALDI	Matrix assisted laser desorption/ionization
MEEKC	Microemulsion electrokinetic chromatography
MEKC	Micellar electrokinetic chromatography
5MeUrd	5-Methyluridine
MS	Mass spectrometry
MSS	Micelle to solvent stacking
Me- $\beta$ -CD	Methyl- $\beta$ -cyclodextrin
3-NPBA	3-Nitrophenylboronic acid
O.D.	Outer diameter
OHP	Outer Helmholtz plane
PBA	Phenylboronate affinity gel
PSP	Pseudostationary phase
RFGE	Retention factor gradient effect
RM-MEKC	Reversed direction mode micellar electrokinetic chromatography
RSD	Relative standard deviation
SD	Standard deviation
SDS	Sodium dodecyl sulfate
SE	Sweeping efficiency



SEF	Sensitivity enhancement factor
SSE	Sum of squared errors
SPE	Solid phase extraction
TOF	Time of flight
tITP	Transient isotachopheresis
TTAB	Tetradecyltrimethylammonium bromide
Urd	Uridine
UV	Ultraviolet
Xao	Xanthosine

## Symbols

$\gamma$	Field-strength enhancement factor
$\delta$	Debye length
$\Delta\mu_{\text{eff}}$	Shift in effective electrophoretic mobility
$\varepsilon$	Electric permittivity of the surrounding medium
$\varepsilon_0$	Electric permittivity of vacuum
$\varepsilon_r$	Dielectric constant
$\zeta$	Electrokinetic potential or zeta potential
$\eta$	Viscosity
$\kappa$	Debye-Hückel parameter
$\lambda$	Wavelength
$\lambda_{\text{exc}}$	Wavelength of maximum excitation
$\lambda_{\text{em}}$	Wavelength of maximum emission
$\mu$	Pseudoeffective electrophoretic mobility of the analyte in micellar background electrolyte
$\mu_a$	Electrophoretic mobility of the analyte
$\mu_{\text{eo}}$	Electroosmotic mobility
$\mu_{\text{ep}}$	Electrophoretic mobility
$\mu_{\text{ep,eff}}$	Effective electrophoretic mobility
$\mu_{\text{mc}}$	Electrophoretic mobility of the micelles

$\mu_{ob}$	Observed electrophoretic mobility
$\sigma$	Surface charge density
D	Octanol/water distribution coefficient
E	Electric field strength
$E_{BGE}$	Electric field strength in the separation zone (BGE)
$E_S$	Electric field strength in the sample zone
f	Additional focusing/defocusing factor
F	Faraday constant
h	Peak height
I	Ionic strength
K	Complex formation constant
$k_{BGE}$	Retention factor of the analyte in the background electrolyte
$K_D$	Distribution coefficient
$k_S$	Retention factor of the analyte in the sample zone
$L_{eff}$	Effective length of the capillary or length to the detector
$l_{focus}$	Length of the focused analyte zone
$l_{grad}$	Final length of the sample zone after sweeping with retention factor gradient effect
$l_{inj}$	Initial sample plug length
$l_{sweep}$	Length of the analyte zone after sweeping
$L_T$	Total length of the capillary
P	Octanol/water partition coefficient
$pK_a$	Acid dissociation constant
$pK_a^*$	Apparent acid dissociation constant
q	Electric charge
R	Gas constant
r	Radius or correlation coefficient
$R_s$	Peak resolution

$S_a$	Standard deviation of intercept
$S_b$	Standard deviation of slope
SSE	Sum of squared errors
$S_{yx}$	Standard deviation of residuals
$S_{x0}$	Method standard deviation
T	Temperature
$t_0$	Migration time of the EOF marker
$t_{eo}$	Electroosmotic hold-up time
$t_{mc}$	Migration time of the micelle marker
$t_{mob}$	Residence time in the mobile phase
$t_{ob}$	Migration time of the analyte
$t_r$	Retention time or migration time
$t_{mc}$	Residence time associated with the micellar pseudophase
U	Voltage
$V_{aq}$	Volume of aqueous phase
$V_{eo}$	Electroosmotic velocity
$V_{ep,mc}$	Electrophoretic velocity of micelles
$V_{mc}$	Observed velocity of micelles
$V_{mic}$	Volume of micellar phase
$V_{mob}$	Velocity of the mobile phase



# **1. Introduction**



## 1.1. Principles of capillary electromigration separation techniques

### 1.1.1. Historical background, current status and application

Electrophoresis is defined as the movement of charged species (ions) upon application of an electric field. In 1937 Tiselius [1] introduced “electrophoresis” or “moving boundary electrophoresis” as a separation technique. He found that a mixture of proteins can be separated after placing them between buffer solutions in a tube and applying an electric field. The limitations associated with this approach, such as thermal diffusion and convection, initiated the development of other techniques such as gel electrophoresis. Gels in the slab or tube format have been used primarily for the size-dependent separation of biological macromolecules, such as nucleic acids and proteins. Although it is one of the most widely used separation techniques, slab gel electrophoresis generally suffers from long analysis times, low efficiencies, and difficulties in detection and automation. An alternative to the slab-format is to perform the electrophoretic separation in narrow-bore open tubes or capillaries. Since narrow capillaries have a low conductance, they generate only small amounts of heat and are in principle anti-convective. In an open tube, the use of gel media is therefore not essential for electrophoresis. This allows the application of free-solution (or capillary) electrophoresis, as well as the use of traditional gel media in the capillary [2].

In 1967, Hjerten [3] was the first to report free solution electrophoresis, conducted in 3-mm inner diameter (ID) capillary tubes. The full advantages of this technique could not be realized until methods to introduce smaller quantities into the capillary tubes were developed to avoid sample overloading. In addition, the use of narrower bore capillary tubing (25–100  $\mu\text{m}$  ID), with greater heat dissipation allows the use of higher field strengths (up to  $900 \text{ V cm}^{-1}$ ) for faster and more efficient separations. In 1981, these advantages were realized by Jorgenson and Lukacs [4] in what is considered the first report of modern FSCE (free solution capillary electrophoresis) or capillary zone electrophoresis (CZE) [5]. The next step in the CE development was the application by Terabe *et al.* [6], in 1984, of buffered solutions with the addition of ionic micelles, which contributed to the separation of neutral analytes and subsequently various modifiers have been used to improve the selectivity of separation [7]. Since then, other landmark developments have been made including the development of microchip CE and the development of CEC (capillary electrochromatography) [5].

The potential of capillary electrophoresis (CE) as an analytical technique is demonstrated in many fields such as: (bio)pharmaceutical, forensics, clinical, foodstuff, environmental, chemical, and biochemical analysis. Expanded from its original application to the analysis of bio-macromolecules, CE has been proven to be useful for the separations of compounds such as amino acids, chiral drugs, vitamins,

pesticides, inorganic ions, organic acids, dyes, surfactants, peptides and proteins, carbohydrates, oligonucleotides and DNA restriction fragments, and even whole cells and virus particles. The trends in CE such as coupling of CE with mass spectrometry (CE-MS) and further miniaturization (microfluidic systems on chips) are strongly dependent on the current and future advances in analytical methodologies and instrumentation [2].

### 1.1.2. Instrumentation

One key feature of CE is the overall simplicity of the instrumentation. A diagrammatic representation of the generic CE instrumentation is shown in Fig. 1 [2]. It consists of a high voltage power supply, two buffer reservoirs that can accommodate the capillary and the electrodes, a polyimide-coated capillary with an internal diameter  $\leq 100 \mu\text{m}$  and a length mostly varying between 20 and 100 cm, and a detector. This basic setup can be equipped with enhanced features such as auto-samplers, multiple injection devices, sample/capillary temperature control, programmable power supply, multiple detectors, and computer interfacing [8]. Sample is loaded into the capillary by replacing one of the reservoirs (usually at the anode) with a sample reservoir and applying either an electric field (electrokinetic injection) or an external pressure (hydrodynamic injection). After replacing the buffer reservoir, the electric field is applied and the separation is performed.

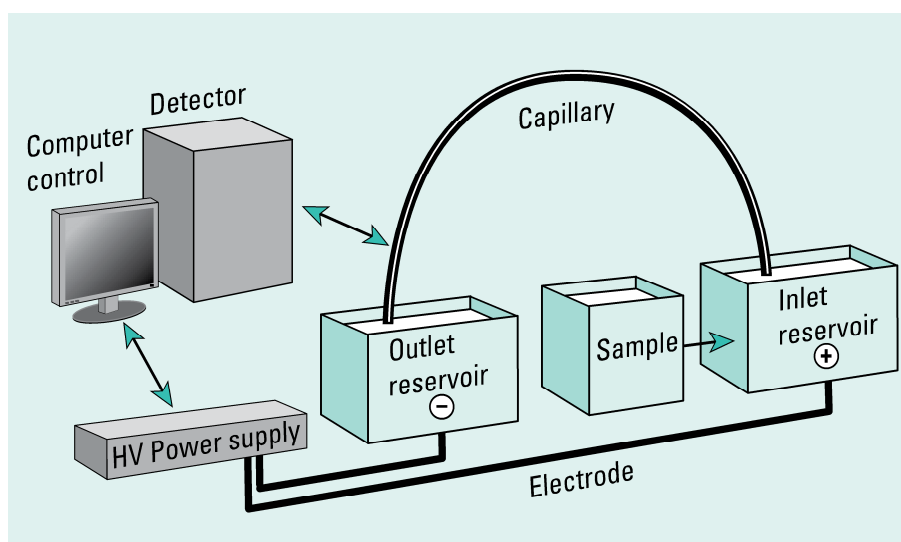


**Figure 1:** Basic components of CE instrumentation [2].

Optical detection (e.g. photometric or fluorimetric detection), which is the most commonly employed, can be made at the opposite end, directly through the capillary wall over a short segment of the capillary [2] in order to avoid instrumental band broadening [9]. The signal is handled by a data handling device and the output is displayed as an electropherogram, which is a plot of the detector response versus time [9].



### 1.1.3. Basic concepts

#### 1.1.3.1. Electrophoresis

The principle of separation by capillary electrophoresis (CE) is based on the fact that charged species are separated according to differences in their electrophoretic mobility. The electrophoretic mobility  $\mu_{ep}$  of an ionic species migrating through a medium in an electrical field is directly proportional to electrical forces ( $F_e$ ) and inversely proportional to frictional forces ( $F_f$ ) acting on the ion. In an electrical field, ions are accelerated by the electrical force  $F_e$ , which is a function of field strength,  $E$ , and charge of the ion,  $q$  (Eq. 1):

$$F_e = qE \quad (1)$$

At the same time, ions in an electric field are retarded by frictional forces. If the accelerating force is equal to the sum of frictional forces, the steady state is reached, which means that the ion has a constant velocity. In the most simplified case, only the friction according to Stokes  $F_f$  (Stokes Law, ion = rigid sphere) has to be considered:

$$F_f = -6\pi\eta rv \quad (2)$$

where  $\eta$  is the viscosity of the electrophoretic medium,  $r$  is the radius of the solvated species, and  $v$  is its velocity. Friction coefficients for particles of other shapes may be estimated using more complex equations. Equating Eqs. (1) and (2), electrophoretic mobility can be given according to Eq (3):

$$\mu_{ep} = \frac{1}{6\pi\eta} \frac{q}{r} \quad (3)$$

From this equation it is evident that small, highly charged species have high mobilities whereas large, minimally charged species have low mobilities [10]. Electrophoretic mobility (observed or apparent electrophoretic mobility) can be defined as the proportionality constant between the electrophoretic velocity and the applied field strength,  $E$  (Eq. 4):

$$\mu_{ep} \equiv \frac{v}{E} \quad (4)$$

Experimentally,  $\mu_{ep}$  can be calculated as follows:

$$\mu_{ep} = \frac{L_{eff}}{t_{ob}} \frac{L_T}{U} \quad (5)$$

In capillary electrophoresis,  $E$  is calculated by dividing the applied voltage  $U$  by the total length of the capillary  $L_T$  and  $v$  is calculated by dividing  $L_{eff}$  (the effective length of the capillary (length to the detector)) by  $t_{ob}$  (migration time of the analyte, which is obtained from the electropherogram).

### 1.1.3.2. Electroosmotic flow (EOF) and regulation of EOF

A fundamental constituent of CE operation is the electroosmotic or electroendosmotic flow (EOF). EOF is the bulk flow of liquid at constant velocity in the capillary as a consequence of the surface charge on the interior capillary wall [11]. The linear velocity of the EOF  $v_{eo}$  can be experimentally obtained using the migration time of a neutral compound (called an electroosmotic flow marker):

$$v_{eo} = \frac{L_{eff}}{t_{eo}} \quad (6)$$

where  $t_{eo}$  is the electroosmotic hold-up time [11] (time required for a liquid in a capillary to move due to electroosmosis through the effective length of the capillary,  $L_{eff}$ )

The linear velocity of flow divided by field strength is defined as the electroosmotic mobility ( $\mu_{eo}$ ):

$$\mu_{eo} \equiv \frac{v_{eo}}{E} \quad (7)$$

And it can be experimentally calculated as follows:

$$\mu_{ep} = \frac{L_{eff} L_T}{t_{eo} U} \quad (8)$$

To get a better understanding of how the electroosmotic flow is driven by an electric field, we first have to understand what happens very close to the walls inside the capillary. Fig. 2a shows a schematic illustration of the electrical double layer [12,13]. There are different models that have described the structure of the electric double layer such as: Helmholtz double layer model, Gouy-Chapman model, Stern model, and Grahame model [14]. In the Helmholtz layer model, the solvated ions arrange themselves along the charged surface but are held away from it by their hydration spheres. The location of the sheet of ionic charge, which is called the outer Helmholtz plane (OHP), is identified as the plane running through the solvated ions. This model assumes that the electric potential changes linearly within the layer confined by the charged surface on one side and the OHP on the other. Since this model assumes the presence of two rigid planes of charge, one plane is the outer Helmholtz plane (OHP) and the other plane is the charged capillary wall, it ignores the effect of thermal motion, which tends to break up and disperse the rigid outer plane of charge.

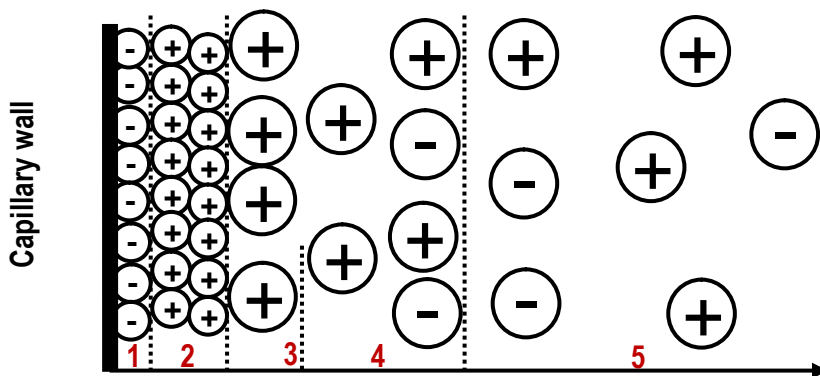
The Gouy-Chapman model describes a rigid charged surface, with a cloud of oppositely charged ions in the solution, the concentration of the oppositely charged ions is decreasing with increasing the distance from the surface. Neither the Helmholtz nor the Gouy–Chapman model is a very good representation of

the structure of the double layer. The former overemphasizes the rigidity of the local solution; the latter underemphasizes its structure.

The Stern model is a combination between the first two models, in which the ions closest to the charged surface forming the Stern layer (which is the same as the rigid Helmholtz plane suggested by the Helmholtz layer model), while ions located outside that layer are diffused into the bulk solution as in the Gouy–Chapman model [15].

In the Grahame model an inner Helmholtz plane (IHP) was added to the Stern model. The IHP is formed by ions that have discarded their solvating molecules and have become attached to the charged surface by chemical bonds.

(a)



(b)

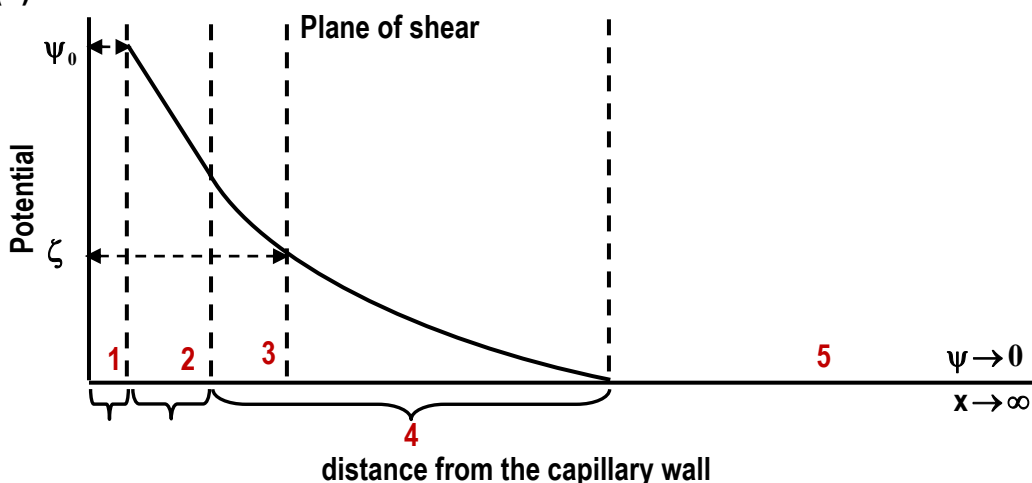


**Figure 2:** Representation of the electrical double layer at the surface of a fused-silica capillary. (a) Distribution of charge at the internal wall of a fused-silica capillary. (b) Potential difference ( $\psi$ ) at the internal wall of a fused-silica capillary due to the distribution of charges. 1 the capillary wall, 2 the Stern layer or the inner Helmholtz plane, 3 the outer Helmholtz plane, 4 the diffuse layer, and 5 the bulk charge distribution within the capillary,  $x$  is the length from the center of charge of the negative wall to a defined distance,  $\zeta$  is the zeta potential modified from [13,16].

In a buffer-filled fused-silica capillary, the EOF results from the effect of the applied electric field on the counterion layer adjacent to the charged capillary wall (Fig. 2a). Electroosmosis occurs because the weakly acidic silanol groups at the surface of the capillary dissociate when in contact with an electrolyte solution (buffer). The dissociation equilibrium can be given according to Eq. 9 [17]:



The ionized silanol groups  $\text{SiO}^-$  of the capillary wall attract cationic species from the buffer (Fig. 2a). The ionic layer that is formed has a positive charge density that decreases exponentially (according to the linearized Poisson-Boltzmann equation) as the distance from the wall increases. The double layer formed closest to the surface is termed the “Inner Helmholtz” or “Stern” layer and, which consist of an immobilized compact layer of tightly bound cations and it is essentially static. A more diffuse layer contains hydrated cations, anions, and neutral species, is formed distal to the Stern Layer is termed the “diffuse layer” or “Gouy layer” (also Gouy-Chapman layer) [16]. The initial part of the diffuse layer, at the side of the Stern layer, is known as the outer Helmholtz plane [13].

Because of the distribution of charges at the double layer at capillary wall-electrolyte interface a potential field is generated as shown in Fig. 2b. According to the Stern model, the electric potential at the surface of the wall  $\Psi_0$  decreases linearly within the compact layer, while the potential drop is exponential within the diffuse layer (according to the linearized Poisson-Boltzmann equation) [13]. The electric potential at the plane of shear that coincides with the outer Helmholtz plane at the boundary of the Stern layer (the interface between the compact and diffuse layers) is called electrokinetic potential or zeta potential  $\zeta$ . When an electric field is applied, ions in the diffuse layer will start to migrate. The extent of the migration velocity is determined by the zeta potential. Cations in the diffuse layer move toward the cathode dragging the rest of the fluid in the capillary that results in a bulk flow of liquid through the capillary. This phenomenon is called electroosmosis and is physically observed as the EOF. At the surface of shear (outer Helmholtz plane) the velocity of the EOF rises from a zero value to a limiting value (electroosmotic velocity:  $v_{eo}$ ) at an infinitive distance from the wall where the distribution of the cations equals to that of the bulk.

The zeta potential depends on the surface charge density and the double layer thickness  $\delta$ . The relationship between the  $\zeta$  potential and the electroosmotic velocity  $v_{eo}$ , is described by the Helmholtz–Smoluchowski equation [9]:

$$v_{eo} = \frac{\varepsilon \zeta E}{4\pi\eta} = \frac{\varepsilon_o \varepsilon_r \zeta E}{\eta} = \mu_{eo} E \quad (10)$$

where  $\varepsilon$  is the electric permittivity of the surrounding medium,  $\varepsilon_0$  is the electric permittivity of vacuum,  $\varepsilon_r$  is the dielectric constant, and  $\zeta$  is the zeta potential,  $E$  is the electric field strength,  $\eta$  is the viscosity of the background electrolyte, and  $\mu_{eo}$  is the electroosmotic mobility. Eq. 10 is only valid if the capillary inner diameter is large compared with the thickness of the electric double layer. However, this restriction is fulfilled in practice [9]. Due to the extremely small size of the double layer, the EOF originates close to or almost at the wall of the capillary [13]. As a result, the EOF has a flat plug-like flow profile, compared to the parabolic profile of hydrodynamic flows. The thickness of the electric double layer (Debye length  $\delta$ ) or its reciprocal (Debye-Hückel parameter  $\kappa$ ) is then given by the following equation [18]:

$$\kappa = \frac{1}{\delta} = \sqrt{\frac{2 c F^2}{R T \varepsilon_0 \varepsilon_r}} \quad (11)$$

where  $\kappa$  is the Debye-Hückel parameter,  $\delta$  is the double layer thickness (Debye length),  $c$  is the molar concentration of the background electrolyte,  $F$  is Faraday constant, and  $R$  is the gas constant.

It is important to note that the EOF velocity is independent of the capillary inner diameter, but it depends upon the surface charge density, the electric field strength, the thickness of the electrical double layer, ionic strength and the viscosity of the separation medium, which in turn is dependent upon the temperature [18]. In addition, it is obvious that the  $v_{eo}$  is strongly dependent on the pH of the BGE, as the buffer pH will determine the fraction of the silanol groups that will be ionized (Eq. 9). Therefore, the EOF velocity is negligible at low pH ( $\text{pH} < 4$ ) and very high at high pH ( $\text{pH} > 9$ ) [18].

In addition to the above mentioned parameters that influence the EOF, the EOF can be regulated, suppressed or even reversed via control of surface charge density. This can be accomplished by either: (i) static or dynamic coating (= covering the inner wall) [19,20] or (ii) addition of metal cations. The static coating can be either physically adsorbed or covalently bonded (permanent coating). Covalent modification strategies of the capillary wall generate new chemical bonds on the surface to change the chemistry, while adsorbed coatings use either electrostatic or hydrophobic interactions to adsorb a polymer onto the surface. Dynamic coatings are different in that the coating agent is in the running buffer and in contact with the surface at all times [21]. Surfactants are the most common species for dynamic coatings as will be discussed later. Moreover, the EOF can be reduced via (ii) addition of divalent metal cations (e.g.  $\text{Ca}^{2+}$  or  $\text{Mg}^{2+}$ ) [22]. These cations will be exchanged against the monovalent cations (e.g.  $\text{H}_3\text{O}^+$  or  $\text{Na}^+$ ), which are the counter ions existing on the negatively charged silica surface resulting in reduction of the EOF velocity.

The overall migration in CE is determined by the combined effect of the effective electrophoretic (due to electrophoretic migration) and the electroosmotic mobility, therefore the observed electrophoretic mobility can be calculated as follows:

$$\mu_{\text{ob}} = \mu_{\text{eo}} + \mu_{\text{ep,eff}} \quad (12)$$

where  $\mu_{\text{eo}}$  is the electroosmotic mobility and  $\mu_{\text{ep,eff}}$  is the effective electrophoretic mobility. By subtracting Eq. 8 from Eq. 5,  $\mu_{\text{ep,eff}}$  can be obtained as follows:

$$\mu_{\text{ep,eff}} = \frac{L_{\text{eff}} L_{\text{T}}}{t_{\text{ob}} U} - \frac{L_{\text{eff}} L_{\text{T}}}{t_{\text{eo}} U} \quad (13)$$

Generally, the electrophoretic mobility is positive if the migration is towards the cathode (positively charged species), and the electrophoretic mobility is negative if the migration is towards the anode (negatively charged species).

## 1.2. CE modes

The separations in capillary electromigration techniques are achieved in narrow capillaries by employing a high electric field strength. These techniques include capillary electrophoretic techniques and electrically driven capillary chromatographic techniques, based on different separation principles. In some cases, these principles overlap [11]. Different modes of capillary electromigration techniques have been reported such as: capillary zone electrophoresis (CZE), micellar electrokinetic chromatography (MEKC), microemulsion electrokinetic chromatography (MEEKC), capillary affinity electrophoresis (CAE), capillary sieving electrophoresis (CSE), capillary gel electrophoresis (CGE), capillary isoelectric focusing (CIEF), capillary isotachopheresis (CITP) and capillary electrochromatography (CEC). Several books and book chapters about CE modes have been published in the literature [2,8,17,23], however in the following discussion, the first two techniques will be discussed in detail.

### 1.2.1. Capillary zone electrophoresis (CZE)

CZE is the most commonly employed mode of CE owing to its versatility; the applications of CZE are as widely varying as the composition of the BGEs. The separation capillary is filled with a predominantly aqueous buffer solution; additives may be incorporated into the BGE to achieve the desired selectivity and resolution of separation [5]. The BGE chosen should demonstrate good buffering capacity and low background current to suppress Joule heating effects. The pH of the BGE can influence both the charge of the analyte and the fused-silica capillary wall according to their  $pK_{\text{a}}$  values. Hence the EOF in the capillary is also influenced. Some buffer additives may influence the solute – capillary wall interactions. The separation selectivity is based on the difference in effective mobilities between compounds, resulting in differences in migration velocities. In the normal polarity mode, charged species are

separated according to their respective charge to-size ratios in an applied electrical field. Cations migrate by coulombic attraction toward the cathode, with the cation of the highest charge-to-size ratio migrating fastest. Conversely, anions migrate toward the anode, with those of the highest charge-to-size ratio migrating fastest. At a sufficient EOF within the capillary, the coulombic attraction of the anions for the anode will be overcome, and the anions will migrate toward the cathode. Overall, the migration order in CZE is cations (from high to low charge-to-size ratio), followed by neutral species (unseparated), and finally anions (from low to high charge-to-size ratio) [5].

### **1.2.2. Micellar electrokinetic chromatography**

#### **1.2.2.1. Separation principle**

The term “Electrokinetic chromatography (EKC)” was introduced by Terabe’s research group and is an analytical separation method which employs the experimental technique of CZE in combination with the principle of chromatography [24]. In addition to the electrolytic solution used in CZE, a major component called the pseudostationary phase, PSP (also called separation carrier) is employed. This then satisfies the definition of chromatography where two phases should exist between which the solute is distributed. The electrokinetic phenomenon, including both electrophoresis and electroosmosis, is the means of transporting the pseudostationary phase and solutes inside the capillary. Separation of neutral and charged analytes is based on the existing differences in their distribution coefficients between the PSP and the surrounding aqueous phase. In addition to distribution equilibria, EKC invariably also involves other types of chemical equilibria, e.g. ion exchange and/or complex formation [9]. A variety of materials can be used as the pseudostationary phase in EKC such as microemulsions [25,26], charged cyclodextrins [27,28], charged polymers [29], proteins [30], nanoparticles [31] and tetraalkylammonium ions [32,33]. Micellar EKC (MEKC) is the term used when micelles are used as PSP (Fig. 3) [34]. Comprehensive introductions to MEKC are those reported by Vindevogel and Sandra [35], Terabe [36] and Khaldi [37]. There is one monograph on electrokinetic chromatography [38] and a very large number of review articles on current state of the art in MEKC as those reported by Quirino and Terabe [39], Terabe [40,41], Pappas *et al.* [42], Silva [43-46] and El-Deeb *et al.* [47,48].

Generally, In EKC, a non-charged solute will be transported either with the velocity of the electroosmotic flow or with the velocity of the separation carrier. The migration velocity of the separation carrier is, in general, virtually unaffected by this interaction. The assumption that the migration velocity of the separation carrier is not altered by the interaction with or incorporation of a solute molecule is used to define the difference between a pseudostationary phase and a simple complex-forming agent, which is used in capillary electrophoresis to modify the effective

electrophoretic mobility of the solutes to be separated. If the solutes to be separated do not possess an effective electrophoretic mobility without the presence of the separation carrier, the separation carrier must have an electrophoretic mobility [9].

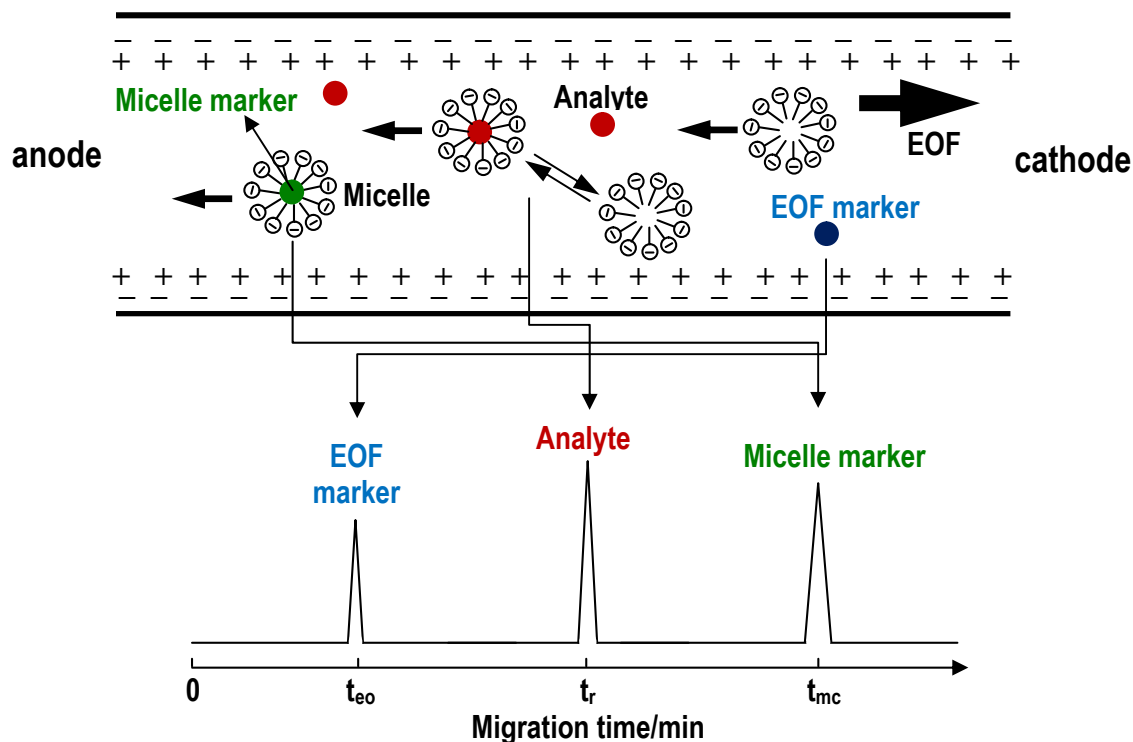


**Figure 3:** Schematic representation of the separation mechanism of micellar electrokinetic chromatography (MEKC) using anionic micelles.  $t_{eo}$  = migration time of a neutral, “unretained” analyte (EOF marker),  $t_r$  = “retention” time of the analyte in MEKC,  $t_{mc}$  = migration time of a micelle marker modified from [34].

Micellar EKC (MEKC) is a special case of EKC, in which the secondary phase is a micellar phase dispersed in the capillary. MEKC was first introduced by Terabe *et al.* in 1985 [49]. The separation of neutral species by MEKC is accomplished by the use of surfactants in the running buffer at concentrations above the critical micelle concentration (8 to 9 mmol L<sup>-1</sup> for sodium dodecyl sulfate (SDS) in water at 25 °C, for example). Micelles are formed from aggregates of surfactant molecules above critical micelle concentration. The presence of micelles, which act as a separation carrier in the running buffer, transforms CZE into MEKC with no need to modify the apparatus. Micelles are often spherical with the hydrophobic tails of the surfactant molecules oriented towards the center, and the charged heads oriented outside towards the buffer. Charged micelles migrate with a velocity different from that of the bulk aqueous phase due to their electrophoretic mobility, whereas the bulk solution migrates with the velocity of the EOF (Fig. 3). As in CZE, even a negatively charged micelle can be transported toward the cathode in the case of a strong EOF under either neutral or alkaline conditions. In CZE, neutral analytes cannot be separated and they usually migrate at the same velocity as does the



bulk solution while in MEKC the separation of neutral analytes differing in their partitioning coefficients (between the PSP and the surrounding phase) is possible [2].

The separation process in EKC can be described in chromatographic terms. In fact, conventional chromatography can be regarded as a special case of EKC, where the observed velocity of the separation carrier is zero [9]. In Fig. 3 the separation mechanism in MEKC for a neutral solute and a micellar pseudophase of an anionic surfactant is illustrated. In MEKC the micelle acts like the stationary phase in chromatography. However, the micelle is not immobilized, and hence can have an observed velocity different from zero. Therefore, the micellar pseudophase in MEKC is termed pseudostationary phase (PSP). The observed velocity of a solute zone (neutral solute) is the weighted mean of the velocity of the mobile phase (the surrounding aqueous phase) and of the observed velocity of the micelles:

$$v_s = \frac{t_{mob}}{t_{mob} + t_{mc}} v_{mob} + \frac{t_{mc}}{t_{mob} + t_{mc}} v_{mc} = \frac{1}{k + 1} v_{mob} + \frac{k}{k + 1} v_{mc} \quad (14)$$

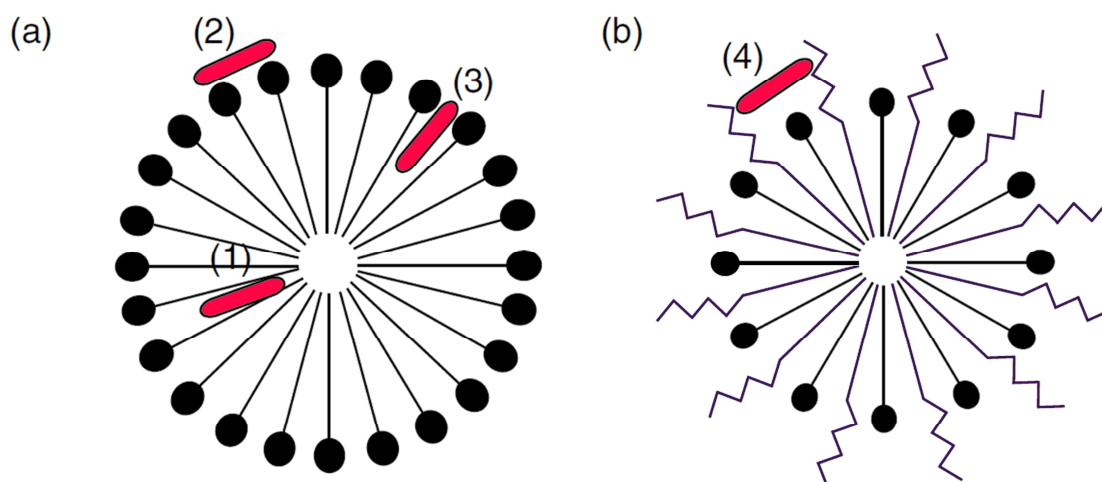
where  $v_s$  is the observed velocity of the solute zone (neutral solute),  $t_{mob}$  is the residence time in the mobile phase,  $t_{mc}$  is the residence time associated with the micellar pseudophase,  $v_{mob}$  is the velocity of the mobile phase,  $v_{mc}$  is the observed velocity of micelles ( $v_{mc} = v_{ep,mc} + v_{eo}$ ) and  $k$  is the retention factor ( $t_{mc}/t_{mob}$ ) [9].

Fig. 3 shows an electropherogram for the separation of a mixture of an EOF marker, a neutral solute and a marker of the micelles of an anionic surfactant, which are assumed to be detectable in the UV region. The neutral analyte free from the micelle migrates only by the EOF, while the analyte totally incorporated by the micelle migrates at the observed velocity of the micelle (the sum of the electroosmotic velocity and the electrophoretic velocity of the micelle). The neutral solute zone migrates at an average velocity between that of the EOF marker and the micelle marker and is detected between  $t_{eo}$  and  $t_{mc}$ , which are the migration times of the EOF marker and the micelle, respectively. Acetone and thiourea can be employed as an EOF marker, while decanophenone, Sudan III, and anthracene [9] can be used as a micelle marker.

### 1.2.2.2. Mechanism of interaction between the micelles and analyte

According to Terabe [50], three kinds of analyte interaction mechanisms with micelles can be differentiated, as presented in Fig. 4a. These are: (i) introducing the analyte to the hydrophobic core of the micelle, (ii) the analyte adsorption on the surface of the micelle by electrostatic or dipole

interaction, and (iii) implementing the analyte as the co-surfactant by participation in the formation of the micelle.



**Figure 4:** Schematic illustration of micellar solubilization. (a) Ionic micelle and (b) mixed micelle of ionic and nonionic surfactants interacting (1) with the hydrophobic core, (2) on the surface, (3) as a cosurfactant, and (4) with nonionic surfactant surface [50].

Highly hydrophobic nonpolar compounds such as aromatic hydrocarbons are introduced to the core and can be used as a micelle marker. Beside hydrophobic interaction with the core of the micelles, it is supposed that the majority of analytes interact with micelles through the surface, palisade layer (term associated with non-ionic surfactant), and polar groups. The effect of the molecular structure of the surfactant on the separation selectivity differs according to the type of interaction involved. The hydrophilic, or ionic group, is generally more important in determining the selectivity than the hydrophobic group due to the interaction of the analytes with the micelle at the surface. Different polar groups of various surfactants can show different selectivity for analytes, even if the surfactants have identical alkyl chain groups. Moreover, the separation selectivity can be significantly improved by applying mixed micelles composed of ionic and non-ionic surfactants (Fig. 4b).

### 1.2.2.3. Retention factor in MEKC

Similar to chromatography the retention factor  $k$  (older term: capacity factor  $k'$ ) in MEKC is defined as the residence time in the micellar pseudophase (pseudostationary phase) divided by the residence time in the surrounding liquid phase. If we assume the micelles to be a homogeneous pseudophase, the separation process can be understood to be due to distribution between two distinct phases having two different observed mobilities:

$$k = K_D \frac{V_{mic}}{V_{aq}} \quad (15)$$

where  $K_D$  is the distribution coefficient,  $V_{mic}/V_{aq}$  is the phase ratio (= volume of micellar phase/volume of aqueous phase). By replacing the velocities in Eq. (14) with the respective distance-over-time and rearranging the results, the following equation is obtained:

$$k = \frac{t_r - t_{eo}}{t_{eo} (1 - t_r / t_{mc})} \quad (16)$$

where  $t_{eo}$  = migration time of the EOF marker,  $t_r$  = migration time of the analyte,  $t_{mc}$  = migration time of the micelle marker.

This equation is valid only in the normal elution mode where the electroosmotic velocity  $v_{eo}$  and the velocity of micelles  $v_{mc}$  have identical direction and  $|v_{eo}| > |v_{mc}|$ . If  $t_{mc}$  approaches infinity, then the definition of ( $k$ ) becomes identical to the definition of ( $k$ ) in conventional chromatography; the solid pseudo-phase becomes the solid phase. In the normal elution mode the time span (window) in which a neutral compound can be eluted is restricted to values between  $t_{eo}$  and  $t_{mc}$ . Consequently,  $t_{eo}/t_{mc}$  or its reciprocal value  $t_{mc}/t_{eo}$  have been mainly used in the literature to characterize the ratio of the observable velocities of the two “phases” in EKC. One widely accepted term for this time ratio is migration (time) window [9].

For measuring the retention factor for charged solutes in MEKC, a different approach is needed. The calculation is then based on following equation:

$$k = \frac{\mu - \mu_{ep,eff}}{\mu_{mc} - \mu} \quad (17)$$

where  $\mu$  = pseudoeffective electrophoretic mobility of the analyte in micellar BGE,  $\mu_{ep,eff}$  = effective electrophoretic mobility of the analyte in micelle-free BGE, and  $\mu_{mc}$  = electrophoretic mobility of the micelles in micellar BGE.

#### 1.2.2.4. Classes of surfactants

Surfactants can be conveniently categorized by the charge on the head group as (a) anionic, (b) cationic, (c) nonionic, and (d) zwitterionic:

##### a- Anionic surfactants

Due to a number of reasons, SDS is the most popular surfactant in MEKC. Among these reasons are high stability, low absorption in the ultraviolet region, high solubilization capability, and the commercial availability of the high quality reagent. The reagent CMC amounts to 8 mmol L<sup>-1</sup> in water; for buffer

solutions, it is even 3 mmol L<sup>-1</sup>. In most cases, 10–50 mmol L<sup>-1</sup> SDS solutions are applied. Still, higher concentrations, even up to 100 mmol L<sup>-1</sup>, give good results provided current intensity does not exceed 50 μA [51].

## **b- Cationic surfactants**

### **(1) Conventional alkyltrimethylammonium salts**

Cationic micelles show substantially different selectivity for neutral and for ionic solutes, as compared with anionic micelles because of the different polar groups of this surfactant. Most cationic surfactants have an alkyltrimethylammonium group and their counter ions are halides. Cetyltrimethylammonium bromide (CTAB) is the most popular cationic surfactant used in CE, mainly to reverse the direction of EOF due to adsorption of the cationic surfactant on the capillary wall. However, it is not widely used as a micelle-forming surfactant in MEKC, probably due to its UV absorption in the short wavelength region and the generation of bromine in the anodic vial during electrophoresis. However, CTAB or the corresponding chloride (CTAC) shows significantly different selectivity compared to anionic surfactants while the migration order of analytes still follows the order of increasing distribution constant, as in the case of anionic micelles. According to studies using the solvation parameter model, CTAB differs significantly from SDS concerning its hydrogen-bond acidity and basicity [52]. Therefore, the use of a cationic surfactant instead of SDS is a promising alternative to change the selectivity.

### **(2) Ionic-Liquid based surfactants**

Ionic liquids (ILs) are known as molten salts with melting points below 100° C. They are a class of ionic non-molecular solvents with a multitude of physicochemical properties. The most remarkable properties include their high thermal stability, a low vapour pressure, the miscibility with water and a variety of organic solvents, notable catalytic properties, as well as good extraction coefficients for various organic compounds [53]. They are environmentally benign and their non-flammability and low volatility allow them to gain an increasing interest in the field of green chemistry. ILs are also considered to be semi-organic salts as they are composed of bulky asymmetric nitrogen- or phosphorous-based organic cations such as alkyl imidazolium, alkyl pyrrolidinium, alkyl ammonium, alkyl pyridinium and alkyl phosphonium with associated inorganic (e.g. Br<sup>-</sup>, Cl<sup>-</sup>, PF<sub>6</sub><sup>-</sup>, BF<sub>4</sub><sup>-</sup>) or organic (e.g., [(CF<sub>3</sub>CO<sub>2</sub>)<sup>-</sup>], [(CF<sub>3</sub>SO<sub>2</sub>)<sub>2</sub>N]<sup>-</sup>) counter anions (Fig. 5) [54]. The low symmetry and the relatively large size of one or both ions lead to a lowering of the lattice energy, and hence the melting point of the resulting ionic liquid. By pairing of different cations and anions, it is possible to create a huge number of different ionic liquids, each with its specific properties and adapted for a particular task. ILs were a subject of many

recent review articles, which highlight a variety of applications in many areas of separation science [53-59].

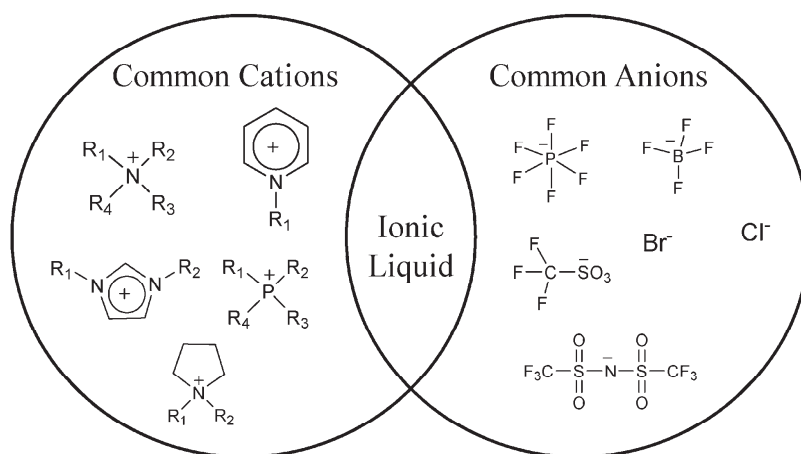


**Figure 5:** Typical cations (left) and anions (right) in ionic liquids [60].

It was reported that ILs possessing long hydrophobic alkyl tails with cationic polar headgroups can form micelles when they are dissolved in water in a concentration above their CMC (critical micelle concentration). This property enables ILs to emerge as a new class of surfactants, especially because they possess the properties of cationic surfactants in addition to the restricted number of the classic cationic surfactants and the growing interest in applications that involve cationic surfactants. It should also be mentioned that the cation/anion pair forming the ionic liquid does no longer constitute a true ionic liquid once the ionic liquid is dissolved in water or any organic solvent. Therefore, the term IL-type surfactant is more appropriate than IL surfactant [53] as suggested in the review article of Pino *et al.* [53]. Dong *et al.* [61] and Vanyur *et al.* [62] reported that micelles are formed in an aqueous solution of long-chain ILs C<sub>14</sub>MImBr (1-tetradecyl-3-methylimidazolium bromide) and C<sub>16</sub>MImBr (1-hexadecyl-3-methylimidazolium bromide). They found that imidazolium-based ILs are superior to the traditional cationic alkyltrimethyl ammonium bromides in their ability to form micelles, i.e., their CMC values are significantly lower than those of the classic cationic surfactants. Alkylimidazolium-based ILs are the most widely used class of IL-type surfactants in capillary electrophoresis [58]. In addition to their role as background electrolyte (BGE) modifier in capillary electrophoretic separation techniques [63-66], several reports have described the utility of long-chain imidazolium-based ILs as pseudostationary phase (PSP) [67-69] in MEKC. Interest in IL-type surfactants stems from the fact that they offer a high versatility of interaction types (electrostatic,  $\pi$ - $\pi$ , ion-dipole or hydrogen bonding interactions with the imidazolium cation head group and hydrophobic interaction due to the long alkyl tail) [70] that give rise to a different separation selectivity.

**Dynamic coating of the capillary wall:**

The presence of cationic surfactants in the BGE can reverse the direction of the EOF through dynamic coating of the capillary wall. Tsuda first reported the use of surfactants (especially cetyltrimethylammonium bromide (CTAB)) for EOF modification in anion analysis in 1987 [71]. However, it was the work of Jones and Jandik in 1991 using tetradecyltrimethylammonium bromide (TTAB) that was the breakthrough in the field of ion analysis by CE. Using  $0.5 \text{ mmol L}^{-1}$  TTAB in  $5 \text{ mmol L}^{-1}$  chromate (indirect UV probe) at pH 8.0, 30 anions were separated in a span of 89 s [72].

It was reported that at one half to one third the CMC, aggregation of the surfactant monomers at the surface of the capillary begins [22]. Above this threshold concentration there is a rapid transition from a normal EOF to a reversed EOF. Once the micellar layer is fully formed at the capillary wall, further increase in the surfactant concentration does not yield changes in the magnitude of the EOF.

As described by Pino *et al.* [53], IL-type surfactants are capable of forming hemimicelles and admicelles when adsorbed onto a solid support. Hemimicelles are defined as a monolayer of surfactant formed on a solid support, whereas the positively charged head groups are attached to the surface of opposite charge. On the other hand, admicelles form bilayer arrangements. In contrast to micelles, admicelles are formed below the CMC. The process in which either hemimicelles or admicelles are formed is called dynamic coating of the capillary. As the capillary wall under these conditions is positively charged, dynamic coating reverses the direction of the EOF.

The difference in the coating stability amongst different types of cationic surfactant can be ascribed to a different aggregate structure of the surfactants at the capillary surface [22]. E.g. Single chain surfactant monomers (e.g. TTAB or CTAB) form spherical aggregates at the capillary wall. This micellar coating formed by TTAB or CTAB creates a rather heterogeneous surface in which gaps between the micelle spheres are evident due to the electrostatic repulsion between adjacent micelles (Fig. 6a).

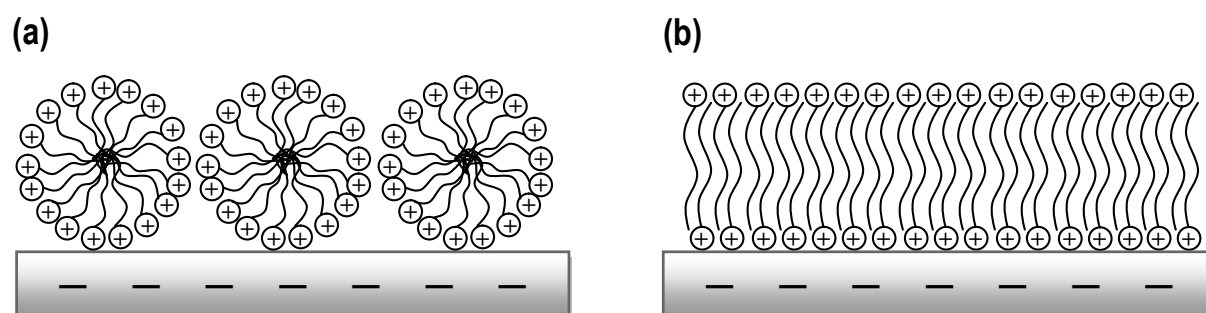


**Figure 6:** Structures previously depicted for surfactant aggregates at the capillary wall. Above the surface CMC (one half to one third of the CMC) surfactants aggregate at the capillary wall to form either (a) a micellar layer (as for CTAB and TTAB) or (b) a bilayer (as with DDAB) modified from [22].

On the other side, didodecyldimethylammonium bromide (DDAB) aggregates to form a flat bilayer structure at the capillary surface. The more homogeneous coating and greater surface coverage provided by DDAB is thought to account for its increased stability compared to that formed by either TTAB or CTAB (Fig. 6b) [22].

### **(c) Non-ionic surfactants**

Nonionic surfactants themselves do not possess an electrophoretic mobility and cannot be used as pseudostationary phases in conventional MEKC [73]. However, nonionic surfactant micelles are useful for the separation of charged compounds, especially for peptides with closely related structures [74]. Nonionic surfactants can also be employed as pseudostationary phases in MEKC with a combination of ionic surfactants. Most nonionic surfactants have polyoxyethylene groups. Mixed micelles of nonionic and ionic surfactants with surfaces covered by polyoxyethylene groups, as shown in Fig. 4b, will have different surface characteristics and hence a different selectivity from that of the ionic surfactant micelle. Some natural chiral surfactants are uncharged and were used as mixed micelles with SDS.

### **(d) Zwitterionic surfactants**

Zwitterionic surfactants (e.g. 3-(N,N-dimethyltetradecylammonio)-propane-sulfonate) are not widely used in MEKC. However, zwitterionic surfactants will be interesting if they are used in mixed micelles, because they should show significantly different selectivity compared to other types of surfactants.

## **1.3. Detection techniques**

The right choice of the detection technique in CZE and EKC depends on the type and concentration of analytes, on the complexity of the sample and on potential interferences from the sample matrix and on the limitations imposed by the electromigration separation method used. Commercial availability of the detector and the cost and ease of operation should also be considered [75]. The detection can be performed either off-line (off-capillary) or in an on-line (on-capillary, end-capillary, and entire capillary) arrangement. In the off-capillary arrangement, the detector is not connected directly to the separation capillary and the separation does not affect the detection as significantly as with on-line detection, so that the separation conditions can be optimized fairly independently of the detection requirements. An example is off-line connection of capillary electromigration techniques with MALDI-TOF-MS (matrix-assisted laser desorption/ionization-time of flight-Mass spectrometry), however, the detection process is discontinuous.

On-line detection can be accomplished either directly on a segment of the separation capillary (typically with UV-spectrophotometric or laser-induced fluorescence detection), or using a detector connected to the end of the capillary such as with MS detection or electrochemical detection. This type of detector should be carefully designed to suppress contributions to band broadening.

Optical detection techniques, including UV spectrophotometric and LIF (laser induced fluorescence) measurements, are widely used in electrophoresis and electrokinetic chromatography. With few exceptions, only UV or LIF detectors are installed in compact commercial instruments. Other detection techniques based on the measurement of electrochemical properties of the analytes (conductometry, amperometry, or potentiometry) are used less often, but their sensitivity is in many cases better than the sensitivity of UV spectrophotometric detectors [75].

The most common detection technique in electrophoresis and EKC is on-column UV absorbance detection, which provides a large applicability, as most organic compounds absorb UV radiation. UV detection is straightforward and easy to implement, and very useful for quantitative purposes. An important drawback is its rather low concentration sensitivity, caused by the small optical path length provided by the capillary diameter. The detection limits usually are not lower than  $10^{-5}$ – $10^{-7}$  mol L<sup>-1</sup>, depending on the molar absorption coefficients of analytes. Moreover, the selectivity of UV detection is very limited, and it hardly gives structural information on analytes, even when diode-array detection (DAD) is used.

Fluorescence detection is not a universal detection method and solutes must possess native fluorescence or must be able to be derivatized to generate a fluorophore. With fluorescence detection, the limits of detection can be lowered compared to conventional photometric detection by about three orders of magnitude. This lowering of detection limits is possible, because in fluorescence detection radiation is measured against a dark background (therefore it is so important to keep stray radiation as low as possible), while in photometric detection with very small absorbance the ratio of two similar high intensities has to be determined. With fluorescence detection, it was possible to extend the applicability of CE into trace analysis. Moreover, fluorescence detection is inherently more selective. Laser-induced fluorescence (LIF) detection can be regarded as the most sensitive optical detection technique to be commonly used with capillary electrophoresis (CE), electrokinetic chromatography (EKC) and capillary electrochromatography (CEC).

The advantage of LIF detection over conventional fluorescence detection is that the spatially coherent radiation of a laser can be focused very efficiently into the inner volume of a separation capillary via



suitable lenses, which minimizes the stray radiation and decreases limits of detection that can be achieved. However, wavelength selection can be limited with laser light sources, especially in the UV. In addition high light intensities have to be avoided, because they can cause photodegradation. LIF is widely used for the analysis of very complex mixtures where the concentration of the analyte of interest is in the  $\mu\text{mol L}^{-1}$  range and where superb sensitivity and selectivity are needed. As an example, LIF can be used to detect trace levels of (derivatized) amino acids in biological media using simplified sample preparation [76]. When LIF detection is used with capillary-format separations, it can detect  $\text{nmol L}^{-1}$  or subnanomolar concentrations; this allows for a number of important innovative analytical methods, such as the simultaneous monitoring of the efflux of neurotransmitters at a frequency of every 10 s in microdialysates from brain tissues [76].

Mass spectrometry (MS) is a highly selective and sensitive spectrometric technique that can be used for analyte characterization, quantification and identification purposes. Over the years, effective coupling methodologies based on electrospray ionization (ESI) have been developed to combine CE and MS. The coupling of EKC with MS clearly would be very beneficial, resulting in a powerful analytical system combining efficient separation with mass-selective and structure-elucidative detection. However, common EKC methods frequently involve the use of nonvolatile PSPs and buffer salts, such as sodium dodecyl sulfate (SDS), cyclodextrins and sodium phosphate, which are (often considered to be) incompatible with MS detection using electrospray ionization (ESI). These constituents may cause analyte ion suppression, background signals and contamination of the ion source and optics. In order to circumvent these compatibility problems, various EKC–MS approaches have been proposed. The most often applied approach so far is the so-called partial-filling technique, in which the PSP is prevented from entering the ion source of the mass spectrometer. Other approaches include the use of special PSPs, like reverse-migrating or high-molecular-weight surfactants, and (semi-)volatile surfactants [77].

### **1.4. Improvement of the detection sensitivity**

CE methods often exhibit detection limits that are one or more orders of magnitude higher than those in corresponding HPLC methods. This is ascribed to the small detection cell volume (limitation of the inner diameter of the separation capillary), which has to be chosen to avoid: (i) radial temperature gradient effects due to Joule heating and (ii) extra-column band broadening (limitation of the length of the detection cell) [5]. The disadvantages due to the limitations of the detection volume, however, can possibly be overcome by using of several approaches. These approaches are mainly based on using: (i) physical methods such as the use of a bubble cell, (ii) on-line enrichment techniques via conversion of a long injected analyte zone into a narrow band inside the capillary utilizing either electrophoretic

phenomena and/or chromatographic effects [78]. Other approaches to decrease the detection limits in CE are to combine its use with (iii) off-line enrichment techniques such as solid phase extraction (SPE), and/or (iv) highly sensitive detection techniques such as LIF or MS. The last approach was thoroughly discussed under Section 1.3. On the following discussion, the second and the third approach will be considered. Although it is possible to work separately with off-line (chromatographic-based methods) or on-line enrichment techniques (electrophoresis-based methods), the combination between these two is very demandable in the analysis of samples with complex matrices that requires both sample clean-up and high preconcentration prior to the analysis.

### 1.4.1. Off-line enrichment techniques

Chromatography-based preconcentration methods prior to CE enable higher sample volumes (compared to electrophoresis methods) to be injected because the analytes are adsorbed onto a stationary phase. Moreover, the sample clean-up in chromatographic methods is effective because the sample matrix can be removed and only the analytes of interest can be maintained. Another advantage of chromatography-based preconcentration techniques is that the preconcentration technique can be performed more selective, since the chromatography is orthogonal to the electrophoresis. Chromatography-based preconcentration includes solid phase extraction (SPE) and solid-phase microextraction (SPME) but SPE is the most widely used because it can achieve higher concentration sensitivity and is versatile. SPE can solve the two main problems in CE; it improves sensitivity and retains the analytes of interest from the sample matrices. Moreover, it can desalt the very saline samples that might interfere with the electrophoretic process. The sorbent in SPE retains the analyte from a large volume of sample in a sorbent. These analytes can then be eluted in a lower volume of elution solvent. Besides, an additional washing step is added between retention and elution of the compounds when needed. SPE can therefore simultaneously enrich the trace analytes and remove potentially interfering compounds. Obviously, if there are no losses, the higher the ratio between sample and elution volumes, the higher the preconcentration factor obtained. However, since injection volumes suitable for CE are at low-nL levels, generally only a part of the eluted sample from SPE can be injected into the separation capillary [79].

Different modes of SPE-CE coupling such as off-line, in-line, on-line, at-line have been discussed in the literature [79,80], however, the off-line combination of SPE and CE is the easiest. It cannot be considered as a coupling but as a combination of SPE and CE. In short, a high sample volume is percolated through a SPE cartridge in such a way that the analytes are retained in the sorbent. Afterwards, the analytes are eluted with a small volume of an appropriate elution solution and can be

injected into the CE system. Due to the high sample volumes employed, the limits of detection (LODs) (associated with using off-line SPE mode) after carrying the CE analysis are in general very low. Moreover, compared with other SPE–CE modes, further preconcentration can be obtained if the eluted sample is evaporated to dryness and redissolved in a lower volume. It is very useful for cleaning up complex matrices before electrophoretic analysis or even before preconcentrating the analytes using other approaches. Besides, the off-line mode has a considerable potential in determining analytes at very low concentrations when a large sample volume is available [79].

#### 1.4.2. On-line enrichment techniques

On-line enrichment/On-line zone focusing methods was a topic of intense research in the last decade. Concomitantly, there are a very large number of review articles covering the field of on-line zone focusing methods in combination with capillary electromigration techniques [78,81-94]. Different modes of on-line enrichment procedures such as field-amplified sample stacking (FASS) [95], large volume sample stacking (LVSS) [96], dynamic pH junction [97,98], and sweeping [99] were reported, which are the main focus of the following discussion.

##### 1.4.2.1. Stacking

One of the simplest methods for sample preconcentration is to induce “stacking” of analytes by exploiting the electric conductivity differences between the sample matrix and the BGE [95,96]. Sample stacking is caused by the motion of sample ions across a boundary that is formed between the sample and the BGE inside the capillary.

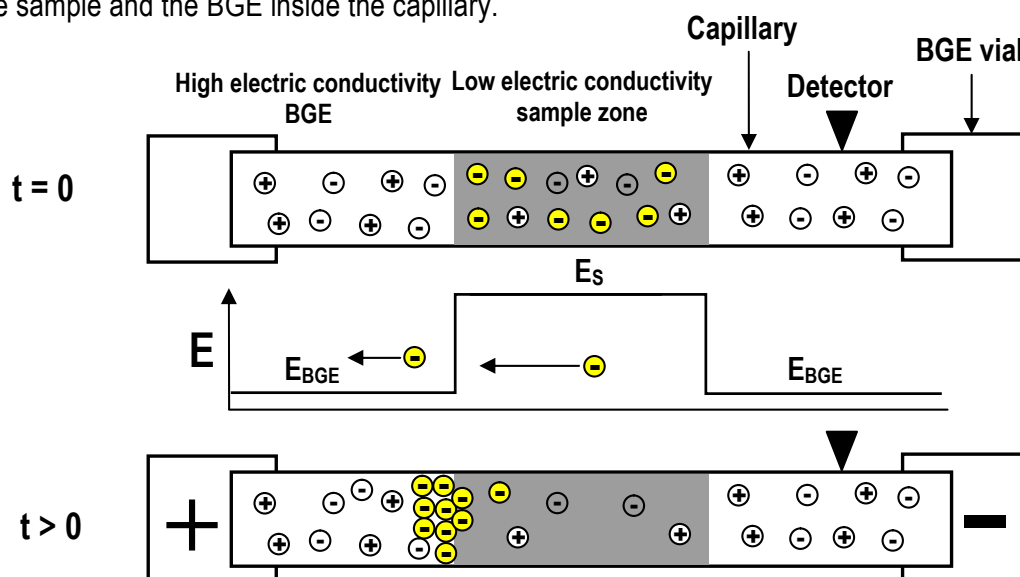


**Figure 7:** Schematic illustration of field amplified sample stacking of negatively charged analyte showing the stacking of the sample ions (in yellow) as they exit the low conductivity sample region and enter the high conductivity regions of the BGE. Modified from [100].

The sample is prepared in a matrix having an electric conductivity lower than that of the BGE. A long plug of the sample solution is injected into the capillary. During the application of voltage, the low conductivity sample zone experiences a higher electric field strength compared with the BGE. Accordingly, the electrophoretic velocity of the analyte ions in the sample zone is higher than that in the BGE. The abrupt decrease in the velocity of the analyte ions moving across the boundary between the sample zone and the BGE results in the narrowing of the analyte zone. The resulting analyte zones will therefore have concentrations higher than the original concentration in the sample (Fig. 7). The concentration effect obtainable with this technique is dependent on the ratio between the electric field strength in the sample zone and in the BGE [95].

### **1.4.2.1.1. Field-amplified sample stacking and field-amplified sample injection**

Being very simple and easily applicable to a range of different analyte types, field amplified sample stacking (FASS) is considered to be the normal mode for CE applications. In spite of its simplicity and wide applicability, FASS suffers from the disadvantage of that the maximum sample volume that can be injected into the capillary is limited to about 5% of the capillary volume [85]. The injection of volumes higher than this will result in band broadening as explained by Chien and Burgi [96] due to the mismatch of local electroosmotic flow velocities between the sample and BGE compartment. This causes a pressure difference resulting in a laminar flow inside the capillary that will broaden the sharp zone generated by the stacking process and reduce the resolution. This pressure difference is related to the field strength boundary between the two zones, and hence the difference in conductivity, and also the magnitude of the EOF throughout the capillary. A sample conductivity 10 times lower than the BGE was found to produce optimum results [85].

A recent study by Huhn and Pyell [101] examined this relationship in more detail at low pH such that there was minimal EOF, with the expectation that this would reduce the significance of the hydrodynamic flow and would have a higher optimal conductivity difference. They found that hydrodynamic dispersion was only a minor contribution under low EOF and that the dominant limiting factor was molecular diffusion arising from elongated migration time that occurs with longer sample plugs. A sample length of 3% of the capillary is optimum with a conductivity ratio of 10, which interestingly are approximately the same conditions identified by Chien and Burgi in a high EOF environment.

While the sample is introduced into the capillary by hydrodynamic flow in the case of FASS, it is introduced by electrokinetic injection (electromigration injection) in the case of field-amplified sample injection (FASI). This has the advantage that the analyte ions enter the capillary as a combination of

electrophoresis and electroosmosis. If the electrophoretic mobility of the analytes is in the opposite direction to the EOF, then smaller amount of analyte ions will enter the capillary than with a hydrodynamic injection. However, if the mobility is in the same direction as the EOF, then FASI will result in greater amount analyte ions being injected [102] than FASS. In this case, assuming the same volume of sample is introduced (approximately 5% of the capillary volume), the sensitivity is typically improved by 100–1000-fold in FASI.

#### 1.4.2.1.2. Large volume sample stacking

As mentioned above, FASS is limited by the volume of sample that can be injected into the capillary. Introduced in the early 1990's by Chien and Burgi [96], large volume sample stacking (LVSS) involves the injection of a large volume (up to the entire capillary volume) of low conductivity sample, which accordingly provides higher concentration sensitivity compared to FASS. LVSS with or without polarity switching is based on stacking with removal of the sample matrix [88].

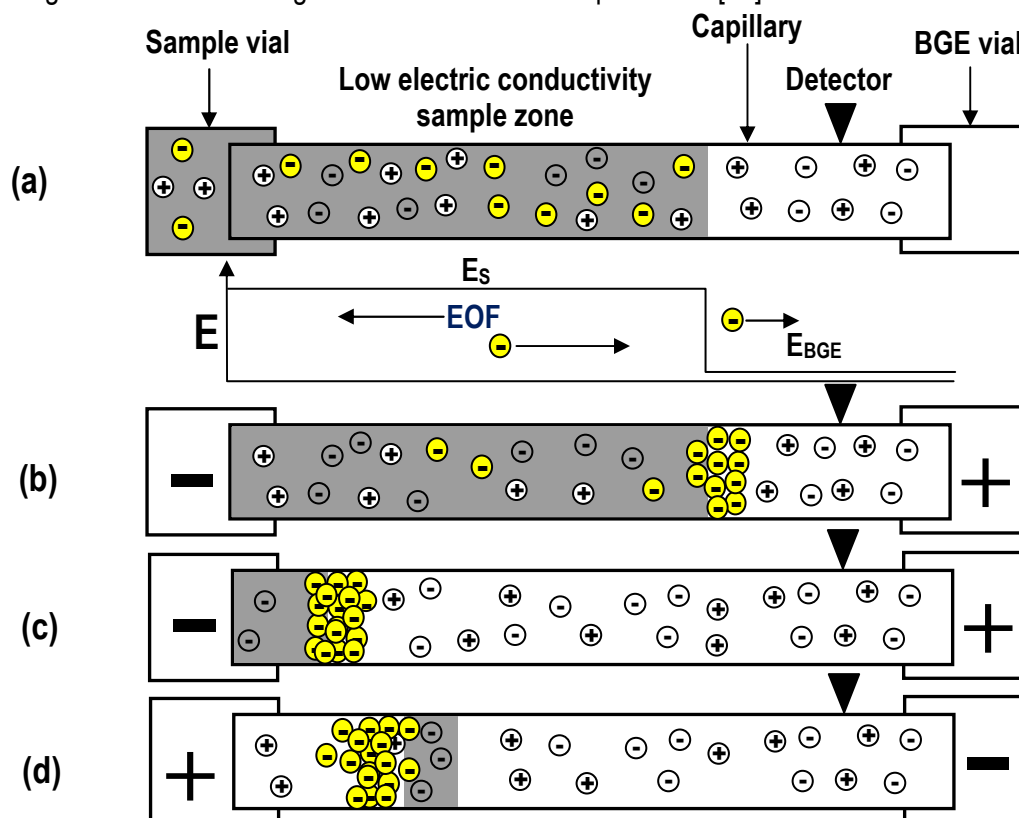


**Figure 8:** Schematic illustration of the focusing mechanism by LVSS of negatively charged analyte. (a) Low conductivity sample matrix is injected into the capillary. (b) Negative voltage is applied with EOF toward the cathode. The negatively charged sample ions (in yellow) stack at the sample/BGE boundary. (c) The stacking process is continued, while most of the sample matrix is pumped out from the capillary inlet. (d) The polarity is reversed and the separation starts.

In LVSS with polarity switching, a large sample volume is injected hydrodynamically into the capillary (Fig. 8a). A negative voltage is applied to remove the sample matrix plug by pumping it out of the

capillary using the electroosmotic flow, while simultaneously maintaining the stacked analytes at the sample/BGE interface, while it moves slowly toward the capillary inlet (Fig. 8b and c). This methodology of pumping is applicable only for ions that have a negative mobility with respect to the bulk electroosmotic flow. The polarity of the electrode is reversed at the end of the matrix removal step when the separation is started (Fig. 8d). To ensure that no fraction of the analyte is lost during the matrix removal step, the electric current strength is monitored, until it reaches 95% of the electric current strength measured when the capillary is entirely filled with BGE.

LVSS with polarity switching was recently employed for the online concentration and analysis of flavonoids in *Brassica oleracea* (broccoli) [103], natural polyphenols in plant extracts [104], sulfonylurea herbicides in water and grape samples [105], haloacetic acids in water [106,107], barbiturates in biological samples [107] and for the characterization and inhibition studies of the nucleoside metabolizing enzymes purine nucleoside phosphorylase and adenosine deaminase present in the membrane of human 1539 melanoma cells [108].

#### 1.4.2.2. Dynamic pH junction

Dynamic pH junction technique utilizes significant changes in the ionization states of the analytes or the electrophoretic velocities between different pH values. The name dynamic pH junction was introduced by Britz-McKibbin and Chen [109], although the use of a discontinuous buffer system was reported by Aebersold and Morrison previously [110].

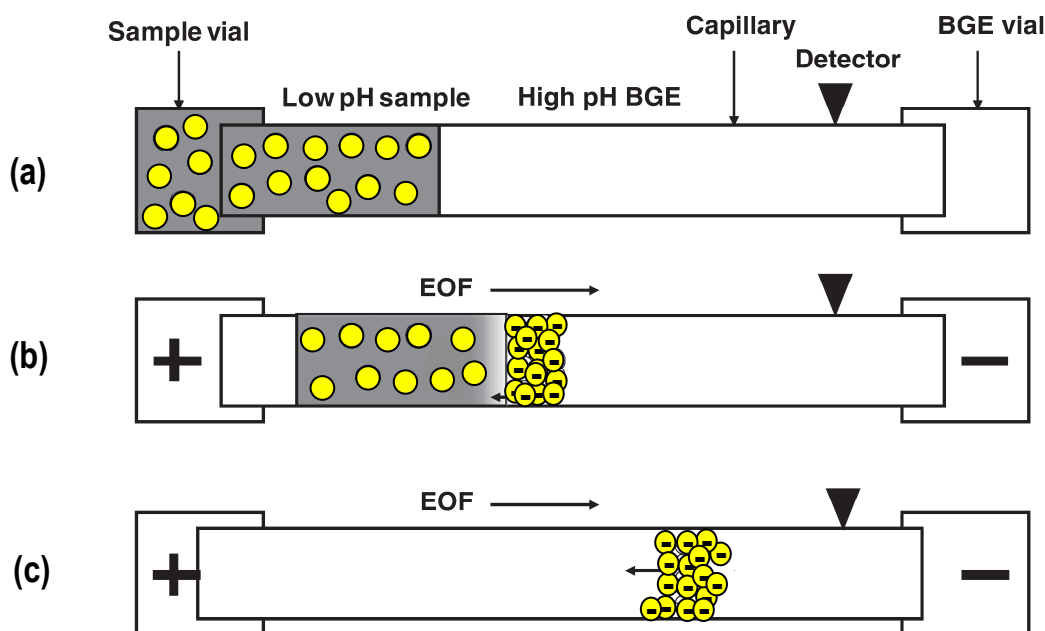


**Figure 9:** Schematic illustration of the enrichment mechanism using dynamic pH junction. (a) Hydrodynamic injection of a low pH sample matrix. (b) The analyte ions (yellow) are focused via dynamic pH junction. (c) The analytes are separated. Modified from [98].

For example, a weakly acidic analyte dissolved in an acidic matrix is injected as a long plug and the capillary is filled with an alkaline BGS (Fig. 9a). When a positive voltage is applied at the injection end, the acidic sample zone is gradually titrated by the hydroxide ion in the alkaline BGE from the cathodic side and the analyte will be ionized in the neutralized zone (Fig. 9b). The negatively ionized analyte will migrate toward the anode but if it enters into the acidic sample zone, it will be protonated again to neutral and stop the electrophoretic migration (Fig. 9b). Thus, the weakly acidic analyte can be focused at the neutralization boundary during the neutralization of the sample zone. Once the acidic sample matrix is consumed, the focused analytes are separated (Fig. 9c) based on their electrophoretic mobilities. The same principle is applied to weakly basic analytes.

A full account of dynamic pH junction including fundamental discussions can be found in recent reviews by Kazarian *et al.* [97], Cao *et al.* [111], and Ptolemy and Britz-McKibbin [112].

### 1.4.2.3. Sweeping

Sweeping is one of the most important sample preconcentration techniques in MEKC. It is defined as the accumulation of analyte molecules by the PSP that penetrates the sample zone being void of PSP [99]. The principle of sweeping is illustrated in Fig. 10.

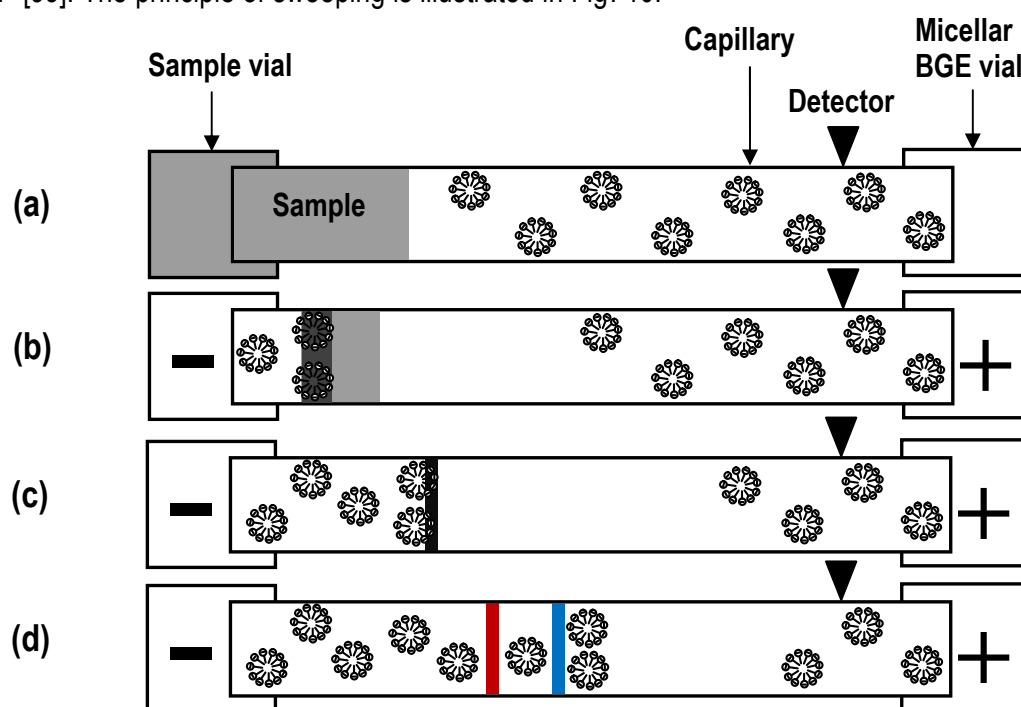


**Figure 10:** Schematic illustration of the sweeping process using negatively charged micelles under homogeneous electric field and zero EOF conditions. (a) Starting situation: injection of a large volume of the sample solution prepared in a matrix with an electric conductivity similar to that of the micellar BGE. (b) Application of voltage (reversed polarity mode) associated with the entrance of micelles into the sample zone and sweeping of the analyte molecules. (c) Formation of the final swept analyte zone when the micelles have filled the sample zone. (d) Separation of analytes by MEKC. Modified from [113].

Based on the concept presented by Terabe and co-workers in 1998 (using neutral analytes dissolved in matrices (without SDS) having the same electric conductivity as the BGE and employing SDS as anionic surfactant [99]), the length of the sample zone after sweeping  $l_{\text{sweep}}$  depends on the initial sample-plug length  $l_{\text{inj}}$  and on the retention factor in the sample zone  $k_s$  during sweeping. The enrichment factor ( $=l_{\text{inj}}/l_{\text{sweep}}$ ) is then directly proportional to  $k_s$ :

$$l_{\text{sweep}} = \frac{1}{1 + k_s} l_{\text{inj}} \quad (18)$$

According to Eq. (18) the highest sweeping efficiency is expected for analytes having very high retention factors within the sample zone.

More investigations on the sweeping phenomenon (i) for charged analytes [114], (ii) with high EOF conditions, (iii) under homogeneous and inhomogeneous electric field conditions [115,116], (iv) with cationic surfactants [117] or (v) using electokinetic injection [118] were carried out. Very recently El-Awady *et al.* [113] presented a detailed study of sweeping under inhomogeneous electric field conditions. They extended the present theory by introduction of a phase ratio shift factor defined as the ratio between the phase ratio in the sample zone and the phase ratio in the BGE. The derived more general equations allow the prediction of sweeping efficiency if the electric conductivity of the sample solution is different from that of the BGE. El-Awady and Pyell have shown both experimentally and theoretically that the focusing process due to sweeping is not only influenced by the retention factor of the analyte in the sample zone, but also by the retention factor of the analyte in the BGE [119]. They have introduced the term **retention factor gradient effect (RFGE)** that can lead to additional focusing or defocusing of the swept analyte zone. This effect complements the sweeping process and occurs in the BGE compartment next to the sample zone. According to [119], Eq. (18) is expanded by introducing the additional focusing/defocusing factor  $f$ .  $l_{\text{grad}}$  is used to describe the length of the swept analyte zone after taking this effect into account [119]:

$$l_{\text{grad}} = \frac{1}{f} \frac{1}{1 + k_s} l_{\text{inj}} \quad (19)$$

$$\text{and } f = \frac{l_{\text{sweep}}}{l_{\text{grad}}} = \frac{k_s k_{\text{BGE}} + k_s}{k_s k_{\text{BGE}} + k_{\text{BGE}}} \quad (20)$$

where  $k_{\text{BGE}}$  is the retention factor in the BGE. The diverse applications of sweeping as on-line enrichment technique (either as a standing alone technique or combined with other off-line and on-line enrichment methods) for the analysis of biochemical components in herbal and pharmaceutical drugs,



dyes, pesticides, food contaminants, explosives, protein and phytochemicals were the focal point of many review articles [46,85,87,88,92,120].

### **1.5. Biological and environmental applications of capillary electromigration techniques**

The clinical/biological field and the pharmaceutical research and production are the main areas that are benefiting most from the application of capillary electromigration techniques. Biological components vary in nature. They consist of simple cationic/anionic entities, amino acids, peptides, proteins, nucleic acids or even whole cells. Most of the clinical tests can be performed by CE as well as other techniques, such as high-performance liquid chromatography (HPLC) or slab gel electrophoresis (SGE). However, CE offers certain advantages for clinical and biological analyses. The main advantage of the CE in clinical and biological analysis is the flexibility of the separation selectivity. It is simple to add different additives to the separation buffer to induce a selective change in the migration velocity. The principle of separation can be changed from free solution CE to any other mode of CE to suit a particular group of compounds. For example, many steroids cannot be separated in free zone electrophoresis. Many of these are neutral or weakly charged compounds and migrate with the EOF. With neutral solutes separation is obtainable by the addition of SDS to achieve separation by MEKC. The second important advantage is the high separation efficiency, a characteristic that is important when dealing with complex samples containing numerous compounds such as serum or urine. The use of an open tubular capillary improves resolution relative to that of packed HPLC columns by eliminating the multiple path term and the resistance to mass transfer term in Van Deemter equation, making (in the ideal case) longitudinal diffusion term the only contributor to band broadening in CE. In addition, CE offers rapid analysis time and a low cost with full automation. A third feature is the ability to perform separations without the need to use large volumes of organic solvents. Organic solvents, which are used often in HPLC, are becoming more expensive to purchase and more difficult, under many state laws, to store and dispose of. This eventually may require shifting of many separations from HPLC to the CE [121].

On the other hand, CE suffers from several problems. Unlike HPLC, CE is greatly affected by sample matrix (i.e., salts and proteins), which are very high in biological samples. Another major problem in clinical analysis is the suboptimal detection sensitivity [121]. The suboptimal detection sensitivity was one of the most important motivations of the present study. The third problem is sample interaction with the capillary walls. To utilize CE successfully for practical separation of clinical samples it is important to understand how these factors affect separations and how strategies can be developed to overcome them. Many comprehensive review articles report the utility of capillary electromigration

techniques in the analysis of a variety of biomolecules after their preconcentration and separation from biological matrices [83,84,86,89,91,93].

Besides their applicability to the analysis of different compounds of interest in biological matrices, capillary electromigration separation techniques have been successfully applied to the analysis of environmental samples. The inherently trace-level concentration of pollutants in different environmental compartments necessitates the involvement of on-line preconcentration techniques in CE to improve the detection sensitivity and permits the analysis of these compounds at the low ng L<sup>-1</sup> level. Further detector improvement to achieve low-concentration limits of detection is highly demandable, which constitutes one of the main motivations of the current work. In addition, the complexity of sample matrices requires the use of off-line extraction procedures for sample clean-up and enrichment prior to the analysis. Significant progress is continually being made, widening the applicability of capillary electromigration methods, mostly CZE, MEKC, and CEC, to the analysis of real environmental samples [122]. Different off-line and on-line preconcentration strategies can be employed in CE with respect to the analysis of different pollutants in many types of environmental samples [84]. The studied analytes include: inorganic pollutants, toxicants, pesticides, polycyclic aromatic, hydrocarbons, phenols, amines, carboxylic acids, explosives, pharmaceuticals, organometallic compounds, and organic compounds typically encountered in industrial manufacturing [84].

## 1.6. References

- [1] A. Tiselius, *Trans. Faraday Soc.* 33 (1937) 524-531.
- [2] H.H. Lauer, G.P. Rozing (Eds.), *High Performance Capillary Electrophoresis-A Primer*, Agilent Technologies, Germany, 2014.
- [3] S. Hjerten, *Chromatogr. Rev.* 9 (1967) 122-219.
- [4] J.W. Jorgenson, K.D. Lukacs, *Anal. Chem.* 53 (1981) 1298-1302.
- [5] R.A. Meyers (Ed.), *Encyclopedia of Analytical Chemistry*, John Wiley & Sons, Ltd., Hoboken, N.J., 2012.
- [6] S. Terabe, K. Otsuka, K. Ichikawa, A. Tsuchiya, T. Ando, *Anal. Chem.* 56 (1984) 111-113.
- [7] B. Buszewski, E. Dziubakiewicz, in: B. Buszewski, E. Dziubakiewicz, M. Szumski (Eds.), *Electromigration Techniques: Theory and Practice*, Springer-Verlag, Berlin Heidelberg, 2013, pp. 1-3.
- [8] S.F.Y. Li (Ed.), *Capillary Electrophoresis: Principles, Practice and Applications*, Elsevier Science, Netherlands, 1992.
- [9] U. Pyell, in: U. Pyell (Ed.), *Electrokinetic Chromatography: Theory, Instrumentation & Applications*, John Wiley & Sons, Ltd., Chichester, 2006, pp. 3-31.
- [10] J.P. Landers, in: J.P. Landers (Ed.), *Handbook of Capillary and Microchip Electrophoresis and Associated Microtechniques*, 3rd edn, CRC Press, Taylor and Francis Group, LLC, Boca Raton, 2008, pp. 3-74.
- [11] M.L. Riekkola, J.A. Joensuu, R.M. Smith, *Pure Appl. Chem.* 76 (2004) 443-451.
- [12] K. Salomon, D.S. Burgi, J.C. Helmer, *J. Chromatogr. A* 559 (1991) 69-80.
- [13] M.I. Jimidar, in: S. Ahuja, M.I. Jimidar (Eds.), *Capillary Electrophoresis Methods for Pharmaceutical Analysis*, Elsevier Science, New York, 2008, pp. 9-42.
- [14] P. Atkins, J. de Paula (Eds.), *Physical Chemistry*, 9th edn., Oxford University Press, Oxford, UK, 2010.
- [15] M.J. Rosen (Ed.), *Surfactants and Interfacial Phenomena*, 3rd edn., John Wiley & Sons, Inc., New Jersey, 2004.
- [16] A.V. Delgado, F. Gonzalez-Caballero, R.J. Hunter, L.K. Koopal, J. Lyklema, *J. Colloid Interface Sci.* 309 (2007) 194-224.
- [17] A. Weston, P.R. Brown (Eds.), *High Performance Liquid Chromatography & Capillary Electrophoresis: Principles and Practices*, Academic Press, California, USA, 1997.
- [18] M.T. Koesdjojo, C.F. Gonzalez, V.T. Remcho, in: J.P. Landers (Ed.), *Handbook of Capillary and Microchip Electrophoresis and Associated Microtechniques*, 3rd edn, CRC Press, Taylor and Francis Group, LLC, Boca Raton, 2008, pp. 183-226.

- [19] J. Horvath, V. Dolnik, *Electrophoresis* 22 (2001) 644-655.
- [20] P.G. Righetti, C. Gelfi, B. Verzola, L. Castelletti, *Electrophoresis* 22 (2001) 603-611.
- [21] C.S. Henry, B.M. Dressen, in: J.P. Landers (Ed.), *Handbook of Capillary and Microchip Electrophoresis and Associated Microtechniques*, 3rd edn, CRC Press, Taylor and Francis Group, LLC, Boca Raton, 2008, pp. 1441-1457.
- [22] J.E. Melanson, N.E. Barylka, C.A. Lucy, *Trends Anal. Chem.* 20 (2001) 365-374.
- [23] H. Whatley, in: J.R. Petersen, A.A. Mohammad (Eds.), *Clinical and Forensic Applications of Capillary Electrophoresis*, Humana Press Inc., Totowa, NJ, 2001, pp. 21-58.
- [24] M.A. Garcia, M.L. Marina, A. Rios, M. Valcarcel, in: M.L. Marina, A. Rios, M. Valcarcel (Eds.), *Analysis and Detection by Capillary Electrophoresis*, Elsevier Science, Amsterdam, 2005, pp. 31-134.
- [25] T. Furumoto, T. Fukumoto, M. Sekiguchi, T. Sugiyama, H. Watarai, *Electrophoresis* 22 (2001) 3438-3443.
- [26] S. Terabe, N. Matsubara, Y. Ishihama, Y. Okada, *J. Chromatogr.* 608 (1992) 23-29.
- [27] S. Terabe, *Trends Anal. Chem.* 8 (1989) 129-134.
- [28] S. Terabe, H. Ozaki, K. Otsuka, T. Ando, *J. Chromatogr. A* 332 (1985) 211-217.
- [29] S. Terabe, T. Isemura, *J. Chromatogr. A* 515 (1990) 667-676.
- [30] G.E. Barker, P. Russo, R.A. Hartwick, *Anal. Chem.* 64 (1992) 3024-3028.
- [31] C. Nilsson, S. Nilsson, *Electrophoresis* 27 (2006) 76-83.
- [32] S. Pedersen-Bjergaard, K. Einar Rasmussen, T. Tilander, *J. Chromatogr. A* 807 (1998) 285-295.
- [33] Y. Walbroehl, J.W. Jorgenson, *Anal. Chem.* 58 (1986) 479-481.
- [34] U. Holzgrabe, S. Laug, F. Wiene, in: P. Schmitt-Kopplin (Ed.), *Capillary Electrophoresis: Methods and Protocols*, Humana Press, 2008, pp. 735-749.
- [35] J. Vindevogel, P. Sandra (Eds.), *Introduction to micellar electrokinetic chromatography*, Hüthig, Heidelberg, 1992.
- [36] S. Terabe, in: N.A. Guzman (Ed.), *Capillary Electrophoresis Technology*, Marcel Dekker, Inc., New York, 1993, pp. 65-87.
- [37] M.G. Khaledi, in: M.G. Khaledi (Ed.), *High-Performance Capillary Electrophoresis: Theory, Techniques, and Applications*, Wiley-interscience, New York, 1998, pp. 77-131.
- [38] U. Pyell (Ed.), *Electrokinetic Chromatography: Theory, Instrumentation & Applications*, John Wiley & Sons, Ltd., Chichester, 2006.
- [39] J.P. Quirino, S. Terabe, *J Chromatogr A* 856 (1999) 465-482.

- [40] S. Terabe, *Chem. Rec.* 8 (2008) 291-301.
- [41] S. Terabe, *Annu. Rev. Anal. Chem.* 2 (2009) 99-120.
- [42] T.J. Pappas, M. Gayton-Ely, L.A. Holland, *Electrophoresis* 26 (2005) 719-734.
- [43] M. Molina, M. Silva, *Electrophoresis* 23 (2002) 3907-3921.
- [44] M. Silva, *Electrophoresis* 28 (2007) 174-192.
- [45] M. Silva, *Electrophoresis* 30 (2009) 50-64.
- [46] M. Silva, *Electrophoresis* 32 (2011) 149-165.
- [47] S.E. Deeb, M.A. Iriban, R. Gust, *Electrophoresis* 32 (2011) 166-183.
- [48] S.E. Deeb, H.A. Dawwas, R. Gust, *Electrophoresis* 34 (2013) 1295-1303.
- [49] S. Terabe, K. Otsuka, T. Ando, *Anal. Chem.* 57 (1985) 834-841.
- [50] S. Terabe, *Anal. Chem.* 76 (2004) 240A-246A.
- [51] B. Edward, P. Kubalczyk, in: B. Buszewski, E. Dziubakiewicz, M. Szumski (Eds.), *Electromigration Techniques: Theory and Practice*, Springer-Verlag, Berlin Heidelberg, 2013, pp. 77-92.
- [52] L. Jia, S. Terabe, in: U. Pyell (Ed.), *Electrokinetic Chromatography: Theory, Instrumentation & Applications*, John Wiley & Sons, Ltd., Chichester, 2006, pp. 79-93.
- [53] V. Pino, M. German-Hernandez, A. Martin-Perez, J.L. Anderson, *Sep. Sci. Technol.* 47 (2012) 264-276.
- [54] S.A. Shamsi, N.D. Danielson, *J. Sep. Sci.* 30 (2007) 1729-1750.
- [55] G.A. Baker, S.N. Baker, S. Pandey, F.V. Bright, *Analyst* 130 (2005) 800-808.
- [56] B. Buszewski, S. Studzinska, *Chromatographia* 68 (2008) 1-10.
- [57] A. Berthod, M.J. Ruiz-Angel, S. Carda-Broch, *J. Chromatogr. A* 1184 (2008) 6-18.
- [58] M. Lopez-Pastor, B.M. Simonet, B. Lendl, M. Valcarcel, *Electrophoresis* 29 (2008) 94-107.
- [59] P. Sun, D.W. Armstrong, *Anal. Chim. Acta* 661 (2010) 1-16.
- [60] M.D. Joshi, J.L. Anderson, *RSC Adv.* 2 (2012) 5470-5484.
- [61] B. Dong, X. Zhao, L. Zheng, J. Zhang, N. Li, T. Inoue, *Colloids Surf. A* 317 (2008) 666-672.
- [62] R. Vanyur, L. Biczok, Z. Miskolczy, *Colloids Surf. A* 299 (2007) 256-261.
- [63] P.L. Laamanen, S. Busi, M. Lahtinen, R. Matilainen, *J. Chromatogr. A* 1095 (2005) 164-171.
- [64] M.E. Yue, Y.P. Shi, *J. Sep. Sci.* 29 (2006) 272-276.

- [65] K. Tian, Y. Wang, Y. Chen, X. Chen, Z. Hu, *Talanta* 72 (2007) 587-593.
- [66] T.F. Jiang, Y.L. Gu, B. Liang, J.B. Li, Y.P. Shi, Q.Y. Ou, *Anal. Chim. Acta* 479 (2003) 249-254.
- [67] H.L. Su, M.T. Lan, Y.Z. Hsieh, *J. Chromatogr. A* 1216 (2009) 5313-5319.
- [68] J. Niu, H. Qiu, J. Li, X. Liu, S. Jiang, *Chromatographia* 69 (2009) 1093-1096.
- [69] M. Borissova, K. Palk, M. Koel, *J. Chromatogr. A* 1183 (2008) 192-195.
- [70] H. Qiu, A.K. Mallik, M. Takafuji, X. Liu, S. Jiang, H. Ihara, *Anal. Chim. Acta* 738 (2012) 95-101.
- [71] T. Tsuda, *J. High Resolut. Chromatogr.* 10 (1987) 622-624.
- [72] W.R. Jones, P. Jandik, *J. Chromatogr. A* 546 (1991) 445-458.
- [73] L. Jia, S. Terabe, in: U. Pyell (Ed.), *Electrokinetic Chromatography: Theory, Instrumentation & Applications*, John Wiley & Sons, Ltd., Chichester, 2006, pp. 79-93.
- [74] N. Matsubara, K. Koezuka, S. Terabe, *Electrophoresis* 16 (1995) 580-583.
- [75] J. Fischer, P. Jandera, in: U. Pyell (Ed.), *Electrokinetic Chromatography: Theory, Instrumentation & Applications*, John Wiley & Sons, Ltd., Chichester, 2006, pp. 235-265.
- [76] C. Bayle, V. Poinot, C. Fournier-Noel, F. Couderc, in: U. Pyell (Ed.), *Electrokinetic Chromatography: Theory, Instrumentation & Applications*, John Wiley & Sons, Ltd., Chichester, 2006, pp. 263-280.
- [77] R. Mol, G. J.de Jong, G.W. Somsen, in: U. Pyell (Ed.), *Electrokinetic Chromatography: Theory, Instrumentation & Applications*, John Wiley & Sons, Ltd., Chichester, 2006, pp. 307-336.
- [78] M. Urbanek, L. Krivankova, P. Bocek, *Electrophoresis* 24 (2003) 466-485.
- [79] P. Puig, F. Borrull, M. Calull, C. Aguilar, *TrAC Trends in Analytical Chemistry* 26 (2007) 664-678.
- [80] P. Puig, F. Borrull, M. Calull, C. Aguilar, *Anal Chim Acta* 616 (2008) 1-18.
- [81] J.B. Kim, S. Terabe, *J. Pharm. Biomed. Anal.* 30 (2003) 1625-1643.
- [82] M.C. Breadmore, *Electrophoresis* 28 (2007) 254-281.
- [83] Z. Mala, L. Krivankova, P. Gebauer, P. Bocek, *Electrophoresis* 28 (2007) 243-253.
- [84] S.L. Simpson, J.P. Quirino, S. Terabe, *J. Chromatogr. A* 1184 (2008) 504-541.
- [85] M.C. Breadmore, J.R.E. Thabano, M. Dawod, A.A. Kazarian, J.P. Quirino, R.M. Guijt, *Electrophoresis* 30 (2009) 230-248.
- [86] Z. Mala, A. Salmpova, P. Gebauer, P. Bocek, *Electrophoresis* 30 (2009) 215-229.

- [87] A.T. Aranas, A.M. Guidote Jr., J.P. Quirino, *Anal. Bioanal. Chem.* 394 (2009) 175-185.
- [88] M.C. Breadmore, M. Dawod, J.P. Quirino, *Electrophoresis* 32 (2011) 127-148.
- [89] Z. Mala, P. Gebauer, P. Bocek, *Electrophoresis* 32 (2011) 116-126.
- [90] B.C. Giordano, D.S. Burgi, S.J. Hart, A. Terray, *Anal Chim Acta* 718 (2012) 11-24.
- [91] A. Salmpova, Z. Mala, P. Pantukova, P. Gebauer, P. Bocek, *Electrophoresis* 34 (2013) 3-18.
- [92] M.C. Breadmore, A.I. Shallan, H.R. Rabanes, D. Gstoettenmayr, K. Abdul, A. Gaspar, M. Dawod, J.P. Quirino, *Electrophoresis* 34 (2013) 29-54.
- [93] Z. Mala, A. Slampova, L. Krivankova, P. Gebauer, P. Bocek, *Electrophoresis* 36 (2015) 15-35.
- [94] M.C. Breadmore, R.M. Tubaon, A.I. Shallan, S.C. Phung, A.S. Abdul Keyon, D. Gstoettenmayr, P. Prapatpong, A.A. Alhusban, L. Ranjbar, H.H. See, M. Dawod, J.P. Quirino, *Electrophoresis* 36 (2015) 36-61.
- [95] R.L. Chien, D.S. Burgi, *Anal. Chem.* 64 (1992) 489A-496A.
- [96] R.L. Chien, D.S. Burgi, *Anal. Chem.* 64 (1992) 1046-1050.
- [97] P. Britz-McKibbin, G.M. Bebault, D.D.Y. Chen, *Anal. Chem.* 72 (2000) 1729-1735.
- [98] A.A. Kazarian, E.F. Hilder, M.C. Breadmore, *J. Sep. Sci.* 34 (2011) 2800-2821.
- [99] J.P. Quirino, S. Terabe, *Science* 282 (1998) 465-468.
- [100] <http://microfluidics.stanford.edu/Projects/Archive/stack.htm> (accessed 26-3-2015)
- [101] C. Huhn, U. Pyell, *J. Chromatogr. A* 1217 (2010) 4476-4486.
- [102] R.L. Chien, D.S. Burgi, *J. Chromatogr. A* 559 (1991) 141-152.
- [103] I.S.L. Lee, M.C. Boyce, M.C. Breadmore, *Food Chem.* 133 (2012) 205-211.
- [104] J. Honegr, J. Safra, M. Polasek, M. Pospisilova, *Chromatographia* 72 (2010) 885-891.
- [105] C. Quesada-Molina, O.I. del, A.M. Garcia-Campana, *Anal. Bioanal. Chem.* 397 (2010) 2593-2601.
- [106] J.O. Bernad, A. Damascelli, O. Nunez, M.T. Galceran, *Electrophoresis* 32 (2011) 2123-2130.
- [107] L.Y. Fan, T. He, Y.Y. Tang, W. Zhang, C.J. Song, X. Zhao, X.Y. Zhao, C.X. Cao, *J. Forensic Sci.* 57 (2012) 813-819.
- [108] J. Iqbal, C.E. Müller, *J. Chromatogr. A* 1218 (2011) 4764-4771.
- [109] P. Britz-McKibbin, D.D.Y. Chen, *Anal. Chem.* 72 (2000) 1242-1252.
- [110] R. Aebersold, H.D. Morrison, *J. Chromatogr. A* 516 (1990) 79-88.

- [111] C.X. Cao, L.Y. Fan, W. Zhang, *Analyst* 133 (2008) 1139-1157.
- [112] A.S. Ptolemy, P. Britz-McKibbin, *Analyst* (Cambridge, U. K. ) 133 (2008) 1643-1648.
- [113] M. El-Awady, C. Huhn, U. Pyell, *J. Chromatogr. A* 1264 (2012) 124-136.
- [114] M.R. Monton, J.P. Quirino, K. Otsuka, S. Terabe, *J. Chromatogr. A* 939 (2001) 99-108.
- [115] J.P. Quirino, S. Terabe, *J. High Resolut. Chromatogr.* 22 (1999) 367-372.
- [116] J.P. Quirino, S. Terabe, *Anal. Chem.* 71 (1999) 1638-1644.
- [117] J.B. Kim, J.P. Quirino, K. Otsuka, S. Terabe, *J. Chromatogr. A* 916 (2001) 123-130.
- [118] J. Palmer, D.S. Burgi, J.P. Landers, *Anal. Chem.* 73 (2001) 725-731.
- [119] M. El-Awady, U. Pyell, *J. Chromatogr. A* 1297 (2013) 213-225.
- [120] J. Quirino, in: U. Pyell (Ed.), *Electrokinetic Chromatography: Theory, Instrumentation & Applications*, John Wiley & Sons, Ltd., Chichester, 2006, pp. 207-231.
- [121] Z.K. Shihabi, in: J.P. Landers (Ed.), *Handbook of Capillary and Microchip Electrophoresis and Associated Microtechniques*, 3rd edn, CRC Press, Taylor and Francis Group, LLC, Boca Raton, 2008, pp. 785-810.
- [122] B. Edward, P. Kubalczyk, S. Studzinska, D. Ewelina, B. Buszewski, in: B. Buszewski, E. Dziubakiewicz, M. Szumski (Eds.), *Electromigration Techniques: Theory and Practice*, Springer-Verlag, Berlin Heidelberg, 2013, pp. 335-353.



## 2. Motivations and Objectives

The main motivation to carry out the current study is to overcome difficulties associated with the analysis of highly hydrophilic analytes when using capillary electromigration separation techniques. Following problems are encountered: (i) High surfactant concentrations (with related drawbacks) are needed for the separation of these compounds as neutral species. (ii) Low limits of detection are required for their analysis either in biological fluids or environmental samples. (iii) There is a poor extraction recovery of polar compounds from environmental samples. Moreover, (iv) there is a strong need for new pseudostationary phases (PSPs) that interact more strongly with polar analytes than those PSPs, which are used traditionally. It is also important (v) that with the new PSPs the retention factors of these analytes need to be adjustable to avoid any interferences from the matrix constituents. For the current study, urinary nucleosides and  $\alpha$ -aminocephalosporins are selected as model examples of highly polar analytes.

The aim of the present work is to separate highly hydrophilic urinary nucleosides with enhanced resolution using a low concentration of the pseudostationary phase (PSP) in the background electrolyte (BGE) (as an alternative strategy to those previously existing) while maintaining short and reproducible migration times. In this regard, it is investigated, whether imidazolium based ionic-liquid-type surfactants can be employed as novel cationic PSPs in micellar electrokinetic chromatography (MEKC) for the analysis of highly polar compounds (here: urinary nucleosides) as charged species. The performance of this type of surfactant is compared to that of the traditional tetraalkylammonium salt cationic surfactants regarding both separation selectivity and reproducibility of the migration times. Besides, those factors are studied that have a major impact on the interaction of the nucleosides with the oppositely charged PSP such as buffer co-ion concentration, pH (and consequently the degree of ionization), and the degree of complexation with tetrahydroxyborate and/or alkyl/aryl boronate. The outcomes of these studies which are related to the fundamental aspects underlying the separation of nucleosides by capillary electromigration separation methods, are intended to be integrated in the development and validation of new capillary zone electrophoresis (CZE) and MEKC methods for the identification and quantification of these compounds in urine samples. The developed separation methods are complemented with fine-tuned on-line zone focusing methods (based on different principles) in addition to the selective extraction and clean-up of the nucleosides from urine using a commercially available phenylboronate affinity gel. Those factors that influence the on-line and off-line enrichment efficiency are to be studied.

The field of application of the strategies developed in the first part of the thesis will be further extended to the analysis of very polar  $\alpha$ -aminocephalosporins in surface water with the intention to

develop and validate a highly sensitive and robust analysis method for this type of antibiotics in environmental samples based on separation by CZE. This approach is intended to combine selective derivatization, electrophoretic separation, laser-induced fluorescence (LIF) detection, and both off-line and on-line enrichment strategies. Those parameters are to be studied which have an impact on the derivatization yield, the obtained separation (resolution), the detection sensitivity, and the extraction yield.

Besides aiming at a better understanding of fundamental principles involved in on-line focusing and separation mechanisms, the undertaken studies are also directed towards showing that methods based on capillary electromigration separation can be fully validated and employed in trace (and ultratrace) analysis provided that they are combined with suitable off-line and on-line extraction and enrichment steps.

### 3. Summary

The current work investigates capillary electromigration separation methods as alternative strategies to the existing methodologies for the analysis of highly hydrophilic analytes. Combined with different on-line and off-line enrichment techniques, the applicability of the developed approaches is demonstrated in either biological fluids or environmental samples. Urinary nucleosides and  $\alpha$ -aminocephalosporins are selected as model analytes for the current study.

Nucleosides possess a cis-diol moiety that enables them to form negatively charged complexes with tetrahydroxyborate under alkaline pH conditions. From the effective electrophoretic mobility data, it is shown that the degree of complexation is close to one even at very low tetraborate concentration (2.5 mmol L<sup>-1</sup>). Insufficient resolution of the studied nucleosides using capillary zone electrophoresis (CZE) as a standing alone technique (in the presence of tetraborate buffer as a background electrolyte (BGE)) necessitates using alternative approaches which are: (i) another CE mode or (ii) buffer additives that can provide a different separation selectivity to permit the complete separation of the studied analytes. Following the first approach, a micellar electrokinetic chromatographic method (MEKC) is developed for the separation of urinary nucleosides in their ionic form using the ionic liquid-type surfactant 1-tetradecyl-3-methylimidazolium bromide (C<sub>14</sub>MImBr) as a cationic surfactant in the presence of tetrahydroxyborate. A complete separation of these hydrophilic metabolites is realized using a low concentration of C<sub>14</sub>MImBr (20 mmol L<sup>-1</sup>) in the BGE (5 mmol L<sup>-1</sup> tetraborate, pH 9.38). Fundamental aspects underlying the separation of urinary nucleosides using C<sub>14</sub>MImBr are studied including the mode of interaction of these compounds with C<sub>14</sub>MImBr and regulation of the retention factors with respect to the oppositely charged PSP. It is proven that the negatively charged complexed nucleosides interact mainly with the C<sub>14</sub>MImBr micelles by electrostatic interaction, while hydrophobic interaction can be considered to be negligible. Moreover, it is demonstrated that the retention factors are increased with decreasing borate concentration and increasing pH of the BGE. Employing the conditions that maximize the interaction between the nucleosides and the C<sub>14</sub>MImBr micelles (quantified via the associated equilibrium constants), a fully optimized and validated MEKC method combined with different on-line enrichment techniques is successfully developed for the identification and quantification of nucleosides in urine samples. It is shown that “pseudostationary ion-exchanger” sweeping is the major contributor to the overall enrichment process. However, due to the low retention factors encountered for the nucleosides adenosine (Ado) and cytidine (Cyd), C<sub>14</sub>MImBr cannot be effectively employed for the sweeping of these analytes. In addition, these two nucleosides comigrate with urinary matrix constituents. As an alternative, SDS is investigated for the analysis of Ado and Cyd as positively charged species (under acidic pH conditions) together with

“pseudostationary ion-exchanger” sweeping as on-line enrichment principle, which is applied successfully to the analysis of the two nucleosides in urine samples. Moreover, it is established that with a BGE containing the combination of an alkyl/aryl boronate and  $C_{14}MImBr$ , the retention factors of all the studied nucleosides are significantly increased. The shift in the retention factors to higher values is attributed to the additional hydrophobic interaction sites introduced by the alkyl/aryl group of the boronate that forms a complex with the cis-diol group of the nucleoside. It is shown that these optimization strategies result in validated methods, which permit the successful analysis of the studied nucleosides in urine samples with limits of detection in the range of 0.1-0.2 mg L<sup>-1</sup>.

Following the second approach, 2-hydroxypropyl- $\beta$ -cyclodextrin (2-HP- $\beta$ -CD) is used as buffer additive in the presence of tetraborate buffer, which permits the modification of the separation selectivity and enables a complete separation of the investigated nucleosides via CZE. Taking advantage of the high complex formation constant between the nucleosides and tetrahydroxyborate and employing 2-HP- $\beta$ -CD as selectivity-tuning additive, a highly sensitive CZE method is developed based on a highly efficient on-line focusing procedure comprising three steps, which are dynamic pH junction, borate sweeping, and large volume sample stacking (LVSS). Limits of detection as low as 10-40  $\mu$ g L<sup>-1</sup> are achieved. The proposed method is validated according to ICH guidelines and is successfully applied to the analysis of the nucleosides under investigation in blank and spiked urine samples. The outcomes of the second approach are successfully transferred to the analysis of selected  $\alpha$ -aminocephalosporins in surface water samples. Together with the use of a highly sensitive detection method such as laser-induced fluorescence (LIF) detection, CZE with LVSS-sweeping is applied successfully to the analysis of cefalexin and cefadroxil in spiked Lahn water samples reaching limits of detection as low as 5-8 ng L<sup>-1</sup>.

#### 4. Zusammenfassung

In der vorliegenden Arbeit werden kapillarelektromigrative Trennmethode als alternative Strategien zu existierenden Verfahren zur Bestimmung extrem hydrophiler Analyte untersucht. Es wird gezeigt, dass die entwickelte Methodik (unter Einschluss unterschiedlicher on-line und off-line Anreicherungstechniken) sich sowohl zur Analyse von biologischen Flüssigkeiten als auch zur Analyse von Umweltproben eignet. Für diese Studie wurden daher als polare Analyte im Urin enthaltene Nucleoside und als mögliche Umweltkontaminanten diskutierte  $\alpha$ -Aminocephalosporine als Modell-Analyte gewählt.

Nucleoside verfügen über eine cis-Diol-Struktureinheit, die es ihnen bei alkalischem pH ermöglicht, negativ geladene Komplexe mit Tetrahydroxyborat-Ionen zu bilden. Über die effektive elektrophoretische Mobilität wird gezeigt, dass der Komplexierungsgrad sogar bei sehr geringer Tetraborat-Konzentration ( $2,5 \text{ mmol L}^{-1}$ ) nahe 1 liegt. Weil die für die untersuchten Nucleoside mit Kapillarzonenelektrophorese (CZE) unter Verwendung eines Borat-Borsäure-Puffers erreichbare Auflösung nicht ausreichend ist, sind zur vollständigen Trennung der untersuchten Nucleoside alternative Herangehensweisen erforderlich: (i) ein anderer Trennmodus oder (ii) Pufferadditive, die eine veränderte Trennselektivität ermöglichen. In einem ersten Schritt wird daher zunächst ein Verfahren entwickelt, welches mizellare elektrokinetische Chromatographie (MEKC) mit dem kationischen Tensid 1-Tetradecyl-3-methylimidazoliumbromid ( $\text{C}_{14}\text{MImBr}$ ) in Gegenwart von Tetrahydroxyborat zur Trennung von in Urin enthaltenen Nucleosiden (nach Konversion in eine ionische Spezies) nutzt. Eine vollständige Trennung der hydrophilen Metabolite ist bereits bei geringer Konzentration des kationischen Tensids  $\text{C}_{14}\text{MImBr}$  ( $20 \text{ mmol L}^{-1}$ ) möglich (Hintergrundelektrolyt  $5 \text{ mmol L}^{-1}$  Dinatriumtetraborat, pH 9,38). Es wird untersucht, welche Gleichgewichte bei Verwendung von  $\text{C}_{14}\text{MImBr}$  als kationischem Tensid für die Trennung der im Urin enthaltenen Nucleoside und die Steuerung des Retentionsfaktors (entgegengesetzt geladene PSP) verantwortlich sind. Es wird gezeigt, dass die negativ geladenen komplexierten Nucleoside mit den  $\text{C}_{14}\text{MImBr}$  Mizellen hauptsächlich elektrostatische Wechselwirkungen eingehen, während hydrophobe Wechselwirkungen als vernachlässigbar betrachtet werden können. Diesem Ergebnis entspricht, dass erhöhte Retentionsfaktoren sowohl mit reduzierter Borat-Konzentration als auch mit heraufgesetztem pH-Wert erhalten werden. Unter Bedingungen maximaler Nucleosid-Mizell-Wechselwirkung (quantifiziert durch Ermittlung der Gleichgewichtskonstanten) wird unter Rückgriff auf kombinierte on-line Anreicherungstechniken ein optimiertes und vollständig validiertes MEKC Verfahren zur Identifizierung und Quantifizierung von Nucleosiden in Urin-Proben entwickelt. Es wird gezeigt, dass "pseudostationary ion-exchanger" sweeping hauptsächlich für den beobachteten Anreicherungsprozess verantwortlich ist.  $\text{C}_{14}\text{MImBr}$  kann jedoch aufgrund der niedrigen Retentionsfaktoren für Adenosin (Ado) and Cytidin (Cyd) nicht effizient für das Sweeping dieser Analyte eingesetzt werden. Außerdem komigrieren diese

Nukleoside mit Bestandteilen der Urin-Matrix. Daher wurde zusätzlich das anionische Tensid SDS für ein Alternativverfahren zur Bestimmung von Ado und Cyd nach Überführung in kationische Spezies (unter sauren pH-Bedingungen) unter Verwendung von "pseudostationary ion-exchanger" sweeping als on-line Anreicherungsprinzip herangezogen. Dieses Alternativverfahren wurde erfolgreich angewendet, um Ado und Cyd in Urinproben zu bestimmen. Ergänzend wurde nachgewiesen dass mit einem Hintergrundelektrolyten, der ein Alkyl- oder Arylboronat zusätzlich zu  $C_{14}MImBr$  enthält, die Retentionsfaktoren aller untersuchten Nukleoside signifikant erhöht sind. Diese Verschiebung der Retentionsfaktoren zu höheren Werten wird der Wechselwirkung mit der zusätzlich über die Alkyl/Aryl-Gruppe des Boronats eingeführten hydrophoben Struktureinheit zugeschrieben (Komplexbildung des Boronats mit der cis-Diol-Gruppe des Nukleosids). Es wird gezeigt, dass die entwickelten Optimierungsstrategien in validierten Verfahren genutzt werden können, die eine Identifizierung und Quantifizierung der untersuchten Nukleoside in Urin-Proben ermöglichen (Nachweisgrenzen im Bereich von  $0,1-0,2 \text{ mg L}^{-1}$ ).

In einem zweiten Schritt wird 2-Hydroxypropyl- $\beta$ -cyclodextrin (2-HP- $\beta$ -CD) als Puffer-Additiv in einem Borat-Borsäure-Puffer verwendet. Dieses Additiv ermöglicht eine Modifizierung der Trennselektivität und eine vollständige Trennung der untersuchten Nukleoside via CZE. Unter Nutzung der sehr hohen Komplexbildungskonstante zwischen Nukleosid und Tetrahydroxyborat unter gleichzeitiger Verwendung des selektivitätsmodifizierenden Additivs 2-HP- $\beta$ -CD wird ein sehr empfindliches CZE-Verfahren entwickelt, dessen Nachweisgrenzen  $10-40 \mu\text{g L}^{-1}$  erreichen. Dieses Verfahren stützt sich auf eine mehrstufige on-line Anreicherung unter Einbeziehung von dynamic pH junction, borate sweeping und large volume sample stacking (LVSS). Eine Validierung wird gemäß den Leitlinien der ICH durchgeführt. Das validierte Verfahren wird erfolgreich auf die Identifizierung und Quantifizierung von Nukleosiden in gespiktem und ungespiktem Urin angewandt. Die Ergebnisse dieses Teils der Untersuchungen werden nachfolgend auf die Analyse ausgewählter  $\alpha$ -Aminocephalosporine in Oberflächenwasser übertragen. Unter Hinzuziehung einer hochempfindlichen Detektionsmethode (Laser-induzierte Fluoreszenz (LIF) Detektion) wird CZE mit LVSS-sweeping zur Analyse von Cefalexin und Cefadroxil in gespiktem Lahnwasser genutzt (Nachweisgrenzen  $5-8 \text{ ng L}^{-1}$ ).

# **5. Cumulative Part (Publications)**





## **5.1. Publication I**

**Imidazolium-based ionic liquid-type surfactant as pseudostationary phase in micellar electrokinetic chromatography of highly hydrophilic urinary nucleosides**

**Azza H. Rageh**, Ute Pyell

**Journal of Chromatography A, 1316 (2013) 135-146**

[doi:10.1016/j.chroma.2013.09.079](https://doi.org/10.1016/j.chroma.2013.09.079)



### 5.1.1. Summary and discussion

In this publication, we investigate the MEKC analysis of the highly hydrophilic urinary nucleosides as negatively charged metabolites under alkaline pH conditions using the imidazolium-based ionic liquid-type surfactant 1-tetradecyl-3-methylimidazolium bromide ( $C_{14}MImBr$ ). The investigated analytes are adenosine (Ado), cytidine (Cyd), uridine (Urd), 5-methyluridine (5MeUrd), guanosine (Guo), inosine (Ino), and xanthosine (Xao). The negative charge of the nucleosides is acquired due to complexation with tetrahydroxyborate and/or dissociation of the amidic group (Fig. 1). The effective electrophoretic mobility data show that complexation between these nucleosides and tetrahydroxyborate occurs with a high degree of complexation even at very low borate concentration ( $2.5 \text{ mmol L}^{-1}$  disodium tetraborate).

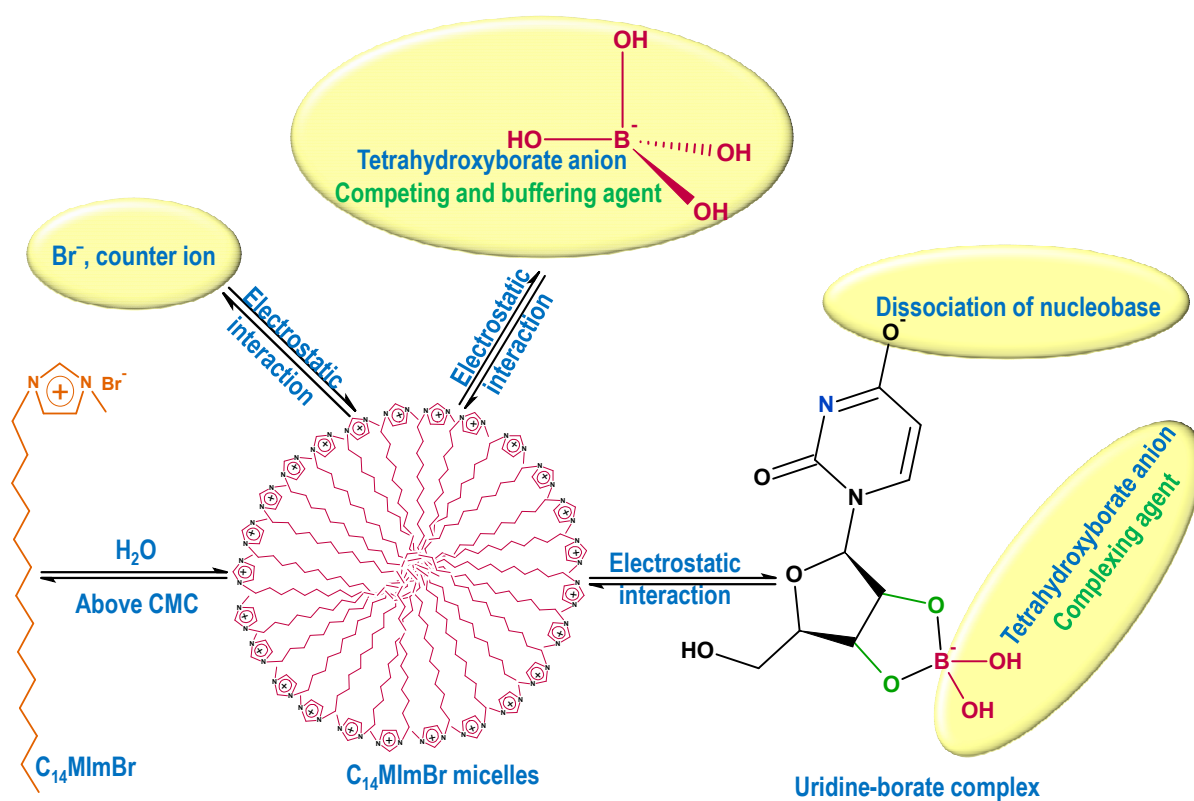


**Figure 1:** Suggested retention mechanism for the nucleosides using  $C_{14}MImBr$  micelles.

The performance of  $C_{14}MImBr$  in nucleoside separation is compared to either (i) the commonly used anionic surfactant sodium dodecyl sulfate SDS or (ii) the conventional tetralkylammonium salt cationic surfactant tetradecyltrimethylammonium bromide (TTAB). It is shown that the separation of the investigated nucleosides is achieved with good resolution using a low concentration of  $C_{14}MImBr$  in the background electrolyte (BGE). The separation of seven urinary nucleosides is successfully achieved using  $20 \text{ mmol L}^{-1}$   $C_{14}MImBr$  in  $5 \text{ mmol L}^{-1}$  borate buffer, pH 9.38. This approach avoids the use of high SDS

concentrations typically associated with the analysis of these highly hydrophilic metabolites as neutral species, which is frequently accompanied by high electric current, Joule heating and long analysis time.

Moreover, C<sub>14</sub>MImBr provides a selectivity, which is different from that of TTAB due to the versatility of the interaction sites provided by the imidazolium head group. Besides electrostatic interaction (that is also existing with TTAB), the imidazolium head group offers additional types of intermolecular interactions ( $\pi$ - $\pi$ , ion-dipole, and hydrogen-bonding interactions). The stronger interaction of C<sub>14</sub>MImBr with the nucleosides is reflected by higher values of the pseudoeffective electrophoretic mobility compared to that obtained using TTAB. The higher repeatability of the migration times accompanied with the use of C<sub>14</sub>MImBr compared to TTAB is attributed by us to the efficiency by which C<sub>14</sub>MImBr dynamically coats the inner capillary wall.

It is proven that the negatively charged nucleosides interact mainly with the oppositely charged PSP by electrostatic (Coulomb) forces, while hydrophobic interaction can be considered to be negligible (Fig. 1). The dependency of the retention factor of the nucleosides on the concentration of borate (buffering, complexing and competing ion) and on the pH of the BGE is determined, being the highest at the lowest borate concentration and at the pH that enables a full deprotonation of the nucleosides under investigation. Based on the classical theory of ion-exchange chromatography, C<sub>14</sub>MImBr can be regarded as a pseudostationary ion-exchanger that provides a fixed concentration of the ion-exchange sites and enables the regulation of the retention factors by proper adjustment of the concentration of the competing buffer ion or the pH of the BGE. Compared to hydrophilic interaction chromatography (HILIC), our new MEKC strategy provides a faster, a more efficient, a highly reproducible and a highly selective method for the analysis of the highly hydrophilic nucleosides.

### **5.1.2. Author contribution**

All the experimental part of this publication was conducted by me, except the separation of the nucleobases and nucleosides experiment, which was carried out by M.Sc. A. Kaltz. Drying of the synthesized 1-tetradecyl-3-methylimidazolium bromide was carried out by M.Sc. M. Abdelmegeed. The draft of the manuscript was written by me and corrected by Prof. Dr. Ute Pyell. The final revision of the manuscript was corrected by me and Prof. Dr. Ute Pyell before submission to the journal. Prof. Dr. Ute Pyell was responsible for the supervision of this work.





Contents lists available at ScienceDirect

## Journal of Chromatography A

journal homepage: [www.elsevier.com/locate/chroma](http://www.elsevier.com/locate/chroma)

# Imidazolium-based ionic liquid-type surfactant as pseudostationary phase in micellar electrokinetic chromatography of highly hydrophilic urinary nucleosides



Azza H. Rageh, Ute Pyell\*

University of Marburg, Department of Chemistry, Hans-Meerwein-Straße, D-35032 Marburg, Germany

## ARTICLE INFO

## Article history:

Received 5 June 2013  
 Received in revised form  
 23 September 2013  
 Accepted 25 September 2013  
 Available online 2 October 2013

## Keywords:

Micellar electrokinetic chromatography  
 Ionic liquid-type surfactant  
 Urinary nucleosides  
 Borate complexation  
 Ion-exchange interaction

## ABSTRACT

Ionic liquid (IL)-type surfactants have been shown to interact more strongly with polar compounds than traditionally used quaternary ammonium cationic surfactants. The aim of this study is to provide an alternative micellar electrokinetic chromatographic method (MEKC) for the analysis of urinary nucleosides in their ionic form at low surfactant concentration. This approach could overcome the use of high surfactant concentrations typically associated with the analysis of these highly hydrophilic metabolites as neutral species, which is frequently accompanied by high electric current, Joule heating and long analysis time. The investigated IL-type surfactant; 1-tetradecyl-3-methylimidazolium bromide ( $C_{14}MImBr$ ) is similar to the commonly employed cationic surfactant; tetradecyltrimethylammonium bromide (TTAB) but it provides a different separation selectivity. We employed  $C_{14}MImBr$  micelles for the MEKC analysis of seven urinary nucleosides. The studied analytes possess a negative charge at pH 9.38 (exceptions are adenosine and cytidine which are neutral at this pH value). Borate imparts an additional negative charge to these compounds after complexation with the *cis*-diol functionality of the ribose unit, which in turn enables them to interact with the oppositely charged  $C_{14}MImBr$  micelles via electrostatic (Coulomb) forces. The effect of the concentration of borate (the complexing, competing and buffering ion) on the effective electrophoretic mobilities and on the retention factors was investigated. The effective electrophoretic mobility data show that complexation between these nucleosides and borate occurs with high degree of complexation even at very low borate concentration ( $2.5 \text{ mmol L}^{-1}$  disodium tetraborate). In addition, we found that the retention factors are strongly dependent on the borate concentration being the highest when using the lowest borate concentration and they can be regulated by variation of either tetraborate concentration or the pH of the background electrolyte using only  $20 \text{ mmol L}^{-1}$   $C_{14}MImBr$ . We confirmed also that the main mode of interaction between these analytes and the  $C_{14}MImBr$  micelles is electrostatic interaction. Our experimental results reveal that the cationic surfactant  $C_{14}MImBr$  exhibits superior selectivity and higher reproducibility relative to that of TTAB, which makes this surfactant a promising cationic surfactant for the MEKC separation of other hydrophilic polar analytes.

© 2013 Elsevier B.V. All rights reserved.

## 1. Introduction

Ionic liquids (ILs) are known as molten salts with melting points below  $100^\circ\text{C}$ . They are a class of ionic non-molecular solvents with a multitude of physicochemical properties. The most remarkable properties include their high thermal stability, a low vapour pressure, the miscibility with water and a variety of organic solvents, notable catalytic properties, as well as good extraction coefficients for various organic compounds [1]. They are environmentally benign and their non-flammability and low volatility allow them to gain an increasing interest in the field of green chem-

istry. The low symmetry and the relatively large size of the ions constituting the ILs lead to a lowering of the lattice energy, and hence the melting point of the resulting ionic liquid. ILs were a subject of many recent review articles, which highlight a variety of applications in many areas of separation science [1–4].

It was reported that ILs possessing long hydrophobic alkyl tails with cationic polar headgroups can form micelles when they are dissolved in water in a concentration above their CMC (critical micelle concentration). This property enables ILs to emerge as a new class of surfactants, especially because they possess the properties of cationic surfactants in addition to the restricted number of the classic cationic surfactants and the growing interest in applications that involve cationic surfactants. As recently pointed out in the review article of Pino et al. [1], it is more adequate to employ the term ionic liquid-based surfactants rather than IL surfactants as

\* Corresponding author. Tel.: +49 6421 2822192; fax: +49 6421 2822124.  
 E-mail address: [pyellu@staff.uni-marburg.de](mailto:pyellu@staff.uni-marburg.de) (U. Pyell).

the cation/anion pair forming the ionic liquid does no longer constitute a true ionic liquid once the ionic liquid is dissolved in water or any organic solvent [1].

Dong et al. [5] and Vanyur et al. [6] reported that micelles are formed in an aqueous solution of long-chain ILs; namely 1-tetradecyl-3-methylimidazolium bromide ( $C_{14}MImBr$ ) and 1-hexadecyl-3-methylimidazolium bromide ( $C_{16}MImBr$ ). They found that imidazolium-based ILs are superior to the traditional cationic alkyltrimethyl ammonium bromides in their ability to form micelles, i.e. their CMC values are significantly lower than those of the classic cationic surfactants with comparable alkyl chain length. Alkylimidazolium-based ILs are the most widely used class of IL-type surfactants in capillary electrophoresis [3]. In addition to their role as background electrolyte (BGE) modifier in capillary electromigration separation techniques [7–10], few reports have described the MEKC utility of long-chain imidazolium-based ILs as pseudostationary phase (PSP) [11–13] in MEKC. Interest in IL-type surfactants stems from the fact that they offer a high versatility of interaction types (electrostatic,  $\pi$ - $\pi$ , ion-dipole or hydrogen bonding interactions with the imidazolium cation head group and hydrophobic interaction due to the long alkyl tail) [14].

Metabolomics has acquired a special focus and increased popularity in life science over the last decade [15,16]. The change in the concentration of specific metabolites in urine reflects a certain physiological or pathological state in the human body, therefore the identification of metabolite profiles is one of the main goals of metabolomics [17]. Nucleosides are metabolites of either RNA's turnover or oxidative damage of DNA. Normal or unmodified nucleosides, e.g. uridine and guanosine, can be either reutilized to form nucleotide triphosphates or further degraded to form uric acid and  $\beta$ -alanine. Modified nucleosides, which mostly exist in the transfer RNA (tRNA) and are formed during posttranscriptional modification by numerous modification enzymes [18], cannot be reutilized or degraded, but are circulated unchanged in the blood stream and are excreted intact in the urine. Abnormal levels of modified nucleosides can indicate degradation of RNA. Therefore, urinary nucleosides, especially modified ones, can be used as a useful biologic marker of cancer. Such a marker reflects the presence of cancer or indicates changes in the tumour mass and can be useful in following up chemotherapy [19].

Nucleosides have been separated using different analytical techniques such as reversed phase high-performance liquid chromatography (RP-HPLC) [20–22], hydrophilic interaction chromatography (HILIC) (due to their highly hydrophilic nature) [23–25], immunoassay [26] and capillary electromigration separation techniques including capillary zone electrophoresis (CZE) [27], capillary electrochromatography (CEC) [28,29] and MEKC [17,21,30–32]. Capillary electromigration separation techniques for nucleoside analysis compared to HPLC offer high resolution and separation efficiency, short analysis time, low sample volume (nL), environmental compatibility, relatively low costs and suitability for the analysis of large series of urine samples which is highly desirable in the clinical laboratory [15]. Nucleoside analysis using capillary electromigration separation techniques is usually performed in two subsequent steps. The first step involves the extraction of the nucleosides from urine using phenylboronate affinity gel as solid phase extraction (SPE) stationary phase [19]. This extraction medium provides a unique means for the selective enrichment of cis-diol containing metabolites. It forms cyclic esters with the vicinal hydroxyl groups of the ribose unit of nucleosides under basic pH conditions. While maintaining the basic conditions, the analytes can be purified from interferences without any loss. When the pH is switched to acidic conditions, the analytes are eluted and after evaporating the extract to dryness, the extract is dissolved in water and analyzed further. The second step is the analysis step, which is commonly performed by MEKC with the

nucleosides in their neutral form and to a lesser extent when they are charged by using either MEKC or CZE.

Terabe and co-workers [33] were the first who reported the MEKC analysis of nucleosides. They used a BGE composed of  $200\text{ mmolL}^{-1}$  SDS,  $25\text{ mmolL}^{-1}$  sodium tetraborate,  $50\text{ mmolL}^{-1}$  sodium dihydrogen phosphate, pH 7 for the separation of 4 nucleosides and one deoxynucleoside. This buffer composition was widely adopted by many authors for the MEKC analysis of urinary nucleosides with slight modifications in the concentrations of SDS, phosphate and borate buffers [17,21,30–32]. The use of a high concentration of the PSP reflects the highly hydrophilic nature of the nucleosides which results in low retention factors. These high concentrations of SDS are typically associated with bubble formation, migration time irreproducibility, noisy baseline [34], high electric current and Joule heating. Working under low applied voltage (to avoid such problems) results in long analysis times [18,31]. Hence, the employment of a new pseudostationary phase that interacts more strongly with these polar analytes and can be used at a lower concentration compared to the concentration needed for SDS is highly desirable.

Jiang and Ma [34] reported a fast MEKC method for the analysis of urinary nucleosides (as charged species) in which they used a borate-phosphate buffer, pH 9.5 containing  $25\text{ mmolL}^{-1}$  cetyltrimethylammonium bromide (CTAB) as BGE. Unfortunately, there is no emphasis in this work about the role of borate complexation in enhancing the interaction between the nucleosides and the PSP. In addition, there is no explanation for the effect of the buffer ionic strength on the retention factor of these analytes and no clarification why most of the investigated analytes are eluted even before the EOF (electro-osmotic flow) marker, which according to our assumption may be attributed to the low interaction between the nucleosides and the CTAB micelles. This low interaction confirms the need for new surfactants that are capable of interacting more strongly with these highly hydrophilic analytes, which may enhance their resolution while maintaining a short run time. Poor reproducibility of EOF and migration times was also reported for the use of tetraalkylammonium ions as a PSP [35]. Therefore, it is also required to employ new cationic surfactants that provide a stable dynamic coating and a reproducible EOF velocity resulting in reproducible migration times.

According to the best of our knowledge, the MEKC analysis of urinary nucleosides employing IL-type surfactants has not been reported so far. In this work, we employ  $C_{14}MImBr$  as PSP for the MEKC separation of six unmodified nucleosides and one methylated nucleoside, based on the assumption that the main mode of interaction between the nucleosides and the micelles formed by  $C_{14}MImBr$  is electrostatic interaction, while regarding the  $C_{14}MImBr$  micelles to be a pseudostationary ion-exchanger. In addition, we investigate the optimum borate concentration that enhances the interaction of urinary nucleosides (as charged analytes) with the positively charged pseudostationary ion-exchanger. The effect of the buffer type, the buffer pH and the buffer ionic strength on the retention factors of the investigated analytes is studied. The performance parameters for  $C_{14}MImBr$  are compared to those exhibited by a conventional cationic surfactant (TTAB) in terms of resolution, selectivity, and migration time reproducibility. Moreover, the selectivity of the developed method regarding the separation of nucleosides from nucleic bases and uric acid is compared to that reported for HILIC.

## 2. Experimental

### 2.1. Chemicals and background electrolytes

Nucleoside standards cytidine (Cyd), adenosine (Ado), 5-methyluridine (5MeUrd), uridine (Urd), guanosine (Guo), inosine



(Ino), xanthosine (Xao) were purchased from Sigma–Aldrich, Steinheim, Germany; their chemical structures are presented in Fig. S1 (supplementary data). Tetradecyltrimethylammonium bromide (TTAB), uric acid, xanthine (Xan), cytosine (Cyt), adenine (Ade), 3-(*N,N*-dimethyltetradecylammonio)-propanesulfonate (ZS), 1-bromotetradecane (98%), 1-methylimidazole (99%), hexanophenone, heptanophenone, octanophenone, decanophenone, dodecanophenone and phosphorous pentoxide were from Sigma–Aldrich, Steinheim, Germany. Uracil (Ura), thymine (Thy), guanine (Gua), sodium dodecyl sulphate (SDS), hydrochloric acid, phosphoric acid and sodium hydroxide were from Fluka, Buchs, Switzerland. Disodium tetraborate decahydrate (borax), sodium dihydrogen phosphate monohydrate, disodium hydrogen phosphate dihydrate was from Merck, Darmstadt, Germany. Thiourea was from Riedel-de Haën, Seelze, Germany. Sodium hydrogen carbonate and sodium sulphate anhydrous were from Grüssing, Filsum, Germany. Methanol, HPLC grade was from VWR-BDH-Prolabo, Leuven, Belgium. Ethyl acetate and toluene were available at the department of chemistry, Marburg, Germany. *d*-Chloroform was from Deutero, Kastellaun, Germany. All single analyte stock solutions (800 mg L<sup>-1</sup> of Ado, Cyt, Urd, 5MeUrd, Ino, 400 mg L<sup>-1</sup> of Xao, Guo, Gua, 100 mg L<sup>-1</sup> of Cyt, Ura, Thy, Ade, 36 mg L<sup>-1</sup> of Xan and 530 mg L<sup>-1</sup> of uric acid) were prepared in water except Gua and uric acid stock solutions which were prepared in 20 mmol L<sup>-1</sup> NaOH. Stock solutions of the nucleoside standards are stored in the refrigerator and are used within one month. The working standard solutions were prepared daily in which the concentration of each of the studied nucleosides in the sample solution mixture was 20 mg L<sup>-1</sup>, unless otherwise specified. Thiourea stock solution was 1000 mg L<sup>-1</sup> in water. A stock solution of decanophenone was prepared in methanol (300 mg L<sup>-1</sup>). Refer to the supplementary data for the synthesis and characterization of C<sub>14</sub>MImBr (Table S1, Figs. S2–S5).

Stock solutions of borate buffer, phosphate buffer, and sodium bicarbonate were prepared and further diluted for the preparation of the background electrolytes. Stock disodium tetraborate buffer (100 mmol L<sup>-1</sup>, pH 9.48) was prepared by dissolving 9.5342 g disodium tetraborate decahydrate in 200 mL water and diluting to 250 mL with water. Stock phosphate buffer (40 mmol L<sup>-1</sup>, pH 7.85) was prepared by dissolving 0.1435 g (4.2 mmol L<sup>-1</sup>) of sodium dihydrogen phosphate monohydrate and 1.5942 g (35.8 mmol L<sup>-1</sup>) of disodium hydrogen phosphate dihydrate in 200 mL water and diluting to 250 mL with water. Stock sodium bicarbonate solution (100 mmol L<sup>-1</sup>, pH 8.65) was prepared by dissolving 1.6802 g of sodium bicarbonate in 100 mL water and diluting to 200 mL with water. Phosphate buffer (50 mmol L<sup>-1</sup>, pH 6.86) for MEKC experiments using either SDS or TTAB was prepared by mixing 25 mL of sodium dihydrogen phosphate monohydrate (250 mmol L<sup>-1</sup>) and 25 mL of disodium hydrogen phosphate dihydrate (250 mmol L<sup>-1</sup>) in 250 mL volumetric flask and diluting with water to 250 mL.

The micellar BGEs were either (i) 2.5, 5, 10, 15, 20, 30 or 40 mmol L<sup>-1</sup> borate buffer containing 20 mmol L<sup>-1</sup> C<sub>14</sub>MImBr, pH 9.38 (without any adjustment) or (ii) 10 mmol L<sup>-1</sup> carbonate buffer containing 20 mmol L<sup>-1</sup> C<sub>14</sub>MImBr, pH 9.38 (pH was adjusted using 0.2 mol L<sup>-1</sup> NaOH) or (iii) 20 mmol L<sup>-1</sup> borate buffer containing either 20, 40, 60, 80 or 100 mmol L<sup>-1</sup> TTAB, pH 9.38 or (iv) 20 mmol L<sup>-1</sup> borate buffer containing either 20, 40 or 60 mmol L<sup>-1</sup> C<sub>14</sub>MImBr, pH 9.38 or (v) 2.5 mmol L<sup>-1</sup> borate buffer containing 20 mmol L<sup>-1</sup> C<sub>14</sub>MImBr adjusted to pH 8.49, 9.02, 9.38, 9.60, 9.84, 10.09, 10.41 (using either 0.2 mol L<sup>-1</sup> HCl or 0.2 mol L<sup>-1</sup> NaOH).

The non-micellar BGEs were either 2.5, 5, 10, 15, 20, 30 or 40 mmol L<sup>-1</sup> borate buffer adjusted to pH 9.38 (using 0.2 mol L<sup>-1</sup> HCl) or 2.5 mmol L<sup>-1</sup> borate buffer adjusted to pH 8.51, 9.03, 9.38, 9.6, 9.86, 10.11, 10.43 (using either 0.2 mol L<sup>-1</sup> HCl or 0.2 mol L<sup>-1</sup> NaOH) or 20 mmol L<sup>-1</sup> phosphate buffer adjusted to pH 7.05, 7.97,

8.35, 8.63, 9.07, 9.37, 9.55, 9.84, 10.43, 11.30 (using either phosphoric acid or 1 mol L<sup>-1</sup> NaOH).

The pH of the micellar BGEs containing C<sub>14</sub>MImBr is lower than the corresponding non-micellar BGEs containing no C<sub>14</sub>MImBr by about 0.05 pH units due to the slight acidity of the imidazolium cation, therefore the pH of the non-micellar BGEs must be adjusted to be exactly the same as the pH of the micellar BGEs containing C<sub>14</sub>MImBr using 0.2 mol L<sup>-1</sup> HCl.

All buffer solutions were filtered prior to use through a 0.45 μm nylon membrane filter (WICOM, Heppenheim, Germany). BGEs were replaced after every four runs.

## 2.2. Instrumentation

All measurements were done using the ATI Unicam CE System, Crystal 300 Series, Model 310 equipped with UV/vis detector Spectra 100 (with deuterium lamp) from Thermo Separation Products, San Jose, USA, set to a wavelength of 257 nm. Oven temperature was kept at 35 °C. Data acquisition was done using an AD-converter (USB-1280FS, Measurement Computing, Middleborough, USA). Data were recorded using CE-Kapillarelektrophorese software (development of the electronic workshop of the Department of Chemistry, University of Marburg based on Delphi). Data analysis was performed with Origin 8.5 software (OriginLab Corporation, Northampton, USA). Fused silica-capillaries (50 μm I.D., 360 μm O.D.) were obtained from Polymicro Technologies (Phoenix, AZ, USA), with a total length of 649 mm and a length to the detector of 502 mm (if not stated otherwise). Blue Ribbon 589/3 ashless quantitative filter paper (Schleicher & Schuell, Dassel, Germany) with a diameter of 125 mm and 2 μm retention was used for filtration. InoLab pH 720 (WTW, Weilheim, Germany) was used for pH measurements. <sup>1</sup>H NMR, <sup>13</sup>C NMR and IR measurements were carried out on Avance 300 or Tensor 37 spectrometer (Bruker GmbH, Germany), respectively.

New capillaries were conditioned by flushing them first with NaOH solution (1 mol L<sup>-1</sup>) 60 min, water 30 min, and BGE 5 min using an applied pressure of 800 mbar. Between runs the capillaries were rinsed with methanol 2 min, HCl (1 mol L<sup>-1</sup>) 2 min, water 2 min, NaOH solution (1 mol L<sup>-1</sup>) 2 min, water 2 min and finally with BGE for 2 min using an applied pressure of 800 mbar. The separations were performed with the micellar and non-micellar BGE under an applied voltage of –10 or +10 kV, respectively, unless otherwise specified. The samples were pressure-injected at 30 mbar for 12 s.

The electroosmotic hold-up time  $t_0$  [36] and the elution time of the micellar phase  $t_{MC}$  were determined using thiourea and decanophenone, respectively, as neutral markers. Electrophoretic mobilities were determined from electropherograms containing a peak of the hold-up time marker. Peak identities were confirmed by spiking.

## 3. Results and discussion

### 3.1. Chemical structures and physical properties of the studied analytes

Nucleosides are glycosylamines consisting of a nucleobase linked to a D-ribose sugar unit via beta-glycosidic linkage. The presence of a ribose sugar unit in the nucleoside structure imparts them a highly hydrophilic nature as reflected by low  $\lg P_{ow}$  values (Fig. S1, supplementary data). The seven investigated nucleosides namely; Ado, Cyt, Urd, 5MeUrd, Guo, Ino and Xao (abbreviations according to IUPAC-IUB commission on biochemical nomenclature [37]) were selected as model examples to test our new MEKC strategy. These compounds can be considered to be the most

problematic ones due to their highly hydrophilic nature and weak interaction with the pseudostationary phase. However, it must be emphasized that urine might contain a larger number of modified nucleosides. Beside the non-availability of many nucleoside standards [27], many of the modified nucleosides such as  $N^1$ -methyladenosine,  $N^6$ -methyladenosine,  $N^2$ -methylguanosine and  $N^2,N^2$ -dimethylguanosine are more hydrophobic than the investigated analytes as indicated by analysis via MEKC using either CTAB [34] or SDS [17] as PSP. It can be expected that their separation can be achieved with a lower surfactant concentration than that needed for the separation of those analytes, which are investigated in the present study. Therefore, our main focus will be directed to the most hydrophilic species.

Five of the studied compounds; namely Urd, 5MeUrd, Ino, Guo and Xao have  $pK_a$  values between 8.80 and 9.70 (except Xao with  $pK_a = 5.70$ ) due to the presence of an amidic group; therefore these compounds are considered to be weak acids. Ado, Guo and Cyd are considered to be weak bases as they can be protonated on one of the ring nitrogen atoms, which act as proton acceptors, rather than on the exocyclic amino group [38] and this  $-NH_2$  group shares the positive charge of the cation by resonance. Xao and Ino can be protonated on one of the ring nitrogen atoms and can also act as a weak base. Owing to the presence of vicinal diol moieties ( $pK_a \sim 12.5$ ) on the ribose unit, these compounds are capable of forming reversible complexes with the borate anion under alkaline pH conditions which enables them to acquire an additional negative charge in addition to the negative charge gained due to dissociation (with exception of Ado and Cyd that acquire their negative charge only due to borate complexation). We calculated the  $pK_a$  values for Ino, Urd, Guo and 5MeUrd in 20 mmol L<sup>-1</sup> phosphate buffer from migration data and obtained 8.80, 9.27, 9.18 and 9.47 for Ino, Urd, Guo and 5MeUrd, respectively (Fig. S6A, supplementary data) that are in good agreement with those values found in the literature (Fig. S1, supplementary data). As shown in Fig. S6B (supplementary data), the absolute effective electrophoretic mobilities of all studied analytes are higher in borate buffer than in phosphate buffer.

It is noteworthy to mention that the effective electrophoretic mobilities of Ado, Cyd and Xao are not dependent on the pH in case of using phosphate buffer (Fig. S6A, supplementary data) as these compounds are either neutral or fully dissociated in the investigated pH range. In case of borate buffer, a significant increase in  $\mu_{eff}$  is observed for all analytes in the pH range from 8.51 to 9.38 (Fig. S6B, supplementary data) that is attributed to either an increase in the degree of dissociation (in case of 5MeUrd, Urd, Guo and Ino) or to an enhanced degree of complexation. The effective electrophoretic mobilities of Ado, Cyd and Xao are slightly increased in borate buffer at pH  $\geq 9.38$  although the  $pK_a$  value of boric acid is 9.24. A possible explanation for this observation is that borate under alkaline pH condition (above its  $pK_a$ ) and in the presence of polyhydroxy organic compounds such as mannitol, glycerol or nucleosides, acts as a much stronger acid (e.g. for the mannitol borate complex,  $pK_a$  is 3.80 [39]) and its  $pK_a$  is lowered. Therefore, in case of Ado, Cyd and Xao any further increase in the pH value above 9.38 will have a very small effect on  $\mu_{eff}$ . We deduce from these data that in presence of borate at pH  $\geq 9.38$ , the effective charge number is increased to  $-2$  in case of Xao and to  $-1$  in case of Ado and Cyd. The observed increase in  $\mu_{eff}$  for the other analytes is due to an increase in the degree of dissociation (effective charge number between  $-1$  and  $-2$ ).

### 3.2. Separation by CZE

As nucleosides under alkaline pH conditions are negatively charged either due to the dissociation of the amidic group or due to complexation with borate, their separation by CZE is possible.

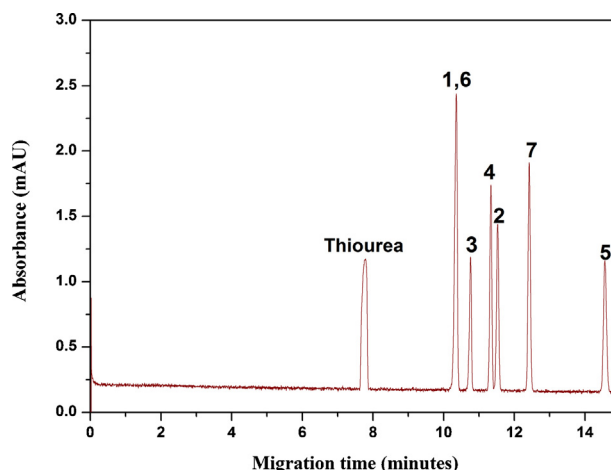


**Fig. 1.** Electropherogram obtained from a standard solution mixture of 20 mg L<sup>-1</sup> of each of the investigated nucleosides and 25 mg L<sup>-1</sup> thiourea in water. CE conditions: 10 mmol L<sup>-1</sup> sodium tetraborate (pH 9.38) as BGE; applied voltage +10 kV; pressure injection 30 mbar for 12 s. Peak designation: 1 = cytidine, 2 = uridine, 3 = 5-methyluridine, 4 = guanosine, 5 = xanthosine, 6 = adenosine, 7 = inosine.

As shown in Fig. 1, some of the nucleosides investigated can be separated when using 10 mmol L<sup>-1</sup> borate buffer as BGE. A closer inspection of the electropherogram in Fig. 1 demonstrates that Ado and Cyd (that are neutral with zero electrophoretic mobility in phosphate buffer, see Fig. S6A, supplementary data), migrate after thiourea in the presence of borate buffer due to the charge gained by borate complexation. The migration order for the other nucleosides is in accordance with their acid-dissociation constants (Fig. S1, supplementary data). However, under the conditions employed Ado and Cyd comigrate and it is very difficult to separate these analytes without adding further additives. No better separation was achieved for this peak pair by increasing the borate concentration up to 40 mmol L<sup>-1</sup> (Fig. S7, supplementary data). The resolution can be improved for other nucleosides (Fig. S8A, supplementary data), although increasing the borate concentration in the BGE does not alter the overall selectivity of the separation. The observed increase in migration times is due to the decrease in the electroosmotic mobility with increasing ionic strength. The enhancement of the peak efficiency and the peak height at higher borate concentration (Fig. S7, supplementary data) can be attributed to the on-line zone focusing by stacking, which is dependent on the conductivity difference between the sample matrix (water) and the BGE.

From plotting  $\mu_{eff}$  against pH (see Fig. S8B, supplementary data), pH 9.38 was selected as optimum value offering the best selectivity within the investigated range. The degree of complex formation is dependent on the concentration of the complexing ion borate. For a fixed pH (9.38) the borate concentration was varied from 2.5 up to 40 mmol L<sup>-1</sup> borax (Fig. S7, supplementary data). Plotting  $\mu_{eff}$  against the concentration of borate (Fig. S8B, supplementary data), reveals that  $\mu_{eff}$  is independent of the borax concentration within the studied range. This implies that the degree of complexation is close to one at very low borate concentration (2.5 mmol L<sup>-1</sup> tetraborate) which gives an indication about the very high complex formation constants of the formed complexes. It was not possible to investigate lower borax concentrations  $< 2.5$  mmol L<sup>-1</sup> due to the low buffer capacity associated and the very low electric current strength generated.

### 3.3. Separation by MEKC

#### 3.3.1. Separation of nucleosides as neutral compounds

We started our investigation by employing SDS as anionic surfactant for the MEKC separation of nucleosides as neutral

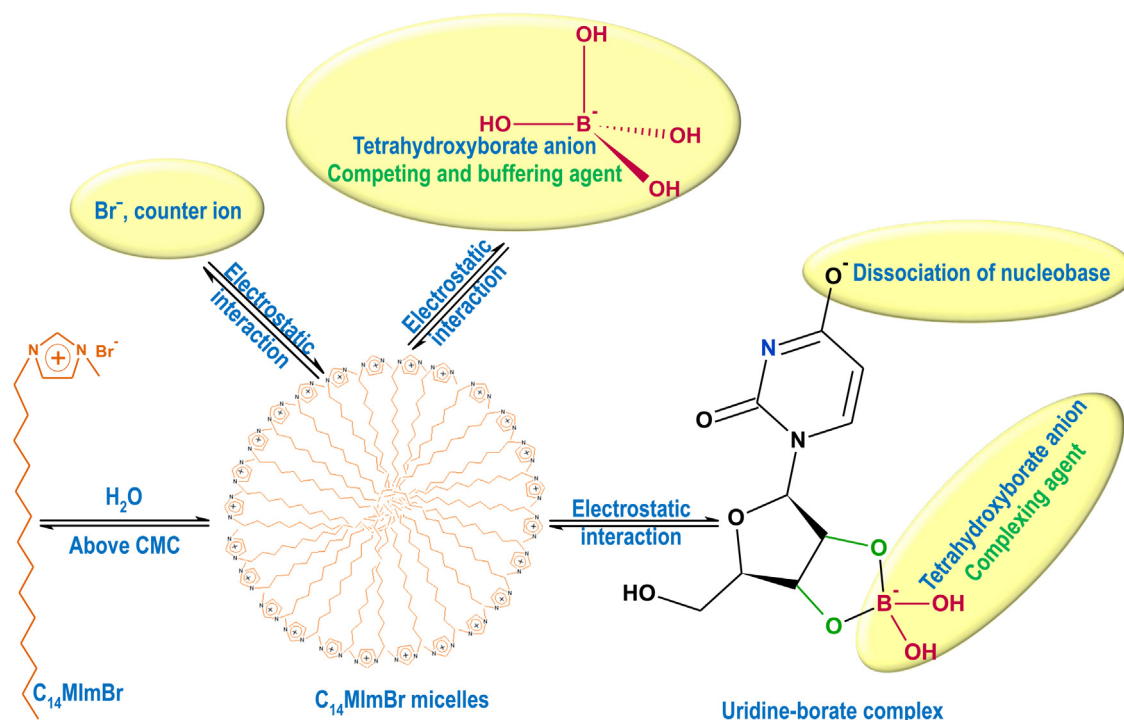


Fig. 2. Suggested retention mechanism for the nucleosides using C<sub>14</sub>MImBr micelles.

compounds. After preliminary trials, a BGE composed of 200 mmol L<sup>-1</sup> SDS in 50 mmol L<sup>-1</sup> phosphate buffer, pH 6.86 was successful in separating the seven nucleosides (Fig. S9, supplementary data) within 30 min. This optimized BGE composition is quite similar to those found in the literature for the analysis of urinary nucleosides [33,40]. The high concentration of the PSP reflects the low partitioning constants between the micellar phase and the aqueous phase. However under these conditions migration times proved to be irreproducible either for intra- or inter-day conditions, which can be attributed in part to the high electric conductivity of this buffer, which is associated with a high current strength and significant Joule heating (see Fig. S10, supplementary data).

It was previously reported that SDS forms mixed micelles with zwitterionic surfactants [41]. This combination increases the micelle radius and reduces the surface charge density relative to pure SDS micelles which will have an impact on the partitioning coefficients of hydrophilic analytes [41]. Based on these considerations, we tested a BGE containing mixed micelles formed by SDS and the zwitterionic surfactant; 3-(N,N-dimethyltetradecylammonio)propanesulfonate (ZS): (i) 25 mmol L<sup>-1</sup> SDS and 15 mmol L<sup>-1</sup> ZS, (ii) 50 mmol L<sup>-1</sup> SDS and 5 mmol L<sup>-1</sup> ZS, (iii) 75 mmol L<sup>-1</sup> SDS and 10 mmol L<sup>-1</sup> ZS and (iv) 100 mmol L<sup>-1</sup> SDS and 10 mmol L<sup>-1</sup> ZS in 50 mmol L<sup>-1</sup> phosphate buffer, pH 6.86. There is, however, no improvement with regard to a BGE containing 200 mmol L<sup>-1</sup> SDS (results not shown). Higher concentrations of SDS ( $\geq 100$  mmol L<sup>-1</sup>) result in long and irreproducible migration times. Trials to use a higher concentration of the zwitterionic surfactant ( $>15$  mmol L<sup>-1</sup>) result in a highly viscous solution that cannot be introduced into the capillary. We obtained similar results (data not shown) with the cationic surfactant tetradecyltrimethylammonium bromide (TTAB) either without ZS (200 mmol L<sup>-1</sup> TTAB) or in combination with ZS (100 mmol L<sup>-1</sup> TTAB and 50 mmol L<sup>-1</sup> ZS) in 50 mmol L<sup>-1</sup> phosphate buffer pH 6.86. It can be generally stated that the tested nucleosides are highly hydrophilic and another mode of interaction (other than hydrophobic interaction) is strongly needed, if a reduction of the PSP concentration is required.

### 3.3.2. Separation of nucleosides as charged compounds

**3.3.2.1. Retention of charged analytes.** In the presence of borate the studied analytes are negatively charged within the investigated pH range. Their separation in electrokinetic chromatography is consequently based on chromatographic as well as electrophoretic principles. The overall retention factor will be the sum of the retention factors for all species present (for more details, see the supplementary data). As shown in Fig. 2, the nucleosides can interact with the positively charged PSP by electrostatic interaction due to the negative charges acquired by dissociation and/or complexation. As listed in Table 1, in aqueous solution, the described dissociation (Eq. (1a)), complexation (Eq. (1b) and Eq. (1c)) and association (Eqs. (1d)–(1g)) equilibria have to be taken into consideration. In case of Ado and Cyd, the equilibria described by Eqs. (1b), (1d) and (1f) in Table 1 have to be considered, while in case of Urd, 5MeUrd, Guo, Ino and Xao, all these equilibria (Eqs. (1a)–(1g)) are involved. In this case, the overall retention factor  $k$  of the nucleoside is the weighted average of the retention factors for four species present in aqueous solution as given by Eq. (2) in Table 1. In case of Ado and Cyd the second and the fourth term can be deleted as they are not deprotonated within the investigated pH range. Due to the high complex formation constant between borate and nucleoside, we can assume that at pH  $\geq 9.38$  the association between the neutral nucleosides or the charged uncomplexed nucleoside and the positively charged PSP is negligible (Eqs. (1d) and (1e)). Consequently, association can be ascribed to the complexed neutral or deprotonated form of the nucleoside (Eqs. (1f) and (1g)). The overall retention factor  $k$  of the nucleoside can then be approximated to be the weighted average for only two species present in aqueous solution (Eq. (3) in Table 1). In case of Ado and Cyd,  $c_{aq}(\text{BN-O}^-)^{2-}$  is negligible and Eq. (3) can be further simplified.

It can be predicted that for anionic PSP  $k_{(\text{BN})^-}$  and  $k_{(\text{BN-O}^-)^{2-}}$  will be very small (electrostatic repulsion). Therefore SDS cannot be employed as PSP for the MEKC separation of nucleosides as charged compounds. For a cationic PSP, however, strong electrostatic interaction of the charged complexed nucleosides with the oppositely charged PSP is expected. Both C<sub>14</sub>MImBr and TTAB

**Table 1**  
Equations describing (i) dissociation, complexation and association equilibria of the nucleosides, nucleosides with borate and nucleosides with the charged PSP, respectively, (ii) dissociation of borax in water and (iii) the dependency of the retention factor on the competing ion concentration.

Eq. no.	Equation	Description of the symbols and letters
1a	$N \rightleftharpoons N - O^- + H^+$	$N$ = nucleoside
1b	$N + B^- \rightleftharpoons [BN]^-$	$B^-$ = tetrahydroxyborate anion, $[BN]^-$ = complexed form of the nucleoside
1c	$N - O^- + B^- \rightleftharpoons [BN - O^-]^{2-}$	$N - O^-$ = deprotonated form of the nucleoside, $[BN - O^-]^{2-}$ = complexed deprotonated form of the nucleoside
1d	$N + M^{x+} \rightleftharpoons [NM^{x+}]$	$M^{x+}$ = micelle.
1e	$N - O^- + M^{x+} \rightleftharpoons [(N - O^-)M^{x+}]$	
1f	$[BN]^- + M^{x+} \rightleftharpoons [(BN)^- M^{x+}]$	
1g	$[BN - O^-]^{2-} + M^{x+} \rightleftharpoons [(BN - O^-)^{2-} M^{x+}]$	
2	$k = \frac{c_{aq}(N)}{c_{aq}(N) + c_{aq}(N - O^-) + c_{aq}(BN)^- + c_{aq}(BN - O^-)^{2-}} k_N$ $+ \frac{c_{aq}(N) + c_{aq}(N - O^-) + c_{aq}(BN)^- + c_{aq}(BN - O^-)^{2-}}{c_{aq}(N - O^-)} k_{(N - O^-)}$ $+ \frac{c_{aq}(N) + c_{aq}(N - O^-) + c_{aq}(BN)^- + c_{aq}(BN - O^-)^{2-}}{c_{aq}(BN)^-} k_{(BN)^-}$ $+ \frac{c_{aq}(N) + c_{aq}(N - O^-) + c_{aq}(BN)^- + c_{aq}(BN - O^-)^{2-}}{c_{aq}(BN - O^-)^{2-}} k_{(BN - O^-)^{2-}}$	$c_{aq}(N)$ is the molar concentration of the neutral form in the mobile phase. $c_{aq}(N - O^-)$ is the molar concentration of the deprotonated form in the mobile phase. $c_{aq}(BN)^-$ is the molar concentration of the complexed form in the mobile phase. $c_{aq}(BN - O^-)^{2-}$ is the molar concentration of the complexed deprotonated form in the mobile phase. $k_N$ is the retention factor of protonated form. $k_{(N - O^-)}$ is the retention factor of deprotonated form. $k_{(BN)^-}$ is the retention factor of the complexed form. $k_{(BN - O^-)^{2-}}$ is the retention factor of the complexed deprotonated form.
3	$k = \frac{c_{aq}(BN)^-}{c_{aq}(BN)^- + c_{aq}(BN - O^-)^{2-}} k_{(BN)^-}$ $+ \frac{c_{aq}(BN - O^-)^{2-}}{c_{aq}(BN)^- + c_{aq}(BN - O^-)^{2-}} k_{(BN - O^-)^{2-}}$	
4	$Na_2B_4O_7 + 7H_2O \rightarrow 2H_3BO_3 + 2B(OH)_4^- + 2Na^+$	
5	$k = \text{const} \cdot c(C)^{-x/y}$	$x$ is the effective charge number of the analyte, $y$ is the effective charge number of the competing ion, $c(C)$ is the molar concentration of the competing ion.
6	$\lg k = \text{const} - \frac{x}{y} \lg [c(C)]$	

can be regarded to be pseudostationary ion-exchangers providing a fixed concentration of ion-exchange sites. In the present study, we investigate  $C_{14}MImBr$  and TTAB as positively charged micelle-forming surfactants for the MEKC separation of the negatively charged nucleosides.  $C_{14}MImBr$  has a CMC of  $2.5 \text{ mmol L}^{-1}$  in water at  $25^\circ\text{C}$  (calculated by conductometric measurements) [6,42]. This value is lower than the CMC of tetradecyltrimethylammonium bromide (CMC =  $3.6 \text{ mmol L}^{-1}$  in water at  $25^\circ\text{C}$ ) [43]. As described by Pino et al. [1], IL-type surfactants are capable of forming hemimicelles and admicelles when adsorbed onto a solid support. Hemimicelles are defined as a monolayer of surfactant formed on a solid support, whereas the positively charged head groups are attracted to the surface of opposite charge. On the other hand, admicelles form bilayer arrangements. In contrast to micelles, admicelles are formed below the CMC [44]. The process in which either hemimicelles or admicelles are formed is called dynamic coating of the capillary. As the capillary wall under these conditions is positively charged, dynamic coating reverses the direction of EOF.

As discussed before, the studied analytes are highly hydrophilic and therefore the contribution of hydrophobic interaction with the cationic micelles to the overall retention factors will be considered to be very small or even negligible. Consequently, following buffer parameters were taken into subsequent optimization studies: the surfactant concentration, the buffer concentration, the buffer pH and the buffer type. In addition, the sample matrix was selected to be pure water as we imitated the extraction procedure of nucleosides from urine using a phenylboronate-based affinity gel [18], i.e. dissolving the nucleoside standards in water mimics the presence of nucleosides in a urine sample extracted by phenylboronate affinity gel and dissolved in water after evaporating the extract to dryness. This assumption is based on the observation that electropherograms (in previously published papers [27,34]) recorded for nucleosides extracted with phenylboronate affinity gel contain only nucleosides without any interference from the matrix

due to the high selectivity of this extraction medium for cis-diol metabolites. In addition, we have not used phenylboronate affinity gel as the extraction by such a medium has been described extensively in the literature and in the present work, we have therefore focused on those factors affecting the separation and retention of nucleosides, which have to be taken into account during real sample applications. Only in those experiments, in which the calculation of the retention factors was needed, the sample matrix was composed of BGE/water/methanol (50:40:10, v/v/v) in order to solubilize decanophenone, the micelle marker. The temperature was maintained at  $35^\circ\text{C}$  because it allows a high EOF velocity and short migration times. In all runs the generated electric current strength was lower than  $40 \mu\text{A}$  (applied voltage  $-20 \text{ kV}$ ).

**3.3.2.2. Optimization of the surfactant concentration.** In order to optimize the separation employing either  $C_{14}MImBr$  or TTAB as a cationic surfactant, following starting conditions were selected:  $20 \text{ mmol L}^{-1}$  borate buffer with varied concentration of  $C_{14}MImBr$  or TTAB at pH 9.38. As shown in Fig. 3A and B, a plateau curve is obtained for each of the investigated nucleosides when plotting the pseudoeffective electrophoretic mobility  $\mu$  against  $c(C_{14}MImBr)$  or  $c(TTAB)$ . All  $\mu$  values are positive relative to  $\mu_{\text{eff}}$  measured in BGE without surfactant due to the interaction of the negatively charged analytes with the positively charged micelle. This plateau curve confirms that the main mode of interaction between the negatively charged nucleosides and the positively charged PSP is electrostatic interaction. These results are completely different from those reported in case of neutral analytes [35] or charged analytes with hydrophobic domain in which an increase in  $\mu$  with increasing PSP concentration is obtained.

A possible explanation for the results obtained in our case is that by increasing the concentration of  $C_{14}MImBr$  or TTAB, a subsequent increase in the concentration of the counter ion; bromide also occurs which competes with the nucleosides on the ion-exchange sites present on the pseudostationary ion exchangers (Fig. 2). It is

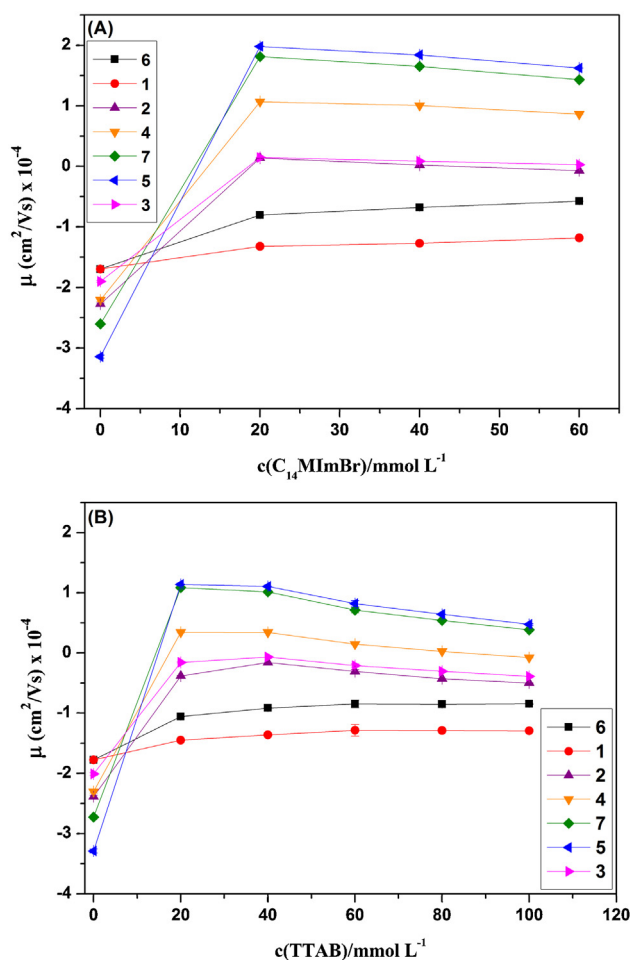


**Fig. 3.** Effect of concentration of (A)  $C_{14}MImBr$  or (B) TTAB in  $20\text{ mmol L}^{-1}$  borax, pH 9.38 on the pseudoeffective mobility. CE conditions: capillary 649(500) mm  $\times$  50  $\mu\text{m}$  I.D.; applied voltage  $-10\text{ kV}$ ; pressure injection 30 mbar for 12 s. Each data point is the average of at least three measurements, standard deviation represented as error bar. For assignment of symbols, see Fig. 1.

clear also from Fig. 3, that the resolution between different analytes is much better in the case of  $C_{14}MImBr$  as PSP than in the case of TTAB, which can be ascribed to the versatility of interaction sites provided by the imidazolium cation. Apart from hydrophobic interaction with the long alkyl tail, it was reported [14] that in addition to the electrostatic interaction exerted by the imidazolium cation, the imidazolium moiety can interact with polar compounds by ion-dipole interactions. Moreover hydrogen bonding is possible with the C-2 hydrogen of the imidazolium ring [14].

The reproducibility of migration times (Fig. 4A and B) was greatly improved when replacing TTAB with  $C_{14}MImBr$ . For all the investigated nucleosides, RSD of the retention times ranged from 0.915 to 1.429% in the case of TTAB and from 0.046% to 0.074% in the case of  $C_{14}MImBr$ . This improvement can be attributed to the micelle structure by which  $C_{14}MImBr$  dynamically coats the capillary. It was reported that the lower homologue  $C_{12}MImBr$  forms multilayer aggregates on the silica surface at a concentration equal to or above 3 times its CMC [45], whereas TTAB forms spherical micelle aggregates on the silica surface at concentration 2 times its CMC [46]. This micellar coating formed by TTAB creates a rather heterogeneous surface in which gaps between the micelle spheres are evident due to the electrostatic repulsion between adjacent micelles [47]. These irregularities may result in the observed non-reproducible EOF velocity.

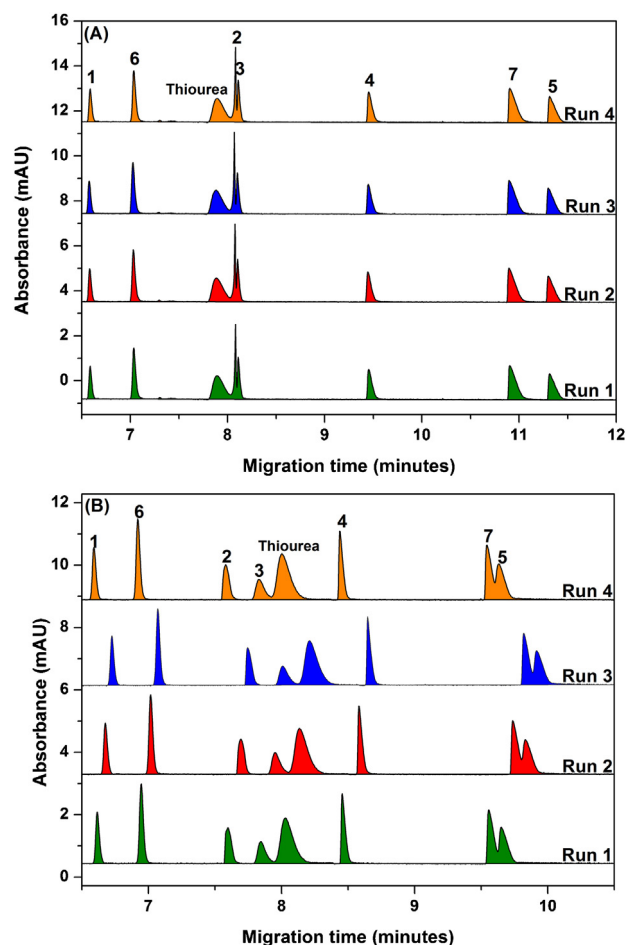


**Fig. 4.** Electropherograms obtained from a standard solution mixture of  $20\text{ mg L}^{-1}$  of each of the studied analytes and  $25\text{ mg L}^{-1}$  thiourea in water. CE conditions: (A)  $20\text{ mmol L}^{-1}$   $C_{14}MImBr$  in  $20\text{ mmol L}^{-1}$  sodium tetraborate, pH 9.38 as BGE (B)  $20\text{ mmol L}^{-1}$  TTAB in  $20\text{ mmol L}^{-1}$  sodium tetraborate, pH 9.38 as a BGE; capillary 649(500) mm  $\times$  50  $\mu\text{m}$  I.D.; applied voltage  $-10\text{ kV}$ ; pressure injection 30 mbar for 12 s. Peak designation: see Fig. 1.

**3.3.2.3. Effect of the buffer concentration.** In borate buffer, the borate ions compete with the bromide ions and with the negatively charged nucleosides (Fig. 2) with regard to the ion-exchange sites on the pseudostationary ion-exchanger. At a fixed concentration of  $C_{14}MImBr$  and accordingly at a fixed concentration of bromide, the retention factors of the nucleosides investigated are highly dependent on the concentration of the competing ion borate. From this observation we draw the conclusion that MEKC with  $C_{14}MImBr$  represents an analogy to ion-exchange chromatography (IEC) [48].

The retention factors were calculated according to Eq. S-2 (supplementary data). At each borate concentration, two experiments were performed subsequently. The first experiment was conducted in the CZE mode to calculate  $\mu_{\text{eff}}$  of each of the studied nucleosides at a given concentration of borax (for more details, see Table S2 and Fig. S7, supplementary data). The second one was conducted in the MEKC mode using  $20\text{ mmol L}^{-1}$   $C_{14}MImBr$  to calculate  $\mu$  and  $\mu_{\text{MC}}$  (the electrophoretic mobility of the micelles) under exactly the same conditions as the experiment performed in the CZE mode (Table S3 and Fig. S11, supplementary data).

In order to select a suitable micelle marker to calculate  $\mu_{\text{MC}}$ , the migration times of a homologues series of alkylphenones were studied. As illustrated in Fig. 5, decanophenone has exactly the same migration time as dodecanophenone. Accordingly, decanophenone and dodecanophenone are suitable micelle markers. The use of decanophenone reduces the problems

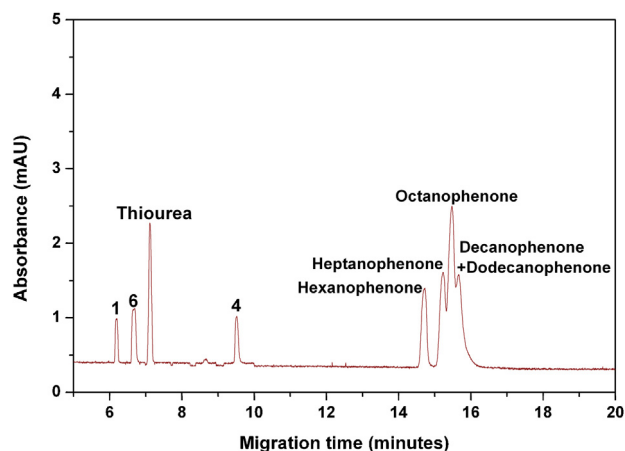


**Fig. 5.** Electropherogram obtained from a standard solution mixture of  $20 \text{ mg L}^{-1}$  of three of the investigated nucleosides and  $28 \text{ mg L}^{-1}$  of all phenones (except  $56 \text{ mg L}^{-1}$  in case of octanophenone) in BGE/water/methanol mixture (50:40:10, v/v/v). CE conditions:  $20 \text{ mmol L}^{-1}$   $\text{C}_{14}\text{MImBr}$  in  $10 \text{ mmol L}^{-1}$  sodium tetraborate, pH 9.38 as BGE; applied voltage  $-10 \text{ kV}$ ; pressure injection  $30 \text{ mbar}$  for  $12 \text{ s}$ . Peak designation: see Fig. 1.

associated with using dodecanophenone such as strong adsorption on the capillary wall and high methanolic content needed in the sample solution [48] (decanophenone needs only 10% methanol in the sample matrix (micellar BGE/water/methanol, 50:40:10, v/v/v) to be solubilized).

As shown in Fig. 6A, a complete separation of the studied analytes was achieved by using only  $20 \text{ mmol L}^{-1}$   $\text{C}_{14}\text{MImBr}$  in the presence of  $10 \text{ mmol L}^{-1}$  tetraborate, pH 9.38. Under these conditions, it is possible to separate Ado and Cyd, which are difficult to be separated in the CZE mode. The reproducibility of the migration times was excellent (Fig. 6B) with  $\text{RSD} \leq 0.270\%$ . In the following discussion, it should be taken into consideration that borax, when dissolved in water, hydrolyses to form a boric acid-borate ion solution as shown in Eq. 4 (Table 1). Therefore, at  $\text{pH} = \text{pK}_a$  of the weak acid, two molecules of boric acid remain unionized and the other two exist as borate ions, therefore we have multiplied the concentration of borax by the factor two to obtain the actual concentration of the competing ion borate. Plotting the retention factors for the analytes investigated against the concentration of the competing ion borate reveals that the retention factors are substantially decreased (Fig. 7A) with increasing borate concentration. The decrease in the retention factor is non-linear and the obtained curves converge to a limiting value. This decrease in retention factors is reflected by a decrease in relative migration times (migration time of analyte/migration time of EOF marker) (see electropherograms shown in Fig. S11, supplementary data). Fig. S12 (supplementary data) shows that for Ado and Cyd  $\mu$  is still negative because these compounds have only one negative charge, which is acquired by borate complexation, which explains their weak interaction with the  $\text{C}_{14}\text{MImBr}$  micelles. In contrast, Xao has an effective charge number of  $-2$  due to deprotonation in addition to the charge gained by borate complexation. Therefore,  $\mu$  is positive corresponding to the higher retention factor.

It is now interesting to see that at high borate concentration Xao comigrates with Ino, which is in agreement with our hypothesis that the retention of the nucleoside borate complexes on the oppositely charged micelles can be modelled as ion-exchange interaction. As we will show below, the extent to which the retention factor is influenced by the competing ion concentration is dependent on the charge of the solute. It is also noticeable that the migration order for Urd and 5MeUrd is reversed so that 5MeUrd elutes after to Urd at  $c(\text{tetraborate}) > 20 \text{ mmol L}^{-1}$ .

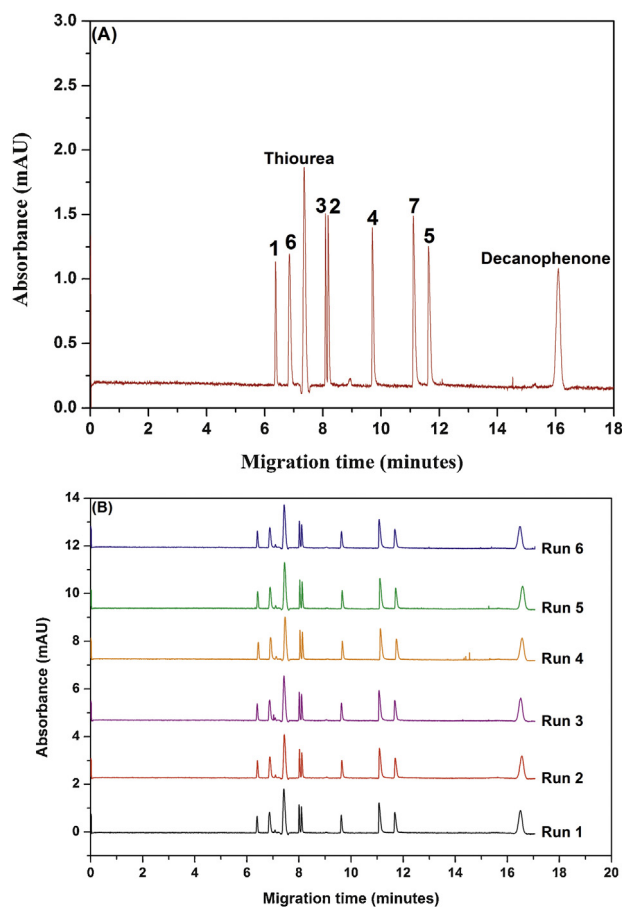


**Fig. 6.** (A) Electropherogram obtained from a standard solution mixture of  $20 \text{ mg L}^{-1}$  of each of the studied nucleosides,  $25 \text{ mg L}^{-1}$  thiourea and  $30 \text{ mg L}^{-1}$  decanophenone in BGE/water/methanol mixture (50:40:10, v/v/v). CE conditions:  $20 \text{ mmol L}^{-1}$   $\text{C}_{14}\text{MImBr}$  in  $10 \text{ mmol L}^{-1}$  sodium tetraborate, pH 9.38 as BGE; applied voltage  $-10 \text{ kV}$ ; pressure injection  $30 \text{ mbar}$  for  $12 \text{ s}$ . Peak designation: see Fig. 1. (B) Electropherograms showing six reproducible runs from the same experiment.

It is noteworthy to mention that the resolution between 5MeUrd and Urd equals 1.52 (Fig. S11E, supplementary data) when using  $10 \text{ mmol L}^{-1}$  tetraborate in the BGE. This value can be improved by lowering the tetraborate concentration. A resolution equal to 2.96 between 5MeUrd and Urd was achieved when using  $5 \text{ mmol L}^{-1}$  tetraborate (Fig. S11F, supplementary data). It can be concluded that the retention factors and accordingly the resolution between nucleosides can be easily regulated by suitable adjustment of the buffer ion concentration. A suitable buffer composition is  $20 \text{ mmol L}^{-1}$   $\text{C}_{14}\text{MImBr}$  in  $5 \text{ mmol L}^{-1}$  borate buffer, pH 9.38. Under these conditions and by using an applied voltage of  $-20 \text{ kV}$ , the generated current was only  $-9.9 \mu\text{A}$ .

According to the obtained results, we can deduce that the concentration of borate has a dramatic effect on the retention factors of nucleosides in a manner exactly corresponding to what is typically observed in ion-exchange chromatography (IEC). In analogy to IEC, from the simple stoichiometric model of retention (in which the exchange process is described by the mass action law) simplified equations can be deduced (Eqs. (5) and (6), Table 1) for low analyte concentration under conditions in which only the concentration of the competing ion is varied [48]. A linear decrease of  $\lg k$  with increasing competing ion concentration is expected when plotting  $\lg k$  against  $\lg[c(\text{C})]$  with a slope of the regression line corresponding to  $-x/y$ . In order to evaluate the validity of Eq. (6),  $\lg(k)$  was plotted against  $\lg(c(\text{borate}))$  (Fig. 7B). There is a clear deviation from linearity, which can be ascribed to the presence of a second

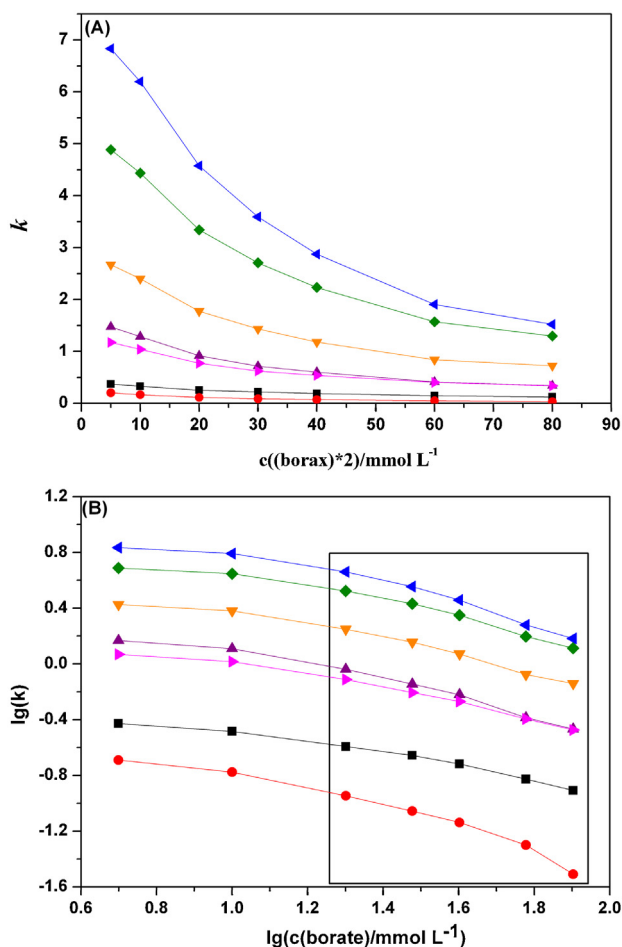


**Fig. 7.** (A) Retention factors dependent on the concentration of borate in the BGE ( $c(\text{C}_{14}\text{MImBr}) = 20 \text{ mmol L}^{-1}$ , pH 9.38). (B) Double logarithmic plot of retention factors dependent on the concentration of borate in the BGE ( $c(\text{C}_{14}\text{MImBr}) = 20 \text{ mmol L}^{-1}$ , pH 9.38); the area marked with the black-lined box illustrates the range of  $\lg(c(\text{borate}))$  used to construct the regression lines (Table 2). For assignment of symbols, see Fig. 3.

competing ion, the bromide ion, which is responsible for decreased values of  $\lg(k)$  at low borate concentration. Due to the influence of this second competing ion, a transition of the regression line from a constant plateau value (at low  $c(\text{borate})$ ) to a region of linear decrease (at high  $c(\text{borate})$ ) can be expected. This observation is in accordance with previously reported results [48]. Therefore, only for  $c(\text{borate}) \geq 20 \text{ mmol L}^{-1}$ , the correlation coefficient  $r$  and the slope of the regression line (plotting  $\lg k$  against  $\lg(c(\text{borate}))$ ) were calculated (Table 2). As shown in Fig. 7B, a linear plot ( $r$  ranged from 0.9929 in the case of Add to 0.9975 in the case of 5MeUrd) with a negative slope is obtained. For Cyd no linear range was reached which might be due to the imprecision of the determination of the retention factor for solutes with very low retention factor. A comparison of the calculated slope with these values expected from effective charge numbers shows that the stoichiometric model does not quantitatively fully describe the retention behaviour observed. The determined values only reflect the trend which would be expected from a comparison of  $\text{p}K_a$  values. As expected the slope is higher for Urd than for 5MeUrd. The higher is the expected effective charge number of the solute, the higher is the determined slope. This retention behaviour is expected if retention is only due to Coulomb interactions (which might be assisted by another type of interaction taking place simultaneously e.g. by hydrophobic forces) and independent hydrophobic or other

**Table 2**

Correlation coefficients and regression line slopes ( $\lg k$  against  $\lg(c(\text{borate}) / \text{mmol L}^{-1})$ ) for the investigated nucleosides.

Nucleoside	$r$ (correlation coefficient)	Slope of the regression line ( $-x/y$ ) <sup>a</sup>
Ado	0.9929	-0.53
Urd	0.9960	-0.73
5MeUrd	0.9976	-0.61
Guo	0.9963	-0.67
Ino	0.9955	-0.70
Xao	0.9952	-0.82

<sup>a</sup>  $x$  is the effective charge of the analyte,  $y$  is the effective charge of the competing ion.

interactions (e.g. coordinative interaction with the neutral solute) can be neglected [49].

To further confirm our hypothesis that exclusively Coulomb interactions (possibly hydrophobically assisted) are responsible for the observed retention,  $k$  was plotted against  $c(\text{borate})^{-x/y}$  (values of  $-x/y$  taken from Table 2). Here the slope is dependent on the volume ratio of the two phases involved, on the ion-exchange equilibrium constant, on the ion-exchange capacity of the pseudostationary phase and on the retention due to hydrophobic assistance [48–50]. This plot can be used to analyze retention data (in which ion-exchange is involved) for a second independent retention mechanism. At a competing ion concentration raised to the power  $-x/y$  extrapolated to zero, Coulomb interactions can be expected to be effectively suppressed. Therefore, the intercept of such a plot must be zero if exclusively (or hydrophobically assisted) Coulomb interactions are responsible for the observed retention. If  $k$  is the sum of two independent processes ( $k = k_1 + k_2$ ) this plot will have a significant  $y$ -axis intercept [49]. In addition, in the second case a large slope relative to the intercept indicates that ion-exchange interactions predominate over other types of interaction.

When plotting  $k$  against  $c(\text{borate})^{-x/y}$  (see Fig. 8) straight lines with positive slopes are obtained. The intercepts of this plot are very close to zero for all investigated nucleosides. Regarding the statistical significance of the  $y$ -axis intercept, we applied t-test. The  $t$ -values were calculated and the highest calculated  $t$  was found to be 0.91 at  $\text{df} = 3$ , which is smaller than the tabulated  $t$  value (3.18 at  $\text{df} = 3$  and  $P = 0.05$ ). We can conclude that at the specified significance level, the intercepts are not significantly different from zero. This result is in accord with the assumption that the retention of the charged nucleosides on a cationic PSP can be modelled

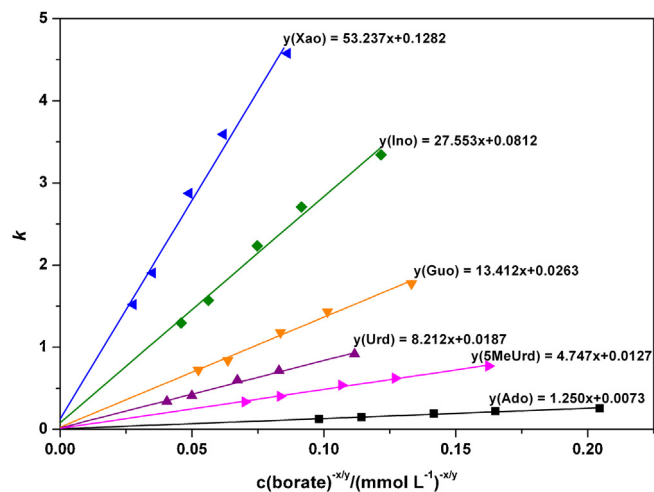


**Fig. 8.**  $k$  vs.  $[\text{borate}]^{-x/y}$  for the tested nucleosides. For analyte abbreviations refer to the experimental part.

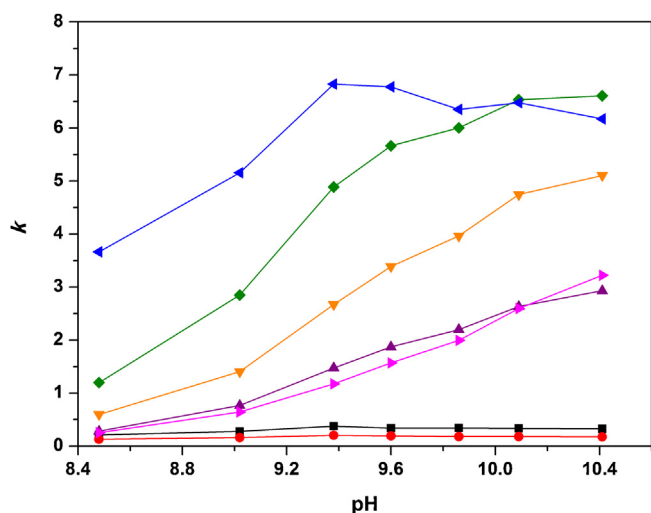


**Fig. 9.** Retention factors dependent on the pH of the BGE ( $c(\text{C}_{14}\text{MImBr}) = 20 \text{ mmol L}^{-1}$  in  $2.5 \text{ mmol L}^{-1}$  sodium tetraborate). For assignment of symbols, see Fig. 3.

by the retention of anions on a pseudostationary anion-exchanger, which additionally confirms the validity of Eq. (3), i.e. interaction of the PSP with the neutral uncomplexed form of the solute can be neglected. Electrostatic interactions have to be considered to be the dominant mode of interaction. The observed variation in selectivity (variation in migration order) with increasing borate concentration can be fully understood on the basis on the classical IEC theory.

**3.3.2.4. Effect of the buffer pH.** The retention factors of the nucleosides investigated are strongly dependent on the pH of the BGE within the range of 8.49–10.41 (Fig. 9). In this study  $c(\text{C}_{14}\text{MImBr})$  was fixed at  $20 \text{ mmol L}^{-1}$  and  $c(\text{borax})$  at  $2.5 \text{ mmol L}^{-1}$ . This concentration of borax was selected to reach the highest possible retention factors. At each pH value, two experiments were done subsequently. The first experiment was performed in the CZE mode to calculate  $\mu_{\text{eff}}$  of each of the studied nucleosides at a given pH value (for more details see Table S4, Figs. S6B and S13, supplementary data) and the second one was conducted in the MEKC mode using  $20 \text{ mmol L}^{-1}$   $\text{C}_{14}\text{MImBr}$  to calculate  $\mu$  under exactly the same conditions as the experiment in the CZE mode (Table S5, Figs. S14 and S15, supplementary data). As illustrated in Fig. S13 (supplementary data), in the CZE mode there is insufficient resolution for the analytes investigated within the pH range studied. Fig. S14 (supplementary data) shows that in the MEKC mode at  $\text{pH} \geq 9.38$ , the relative migration times of the nucleosides (except for Ado, Cyd and Xao) are increased by increasing the pH of the BGE due to the induced increase in the effective charge number. The migration order was changed by variation of the pH in the case of Urd, 5MeUrd and Ino, Xao. This change in migration order can be attributed to differences in the  $\text{pK}_a$  values of the formed borate complexes. Fig. S15 (supplementary data) illustrates that the electrophoretic mobility of the micelles is independent of the pH of the BGE. Adequate resolution between all studied analytes was achieved at pH 9.38 (Fig. S11G, supplementary data). Therefore, the optimum pH value was selected to be pH 9.38. Under these conditions Ado coelutes with thiourea. As illustrated in Fig. S11F (supplementary data), a complete separation between Ado and thiourea can be obtained using  $20 \text{ mmol L}^{-1}$   $\text{C}_{14}\text{MImBr}$  in  $5 \text{ mmol L}^{-1}$  tetraborate, therefore this BGE composition was finally selected as optimum.

**Table 3**

Retention factors in presence and absence of borax.<sup>a</sup>

Analyte	$k$ ( $10 \text{ mmol L}^{-1}$ borax)	$k$ ( $10 \text{ mmol L}^{-1}$ carbonate buffer)
Ado	0.26	0.00
Cyd	0.11	0.00
Urd	0.92	0.14
Guo	1.78	0.35
Ino	3.34	0.58
Xao	4.58	0.64
5MeUrd	0.77	0.13

<sup>a</sup> For experimental details see Figs. 6A and S16 (supplementary data).

**3.3.2.5. Effect of the buffer type.** In order to highlight the importance of borate complexation in adjusting the interaction between the nucleosides and the positively charged PSP, a BGE composed of  $20 \text{ mmol L}^{-1}$   $\text{C}_{14}\text{MImBr}$  in  $10 \text{ mmol L}^{-1}$  carbonate buffer, pH 9.38 was also tested for the separation of the investigated nucleosides. Under these conditions and in the absence of borate, Ado and Cyd are neutral. Therefore, they cannot be separated using this BGE and they are coeluted with thiourea (Fig. S16, supplementary data). In addition, Urd, 5MeUrd, Guo and Ino which have a degree of dissociation lower than one migrate very close to/with the EOF marker. Xao, which has an effective charge number of  $-1$ , comigrates with Guo. We calculated the retention factors of the investigated compounds by performing a CZE experiment using  $10 \text{ mmol L}^{-1}$  carbonate buffer, pH 9.38 as BGE. Then a subsequent MEKC experiment using  $20 \text{ mmol L}^{-1}$   $\text{C}_{14}\text{MImBr}$  in  $10 \text{ mmol L}^{-1}$  carbonate buffer, pH 9.38 as BGE (decanophenone was used as a micelle marker) (Fig. S16, supplementary data) was carried out. As expected, the retention factors in borate buffer are higher than those in carbonate buffer (Table 3) in accord with the increase in effective charge number due to complexation with borate. This result further confirms our hypothesis that the retention of the charged hydrophilic nucleosides by oppositely charged IL-type surfactant micelles can be modelled as retention of charged solutes by a pseudostationary ion-exchanger. Borate complexation and the negative charge gained due to such a complex plays a significant role in enhancing the interaction between the nucleosides and the positively charged micelles. In addition, we can conclude that neither CZE using borate buffer nor MEKC using  $\text{C}_{14}\text{MImBr}$  in carbonate buffer enable the separation of all studied nucleosides within the parameter range studied. Only a combination of borate complexation and interaction with the  $\text{C}_{14}\text{MImBr}$  micelles is successful for the separation of the investigated analytes.

### 3.3.3. Selectivity of the developed MEKC method compared to that exhibited by HILIC

The employment of  $\text{C}_{14}\text{MImBr}$  in combination with borate in the separation buffer can be used for the selective separation of nucleosides from nucleobases and uric acid. Fig. 10 shows the electropherogram of a sample solution containing nucleosides, nucleobases and uric acid. There is a comigration for thiourea and Cyt and for Thy and Xan. For Ado and Ura and for 5MeUrd and Uric acid, there is no baseline separation. All other nucleosides are baseline separated.

The separation of the very similar nucleosides and nucleobases is possible because of the combination of borate complexation and the use of  $\text{C}_{14}\text{MImBr}$  as a PSP. As mentioned in Section 3.3.2.3, the higher is the negative charge of the analyte, the stronger is the electrostatic interaction with the positively charged  $\text{C}_{14}\text{MImBr}$  micelles, which results in longer migration times. In contrast to the nucleobases, nucleosides acquire an additional negative charge by complexation with borate because of their cis-diol groups. The nucleobases possess their negative charge only due to the dissociation of the amidic group, therefore they show a much weaker



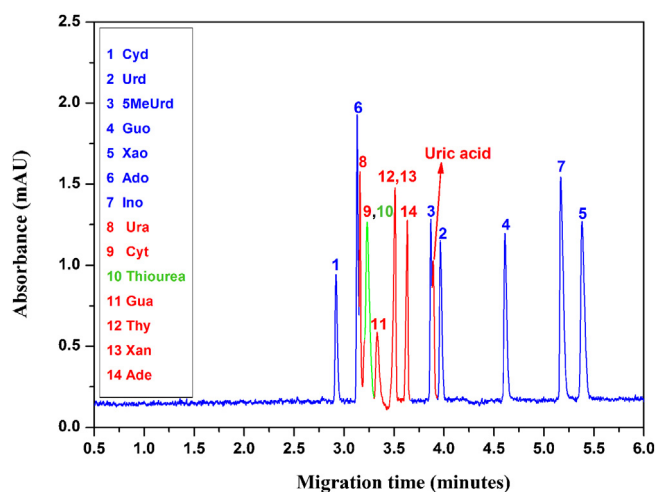


**Fig. 10.** Electropherogram obtained from a standard solution mixture of 20 mg L<sup>-1</sup> of each of the studied nucleosides, 10 mg L<sup>-1</sup> of Cyt, Gua, Thy, Ura, Ade, 7.2 mg L<sup>-1</sup> of Xan, 13.3 mg L<sup>-1</sup> of uric acid and 25 mg L<sup>-1</sup> thiourea in water. CE conditions: 20 mmol L<sup>-1</sup> C<sub>14</sub>MImBr in 5 mmol L<sup>-1</sup> sodium tetraborate, pH 9.38 as BGE; capillary 647(502) mm × 50 μm I.D.; applied voltage -20 kV; current -9.9 μA; pressure injection 30 mbar for 12 s. For analyte abbreviations refer to the experimental part.

interaction with the positively charged micelles and elute earlier (Fig. 10). On the other hand, uric acid elutes later relative to the nucleobases because uric acid, a product of the metabolic breakdown of purine nucleotides, is a diprotic acid ( $pK_a = 5.4, 10.3$ ) [51]. Therefore, under the experimental conditions employed (Fig. 10), it has an effective charge number higher than -1. Those nucleosides having an effective charge number between -1 and -2 (Urd, 5MeUrd, Guo, Ino and Xao) are eluted after the nucleobases, whereas Cyt and Ado having an effective charge number of -1 have migration times within those of the nucleobases.

Due to their highly hydrophilic nature, nucleosides were the target analytes of many articles that investigate HILIC for their separation [23]. The primary retention mechanism of HILIC stationary phases is to bind water on their surfaces. The retention of the analytes can be ascribed due to the partition of the solute between the organic and the aqueous phase or due to the adsorption of the analyte on the stationary phase. Secondary interactions (dipole-dipole and ionic attractive/repulsive forces between the solute and the stationary phase active groups) are also possible for retention by HILIC [23], therefore most HILIC mobile phases are prepared including a significant concentration of a salt to suppress these secondary interactions [23]. Compared to our developed MEKC strategy, HILIC provides a completely different selectivity. Based on this retention mechanism, it is expected that nucleobases that are less hydrophilic than the corresponding nucleosides ( $\lg P_{ow}$  values are -0.71, -2.29, -0.12, -0.09, -0.91 for Ura, Cyt, Thy, Ade, and Gua; respectively [23]) will elute earlier than the nucleosides. A closer inspection of the chromatogram shown in Ref. [23] illustrates that for every nucleobase/nucleoside pair, the nucleobase elutes before its corresponding nucleoside. In our developed method, Cyt and Ado migrate before Cyt and Ade because of the weak interaction with the PSP and the interplay of separation by differences in the electrophoretic mobility and by differences in the retention factor. Cyt is neutral at pH 9.38 and comigrates with the EOF marker. Ade with  $pK_a = 9.8$ , has a charge number  $< -1$ . Urd, Guo and Xao migrate after Ura, Gua and Xan as they have negative effective charge numbers higher than the corresponding nucleobases due to dissociation and complexation. With the exception of Ado and Cyt, there is a group separation of the nucleosides from the corresponding nucleobases. This group separation is not given in the presented HILIC method. Adding to this, the run time using HILIC is relatively long

(>50 min) [23] if compared to our developed MEKC method (total run time <6 min) (Fig. 10). Moreover, peak efficiencies are much better using MEKC with C<sub>14</sub>MImBr micelles. Although separation by HILIC might be seen as the state of art for the determination of the highly hydrophilic nucleosides, our new MEKC strategy provides a faster, more efficient, highly reproducible and highly selective method for the analysis of these hydrophilic metabolites.

#### 4. Conclusions

The separation of seven urinary nucleosides can be successfully achieved using 20 mmol L<sup>-1</sup> C<sub>14</sub>MImBr in 5 mmol L<sup>-1</sup> borate buffer. C<sub>14</sub>MImBr can be regarded as a pseudostationary ion-exchanger, which interacts with the analytes predominantly by electrostatic interaction. Retention factors of the analytes can be regulated by proper adjustment of the concentration of the competing buffer ion or the pH of the BGE. The employment of an IL-type surfactant as cationic pseudostationary phase has the advantage of improved repeatability over the use of an alkytrimethyl ammonium bromide as PSP. MEKC using an IL-type surfactant can provide a potential alternative to HILIC in the analysis of highly hydrophilic urinary nucleosides.

#### Acknowledgments

A.H. Rageh thanks the Egyptian ministry of higher education and state for scientific research and the Deutscher Akademischer Austauschdienst (DAAD) for funding her PhD scholarship through German Egyptian Research Long-Term Scholarship program (GERLS). We also thank M. Abdelmegeed and A. Kaltz for doing some of the experimental work. We thank the workshops of the Department of Chemistry for the development of the data recording unit.

#### Appendix A. Supplementary data

Supplementary data associated with this article can be found, in the online version, at <http://dx.doi.org/10.1016/j.chroma.2013.09.079>.

#### References

- [1] V. Pino, M. German-Hernandez, A. Martin-Perez, J.L. Anderson, *Sep. Sci. Technol.* 47 (2012) 264.
- [2] A. Berthod, M.J. Ruiz-Angel, S. Carda-Broch, *J. Chromatogr. A* 1184 (2008) 6.
- [3] M. Lopez-Pastor, B.M. Simonet, B. Lendl, M. Valcarcel, *Electrophoresis* 29 (2008) 94.
- [4] P. Sun, D.W. Armstrong, *Anal. Chim. Acta* 661 (2010) 1.
- [5] B. Dong, X. Zhao, L. Zheng, J. Zhang, N. Li, T. Inoue, *Colloids Surf. A* 317 (2008) 666.
- [6] R. Vanyur, L. Biczok, Z. Miskolczy, *Colloids Surf. A* 299 (2007) 256.
- [7] P.L. Laamanen, S. Busi, M. Lahtinen, R. Matilainen, *J. Chromatogr. A* 1095 (2005) 164.
- [8] M.E. Yue, Y.P. Shi, *J. Sep. Sci.* 29 (2006) 272.
- [9] K. Tian, Y. Wang, Y. Chen, X. Chen, Z. Hu, *Talanta* 72 (2007) 587.
- [10] T.F. Jiang, Y.L. Gu, B. Liang, J.B. Li, Y.P. Shi, Q.Y. Ou, *Anal. Chim. Acta* 479 (2003) 249.
- [11] H.L. Su, M.T. Lan, Y.Z. Hsieh, *J. Chromatogr. A* 1216 (2009) 5313.
- [12] J. Niu, H. Qiu, J. Li, X. Liu, S. Jiang, *Chromatographia* 69 (2009) 1093.
- [13] M. Borissova, K. Palk, M. Koel, *J. Chromatogr. A* 1183 (2008) 192.
- [14] H. Qiu, A.K. Mallik, M. Takafuji, X. Liu, S. Jiang, H. Ihara, *Anal. Chim. Acta* 738 (2012) 95.
- [15] M.J. Markuszewski, W. Struck, M. Waszczuk-Jankowska, R. Kalisz, *Electrophoresis* 31 (2010) 2300.
- [16] W. Struck, M. Waszczuk-Jankowska, R. Kalisz, M.J. Markuszewski, *Anal. Bioanal. Chem.* 401 (2011) 2039.
- [17] E. Szymanska, M.J. Markuszewski, K. Bodzioch, R. Kalisz, *J. Pharm. Biomed. Anal.* 44 (2007) 1118.
- [18] G. Xu, H.M. Liebich, R. Lehmann, S. Muller-Hagedorn, *Methods Mol. Biol.* 162 (2001) 459.
- [19] C.W. Gehrke, K.C. Kuo, G.E. Davis, R.D. Suits, T.P. Waalkes, E. Borek, *J. Chromatogr.* 150 (1978) 455.
- [20] S.H. Cho, M.H. Choi, W.Y. Lee, B.C. Chung, *Clin. Biochem.* 42 (2009) 540.

- [21] H.M. Liebich, S. Mueller-Hagedorn, F. Klaus, K. Meziane, K.R. Kim, A. Fricken-schmidt, B. Kammerer, J. Chromatogr. A 1071 (2005) 271.
- [22] B. Feng, M. Zheng, Y. Zheng, A. Lu, J. Li, M. Wang, J. Ma, G. Xu, B. Liu, Z. Zhu, J. Gastroenterol. Hepatol. 20 (2005) 1913.
- [23] G. Marrubini, B.E.C. Mendoza, G. Massolini, J. Sep. Sci. 33 (2010) 803.
- [24] Y. Guo, S. Gaiki, J. Chromatogr. A 1074 (2005) 71.
- [25] E. Rodriguez-Gonzalo, D. Garcia-Gomez, R. Carabias-Martinez, J. Chromatogr. A 1218 (2011) 9055.
- [26] A.J. Sasco, F. Rey, C. Reynaud, J.Y. Bobin, M. Clavel, A. Niveleau, Cancer Lett. 108 (1996) 157.
- [27] S. Wang, X. Zhao, Y. Mao, Y. Cheng, J. Chromatogr. A 1147 (2007) 254.
- [28] T. Helboe, S.H. Hansen, J. Chromatogr. A 836 (1999) 315.
- [29] M. Zhang, Z. El-Rassi, Electrophoresis 20 (1999) 31.
- [30] H.M. Liebich, R. Lehmann, G. Xu, H.G. Wahl, H.U. Haring, J. Chromatogr. B: Biomed. Sci. Appl. 745 (2000) 189.
- [31] Y.F. Zheng, H.W. Kong, J.H. Xiong, L. Shen, G.W. Xu, Clin. Biochem. 38 (2005) 24.
- [32] Y.F. Zheng, G.W. Xu, D.Y. Liu, J.H. Xiong, P.D. Zhang, C. Zhang, Q. Yang, L. Shen, Electrophoresis 23 (2002) 4104.
- [33] A.S. Cohen, S. Terabe, J.A. Smith, B.L. Karger, Anal. Chem. 59 (1987) 1021.
- [34] Y. Jiang, Y. Ma, Anal. Chem. 81 (2009) 6474.
- [35] P.G. Muijselaar, H.B. Verhelst, H.A. Claessens, C.A. Cramers, J. Chromatogr. A 764 (1997) 323.
- [36] M.L. Riekkola, J.A. Joensson, R.M. Smith, Pure Appl. Chem. 76 (2004) 443.
- [37] IUPAC-IUB Commission on Biochemical Nomenclature (CBN), Pure Appl. Chem. 40 (1974) 277.
- [38] G.M. Blackburn, M.J. Gait, D.M. Williams (Eds.), Nucleic Acids in Chemistry and Biology, 3rd ed., Royal Society of Chemistry, Cambridge, 2006, p. 16.
- [39] J. Mendham, R.C. Denney, J.D. Barnes, M.J.K. Thomas (Eds.), Vogel's Textbook of Quantitative Chemical Analysis, 6th ed., Prentice Hall, NY, 2000, p. 357.
- [40] S. La, J. Cho, J.H. Kim, K.R. Kim, Anal. Chim. Acta 486 (2003) 171.
- [41] M.R. Monton, K. Otsuka, S. Terabe, J. Chromatogr. A 985 (2003) 435.
- [42] A. Cornellas, L. Perez, F. Comelles, I. Ribosa, A. Manresa, M.T. Garcia, J. Colloid Interface Sci. 355 (2011) 164.
- [43] M.J. Rosen (Ed.), Surfactants and Interfacial Phenomena, 3rd ed., John Wiley & Sons, Inc., NJ, 2004, p. 128.
- [44] S. Gangula, S.Y. Suen, E.D. Conte, Microchem. J. 95 (2010) 2.
- [45] M. Ao, G. Xu, J. Pang, T. Zhao, Langmuir 25 (2009) 9721.
- [46] S. Manne, H.E. Gaub, Science 270 (1995) 1480.
- [47] J.E. Melanson, N.E. Baryla, C.A. Lucy, TrAC, Trends Anal. Chem. 20 (2001) 365.
- [48] I. Orentaite, A. Maruska, U. Pyell, Electrophoresis 32 (2011) 604.
- [49] X. Yang, J. Dai, P.W. Carr, J. Chromatogr. A 996 (2003) 13.
- [50] F. Al-Rimawi, U. Pyell, J. Chromatogr. A 1160 (2007) 326.
- [51] R.L. Lundblad, F. MacDonald (Eds.), Handbook of Biochemistry and Molecular Biology, 4th ed., CRC Press, Taylor and Francis Group, LLC, Boca Raton, 2010.

## **Imidazolium-based ionic liquid-type surfactant as pseudostationary phase in micellar electrokinetic chromatography of highly hydrophilic urinary nucleosides**

Azza H. Rageh, Ute Pyell\*

University of Marburg, Department of Chemistry, Hans-Meerwein-Straße, D-35032 Marburg, Germany

\* corresponding author

### **Supplementary data**

- Chemical structures,  $pK_a$  and  $\lg P_{ow}$  values of the investigated nucleosides.
- Synthesis and Characterization of  $C_{14}MImBr$ .
- Effect of tetraborate concentration on the migration times and on the effective electrophoretic mobility of the studied nucleosides in the CZE mode.
- MEKC separation of the studied nucleosides as neutral compounds using SDS as a pseudostationary phase.
- Calculation of the retention factors of the nucleosides (as charged complexed compounds) under variation of buffer ion concentration or buffer pH using  $C_{14}MImBr$  as a PSP.
- Electropherograms illustrating the separation of nucleosides under variation of borate buffer concentration or pH in either CZE mode or MEKC mode.
- Figures illustrating the effect of borax concentration or pH on the pseudoeffective electrophoretic mobility.
- Carbonate buffer instead of borate buffer in MEKC separation of the nucleosides using  $C_{14}MImBr$  as a PSP.

S-2

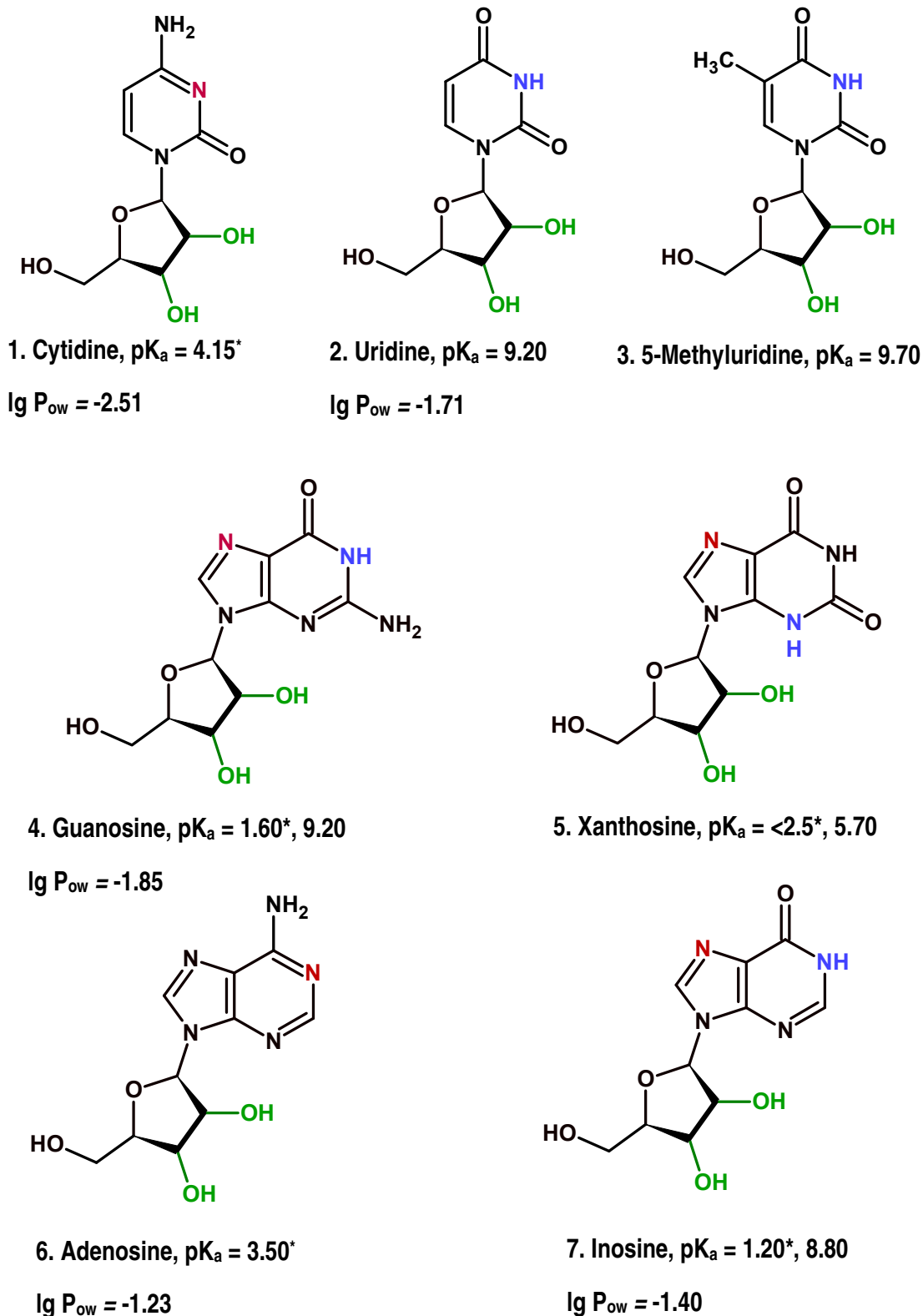


**Figure S1:** Structural formulas,  $pK_a$  [1] and  $\lg P_{ow}$  [2] of the investigated nucleosides. \* Values of  $pK_a$  are those of the cationic protonated conjugate acid form. Red and blue colours are used to mark the protonation and dissociation sites, respectively.  $pK_a$  values of cis-diol moieties (marked with the green colour) are  $\sim 12.5$  [1].

**Synthesis of 1-tetradecyl-3-methylimidazolium bromide (C<sub>14</sub>MImBr)**

C<sub>14</sub>MImBr was synthesised according to the procedure reported by Vanyur et al. [3] with slight modifications. In a three-necked round-bottomed flask fitted with a reflux condenser 1-methylimidazole (0.05 mol) was dissolved in toluene (30 mL) and then a slight excess of 1-bromotetradecane (0.06 mol) was used to assure complete consumption of 1-methylimidazole. 1-Bromotetradecane was added dropwise to the reaction mixture while stirring (using a magnetic stirrer). Afterwards the reaction mixture was stirred and heated at 80°C for 24 h. The resulting viscous liquid was allowed to cool to room temperature, then the formed white crystalline salt was filtered off and washed six times with 300 mL portions of ethyl acetate (previously dried for 2 days over sodium sulphate and filtered). The white powder obtained was dried in a vacuum desiccator (over phosphorous pentoxide) for 3 days prior to use. The synthesized C<sub>14</sub>MImBr was characterized using <sup>1</sup>H NMR and <sup>13</sup>C NMR spectroscopy, IR spectroscopy, determination of the melting point and elemental analysis. The chemical structure is shown in Fig. S2. The obtained data (Table S1, Figs. S3-S5) are in excellent agreement with those found in the literature [4-9].

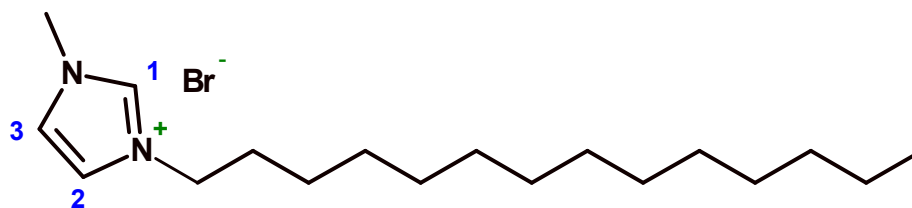


**Figure S2:** Structural formula of 1-tetradecyl-3-methylimidazolium bromide (C<sub>14</sub>MImBr)

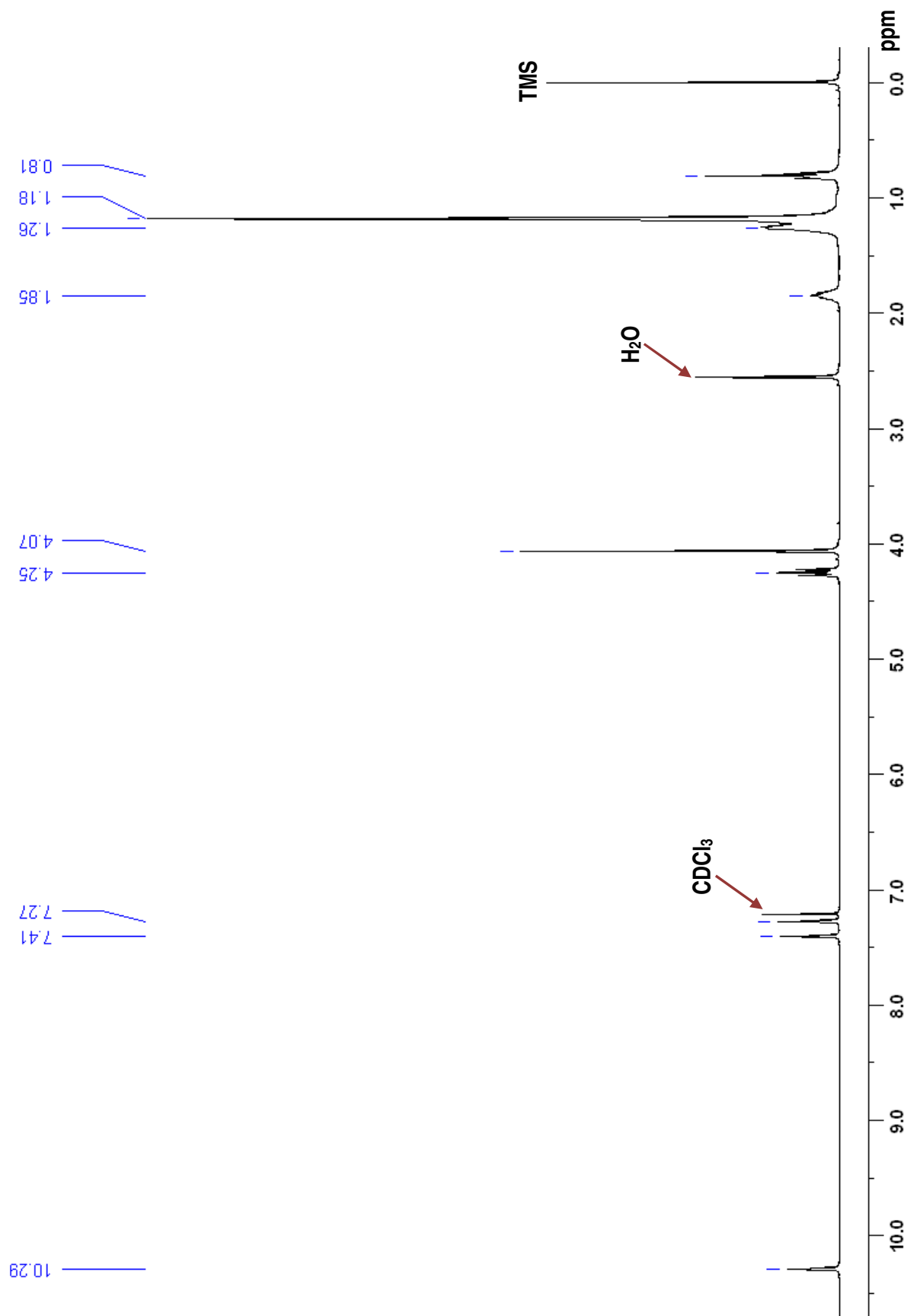
**Table S1.** Characterization of the synthesised C<sub>14</sub>MImBr [C<sub>18</sub>H<sub>35</sub>BrN<sub>2</sub>·H<sub>2</sub>O (377.4 g/mol)]

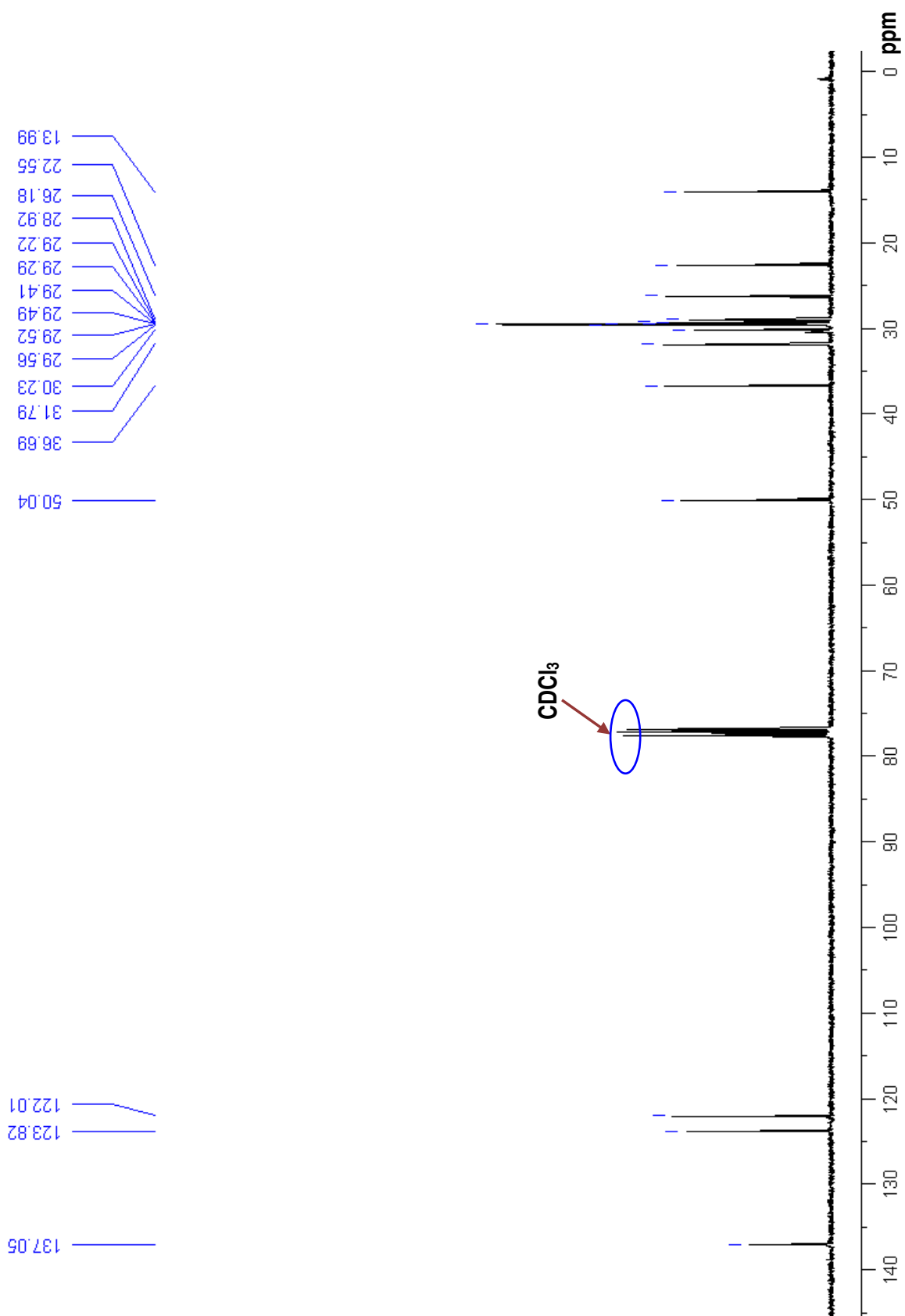
Tool of characterization	Peak interpretation/results
<sup>1</sup> H-NMR (300 K, 300 MHz, CDCl <sub>3</sub> ) δ/ppm See Fig. S2	0.84 (3H, t, <i>J</i> = 6.60 Hz, CH <sub>3</sub> ), 1.18-1.26 (22H, m, CH <sub>2</sub> ), 1.88 (2H, qi, <i>J</i> = 7.20 Hz, NCH <sub>2</sub> CH <sub>2</sub> ), 4.07 (3H, s, NCH <sub>3</sub> ), 4.25 (2H, t, <i>J</i> = 7.50, NCH <sub>2</sub> ), 7.28 (1H, t <sup>a</sup> , <i>J</i> = 1.50 Hz, C(2)H), 7.41 (1H t <sup>a</sup> , <i>J</i> = 1.50 Hz, C(3)H), 10.29 (1H, bs, C(1)H). s: singlet, bs: broad singlet, t: triplet, qi: quintet and m: multiplet.
<sup>13</sup> C-NMR (300 K, 75.4 MHz, CDCl <sub>3</sub> ) δ/ppm See Fig. S3	13.99 (CH <sub>3</sub> ), 22.55 (CH <sub>2</sub> ), 26.18 (CH <sub>2</sub> ), 28.92 (CH <sub>2</sub> ), 29.22 (CH <sub>2</sub> ), 29.29 (CH <sub>2</sub> ), 29.41 (CH <sub>2</sub> ), 29.49 (CH <sub>2</sub> ), 29.52 (2 x CH <sub>2</sub> ), 29.56 (CH <sub>2</sub> ), 30.23 (CH <sub>2</sub> ), 31.79 (CH <sub>2</sub> ), 36.69 (NCH <sub>3</sub> ), 50.04 (NCH <sub>2</sub> ), 122.01 (C2), 123.82 (C3), 137.05 (C1)
MIR (500-4000 cm <sup>-1</sup> , KBr pellet) $\bar{\nu}$ /cm <sup>-1</sup> See Fig. S4	3574 (w), 3476 (s), 3428 (s): $\nu$ (O-H) <sup>b</sup> ; 3142 (w), 3082 (s), 3062 (s): $\nu$ (aromatic =C-H); 2949 (m): $\nu_{as}$ (CH <sub>3</sub> ); 2914 (s): $\nu_{as}$ (CH <sub>2</sub> ); 2870 (m): $\nu_s$ (CH <sub>3</sub> ); 2849 (s): $\nu_s$ (CH <sub>2</sub> ); 1666 (w), 1629 (m), 1572 (s): symmetric ring stretch; 1472 (s): (C-H scissoring); 1426 (m); 1381(w): (C-H rock); 1337 (w); 1314 (w); 1282 (w); 1176 (s); 862 (m); 792 (s); 741 (m); 715 (s): (C-H rock); 662 (m); 622 (s). s: singlet, m: medium, w: weak, $\nu_{as}$ : asymmetrical stretching $\nu_s$ : symmetrical stretching.
Elemental analysis (CHN) <sup>c</sup>	(%) Calcd for C <sub>18</sub> H <sub>35</sub> BrN <sub>2</sub> ·H <sub>2</sub> O: C 57.28, H 9.88, N 7.42, Br 21.17; found (average of two measurements): C 57.23, H 9.94, N 7.35, Br 20.96
Melting point determination	56-57 °C

<sup>a</sup> In principle the NMR signals for C(2)H) and C(3)H) should appear as quartets or doublet of doublet, but they are reduced to triplets because of the similarity in the values of <sup>3</sup>*J*<sub>C(2)H,C(3)H</sub>, <sup>4</sup>*J*<sub>C(1)H,C(2)H</sub>, <sup>4</sup>*J*<sub>C(1)H,C(3)H</sub> [4].

<sup>b</sup> The presence of an O-H stretching band is indicative of the presence of water in the sample.

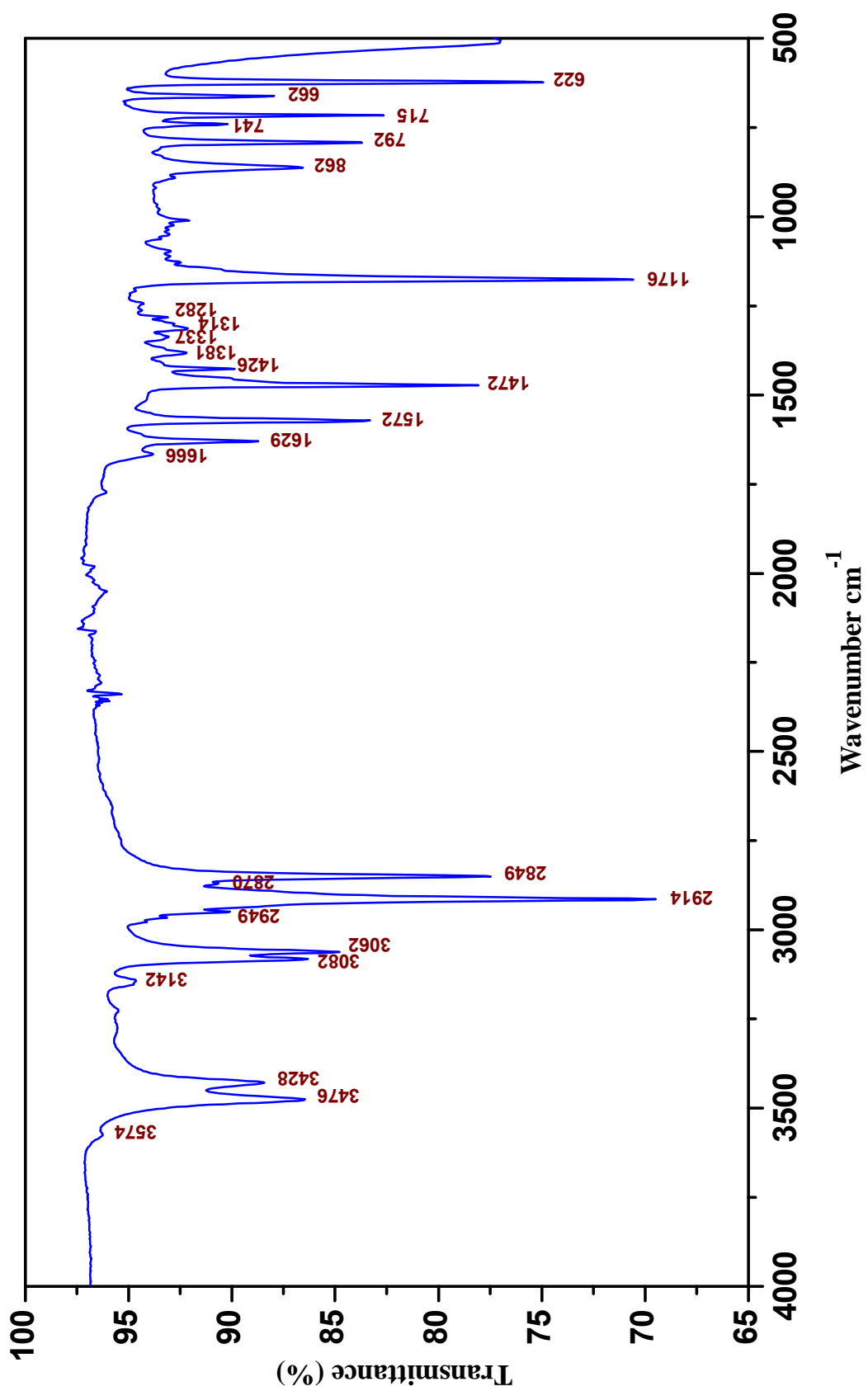
<sup>c</sup> Elemental analysis shows that the synthesised salt contains one mole of water. Water can be removed during the synthesis and extraction steps but due to the highly hygroscopic nature of C<sub>14</sub>MImBr, it readily absorbs atmospheric moisture to form stable monohydrates that can be stored in air [5].

Figure S3:  $^1\text{H}$  NMR spectrum of  $\text{C}_{14}\text{MImBr}$



**Figure S4:**  $^{13}C$  NMR spectrum of  $C_{14}MImBr$





**Figure S5:** IR spectrum of C<sub>14</sub>MImBr

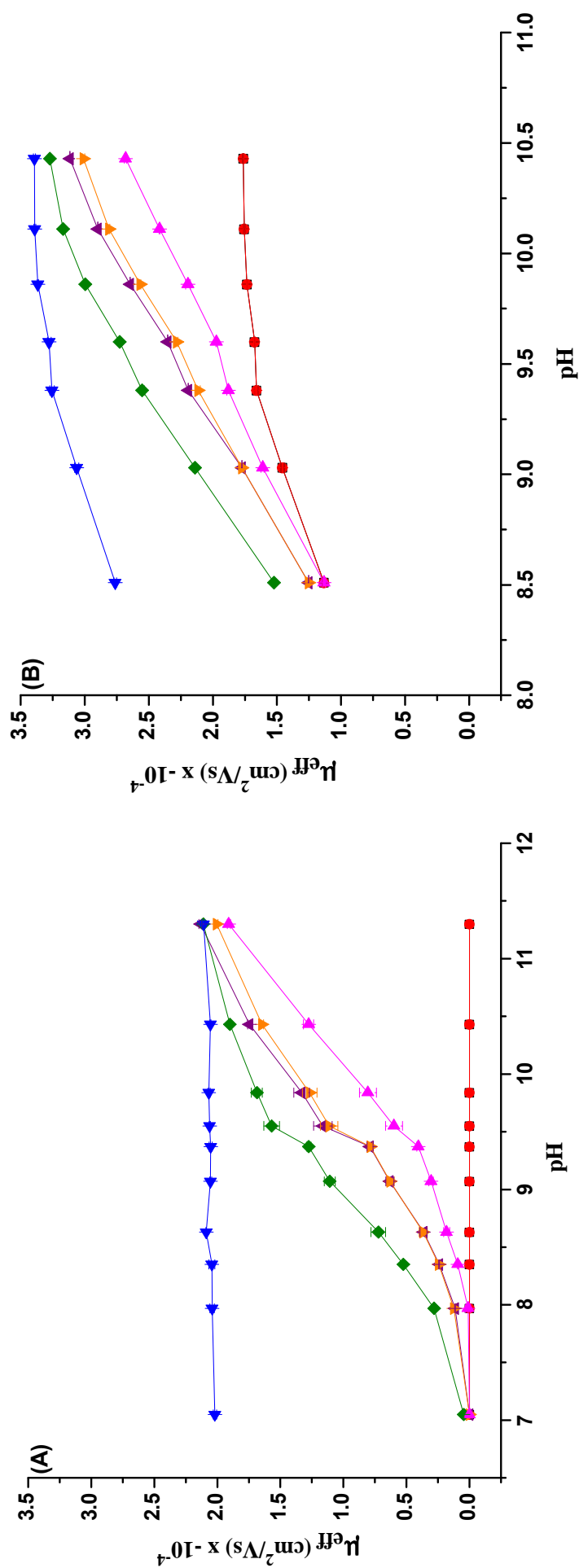


**Figure S6:** Effect of pH on the effective electrophoretic mobility using either (A) 20 mmol L<sup>-1</sup> phosphate buffer as BGE or (B) 2.5 mmol L<sup>-1</sup> borate buffer as BGE (see experimental part for preparation of BGE solution). Sample is a standard solution mixture of 20 mg L<sup>-1</sup> of each of the investigated nucleosides and 25 mg L<sup>-1</sup> thiourea in water. CE conditions: capillary 649(501) mm  $\times$  50  $\mu$ m I.D.; voltage +20 kV; pressure injection 30 mbar for 12 s. Each data point is the average of at least five measurements; standard deviation represented as error bar. For assignment of symbols, see legend in Fig. 3.

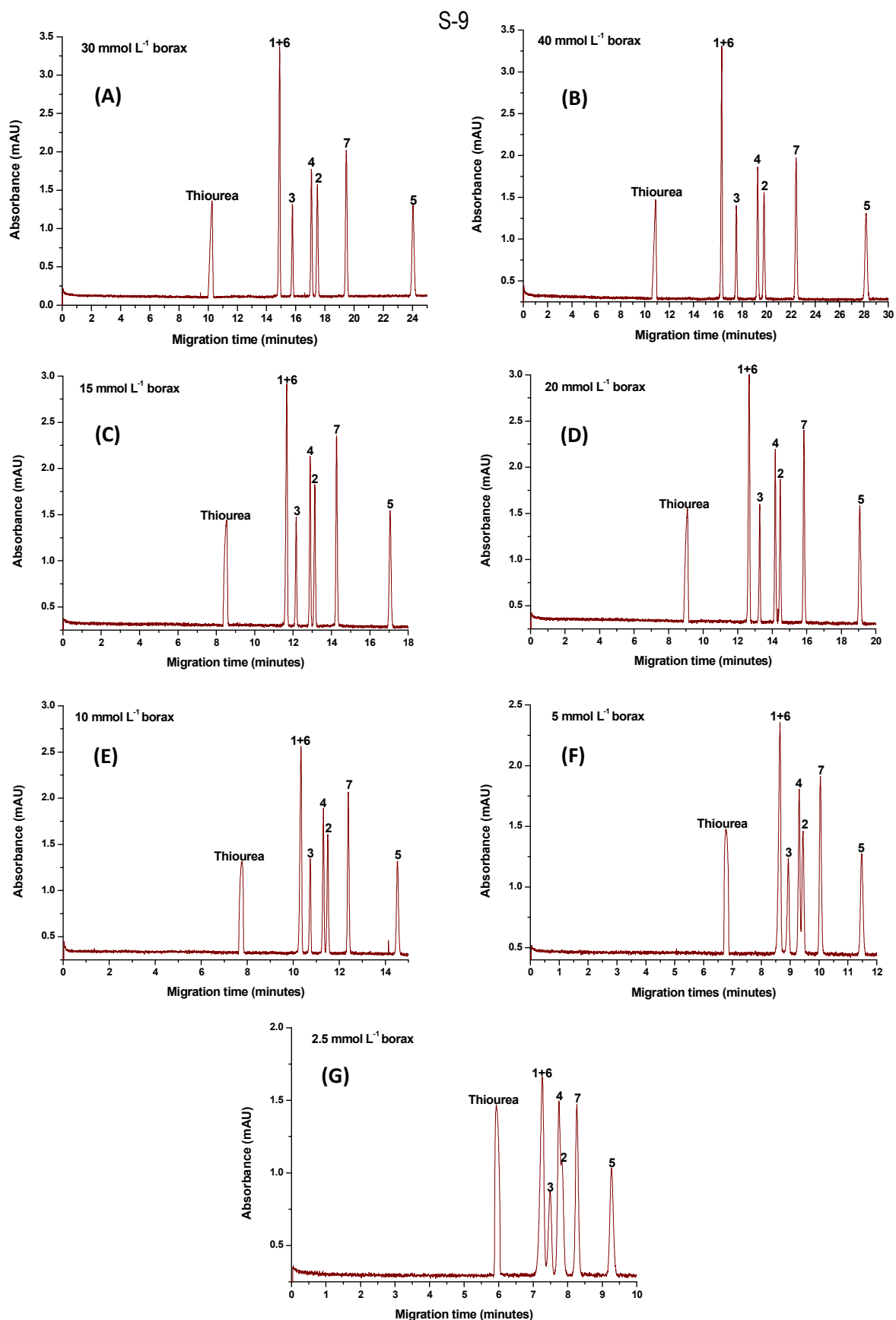


**Figure S7:** Electropherograms showing the separation of the studied nucleosides using different borax concentration at pH 9.38. CE conditions: capillary 649(502) mm × 50 μm I.D.; voltage +10 kV; pressure injection 30 mbar for 12 s. Sample solution is 20 mg L<sup>-1</sup> of each of the studied analytes and 25 mg L<sup>-1</sup> thiourea in water. Peak designation: see Fig. 1.

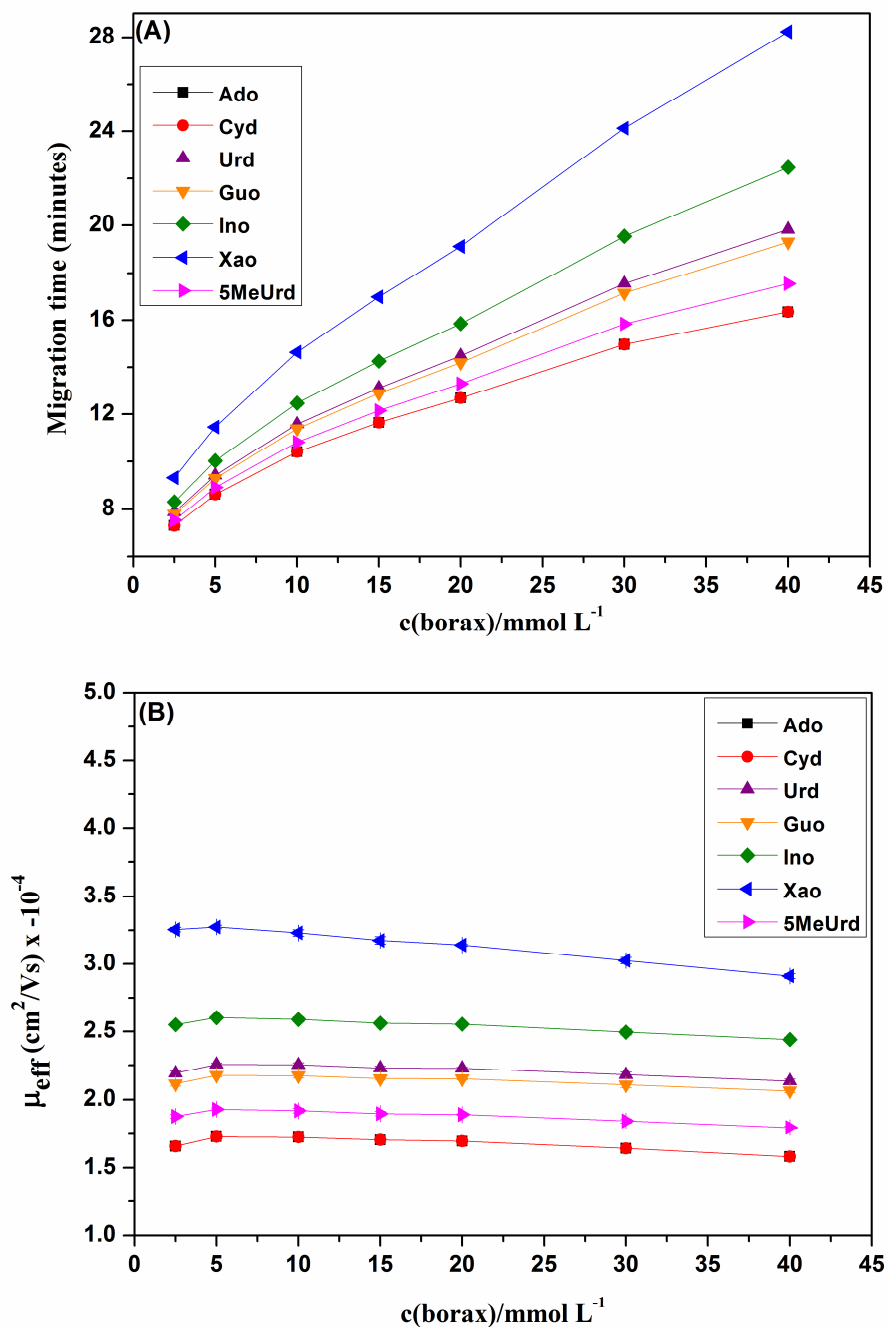


**Figure S8:** Effect of borax concentration on migration times (A) and on the effective electrophoretic mobility (B). CE conditions: capillary 649(502) mm  $\times$  50  $\mu\text{m}$  I.D.; voltage +10 kV; pressure injection 30 mbar for 12 s. Sample solution is 20 mg L<sup>-1</sup> of each of the studied analytes and 25 mg L<sup>-1</sup> thiourea in water. For analyte abbreviations refer to the experimental part. In Fig. S8B, each data point is the average of at least five measurements, standard deviation represented as error bar.

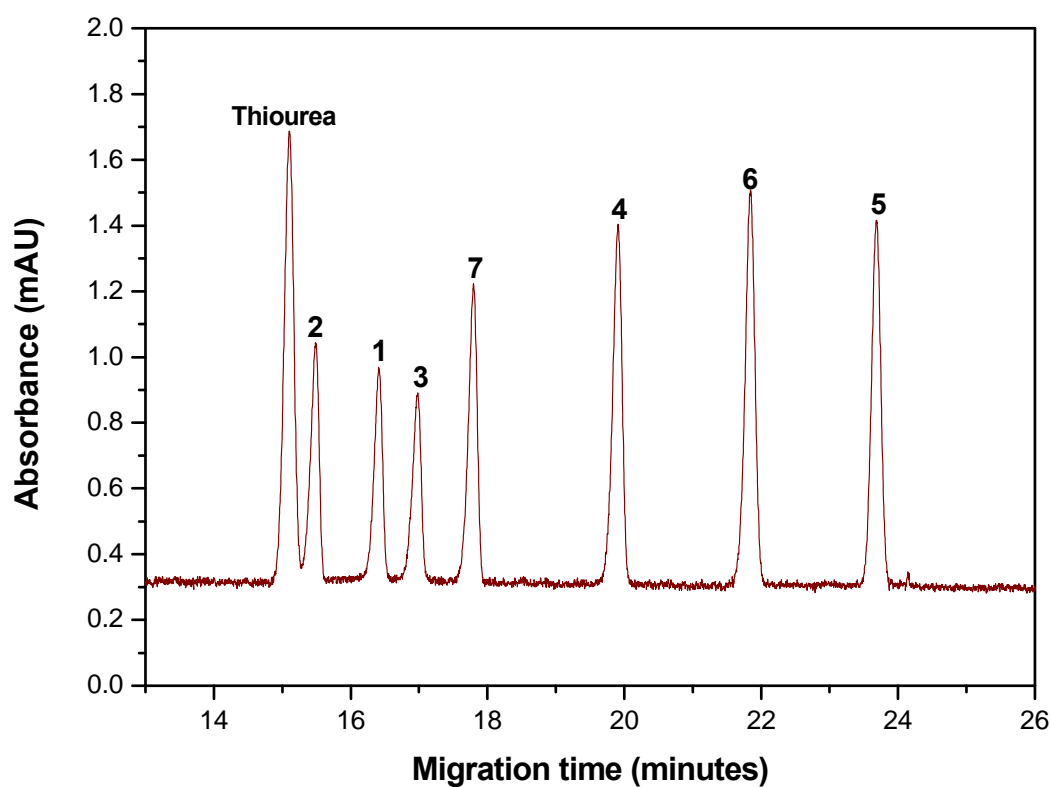


**Figure S9:** Electropherogram obtained from a mixture of 25 mg L<sup>-1</sup> of each of the studied nucleosides and 50 mg L<sup>-1</sup> thiourea in 4 mmol L<sup>-1</sup> phosphate buffer pH 6.86. CE conditions: 200 mmol L<sup>-1</sup> SDS in 50 mmol L<sup>-1</sup> phosphate buffer, pH 6.86 as BGE; capillary 649(501) mm × 50 μm I.D.; voltage +10 kV; pressure injection 30 mbar for 12 s; 35 °C. Peak designation: see Fig. 1.

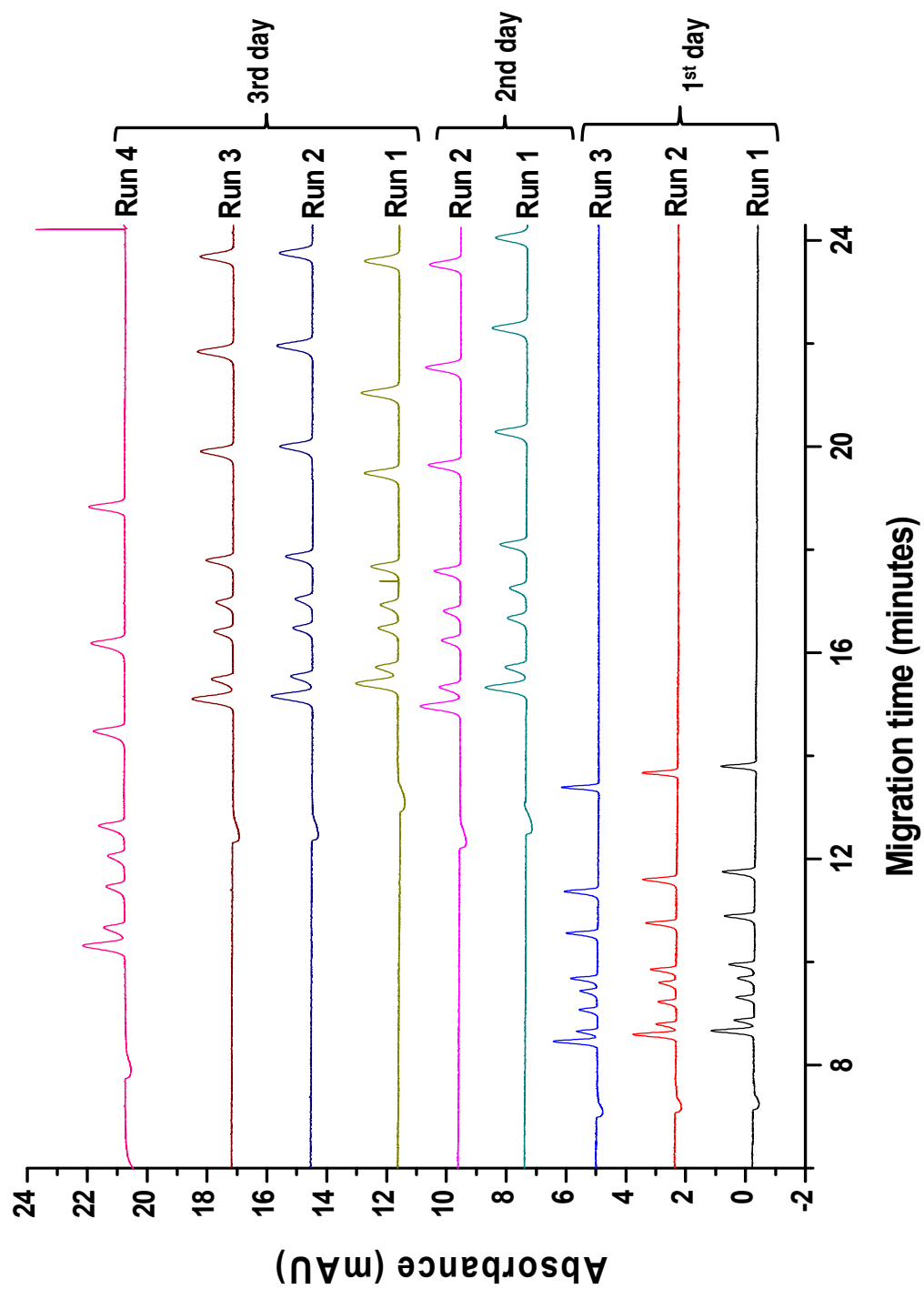


**Figure S10:** Electropherograms showing the reproducibility with MEKC experiments using SDS as PSP. Experimental parameters and migration order are the same as in Fig. S9.

**Calculation of the retention factors of the nucleosides as charged analytes**

To calculate the retention factor for a weak acid, the following equation can be employed [10-13]:

$$\mu = \frac{1}{k+1} \mu_{\text{eff}} + \frac{k}{1+k} \mu_{\text{MC}} \quad (\text{S-1})$$

where  $\mu$  is the pseudoeffective electrophoretic mobility of the analyte in micellar BGE,  $k$  is the overall retention factor of the analyte,  $\mu_{\text{eff}}$  is the effective electrophoretic mobility of the analyte in micelle-free BGE, and  $\mu_{\text{MC}}$  is the electrophoretic mobility of the micelles in micellar BGE. From Eq. (S-1) following expression can be derived, which allows to calculate the true retention factor  $k$  in MEKC from the mobilities  $\mu$ ,  $\mu_{\text{eff}}$ , and  $\mu_{\text{MC}}$  [10], which have to be determined in separate measurements with a separation electrolyte containing surfactant ( $\mu$  and  $\mu_{\text{MC}}$ ) and with a separation electrolyte containing no surfactant ( $\mu_{\text{eff}}$ ):

$$k = \frac{\mu - \mu_{\text{eff}}}{\mu_{\text{MC}} - \mu} \quad (\text{S-2})$$

Several assumptions have to be made: the influence of the pseudostationary phase on the ionic strength, viscosity, and dielectric constant of the BGE must be assumed to be very low, interaction of the analyte either with the capillary wall (solute-admicelle interaction) and with surfactant monomers is neglected. Regarding the last point, it was reported in a previous study [14] that  $\mu_{\text{eff}}$  in the presence of surfactant monomers is not significantly different from the values obtained in absence of such monomers i.e. ion pair formation can be neglected. It must be emphasized that analytes used in that study are hydrophilic, a situation which is quite similar to our case (highly hydrophilic nucleosides).

**Table S2.** Effective electrophoretic mobilities (mean value  $\pm$  standard deviation, N = number of runs) determined under variation of the concentration of borax, pH = 9.38, capillary 649(502) mm  $\times$  50  $\mu$ m I.D.; voltage +10 kV; pressure injection 30 mbar for 12 s; 1 = cytidine, 2 = uridine, 3 = 5-methyluridine, 4 = guanosine, 5 = xanthosine, 6 = adenosine, 7 = inosine.

c(borax)/ mmol L <sup>-1</sup>	$\mu_{eff}$ (1)/ cm <sup>2</sup> kV <sup>-1</sup> s <sup>-1</sup>	$\mu_{eff}$ (2)/ cm <sup>2</sup> kV <sup>-1</sup> s <sup>-1</sup>	$\mu_{eff}$ (3)/ cm <sup>2</sup> kV <sup>-1</sup> s <sup>-1</sup>	$\mu_{eff}$ (4)/ cm <sup>2</sup> kV <sup>-1</sup> s <sup>-1</sup>	$\mu_{eff}$ (5)/ cm <sup>2</sup> kV <sup>-1</sup> s <sup>-1</sup>	$\mu_{eff}$ (6)/ cm <sup>2</sup> kV <sup>-1</sup> s <sup>-1</sup>	$\mu_{eff}$ (7)/ cm <sup>2</sup> kV <sup>-1</sup> s <sup>-1</sup>
2.5	-0.166 $\pm$ 0.00120 N = 6	-0.219 $\pm$ 0.00137 N = 6	-0.188 $\pm$ 0.00134 N = 6	-0.211 $\pm$ 0.00160 N = 6	-0.326 $\pm$ 0.00164 N = 6	-0.166 $\pm$ 0.00120 N = 6	-0.255 $\pm$ 0.00153 N = 6
5	-0.173 $\pm$ 0.00092 N = 6	-0.226 $\pm$ 0.00097 N = 6	-0.193 $\pm$ 0.00087 N = 6	-0.218 $\pm$ 0.00091 N = 6	-0.327 $\pm$ 0.00131 N = 6	-0.173 $\pm$ 0.00092 N = 6	-0.260 $\pm$ 0.00104 N = 6
10	-0.172 $\pm$ 0.00149 N = 5	-0.225 $\pm$ 0.00175 N = 5	-0.192 $\pm$ 0.00168 N = 5	-0.217 $\pm$ 0.00173 N = 5	-0.323 $\pm$ 0.00236 N = 5	-0.172 $\pm$ 0.00149 N = 5	-0.259 $\pm$ 0.00194 N = 5
15	-0.171 $\pm$ 0.00202 N = 6	-0.223 $\pm$ 0.00128 N = 6	-0.190 $\pm$ 0.00155 N = 6	-0.215 $\pm$ 0.00123 N = 6	-0.317 $\pm$ 0.00276 N = 6	-0.171 $\pm$ 0.00202 N = 6	-0.256 $\pm$ 0.00127 N = 6
20	-0.169 $\pm$ 0.00049 N = 8	-0.223 $\pm$ 0.00077 N = 8	-0.189 $\pm$ 0.00057 N = 8	-0.215 $\pm$ 0.00073 N = 8	-0.314 $\pm$ 0.00081 N = 8	-0.169 $\pm$ 0.00049 N = 8	-0.255 $\pm$ 0.00085 N = 8
30	-0.164 $\pm$ 0.00123 N = 10	-0.218 $\pm$ 0.00206 N = 10	-0.184 $\pm$ 0.00162 N = 10	-0.211 $\pm$ 0.00201 N = 10	-0.303 $\pm$ 0.00233 N = 10	-0.164 $\pm$ 0.00123 N = 10	-0.250 $\pm$ 0.00231 N = 10
40	-0.158 $\pm$ 0.00104 N = 6	-0.213 $\pm$ 0.00147 N = 6	-0.180 $\pm$ 0.00123 N = 6	-0.206 $\pm$ 0.00140 N = 6	-0.291 $\pm$ 0.00192 N = 6	-0.158 $\pm$ 0.00104 N = 6	-0.244 $\pm$ 0.00170 N = 6



**Table S3.** Pseudoeffective electrophoretic mobilities (mean value  $\pm$  standard deviation, N = number of runs) determined under variation of the concentration of borax with  $c(\text{C}_{14}\text{MImBr}) = 20 \text{ mmol L}^{-1}$ , pH = 9.38; capillary 649(502) mm  $\times$  50  $\mu\text{m}$  I.D.; voltage -10 kV; pressure injection 30 mbar for 12 s; 1 = cytidine, 2 = uridine, 3 = 5-methyluridine, 4 = guanosine, 5 = xanthosine, 6 = adenosine, 7 = inosine, 8 = decanophenone.

$c(\text{borax})/\text{mmol L}^{-1}$	$\mu_{\text{eff}}^P$ (1)/ $\text{cm}^2\text{kV}^{-1}\text{s}^{-1}$	$\mu_{\text{eff}}^P$ (2)/ $\text{cm}^2\text{kV}^{-1}\text{s}^{-1}$	$\mu_{\text{eff}}^P$ (3)/ $\text{cm}^2\text{kV}^{-1}\text{s}^{-1}$	$\mu_{\text{eff}}^P$ (4)/ $\text{cm}^2\text{kV}^{-1}\text{s}^{-1}$	$\mu_{\text{eff}}^P$ (5)/ $\text{cm}^2\text{kV}^{-1}\text{s}^{-1}$	$\mu_{\text{eff}}^P$ (6)/ $\text{cm}^2\text{kV}^{-1}\text{s}^{-1}$	$\mu_{\text{eff}}^P$ (7)/ $\text{cm}^2\text{kV}^{-1}\text{s}^{-1}$	$\mu_{\text{eff}}^P$ (8)/ $\text{cm}^2\text{kV}^{-1}\text{s}^{-1}$
2.5	-0.062 $\pm 0.00042$ N = 4	0.176 $\pm 0.00088$ N = 4	0.153 $\pm 0.00102$ N = 4	0.265 $\pm 0.00074$ N = 4	0.345 $\pm 0.00067$ N = 4	0.000 N = 4	0.325 $\pm 0.00074$ N = 4	0.444 $\pm 0.00007$ N = 2
5	-0.088 $\pm 0.00023$ N = 5	0.138 $\pm 0.00086$ N = 5	0.120 $\pm 0.00062$ N = 5	0.234 $\pm 0.00062$ N = 5	0.317 $\pm 0.00072$ N = 5	-0.026 $\pm 0.00017$ N = 5	0.296 $\pm 0.00054$ N = 5	0.421 $\pm 0.00009$ N = 2
10	-0.114 $\pm 0.00005$ N = 3	0.075 $\pm 0.00030$ N = 3	0.067 $\pm 0.00010$ N = 3	0.180 $\pm 0.00030$ N = 3	0.272 $\pm 0.00031$ N = 3	-0.055 $\pm 0.00011$ N = 3	0.251 $\pm 0.00004$ N = 3	0.403 $\pm 0.00058$ N = 2
15	-0.125 $\pm 0.00021$ N = 5	0.032 $\pm 0.00059$ N = 6	0.032 $\pm 0.00059$ N = 6	0.140 $\pm 0.00034$ N = 5	0.235 $\pm 0.00012$ N = 5	-0.070 $\pm 0.00004$ N = 5	0.215 $\pm 0.00021$ N = 6	0.389 $\pm 0.00028$ N = 2
20	-0.132 $\pm 0.00022$ N = 4	0.003 $\pm 0.00060$ N = 4	0.010 $\pm 0.00084$ N = 4	0.106 $\pm 0.00134$ N = 4	0.200 $\pm 0.00148$ N = 4	-0.081 $\pm 0.00002$ N = 4	0.183 $\pm 0.00152$ N = 4	0.379 $\pm 0.00206$ N = 2
30	-0.139 $\pm 0.00164$ N = 4	-0.048 $\pm 0.00125$ N = 5	-0.026 $\pm 0.00436$ N = 5	0.053 $\pm 0.00194$ N = 4	0.136 $\pm 0.00286$ N = 5	-0.095 $\pm 0.00009$ N = 4	0.127 $\pm 0.00386$ N = 4	0.367 extrapolated value
40	-0.143 $\pm 0.00093$ N = 4	-0.068 $\pm 0.00055$ N = 5	-0.045 $\pm 0.00062$ N = 5	0.030 $\pm 0.00112$ N = 5	0.100 $\pm 0.00262$ N = 5	-0.101 $\pm 0.00056$ N = 4	0.100 $\pm 0.00164$ N = 5	0.358 extrapolated value

**Table S4.** Effective electrophoretic mobilities (mean value  $\pm$  standard deviation, N = number of runs) determined under variation of pH with  $c(\text{Na}_2\text{B}_4\text{O}_7) = 2.5 \text{ mmol L}^{-1}$ ; capillary 649(501) mm  $\times$  50  $\mu\text{m}$  I.D.; voltage +20 kV; pressure injection 30 mbar for 12 s; 1 = cytidine, 2 = uridine, 3 = 5-methyluridine, 4 = guanosine, 5 = xanthosine, 6 = adenosine, 7 = inosine.

pH	$\mu_{\text{eff}}$ (1)/ $\text{cm}^2\text{kV}^{-1}\text{s}^{-1}$	$\mu_{\text{eff}}$ (2)/ $\text{cm}^2\text{kV}^{-1}\text{s}^{-1}$	$\mu_{\text{eff}}$ (3)/ $\text{cm}^2\text{kV}^{-1}\text{s}^{-1}$	$\mu_{\text{eff}}$ (4)/ $\text{cm}^2\text{kV}^{-1}\text{s}^{-1}$	$\mu_{\text{eff}}$ (5)/ $\text{cm}^2\text{kV}^{-1}\text{s}^{-1}$	$\mu_{\text{eff}}$ (6)/ $\text{cm}^2\text{kV}^{-1}\text{s}^{-1}$	$\mu_{\text{eff}}$ (7)/ $\text{cm}^2\text{kV}^{-1}\text{s}^{-1}$
8.51	-0.113 $\pm 0.00107$ N = 5	-0.125 $\pm 0.00095$ N = 5	-0.113 $\pm 0.00110$ N = 5	-0.125 $\pm 0.00095$ N = 5	-0.276 $\pm 0.00097$ N = 5	-0.113 $\pm 0.00107$ N = 5	-0.152 $\pm 0.00060$ N = 5
9.03	-0.146 $\pm 0.00121$ N = 5	-0.177 $\pm 0.00110$ N = 5	-0.161 $\pm 0.00118$ N = 5	-0.177 $\pm 0.00110$ N = 5	-0.306 $\pm 0.00170$ N = 5	-0.146 $\pm 0.00121$ N = 5	-0.214 $\pm 0.00120$ N = 5
9.38	-0.166 $\pm 0.00120$ N = 6	-0.219 $\pm 0.00137$ N = 6	-0.188 $\pm 0.00134$ N = 6	-0.211 $\pm 0.00160$ N = 6	-0.326 $\pm 0.00164$ N = 6	-0.166 $\pm 0.00120$ N = 6	-0.255 $\pm 0.00153$ N = 6
9.60	-0.167 $\pm 0.00060$ N = 6	-0.235 $\pm 0.00060$ N = 6	-0.197 $\pm 0.00049$ N = 6	-0.228 $\pm 0.00075$ N = 6	-0.328 $\pm 0.00145$ N = 6	-0.167 $\pm 0.00060$ N = 6	-0.273 $\pm 0.00084$ N = 6
9.86	-0.173 $\pm 0.00064$ N = 6	-0.265 $\pm 0.00072$ N = 6	-0.219 $\pm 0.00178$ N = 6	-0.257 $\pm 0.00038$ N = 6	-0.337 $\pm 0.00075$ N = 6	-0.173 $\pm 0.00064$ N = 6	-0.300 $\pm 0.00052$ N = 6
10.11	-0.175 $\pm 0.00080$ N = 6	-0.290 $\pm 0.00082$ N = 6	-0.242 $\pm 0.00043$ N = 6	-0.281 $\pm 0.00067$ N = 6	-0.339 $\pm 0.00081$ N = 6	-0.175 $\pm 0.00080$ N = 6	-0.317 $\pm 0.00078$ N = 6
10.43	-0.176 $\pm 0.00039$ N = 5	-0.312 $\pm 0.00106$ N = 5	-0.268 $\pm 0.00088$ N = 5	-0.301 $\pm 0.00104$ N = 5	-0.339 $\pm 0.00086$ N = 5	-0.176 $\pm 0.00039$ N = 5	-0.327 $\pm 0.00064$ N = 5

**Table S5.** Pseudoeffective electrophoretic mobilities (mean value  $\pm$  standard deviation, N = number of runs) determined under variation of pH with  $c(\text{C}_{14}\text{MImBr}) = 20 \text{ mmol L}^{-1}$ ,  $c(\text{Na}_2\text{B}_4\text{O}_7) = 2.5 \text{ mmol L}^{-1}$ , capillary 649(503) mm  $\times$  50  $\mu\text{m}$  I.D.; voltage -20 kV; pressure injection 30 mbar for 12 s; 1 = cytidine, 2 = uridine, 3 = 5-methyluridine, 4 = guanosine, 5 = xanthosine, 6 = adenosine, 7 = inosine, 8 = decanophenone.

pH	$\mu_{\text{eff}}^{\text{P}} (1)/$ $\text{cm}^2\text{kV}^{-1}\text{s}^{-1}$	$\mu_{\text{eff}}^{\text{P}} (2)/$ $\text{cm}^2\text{kV}^{-1}\text{s}^{-1}$	$\mu_{\text{eff}}^{\text{P}} (3)/$ $\text{cm}^2\text{kV}^{-1}\text{s}^{-1}$	$\mu_{\text{eff}}^{\text{P}} (4)/$ $\text{cm}^2\text{kV}^{-1}\text{s}^{-1}$	$\mu_{\text{eff}}^{\text{P}} (5)/$ $\text{cm}^2\text{kV}^{-1}\text{s}^{-1}$	$\mu_{\text{eff}}^{\text{P}} (6)/$ $\text{cm}^2\text{kV}^{-1}\text{s}^{-1}$	$\mu_{\text{eff}}^{\text{P}} (7)/$ $\text{cm}^2\text{kV}^{-1}\text{s}^{-1}$	$\mu_{\text{eff}}^{\text{P}} (8)/$ $\text{cm}^2\text{kV}^{-1}\text{s}^{-1}$
8.49	-0.050 $\pm 0.00074$ N = 4	0.000 N = 4	0.000 N = 4	0.088 $\pm 0.00063$ N = 4	0.291 $\pm 0.00013$ N = 4	-0.016 $\pm 0.00117$ N = 4	0.174 $\pm 0.00180$ N = 4	0.446 $\pm 0.00070$ N = 4
9.02	-0.063 $\pm 0.00016$ N = 3	0.094 $\pm 0.00062$ N = 3	0.078 $\pm 0.00103$ N = 3	0.187 $\pm 0.00040$ N = 3	0.325 $\pm 0.00034$ N = 3	-0.017 $\pm 0.00067$ N = 3	0.275 $\pm 0.00032$ N = 3	0.447 $\pm 0.00563$ N = 3
9.38	-0.062 $\pm 0.00042$ N = 4	0.176 $\pm 0.00088$ N = 4	0.153 $\pm 0.00102$ N = 4	0.265 $\pm 0.00074$ N = 4	0.345 $\pm 0.00067$ N = 4	0.000 N = 4	0.325 $\pm 0.00074$ N = 4	0.444 $\pm 0.00007$ N = 2
9.60	-0.070 $\pm 0.00077$ N = 6	0.204 $\pm 0.00234$ N = 6	0.191 $\pm 0.00272$ N = 6	0.287 $\pm 0.00240$ N = 6	0.340 $\pm 0.00235$ N = 6	-0.014 $\pm 0.00116$ N = 6	0.332 $\pm 0.00214$ N = 6	0.439 $\pm 0.00261$ N = 6
9.84	-0.079 $\pm 0.00124$ N = 4	0.222 $\pm 0.00088$ N = 4	0.222 $\pm 0.00088$ N = 4	0.302 $\pm 0.00112$ N = 4	0.337 $\pm 0.00156$ N = 4	-0.017 $\pm 0.00092$ N = 4	0.337 $\pm 0.00156$ N = 4	0.443 $\pm 0.00218$ N = 4
10.09	-0.083 $\pm 0.00183$ N = 4	0.231 $\pm 0.00250$ N = 4	0.243 $\pm 0.00324$ N = 4	0.304 $\pm 0.00191$ N = 4	0.327 $\pm 0.00225$ N = 4	-0.024 $\pm 0.00116$ N = 4	0.330 $\pm 0.00244$ N = 4	0.429 $\pm 0.00515$ N = 4
10.41	-0.087 $\pm 0.00054$ N = 2	0.242 $\pm 0.00043$ N = 2	0.265 $\pm 0.00008$ N = 2	0.311 $\pm 0.00053$ N = 2	0.323 $\pm 0.00075$ N = 2	-0.027 $\pm 0.00006$ N = 2	0.331 $\pm 0.00086$ N = 2	0.431 $\pm 0.00105$ N = 2

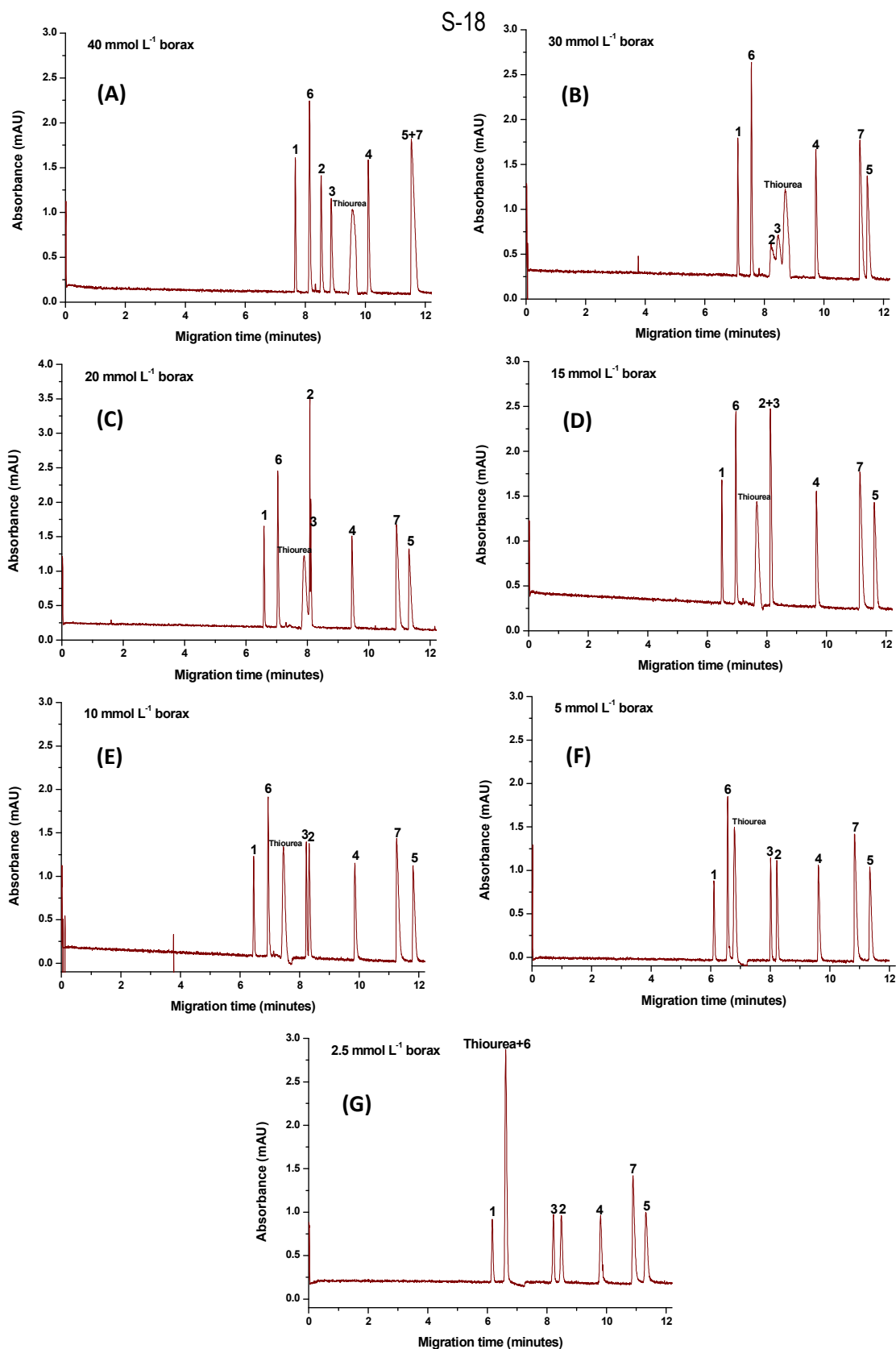


**Figure S11:** Electropherograms showing the separation of the studied nucleosides using 20 mmol L<sup>-1</sup> C<sub>14</sub>MImBr at different concentration of borax, pH 9.38. CE conditions: capillary 649(502) mm × 50 μm I.D.; voltage -10 kV; pressure injection 30 mbar for 12 s. Sample solution is 25 mg L<sup>-1</sup> of all studied nucleosides and 25 mg L<sup>-1</sup> thiourea in water. Peak designation: see Fig. 1.

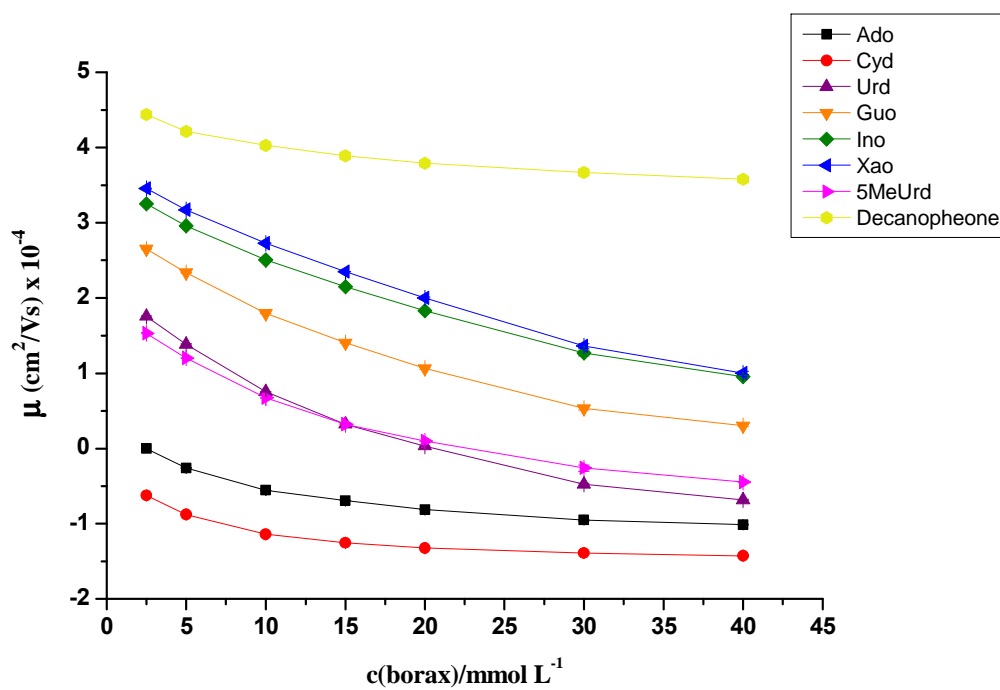


**Figure S12:** Effect of concentration of borax on the pseudo-effective mobility. For experimental details refer to Fig. S11. Each data point is the average of at least two measurements; standard deviation represented as error bar.

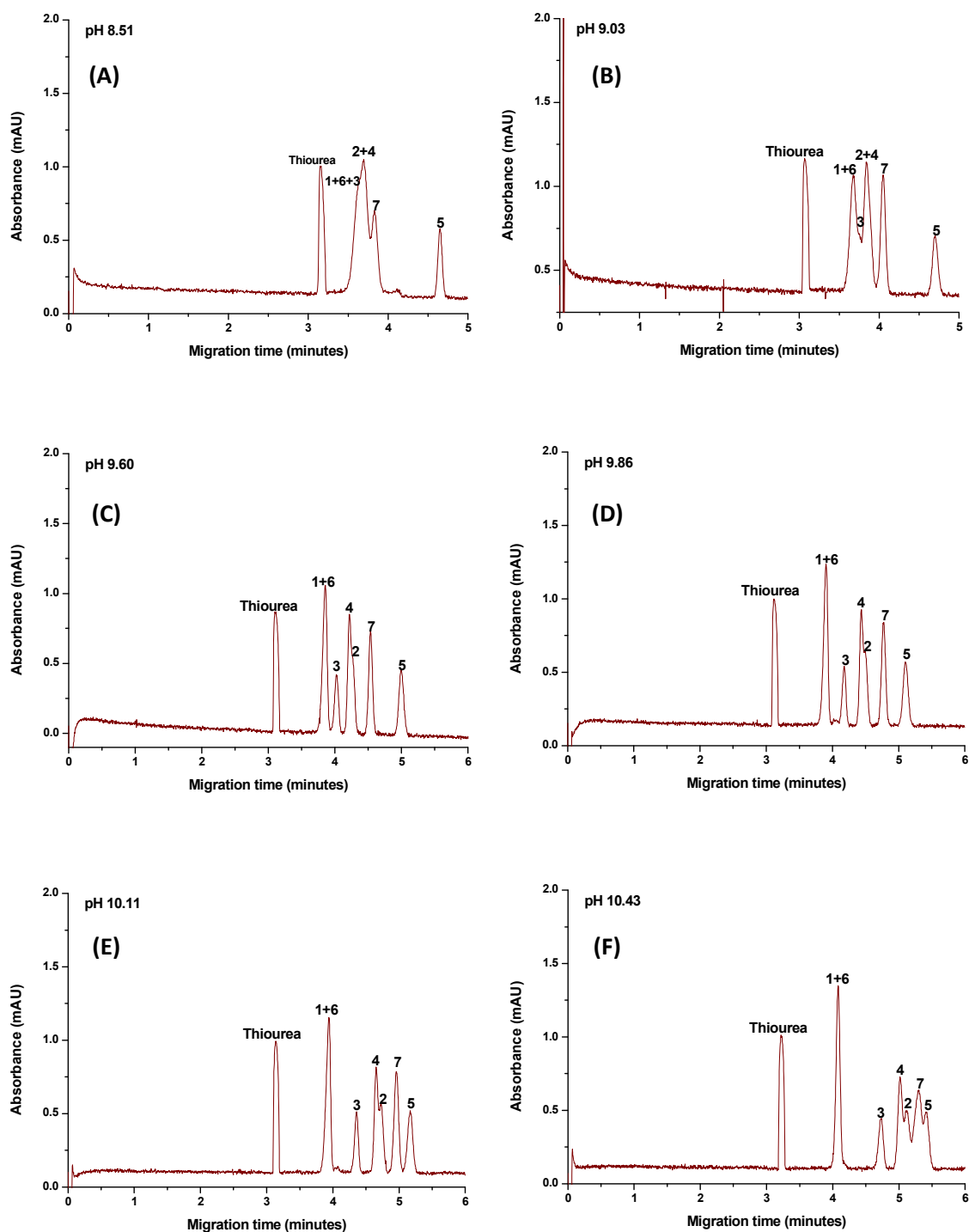


**Figure S13:** Electropherograms showing the separation of the studied nucleosides using 2.5 mmol L<sup>-1</sup> borax at different pH values. CE conditions: capillary 649(502) mm × 50 μm I.D.; voltage +20 kV; pressure injection 30 mbar for 12 s. Sample solution is 20 mg L<sup>-1</sup> of each of the studied nucleosides and 25 mg L<sup>-1</sup> thiourea in water. Peak designation: see Fig. 1. For pH 9.38, see Fig. S7G.

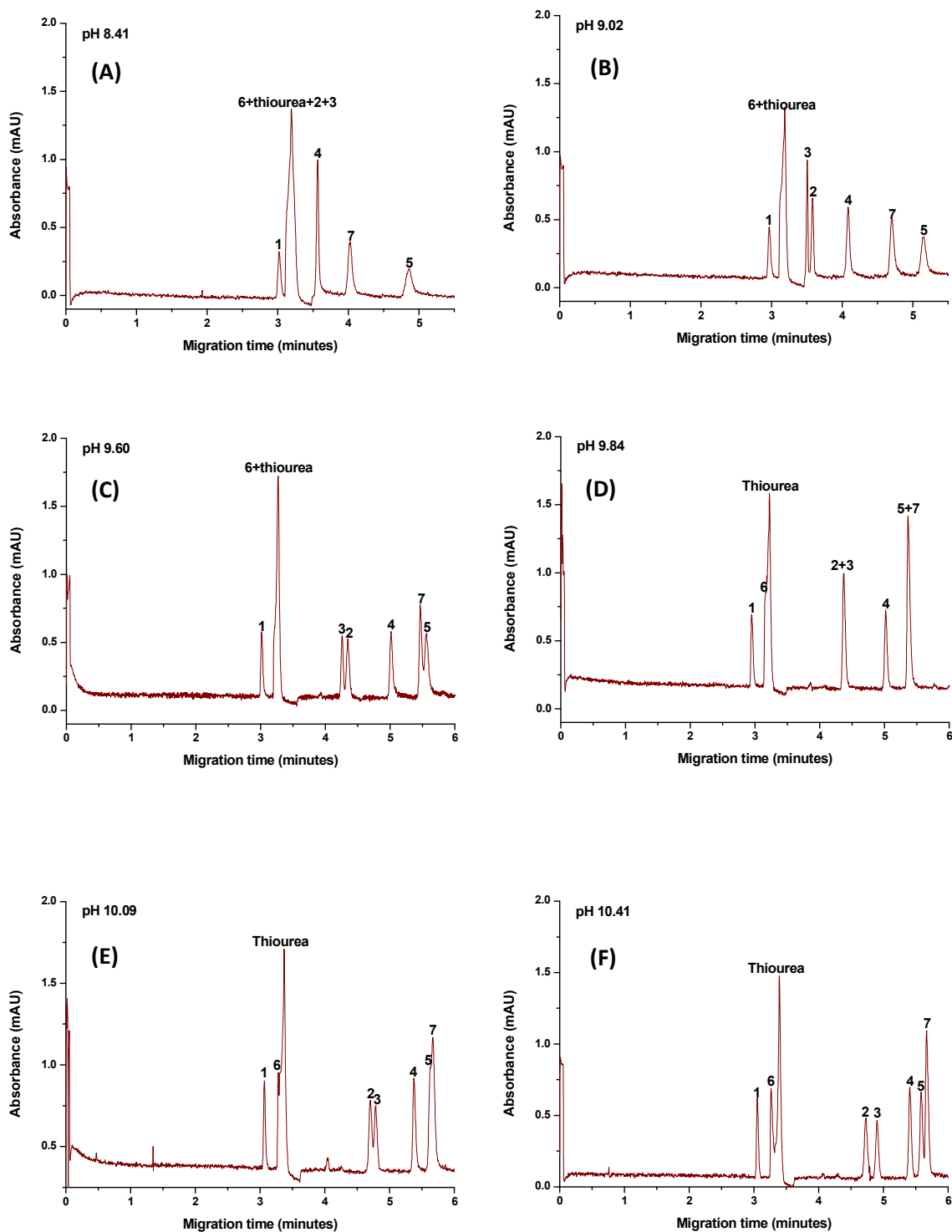


**Figure S14:** Electropherograms showing the separation of the studied nucleosides using 20 mmol L<sup>-1</sup> C<sub>14</sub>MImBr in 2.5 mmol L<sup>-1</sup> borax at different pH values. CE conditions: capillary 649(503) mm × 50 μm I.D.; voltage -20 kV; pressure injection 30 mbar for 12 s. Sample solution is 20 mg L<sup>-1</sup> of each of the investigated nucleosides and 25 mg L<sup>-1</sup> thiourea in BGE/water/methanol mixture (50:40:10, v/v/v). Peak designation: see Fig. 1. For pH 9.38, see Fig. S11G.

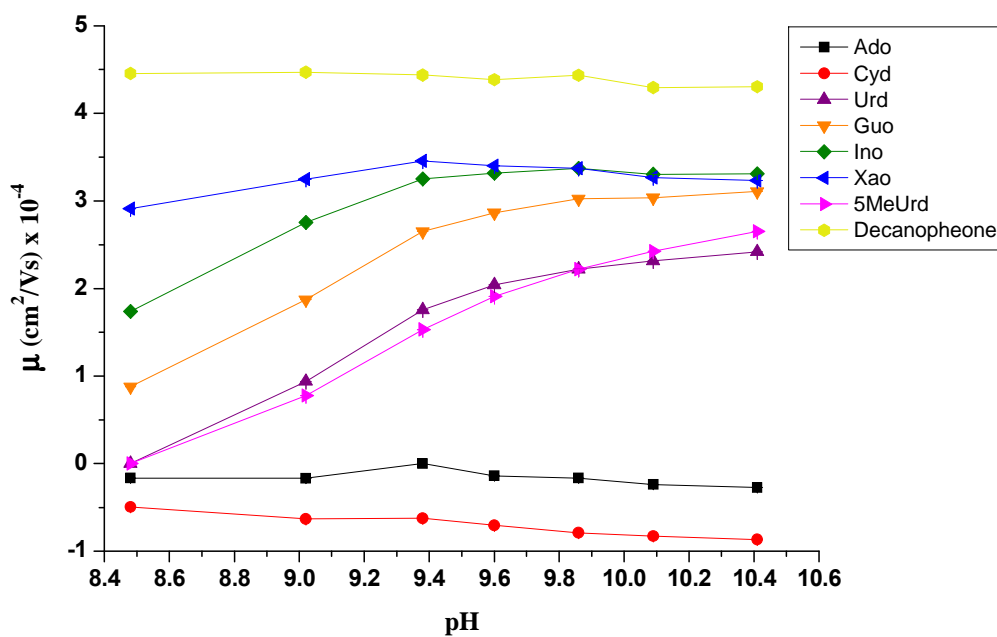


**Figure S15:** Effect of pH on the pseudoeffective mobility. For experimental details refer to Fig. S14. Each data point is the average of at least two measurements; standard deviation represented as error bar.



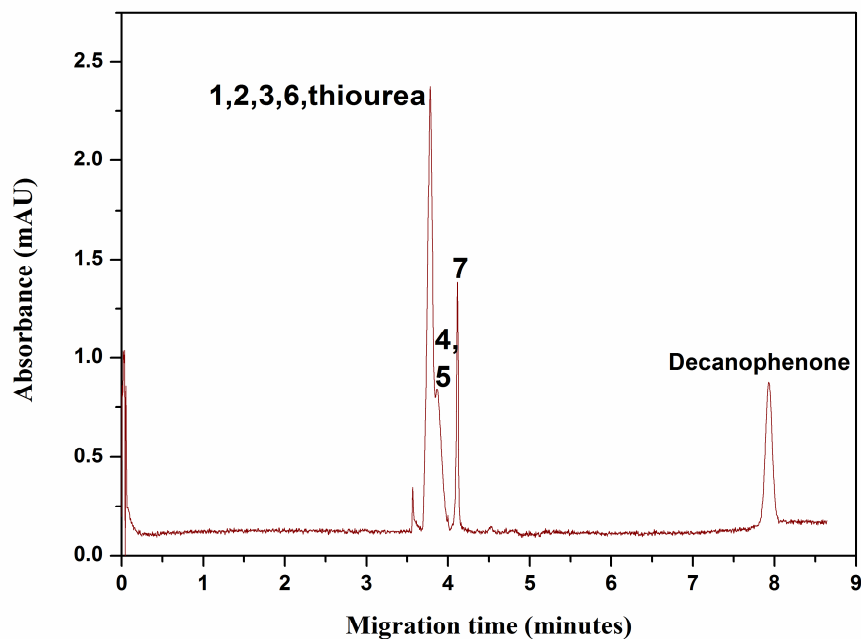


**Figure S16:** Electropherogram obtained from a standard solution mixture of 20 mg L<sup>-1</sup> of each of the studied analytes, 25 mg L<sup>-1</sup> thiourea and 30 mg L<sup>-1</sup> decanophenone in BGE/water/methanol mixture (50:40:10, v/v/v). CE conditions: 20 mmol L<sup>-1</sup> C<sub>14</sub>MImBr in 10 mmol L<sup>-1</sup> carbonate buffer, pH 9.38; applied voltage -20 kV; pressure injection 30 mbar for 12 s. Peak designation: see Fig. 1

## References

- [1] R.L. Lundblad, F. MacDonald (Eds.), Handbook of Biochemistry and Molecular Biology, 4th ed., CRC Press, Taylor and Francis Group, LLC, Boca Raton, 2010.
- [2] G. Marrubini, B.E.C. Mendoza, G. Massolini, J. Sep. Sci. 33 (2010) 803.
- [3] R. Vanyur, L. Biczok, Z. Miskolczy, Colloids Surf. A 299 (2007) 256.
- [4] Y. Takeuchi, H.J.C. Yeh, K.L. Kirk, L.A. Cohen, J. Org. Chem. 43 (1978) 3565.
- [5] A.E. Bradley, C. Hardacre, J.D. Holbrey, S. Johnston, S.E.J. McMath, M. Nieuwenhuyzen, Chem. Mater. 14 (2002) 629.
- [6] H. Luo, J.F. Huang, S. Dai, Sep. Sci. Technol. 43 (2008) 2473.
- [7] A. Getsis, A.V. Mudring, Cryst. Res. Technol. 43 (2008) 1187.
- [8] D. Guzman-Lucero, P. Flores, T. Rojo, R. Martinez-Palou, Energy Fuels 24 (2010) 3610.
- [9] A. Cornellias, L. Perez, F. Comelles, I. Ribosa, A. Manresa, M.T. Garcia, J. Colloid Interface Sci. 355 (2011) 164.
- [10] M.T. Ackermans, F.M. Everaerts, J.L. Beckers, J. Chromatogr. 585 (1991) 123.
- [11] K. Otsuka, S. Terabe, T. Ando, J. Chromatogr. 348 (1985) 39.
- [12] M.G. Khaledi, S.C. Smith, J.K. Strasters, Anal. Chem. 63 (1991) 1820.
- [13] I. Orentaite, A. Maruska, U. Pyell, Electrophoresis 32 (2011) 604.
- [14] U. Pyell, in: U. Pyell (Ed.), Electrokinetic Chromatography: Theory, Instrumentation & Applications, John Wiley & Sons, Ltd., Chichester, 2006.

## ELSEVIER LICENSE TERMS AND CONDITIONS

Apr 08, 2015

This is a License Agreement between Azza Rageh ("You") and Elsevier ("Elsevier") provided by Copyright Clearance Center ("CCC"). The license consists of your order details, the terms and conditions provided by Elsevier, and the payment terms and conditions.

**All payments must be made in full to CCC. For payment instructions, please see information listed at the bottom of this form.**

Supplier	Elsevier Limited The Boulevard, Langford Lane Kidlington, Oxford, OX5 1GB, UK
Registered Company Number	1982084
Customer name	Azza Rageh
Customer address	Hans-Meerwein Str. 4, Chemie, Maburg, Hessen 35032
License number	3604350534165
License date	Apr 08, 2015
Licensed content publisher	Elsevier
Licensed content publication	Journal of Chromatography A
Licensed content title	Imidazolium-based ionic liquid-type surfactant as pseudo-stationary phase in micellar electrokinetic chromatography of highly hydrophilic urinary nucleosides
Licensed content author	Azza H. Rageh, Ute Pyell
Licensed content date	5 November 2013
Licensed content volume number	1316
Licensed content issue number	
Number of pages	12
Start Page	135
End Page	146
Type of Use	reuse in a thesis/dissertation
Portion	full article
Format	both print and electronic
Are you the author of this Elsevier article?	Yes
Will you be translating?	No
Title of your thesis/dissertation	On-line and Off-line Enrichment Techniques Combined with Capillary Electromigration Separation Methods in the Analysis of Highly Hydrophilic Analytes in Biological and Environmental Samples
Expected completion date	May 2015



## **5.2. Publication II**

**Determination of urinary nucleosides via borate complexation capillary electrophoresis combined with dynamic pH junction-sweeping-large volume sample stacking as three sequential steps for their on-line enrichment**

**Azza H. Rageh, Achim Kaltz, Ute Pyell**

**Analytical and Bioanalytical Chemistry, 406 (2014) 5877-5895**

[doi: 10.1007/s00216-014-8022-2](https://doi.org/10.1007/s00216-014-8022-2)



### 5.2.1. Summary and discussion

In this publication, a highly sensitive CZE method is developed for the determination of urinary nucleosides in real urine samples accompanied with three consecutive on-line enrichment techniques for nucleoside focusing prior to their analysis. These techniques are dynamic pH junction, sweeping and large volume sample stacking (LVSS). To fulfill the requirements for nucleoside focusing by these techniques, a low conductivity aqueous sample matrix free from borate with a pH different from that of the BGE is employed. The BGE composed of  $42.0 \text{ mg L}^{-1}$  2-hydroxypropyl- $\beta$ -cyclodextrin (2-HP- $\beta$ -CD) in  $40 \text{ mmol L}^{-1}$  sodium tetraborate, pH 9.25. 2-HP- $\beta$ -CD is an additive added to the BGE to permit the baseline separation of the critical peak pair adenosine (Ado) and cytidine (Cyd). By varying the concentration of 2-HP- $\beta$ -CD in the BGE and after normalization of the viscosity changes of the tested BGEs, it is shown that 2-HP- $\beta$ -CD interacts more strongly with Ado than Cyd, which permits their separation.

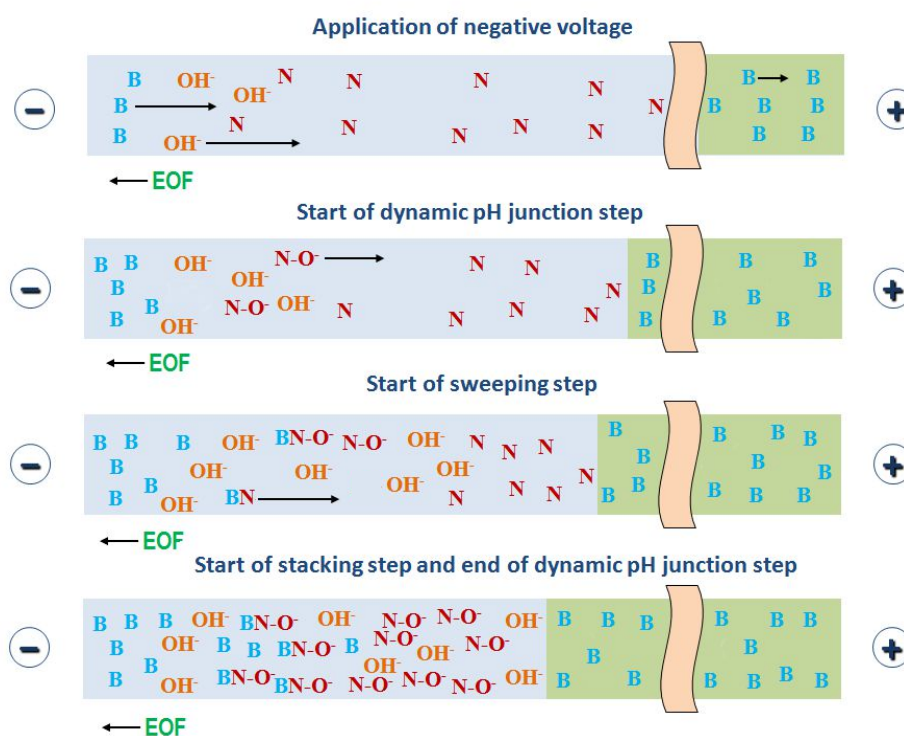


**Figure 2:** Schematic presentation of the developed three-step focusing mechanism (combining dynamic pH junction, sweeping using borate complexation, and LVSS).

A schematic illustration for the suggested mechanism of the whole focusing procedure is given in Fig. 2. Method optimization is carried out by studying the factors that influence the separation and focusing efficiency such as pH and composition of the BGE and the sample matrix, sample injection volume, concentration of borax, concentration of 2-HP- $\beta$ -CD in the BGE, oven temperature and applied voltage. The charge of the nucleoside, the formation constant of the formed tetrahydroborate nucleoside complex, and the electric conductivity and the pH of the sample matrix and the BGE are identified to be

the key parameters determining the focusing efficiency. The enrichment efficiency is shown to be highly dependent on the electrophoretic mobility of the nucleosides, i.e. the higher is the mobility, the higher is the sensitivity enhancement factor (SEF). Method validation is performed for the standard nucleosides (dissolved in water) both without and after their extraction with the commercially available phenylboronate affinity gel (PBA). The extraction procedure has a positive impact on the method detection limits. This is because the ionic constituents remaining in the reconstituted sample after extraction reduce the initial loss of the analyte at the beginning of the negative voltage application. The proposed method is validated according to ICH guidelines and is successfully applied to the analysis of the nucleosides under investigation in blank and spiked urine samples.



### **5.2.2. Author contribution**

The major experimental part of this publication was carried out by me. Method validation and optimization of separation of the standard nucleosides was conducted by M.Sc. A. Kaltz. The draft of the manuscript was written by me and corrected by Prof. Dr. Ute Pyell. The final revision of the manuscript was conducted by me and Prof. Dr. Ute Pyell before submission to the journal. Prof. Dr. Ute Pyell was responsible for the supervision of this work.



# Determination of urinary nucleosides via borate complexation capillary electrophoresis combined with dynamic pH junction-sweeping-large volume sample stacking as three sequential steps for their on-line enrichment

Azza H. Rageh · Achim Kaltz · Ute Pyell

Received: 25 April 2014 / Revised: 20 June 2014 / Accepted: 7 July 2014 / Published online: 29 July 2014

© Springer-Verlag Berlin Heidelberg 2014

**Abstract** The combination of dynamic pH junction, sweeping (using borate complexation), and large volume sample stacking (LVSS) is investigated as three consecutive steps for on-line focusing in the sensitive quantitation of urinary nucleosides by CE-UVD. A low conductivity aqueous sample matrix free from borate and a high conductivity BGE (containing borate, pH 9.25) are needed to fulfill the required conditions for dynamic pH junction, LVSS, and sweeping. Parameters affecting the separation and the enrichment efficiency are studied such as buffer concentration, separation voltage, capillary temperature, sample composition, and sample injection volume. Prerequisite for the developed strategy is the extraction of the nucleosides from urine using a phenylboronate affinity gel, which is described to be a unique means for the selective enrichment of *cis*-diol metabolites under alkaline conditions. The impact of ionic constituents remaining in the eluate after extraction on focusing efficiency and resolution is investigated. The developed method is applied to the analysis of blank and spiked urine samples. Fundamental aspects underlying the proposed enrichment procedure are discussed. A detection limit as low as 10 ng mL<sup>-1</sup> is achieved. To the best of our knowledge, this LOD represents the lowest LOD reported so far for the analysis of nucleosides using CE with UV detection and provides a comparable sensitivity to CE/MS. Because of the high sensitivity, the proposed method shows a great potential for

the analysis of nucleosides in human urine and other types of biological fluids.

**Keywords** Dynamic pH junction · Sweeping via borate complexation · Large volume sample stacking · Urinary nucleosides · Polarity switching · Phenylboronate affinity gel

## Introduction

Nucleosides are metabolites of either RNA's turnover or oxidative damage of DNA. Based on the literature data, nucleosides are a group of potential markers for predicting cancer. This group is composed of unmodified nucleosides such as uridine, cytidine, adenosine, guanosine and their modified derivatives: methylated (5-methyluridine), acetylated (N4-acetylcytidine) or reduced (dihydrouridine) nucleosides [1]. Modified nucleosides mostly exist in transfer RNA (tRNA) and they are formed during posttranscriptional modification by numerous modification enzymes [2]. Modified nucleosides, in contrast to unmodified nucleosides, cannot be reutilized or degraded, but are circulated unchanged in the blood stream and are excreted intact in the urine. Therefore, elevated urinary levels of modified nucleosides are associated with an increased turnover of RNA, which occurs under pathological conditions such as inflammation and cancer. The increasing interest in metabolomics and the diagnostic value of urinary nucleosides highlight the need for appropriate analytical techniques, which should achieve good selectivity, sensitivity, and reproducibility for the determination of these important metabolites.

Nucleosides have been separated and determined using different analytical techniques such as reversed-phase high-performance liquid chromatography (RP-HPLC) [3], hydrophilic interaction chromatography (HILIC) (due to their

**Electronic supplementary material** The online version of this article (doi:10.1007/s00216-014-8022-2) contains supplementary material, which is available to authorized users.

A. H. Rageh · A. Kaltz · U. Pyell (✉)  
Department of Chemistry, University of Marburg,  
Hans-Meerwein-Straße, 35032 Marburg, Germany  
e-mail: pyell@chemie.uni-marburg.de

highly hydrophilic nature) [4], immunoassay [5], and capillary electromigration separation techniques including capillary zone electrophoresis (CZE) [6], capillary electrochromatography (CEC) [7, 8] and micellar electrokinetic chromatography (MEKC) [9–14]. MS-coupled techniques such as CE-MS [15] were also reported. Although CE shows a high sensitivity in terms of absolute amounts even with absorbance detectors, e.g., down to fg-levels; its concentration sensitivity is not very high, e.g., down to the micromolar level, which is attributed mainly to the small volume of sample injected (<1 % of the capillary length) and the short optical path length [16]. To circumvent the poor concentration sensitivity, several approaches have been reported. One possibility is to utilize on-line sample preconcentration techniques such as sweeping, field-enhanced (amplified) sample stacking (FASS), transient isotachopheresis (t-ITP) or dynamic pH junction [16].

Sweeping is an on-line sample concentration technique for neutral and charged analytes [17]. The mechanism relies on the interaction between an additive in the BGE (e.g., the pseudostationary phase (PSP) or a complexing agent) and the analyte in a sample matrix that does not contain this additive [18]. The degree of focusing is dependent on the strength of the interaction involved [18]. Sweeping by borate complexation was reported for the on-line focusing of neutral analytes that possess a *cis*-diol moiety (e.g., catechols, carbohydrates, flavonoid glycosides, nucleosides [19], and catechins [20]). Borate ions interact with the *cis*-diol groups to form anionic or zwitterionic complexes (depending on the charge of the analyte) and hence alter the analyte electrophoretic mobility. The main difference between borate as a sweeping carrier and a separation carrier (also called pseudostationary phase), is that the migration velocity of a separation carrier is virtually unaffected by the interaction with the dissolved solutes [21], whereas the electrophoretic mobility of the borate complex is very different from that of the borate ion.

It is noteworthy to mention that the concentration mechanism with a dynamic pH junction [22] assisted by borate complexation is partly the same as that for sweeping of vicinal diols with borate complexation [23]. In sweeping, the sample solution is void of borate. Here on-line enrichment is accomplished by complexation with borate that enters the sample zone. The difference in pH between the sample zone and the BGE is not essential from the viewpoint of sweeping and the term sweeping can be used for any system where interaction between the analyte and the sweeping carrier is the major mechanism of focusing [23]. However, focusing by dynamic pH junction occurs when the difference in pH between the sample zone and the BGE is essential for narrowing the sample zone (irrespective of the borate content in the sample solution). However, in the present case, both pH difference and difference in the borate concentration (with respect to

sample zone and the BGE compartment) will contribute to the change in the effective electrophoretic mobility of the analyte.

Large volume sample stacking (LVSS) with or without polarity switching is based on stacking with removal of the sample matrix. In LVSS with polarity switching, a large sample volume is injected hydrodynamically into the capillary. A negative voltage is applied to remove the sample matrix plug by pumping it out of the capillary using the electroosmotic flow, while simultaneously maintaining the stacked analytes at the sample/BGE interface, while it moves slowly toward the capillary inlet. This methodology of pumping is applicable only for ions that have a negative mobility with respect to the bulk electroosmotic flow. The polarity of the electrode is reversed at the end of the matrix removal step when the separation is started. To ensure that no analyte is lost during the matrix removal step, the electric current strength is monitored until it reaches 90–99 % of the electric current strength measured when the capillary is entirely filled with BGE.

A summary of the medically relevant concentrations of the studied nucleosides normalized by the concentration of creatinine can be found in [9] and also in the human metabolome data base. The limits of detection (LOD) for CE methods with UV detection for the analysis of urinary nucleosides are reported to be from 3.1 to 74  $\mu\text{mol L}^{-1}$  (Zheng et al. [13]), from 0.17 to 2.3  $\mu\text{mol L}^{-1}$  (Szymanska et al. [9]), from 2.0 to 61  $\mu\text{mol L}^{-1}$  (Liebich et al. [24]), and from 5.4 to 65  $\mu\text{mol L}^{-1}$  [25]. Jiang et al. [26] also reported a fast CE method for the separation of ten different nucleosides present in urine samples employing cetyltrimethyl ammonium bromide as PSP. The achieved LOD ranged from 0.55 to 1.67  $\mu\text{mol L}^{-1}$ . But according to Iqbal et al. [27], limits of detection reported so far for the determination of nucleosides by capillary electromigration separation techniques with UV detection are not sufficient for clinical studies. Therefore, trials to increase the concentration sensitivity for these metabolites especially for the modified ones are of a major concern up to date [28]. The LODs reported in [28] are in the range of 40–170  $\text{ng mL}^{-1}$  (using CE/MS). Britz-McKibbin et al. [29] developed a CE-UV method based on the focusing of nucleotides and nucleosides using a dynamic pH junction assisted by borate complexation. This focusing mechanism generates (even for the late-migrating analytes such as uridine) a short analyte zone (when passing the detector: 0.64 cm) after introduction of an injection plug having a length of 4.0 cm. However, there is no record for the limit of detection [29]. In contrast to the present case, the sample matrix in [29] contains both borate (160  $\text{mmol L}^{-1}$ ) and a high content of sodium chloride (150  $\text{mmol L}^{-1}$ ).

Recently, Iqbal et al. [27] reported a sensitive CE-UV method for the monitoring of nucleoside metabolizing enzymes, whose products are nucleobases or nucleosides. The

employed BGE is 100 mmol L<sup>-1</sup> SDS in 50 mmol L<sup>-1</sup> borate buffer with a pH of 9.1. However, negatively charged nucleosides (highly hydrophilic metabolites) have a negligible interaction with SDS micelles. Even under experimental conditions, at which they are neutral, they have a very low interaction with the micelles formed by SDS and a high concentration of SDS (200 mmol L<sup>-1</sup>) is required for their separation [14]. Iqbal et al. [27] have stated that “the achieved LOD represents the highest sensitivity for nucleoside and nucleobase analysis using CE with UV detection reported so far”. They have used reversed-electrode polarity switching mode-MEKC (REPSM-MEKC) in a 75 μm I.D fused-silica capillary. An about ten-fold enhancement in sensitivity was achieved when compared with CE without stacking [27]. Limits of detection as low as 60 nmol L<sup>-1</sup> were obtained. As borate is highly selective for *cis*-diol complexation, it can be used for the on-line focusing of nucleosides by borate sweeping [19] especially because the complex formation constant between tetrahydroxyborate and nucleosides is very high [14].

Urinary nucleoside analysis using capillary electromigration separation techniques is usually performed in two subsequent steps. The first step involves the extraction of the nucleosides from the urine using a phenylboronate affinity gel (PBA) as solid phase extraction (SPE) stationary phase. The second step is the analysis step, which is commonly performed by MEKC when the nucleosides are in their neutral form and to a lesser extent when they are charged by using either MEKC or CZE. In the present paper, we develop a highly sensitive method for the determination of urinary nucleosides based on this two-step-principle, whereas we performed the extraction according to the procedure described in detail by Gehrke et al. [30]. The phenylboronate-based affinity gel used provides a unique means for the selective enrichment of *cis*-diol containing metabolites. It forms cyclic esters with the vicinal hydroxyl groups of the ribose unit of nucleosides under basic pH conditions. While maintaining the basic conditions, the analytes can be purified from interferences without any loss. When the pH is switched to acidic conditions (by applying an acidic eluent), the analytes are eluted and after evaporating the extract to dryness, the extract can be dissolved in water and analyzed further.

In this paper, we investigate those factors, which influence the focusing efficiency when applying a combination of dynamic pH junction, sweeping with borate complexation and large volume sample stacking. Together with developing a robust reproducible procedure for this type of three-step on-line focusing we optimize the separation conditions including composition of the BGE (borax concentration, concentration of 2-hydroxypropyl-β-cyclodextrin, pH), applied voltage, and capillary temperature. The developed method is validated according

to the ICH guidelines [31]. The sensitivity enhancement factors achieved are determined following a procedure published in a [32]. With several blank and spiked urine samples, we demonstrate the applicability of the proposed strategy.

## Experimental

### Chemicals and background electrolytes

Nucleoside standards cytidine (Cyd), adenosine (Ado), 5-methyluridine (5MeUrd), uridine (Urd), guanosine (Guo), inosine (Ino), xanthosine (Xao) were purchased from Sigma-Aldrich, Steinheim, Germany; their chemical structures are presented in Fig. S1 (Electronic Supplementary Material). Sodium hydroxide was from Fluka, Buchs, Switzerland. Disodium tetraborate decahydrate (borax) and ammonium acetate were from Merck, Darmstadt, Germany. β-Cyclodextrin (97 %), formic acid (98–100 %), sodium chloride and ammonium hydroxide (25 %) were from Sigma-Aldrich, Steinheim, Germany. 2-Hydroxypropyl-β-cyclodextrin (97 %) was from Acros Organics, Geel, Belgium with a degree of substitution of 2 to 6 (located mainly at O(2) position) and the water content is 7.5 % max. Thiourea was from Riedel-de Haën, Seelze, Germany. Thiourea stock solution was 1000 mg L<sup>-1</sup> in water. The Affi-gel 601, used as the stationary phase for the extraction of nucleosides from urine, was purchased from Bio-Rad (Hercules, CA, USA). Methanol, HPLC grade was from VWR-BDH-Prolabo, Leuven, Belgium. Ammonium acetate (0.25 mol L<sup>-1</sup>, pH 8.80) was prepared by dissolving 9.6350 g in 400 mL water and then it was adjusted with concentrated ammonium hydroxide (25 %) to pH 8.80 and then diluting to 500 mL with water.

Stock disodium tetraborate (borax) buffer (100 mmol L<sup>-1</sup>, pH 9.30) was prepared by dissolving 3.8138 g disodium tetraborate decahydrate in 70 mL water and diluting to 100 mL with water. Lower concentrations of borax buffer were prepared by further dilution with water. 16.4 mg mL<sup>-1</sup> β-cyclodextrin (β-CD) in 40 mmol L<sup>-1</sup> borax buffer, pH 9.25 was prepared by dissolving 0.8201 g of β-CD in 30 mL of 40 mmol L<sup>-1</sup> borax buffer and diluting with the same buffer to 50 mL. Different concentrations of 2-hydroxypropyl-β-cyclodextrin (2-HP-β-CD) solutions; 15.0, 30.0, 35.0, 42.0 mg mL<sup>-1</sup> of 2-HP-β-CD in 40 mmol L<sup>-1</sup> borax buffer, pH 9.25 were prepared by dissolving 0.7500, 1.5000, 1.7500 and 2.1000 g, respectively in 30 mL of 40 mmol L<sup>-1</sup> borax buffer and diluting with the same buffer to 50 mL. All buffer solutions were filtered prior to use through a 0.45 μm nylon membrane filter (WICOM, Heppenheim, Germany). To avoid buffer depletion, the BGEs in the inlet and the outlet vials were replaced after every four runs [33].

### Instrumentation

All measurements were done using the ATI Unicam CE System, Crystal 300 Series, Model 310 equipped with a UV/vis detector Spectra 100 (with deuterium lamp) from Thermo Separation Products, San Jose, USA, set to a wavelength of 257 nm (optimized wavelength). Unless otherwise specified the oven temperature was kept at 35 °C. Data acquisition was done using an AD-converter (USB-1280FS, Measurement Computing, Middleborough, USA). Data were recorded using CE-Kapillarelektrophorese software (development of the electronics workshop of the Department of Chemistry, University of Marburg based on Delphi). Data analysis was performed with Origin 8.5 software (OriginLab Corporation, Northampton, USA). Fused silica-capillaries (50.2  $\mu\text{m}$  I.D., 362  $\mu\text{m}$  O.D.) were obtained from Polymicro Technologies (Phoenix, AZ, USA), with a total length of 648 mm and a length to the detector of 500 mm. InoLab pH720 (WTW, Weilheim, Germany) was used for pH measurements. Solid-phase extractions were performed on a vacuum manifold column processor (J.T. Baker, Griesheim, Germany). The flow rate during sample loading and elution is 0.5 mL/min. The eluate obtained after the extraction procedure was lyophilized in a Christ Alpha 2–4 LSC Freeze Dryer (Martin Christ, Osterode am Harz, Germany).

New capillaries were conditioned by flushing them first with NaOH solution (1 mol L<sup>-1</sup>) 25 min, water 25 min, and BGE 5 min using an applied pressure of 800 mbar. At the beginning of each day, the capillaries were rinsed with NaOH solution (0.1 mol L<sup>-1</sup>) 20 min, water 20 min, and BGE 5 min. Between runs the capillaries were rinsed with BGE for 2 min. Because of the acidity of the reconstituted sample matrix after redissolving the lyophilized eluate in water there is a subsequent partial deactivation of the negatively charged silanol groups of the inner capillary wall. Therefore, in the case of the analysis of a sample after elution from a PBA column, the capillaries were rinsed between runs subsequently for 2 min with an aqueous solution of NaOH (1 mol L<sup>-1</sup>), water 2 min, and BGE 2 min to ensure the reproducibility of the migration times. The separations were performed under an applied voltage of +20 kV, unless otherwise specified. The samples were pressure-injected at 120 mbar for 300 s, unless otherwise mentioned. The electroosmotic hold-up time  $t_0$  [34] was determined using thiourea as neutral marker. Electrophoretic mobilities were determined from electropherograms containing a peak of the hold-up time marker. Peak identities are confirmed by spiking.

### Preparation of standard solutions and calibration curves

All single analyte stock solutions (800.0 mg L<sup>-1</sup> of Ado, Cyd, Urd, 5MeUrd, Ino, 400.0 mg L<sup>-1</sup> of Xao, Guo) were prepared in water and stored in the refrigerator (stock solutions of

nucleoside standards are used within one month). The working standard solutions were prepared daily (concentration of each of the studied nucleosides in the sample solution mixture 20 mg L<sup>-1</sup>, unless otherwise specified).

The tested analytes are endogenously present in urine. Therefore, urine is unsuitable for the preparation of the reference samples [35]. As the studied analytes are highly polar, distilled water was used as a surrogate or artificial matrix for the preparation of the standard solutions [9]. The concentration ranges for the investigated analytes are listed in Table 1 for direct injection, and in Table S2 (Electronic Supplementary Material) for injection after extraction with a PBA column. Following optimized method parameters were used: BGE 42.0 mg mL<sup>-1</sup> 2-HP- $\beta$ -CD in 40 mmol L<sup>-1</sup> borax buffer, pH 9.25, capillary 647(499)mm $\times$ 50.2  $\mu\text{m}$  I.D., applied voltage during dynamic pH junction/sweeping/LVSS/sample matrix removal -20 kV, separation voltage +20 kV, capillary temperature 35 °C, pressure injection 120 mbar for 5 min or 600 mbar for 1 min, detection 257 nm. After having filled the capillary with BGE by application of pressure (800 mbar) and before sample injection, the capillary is dipped into a vial containing water (10 mbar for 0.02 min). Calibration curves are constructed by plotting either peak height, peak area, or corrected peak area against the corresponding concentration in  $\mu\text{g}$  per mL.

### Urine samples and extraction conditions

Samples of human urine were obtained from a female 27-year old healthy volunteer and were collected in 100 mL plastic bottles and frozen immediately until analysis. Before use, the samples were thawed at room temperature. For the study of spiked or blank urine samples, sample preparation was performed with a PBA column. The extraction conditions are selected according to previously reported methods [2, 9, 30, 36]. A brief description of the extraction procedure is given in the [Electronic Supplementary Material](#).

## Results and discussion

### Mechanism of dynamic pH junction-sweeping-LVSS

Nucleosides are glycosylamines consisting of a nucleobase linked to a D-ribose sugar unit via beta-glycosidic linkage. The seven investigated nucleosides Ado, Cyd, Urd, 5MeUrd, Guo, Ino, and Xao (abbreviations according to IUPAC-IUB commission on biochemical nomenclature [37]) were selected as model compounds for the development and optimization of the presented on-line focusing strategy. Five of the studied

**Table 1** Linear regression parameters of the developed method for calibration standards injected directly without SPE

	No. of calib. standards ( <i>n</i> )	Linearity range ( $\mu\text{g mL}^{-1}$ )	Intercept ( <i>a</i> ) $\pm$ SD <sup>a</sup>	Slope ( <i>b</i> ) $\pm$ SD <sup>b</sup>	SSE <sup>c</sup>	$S_{yx}$ <sup>d</sup>	$S_{x0}$ <sup>e</sup>	Confidence interval of ( <i>a</i> ) <sup>f</sup>	Confidence interval of ( <i>b</i> ) <sup>f</sup>	$r^g$	Mandel's test value <sup>h</sup>
Ado											
PH <sup>i</sup>	8	0.53–21.3	-0.102 $\pm$ 0.112	0.392 $\pm$ 0.010	0.260	0.208	0.530	$\pm$ 0.417	$\pm$ 0.037	0.9981	2.96
PA <sup>j</sup>	8	0.53–21.3	-1.180 $\pm$ 0.859	2.205 $\pm$ 0.077	15.253	1.594	0.723	$\pm$ 3.185	$\pm$ 0.284	0.9964	12.63
Corr. PA <sup>k</sup>	8	0.53–21.3	-0.130 $\pm$ 0.101	0.264 $\pm$ 0.009	0.210	0.187	0.709	$\pm$ 0.374	$\pm$ 0.034	0.9965	11.00
Cyd											
PH	7	1.02–20.4	-0.123 $\pm$ 0.106	0.226 $\pm$ 0.009	0.142	0.168	0.744	$\pm$ 0.428	$\pm$ 0.038	0.9958	15.31
PA	7	1.02–20.4	-0.698 $\pm$ 0.536	1.169 $\pm$ 0.047	3.620	0.851	0.728	$\pm$ 2.163	$\pm$ 0.188	0.9960	21.11
Corr. PA	7	1.02–20.4	-0.074 $\pm$ 0.061	0.135 $\pm$ 0.005	0.047	0.097	0.716	$\pm$ 0.246	$\pm$ 0.022	0.9961	19.75
5MeUrd											
PH	9	0.40–20.2	0.177 $\pm$ 0.101	0.410 $\pm$ 0.010	0.315	0.212	0.518	$\pm$ 0.355	$\pm$ 0.035	0.9979	5.12
PA	9	0.40–20.2	0.149 $\pm$ 0.393	1.968 $\pm$ 0.039	4.752	0.824	0.419	$\pm$ 1.377	$\pm$ 0.138	0.9986	0.04
Corr. PA	9	0.40–20.2	0.024 $\pm$ 0.043	0.210 $\pm$ 0.004	0.057	0.090	0.429	$\pm$ 0.151	$\pm$ 0.016	0.9985	0.00
Guo											
PH	8	0.21–12.48	0.102 $\pm$ 0.153	1.064 $\pm$ 0.027	0.641	0.327	0.307	$\pm$ 0.566	$\pm$ 0.101	0.9980	13.58
PA	10	0.21–20.80	1.107 $\pm$ 1.142	4.536 $\pm$ 0.117	56.131	2.946	0.584	$\pm$ 3.831	$\pm$ 0.392	0.9974	3.16
Corr. PA	10	0.21–20.80	0.123 $\pm$ 0.118	0.448 $\pm$ 0.012	0.604	0.275	0.614	$\pm$ 0.398	$\pm$ 0.041	0.9971	3.47
Urd											
PH	8	0.20–12.12	0.162 $\pm$ 0.138	0.918 $\pm$ 0.026	0.527	0.296	0.323	$\pm$ 0.513	$\pm$ 0.094	0.9977	13.61
PA	10	0.20–20.20	1.319 $\pm$ 0.991	4.070 $\pm$ 0.104	42.311	2.300	0.565	$\pm$ 3.327	$\pm$ 0.350	0.9974	3.79
Corr. PA	10	0.20–20.20	0.135 $\pm$ 0.097	0.385 $\pm$ 0.010	0.403	0.225	0.583	$\pm$ 0.325	$\pm$ 0.034	0.9972	4.00
Ino											
PH	8	0.10–12.30	0.219 $\pm$ 0.268	1.917 $\pm$ 0.049	1.983	0.575	0.300	$\pm$ 0.992	$\pm$ 0.181	0.9981	11.52
PA	10	0.10–20.50	4.799 $\pm$ 3.011	8.928 $\pm$ 0.312	391.293	6.994	0.783	$\pm$ 10.103	$\pm$ 1.048	0.9951	12.00
Corr. PA	10	0.10–20.50	0.430 $\pm$ 0.264	0.766 $\pm$ 0.027	2.989	0.613	0.800	$\pm$ 0.886	$\pm$ 0.092	0.9949	11.52
Xao											
PH	7	0.05–4.00	0.007 $\pm$ 0.169	3.828 $\pm$ 0.097	0.583	0.342	0.089	$\pm$ 0.682	$\pm$ 0.391	0.9984	1.91
PA	7	0.05–4.00	-0.451 $\pm$ 0.882	25.523 $\pm$ 0.506	15.856	1.781	0.070	$\pm$ 3.557	$\pm$ 2.038	0.9990	0.38
Corr. PA	7	0.05–4.00	-0.029 $\pm$ 0.071	1.844 $\pm$ 0.040	0.101	0.142	0.077	$\pm$ 0.285	$\pm$ 0.164	0.9988	0.67

<sup>a</sup> Standard deviation of the intercept<sup>b</sup> Standard deviation of the slope<sup>c</sup> Sum of square errors<sup>d</sup> Residual standard deviation (standard error of estimate (SEE))<sup>e</sup> Method standard deviation ( $=S_{yx}/b$ )<sup>f</sup> Confidence interval calculated at  $P=0.99$ <sup>g</sup>  $r$  is the correlation coefficient<sup>h</sup> Tabulated  $f$  values at  $P=0.99$  are 12.24, 13.74, 16.25, 21.19 at (df1 (1), df2 ( $n-3$ ))=(1,7), (1,6), (1,5), (1,4), respectively<sup>i</sup> Peak height<sup>j</sup> Peak area<sup>k</sup> Corrected peak area

compounds (Ino, Urd, Guo, Xao, and 5MeUrd) have a  $pK_a$  between 8.80 and 9.70 (except Xao with  $pK_a=5.70$ ) [38] due to the presence of an amidic group. Therefore, these compounds are weak acids. Owing to the presence of a vicinal diol moiety ( $pK_a\sim 12.5$ ) on the ribose unit, these compounds are also capable of forming reversibly complexes with the

tetrahydroxyborate anion under alkaline pH conditions, which enables them to acquire an additional negative charge in addition to the negative charge gained due to dissociation. In contrast to these weak acids, the nucleosides Ado and Cyd acquire a negative charge only by borate complexation. In the following discussion, we will describe borate as a sweeping

carrier. Borate is not a pseudostationary phase, because its electrophoretic mobility is considerably lowered by complexation with a nucleoside.

The focusing mechanism shown in Fig. 1 is given for a nucleoside having a deprotonation site (e.g., Urd). After filling the capillary with a high-conductivity BGE (42.0 mg L<sup>-1</sup> 2-HP- $\beta$ -CD in 40 mmol L<sup>-1</sup> sodium tetraborate, pH 9.25), a large volume of a sample with low electric conductivity (nucleosides are neutral when dissolved in water except Xao) is injected hydrodynamically (Fig. 1a). A significant increase in the detector signal can be observed when the sample/BGE boundary passes the detection window during sample injection. The inlet vial is then replaced by a vial containing the BGE and a negative voltage is applied, whereas the electric current strength is very low due to the increase in resistivity caused by the sample matrix (-0.4  $\mu$ A). At this moment, the direction of the EOF is toward the inlet end and borate and hydroxide ions from the inlet vial migrate toward the outlet end (Fig. 1b). As the sample matrix is an unbuffered solution, hydroxide ions are faster than borate ions. This is very important to permit the presence of borate as tetrahydroxyborate (not boric acid), which is needed for the subsequent sweeping of the nucleosides. Neutral nucleosides are transported together with the sample matrix toward the injection end. Due to the migration of the hydroxide ions, nucleosides (with exception of Cyd and Ado) in the first titrated segment of the capillary acquire a negative charge via dissociation of their amidic group (Fig. 1c, N $\rightarrow$ N-O<sup>-</sup>). Accordingly, nucleosides start migrating in the direction toward the detection end, which results in their focusing by dynamic pH junction. With a lower electrophoretic velocity than hydroxide, borate migrates into the sample zone and starts sweeping the (neutral or negatively charged) nucleosides (Fig. 1d). Borate complexation imparts an additional negative charge due to the formation of a very stable nucleoside-tetrahydroxyborate complex BN-O<sup>-</sup> (Fig. 1d). The focusing by dynamic pH junction ends when the hydroxide ions reach the sample matrix/BGE boundary (Fig. 1e). Simultaneously, the stacking process commences once the deprotonated nucleosides reach sample/BGE boundary. The complexed (neutral or deprotonated) nucleosides migrate across the stacking boundary, where they slow down because of the reduced electric field strength in the BGE zone (Fig. 1f). By completion of the sweeping and stacking processes (Fig. 1g), the sample matrix is almost completely pumped out from the injection end of the capillary. In this moment, the polarity of the applied voltage is reversed (Fig. 1h). This is possible, because the electric current strength had been monitored during matrix removal. The electrode polarity is reversed and the separation starts in the normal polarity mode using an applied voltage of +20 kV, when the electric current strength reaches approximately 95 % of its original value (the electric current strength observed when the whole capillary is filled with BGE). We

describe the resulting combined on-line focusing procedure as a three-step focusing process (focusing with three sequential steps) because firstly the dynamic pH junction step starts, is assisted and accompanied subsequently by sweeping and finally continued by field-amplified stacking.

Experimentally, the polarity is switched when the absolute electric current strength reaches 34.5 $\pm$ 0.3  $\mu$ A (which represents 95 % of the original electric current strength at 20 kV). The time elapsed between the application of the negative voltage (-20 kV) and the application of the positive voltage (+20 kV) is approximately 2.1 min (in case of calibration standards injected directly) or 3.5 min (in case of calibration standards injected after extraction with PBA column). Figure 2 shows electropherograms recorded under optimized separation conditions after (Fig. 2a) and without (Fig. 2b) having carried out a polarity switching step. Without polarity switching, the average bulk electroosmotic velocity is increased and dominated by the low ionic strength sample plug, while the electric field strength in the BGE is strongly reduced. Moreover, the length of the separation compartment becomes very short, whereas the negatively charged nucleosides are stacked at the boundary sample zone/separation compartment. All analytes are recorded close to the end of the sample zone with very low resolution (Fig. 2b).

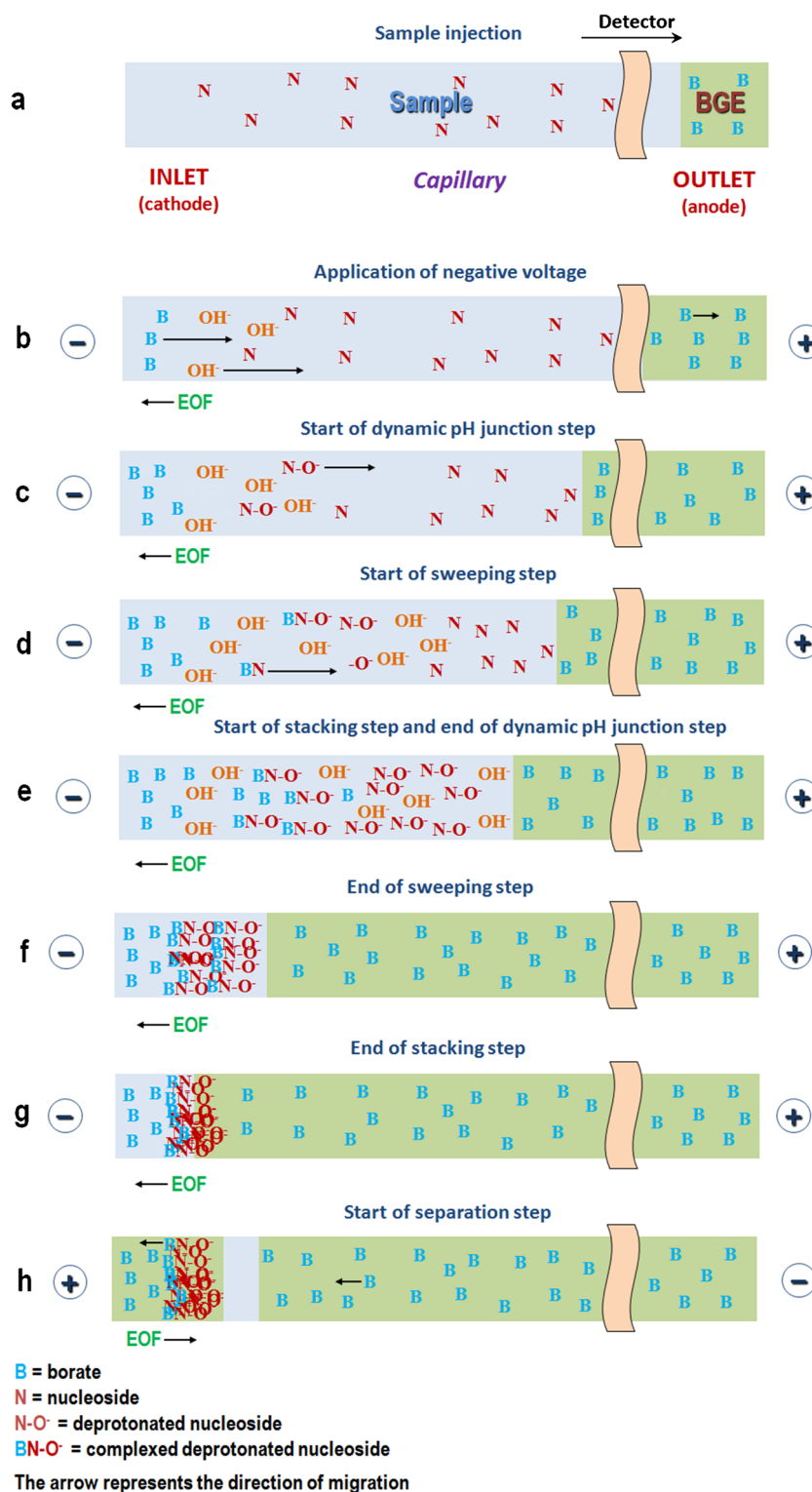
#### Method optimization

##### *Borax concentration*

The effect of the borax concentration (pH=9.25) was investigated with regard to the separation of the nucleosides investigated in a range from 20 to 100 mmol L<sup>-1</sup>. The electropherograms shown in Fig. S2 (Electronic Supplementary Material) illustrate that there is an increase in migration time and resolution with increasing borax concentration. If c(borax) > 60 mmol L<sup>-1</sup>, there is a high electric current strength (>80  $\mu$ A) with associated unfavorable Joule heating. At c(borax)=20 mmol L<sup>-1</sup>, Urd and Guo are not base-line separated. At c(borax)=60 mmol L<sup>-1</sup>, the efficiency of the separation was not further improved with regard to the results obtained with c(borax)=40 mmol L<sup>-1</sup> at the expense of longer migration times. Therefore, 40 mmol L<sup>-1</sup> was selected as optimum borax concentration. At this concentration, the separation of Ado from Cyd is not possible. Here, the use of a secondary complex equilibrium is required as will be discussed later. Moreover, BGEs composed of 40 mmol L<sup>-1</sup> borax with different pH values: 9.25, 9.53, and 9.86 (adjusted using sodium hydroxide) were tested. Because of the adjustment procedure, the electric current strength increased from 41  $\mu$ A (in case of pH 9.25) to 67.5  $\mu$ A (in case of pH 9.86). This increase in ionic strength results in a decrease of the



**Fig. 1** Schematic presentation of the suggested three-step focusing mechanism (combining dynamic pH junction, sweeping using borate complexation, and LVSS). **a** Capillary filled with BGE followed by hydrodynamic injection of an extremely large sample plug. **b** Application of a negative voltage, where EOF is toward the cathode and hydroxide and borate ions migrate toward the anode. **c** Focusing by dynamic pH junction starts where hydroxide ions deprotonate the nucleosides. **d** Borate commences to sweep the nucleosides within the sample zone via complexation. **e** Focusing by dynamic pH junction ends, whereas the deprotonated analytes stacked at the sample matrix/BGE boundary. **f** Nucleosides continue to be accumulated by sweeping and concurrently the sample matrix is pumped out from the injection end. **g** Analytes are completely swept and stacked at the sample matrix/BGE boundary. **h** Polarity is switched and the separation starts

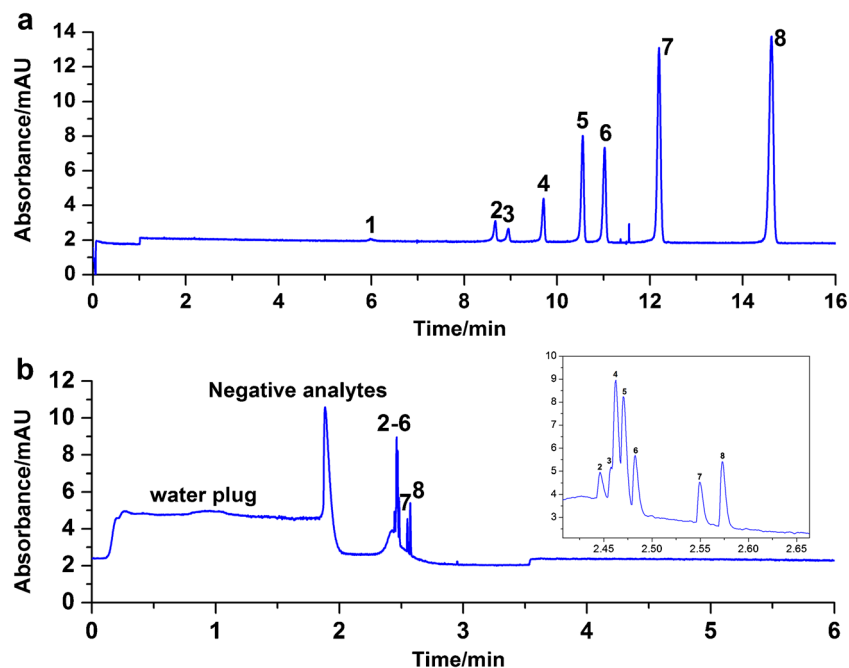


electroosmotic mobility having an unfavorable impact on migration times and efficiency (results are not shown). Based on these observations, a pH of 9.25, which corresponds to the pH reached by the hydrolysis of dissolved borax, was selected as optimum pH.

#### Sample matrix

Focusing by LVSS requires to inject a low conductivity sample into the capillary. We compared the results obtained with water (Condition 1) and with 2.5 mmol L<sup>-1</sup> borax (pH 9.25)

**Fig. 2** Electropherograms obtained with (a) or without (b) polarity switching step. Sample: nucleosides dissolved in water ( $5.0 \text{ mg L}^{-1}$  of each of the studied analytes and  $25.0 \text{ mg L}^{-1}$  thiourea). CE conditions:  $42.0 \text{ mg L}^{-1}$  2-HP- $\beta$ -CD in  $40 \text{ mmol L}^{-1}$  sodium tetraborate, pH 9.25 as BGE, capillary  $648(500) \text{ mm} \times 50.2 \text{ }\mu\text{m}$  I.D., applied voltage during dynamic pH junction/sweeping/LVSS/sample matrix removal  $-20 \text{ kV}$ , separation voltage  $+20 \text{ kV}$ , pressure injection  $120 \text{ mbar}$  for  $5 \text{ min}$ , oven temperature  $35 \text{ }^\circ\text{C}$ . Peak designation: (1) thiourea, (2) adenosine, (3) cytidine, (4) 5-methyluridine, (5) guanosine, (6) uridine, (7) inosine, and (8) xanthosine

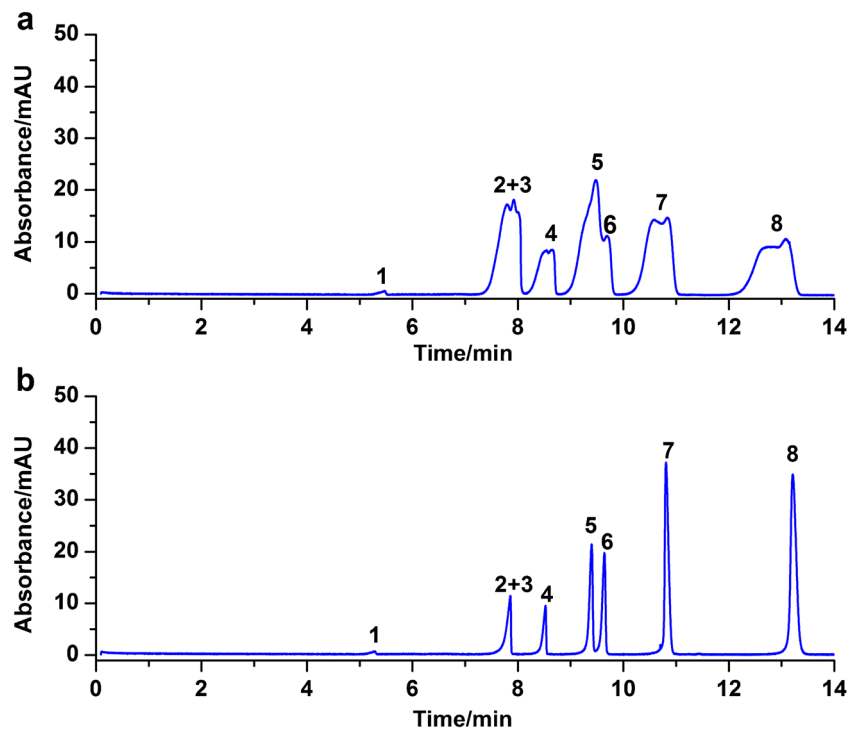


(Condition 2) as sample matrix with the aim to highlight the significant role of dynamic pH junction and sweeping by borate complexation in addition to the degree of focusing resulting from FASS. As can be seen in Fig. 3a, the presence of borate in the sample matrix has a detrimental effect on the peak shape, because under these conditions there is no analyte focusing due to dynamic pH junction and sweeping, while focusing due to FASS is maintained. The significant improvement in efficiency visible in Fig. 3b can be directly attributed

to an improved focusing by a combination of three sequential focusing steps: dynamic pH junction, borate sweeping, and LVSS.

At the beginning of the application of the negative voltage (Condition 1, water as sample matrix (Fig. 3b)), the electric field enhancement will be the lowest because only a small segment of the capillary is filled with BGE. These conditions result in a partial loss of analyte at the start of the focusing process especially of the first migrating nucleosides (Cyd and

**Fig. 3** Electropherograms obtained under identical injection conditions with a sample containing  $20.0 \text{ mg L}^{-1}$  of each of the nucleosides and  $25.0 \text{ mg L}^{-1}$  thiourea in either **a**  $2.5 \text{ mmol L}^{-1}$  sodium tetraborate, pH 9.25 or **b** water. CE conditions:  $40 \text{ mmol L}^{-1}$  sodium tetraborate, pH 9.25 as BGE, other conditions as in Fig. 2a



Ado). As the high-concentration BGE continuously replaces the sample matrix inside the capillary, the electric field strength in the sample zone increases gradually associated with an enhancement of the electrophoretic velocity (toward the detection end) of the (complexed) analytes. Under Condition 2, the presence of borate in the sample zone causes the migration of the nucleosides toward the stacking boundary already at the start of the focusing process, so that there will be no analyte loss in the beginning of the on-line enrichment procedure, which can be confirmed by comparing the recorded peak areas (Fig. 3a). However, focusing by dynamic pH junction and sweeping are not existing under these conditions, reflected by broadened peaks due to volume overload. It should be emphasized that, although the concentration of borate within the sweeping step is very low (Condition 1, water as sample matrix), the degree of borate complexation will be very high. We have confirmed in a previously published work that the complex formation constant between the tetrahydroxyborate ion and the nucleosides is very high [14] so that there will be a high sweeping efficiency even at low borate concentration.

#### *Injection volume, applied voltage, and capillary temperature*

Different injection parameters were tested in order to define the optimum injection volume. As shown in Fig. S3 (Electronic Supplementary Material), filling of almost the whole capillary, i.e. 94 % of the capillary volume, improves the concentration sensitivity for all the investigated nucleosides when compared to that of filling only 16 or 57 % of the capillary (refer to [Electronic Supplementary Material](#) for calculation of the injected sample volume and the sample plug length). Therefore, 120 mbar for 5 min were selected as optimum injection parameters. To reduce the analysis time 600 mbar for 1 min are applied in the analysis of the spiked urine samples. Separation voltage and oven temperature are set to 20 kV and 35 °C (optimization of these parameters with regard to resolution and efficiency, data not shown).

#### *Concentration of 2-hydroxypropyl- $\beta$ -cyclodextrin*

$\beta$ -CD was previously reported to form an inclusion complex with adenine (the nucleobase of adenosine), which can be used to separate adenine from thymine [39]. Moreover, the complex formation constant between Ado and  $\beta$ -CD or its hydroxyalkylated derivative was reported to be higher than that of  $\alpha$ -CD [40]. This difference might be attributed to the small cavity size of  $\alpha$ -CD and the good size matching between adenosine and the cavity of  $\beta$ -CD. Another study performed by Kawamura [41] indicates that the complexation of adenosine nucleotides with  $\beta$ -CD is stronger than that with  $\alpha$ -CD or  $\gamma$ -CD. Tadey and Purdy [42] separated a mixture of 12 monophosphorylated nucleotides using a buffer containing

20 mmol L<sup>-1</sup> borate-10 mmol L<sup>-1</sup>  $\beta$ -CD. Chen and co-workers [43] have employed  $\beta$ -CD as additive to separate Ado from Cyd.

Because of the low solubility of  $\beta$ -CD in water (18.0 mg mL<sup>-1</sup> at 25 °C), the used concentration of 16.4 mg mL<sup>-1</sup> (employed when optimizing the sample injection volume, see Fig. S3, Electronic Supplementary Material) represents the highest possible concentration. At this concentration of  $\beta$ -CD, there is no baseline separation of the critical peak pair (Ado and Cyd) under dynamic pH junction-sweeping-LVSS conditions. The developed focusing strategy imposes higher demands on the separation than methods without a focusing step [39, 41–43]. Because of its higher solubility in water (330.0 mg mL<sup>-1</sup> at 25 °C), we have selected 2-HP- $\beta$ -CD as complex forming additive in further experiments. As depicted in Fig. 4a, a BGE containing 42.0 mg mL<sup>-1</sup> 2-HP- $\beta$ -CD in 40 mmol L<sup>-1</sup> borax buffer, pH 9.25 permitted the complete baseline separation of Ado and Cyd also under dynamic pH junction-sweeping-LVSS conditions.

The charge-to-size ratio after the complexation of Ado with 2-HP- $\beta$ -CD is reduced (with respect to Ado), which accounts for the lower electrophoretic mobility and shorter migration time of this compound when compared to experiments done without using 2-HP- $\beta$ -CD. The effect of different concentrations of 2-HP- $\beta$ -CD on the effective electrophoretic mobility  $\mu_{\text{eff}}$  of the nucleosides is depicted in Fig. 4a. The decrease of  $\mu_{\text{eff}}$  of the tested nucleosides is due to the formation of an inclusion complex in addition to the increase in the viscosity of the BGE with increasing 2-HP- $\beta$ -CD concentration. In order to demonstrate the effect of buffer viscosity on  $\mu_{\text{eff}}$ , (i) the effective electrophoretic mobility of all nucleosides is first calculated without taking into account the viscosity change and (ii) in a second step  $\mu_{\text{eff}}$  is calculated while taking into account the viscosity change induced by adding 2-HP- $\beta$ -CD to the BGE.

The viscosity correction factor is calculated from the migration time of a non-interacting marker, which is assumed to be equally affected as the analyte by the altered viscosity of the BGE [44]. We also assume that the dielectric constant of the BGE is not significantly affected by the addition of 2-HP- $\beta$ -CD [45]. Employing thiourea as non-interacting marker (not incorporated into the cavity of 2-HP- $\beta$ -CD), the viscosity correction factor can be obtained by dividing the observed mobility of thiourea (which is equal to the electroosmotic mobility) at  $c(2\text{-HP-}\beta\text{-CD})=0$  mmol L<sup>-1</sup> by the observed mobility of thiourea at each concentration of 2-HP- $\beta$ -CD. This factor is then multiplied with  $\mu_{\text{eff}}$  measured in (i). Figure 4a, b show the calculated mobility before (Fig. 4a) and after using (Fig. 4b) the viscosity correction factor. After normalization on the viscosity effects, it is now clear from Fig. 4b that the observed decrease in the mobility of Ado by increasing the 2-HP- $\beta$ -CD concentration is due to the influence on the degree of complexation. There is also a slight improvement in the resolution between Urd and Guo, which

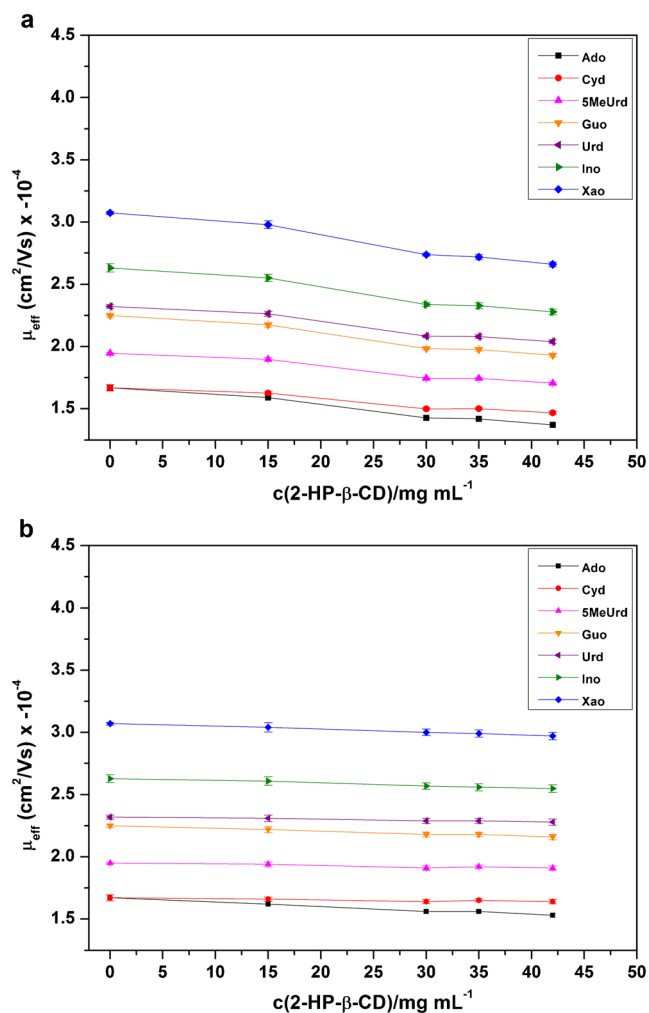


**Fig. 4** Effect of the concentration of 2-HP-β-CD on the effective electrophoretic mobility without (a) or with (b) taking into account the viscosity correction factor. Each data point is the average of at least four measurements (standard deviation represented as *error bar*). The standard deviations in **b** are calculated from the corresponding standard errors by applying the rules for error propagation [55]. Sample solution is 20.0 mg L<sup>-1</sup> of each of the investigated nucleosides and 25.0 mg L<sup>-1</sup> thiourea in water. CE conditions: as in Fig. 2a. For analyte abbreviations, refer to the “Experimental” section

can be ascribed to the inclusion of Guo into the cavity of 2-HP-β-CD. These findings are in agreement with what was previously published regarding the interaction between deoxyribonucleotides and 2-HP-β-CD [45]. According to [42, 45], the complexation of CD is stronger with purine nucleotides than pyrimidine nucleotides as pyrimidine nucleotides are smaller in size. Ado and Guo are examples of purine nucleosides and Cyd and Urd are examples of pyrimidine nucleosides.

#### Extraction of nucleosides using a phenylboronate affinity gel

After extraction of the nucleosides from either blank or spiked urine samples with a phenylboronate affinity gel (for

description of extraction and elution procedure, see [Electronic Supplementary Material](#)), the eluate after freeze drying was reconstituted in 2 mL water (the same volume as the starting urine sample volume). In our case, extraction constitutes only a clean-up step. It was not employed for off-line sample concentration. Redissolving the eluate after lyophilization in 0.2 mL water (sample extract is then 10 times concentrated compared to the starting urine sample volume) results in a matrix with a conductivity approximately half of that of the BGE, a situation that contradicts the prerequisite of the developed enrichment strategy. In addition, trials to avoid the lyophilization step (with the aim to reduce the total analysis time) by employing only vacuum drying showed that this is impossible because of the high concentration of formic acid, which remains in the final extract. Even with the lyophilization step, it was impossible to remove completely formic acid from the eluate.

The remaining formic acid (in the dried extract after lyophilization) results in an acidic sample matrix (pH 4.44–5.90). However, this has no measurable influence on the enrichment efficiency which we confirmed by comparing the results obtained with synthetic sample solutions containing different formic acid concentrations (0–40 μmol L<sup>-1</sup>). In all cases, the electric current strength was very low (–0.4 μA) at the start of the enrichment procedure.

It is important to note that we have observed that ions remaining in the sample extract after the lyophilization step (these ions can be either the ions present in urine or brought in by the washing solutions such as sodium (Na<sup>+</sup>), potassium (K<sup>+</sup>), chloride (Cl<sup>-</sup>), magnesium (Mg<sup>2+</sup>), calcium (Ca<sup>2+</sup>), ammonium (NH<sub>4</sub><sup>+</sup>), sulfates (SO<sub>4</sub><sup>2-</sup>), phosphates (e.g., PO<sub>4</sub><sup>3-</sup>) and urates) have a positive effect on the enrichment efficiency, especially on that of the first migrating nucleosides (Ado, Cyd, 5MeUrd). Congruent with the developed scheme of the three-step enrichment procedure (see Fig. 1), we assume following reason: the reduction in the EOF velocity due to the increase in the ionic strength in the sample compartment decreases the initial loss of these analytes in the initial period of the matrix removal process. In addition, there will be some improvement in the stacking efficiency in the presence of a low salt concentration in the sample zone associated with the reduced difference in the electroosmotic velocities (which is causing a partial laminar flow due to intersegmental pressure differences). In Fig. 5, electropherograms obtained with a sample solution containing the studied nucleosides dissolved in water and injected directly into the capillary (current at start of matrix removal is –0.4 μA (Fig. 5b)) are compared to those electropherograms, which have been obtained after extraction with a PBA column and reconstitution after lyophilization in water with a sample containing the nucleosides at identical concentration (current at the start of matrix removal is –1.9 μA (Fig. 5a)). From Fig. 5, it can be deduced that there is an improvement in the concentration sensitivity by

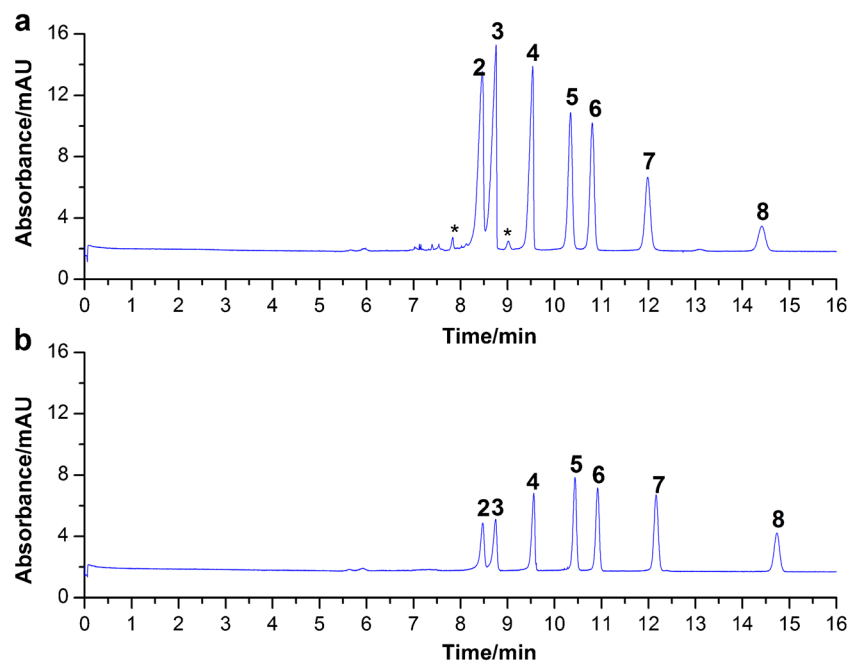


**Fig. 5** Electropherograms obtained under dynamic pH junction/sweeping/LVSS conditions using (a) nucleosides extracted on PBA column and reconstituted in water or (b) nucleosides dissolved in water and injected in CE directly. Sample solution is  $8.0 \text{ mg L}^{-1}$  of Ado and  $5 \text{ MeUrd}$ ,  $16.1 \text{ mg L}^{-1}$  Cyd,  $4.1 \text{ mg L}^{-1}$  Guo,  $4.0 \text{ mg L}^{-1}$  Urd,  $2.0 \text{ mg L}^{-1}$  Ino,  $1.0 \text{ mg L}^{-1}$  Xao. CE conditions:  $42.0 \text{ mg L}^{-1}$  2-HP- $\beta$ -CD in  $40 \text{ mmol L}^{-1}$

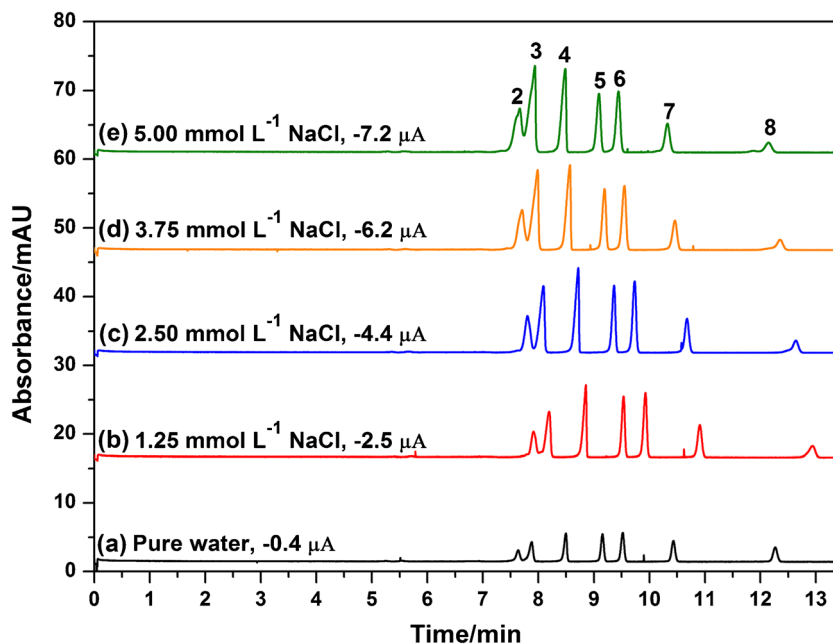
sodium tetraborate, pH 9.25 as BGE, capillary  $648(500) \text{ mm} \times 50.2 \text{ }\mu\text{m}$  I.D., applied voltage during dynamic pH junction/sweeping/LVSS/sample matrix removal  $-20 \text{ kV}$ , separation voltage  $+20 \text{ kV}$ , pressure injection  $600 \text{ mbar}$  for  $1 \text{ min}$ , oven temperature  $35 \text{ }^\circ\text{C}$ . Peak designation: see Fig. 2.\*impurity.

comparing the peak areas of the nucleosides in Figs. 5a, b. Xao is the only compound that is negatively affected by ionic constituents in the sample matrix as will be discussed in detail later.

In order to confirm this observation, we have imitated the conditions resulting in the electropherograms shown in Fig. 5a and prepared samples with different concentration of sodium

chloride to imitate the presence of ionic constituents in the sample extract. The resulting electropherograms are given in Fig. 6. The comparison clearly shows that there is an improvement of the peak area and peak height for all of the investigated nucleosides (with the exception of Xao) at  $c(\text{Cl}^-) = 1.25 \text{ mmol L}^{-1}$  (Fig. 6b) relative to pure water (Fig. 6a), which can be ascribed to the improvement of the stacking efficiency.

**Fig. 6** Electropherograms obtained at different concentrations of sodium chloride in the sample solutions with the values of the current at the start of the matrix removal step at each concentration level. Nucleosides concentrations are  $4.0 \text{ mg L}^{-1}$  of Ado,  $8.0 \text{ mg L}^{-1}$  5MeUrd,  $16.1 \text{ mg L}^{-1}$  Cyd,  $4.1 \text{ mg L}^{-1}$  Guo,  $4.0 \text{ mg L}^{-1}$  Urd,  $2.0 \text{ mg L}^{-1}$  Ino,  $1.0 \text{ mg L}^{-1}$  Xao. CE conditions and peak designation: see Fig. 5



By increasing  $c(\text{Cl}^-)$  to  $2.50 \text{ mmol L}^{-1}$  (Fig. 6c), there is some further increase in the peak heights and areas for 5MeUrd, Urd, Guo, and no further improvement for Ino, while there is a considerable improvement for Ado and Cyd as these compounds are those, which are most subjected to loss during matrix removal. With  $c(\text{Cl}^-)=3.75$  and  $5.00 \text{ mmol L}^{-1}$  (Fig. 6d, e) there is still an increase in the peak height and area for Ado and Cyd, but because of additional band broadening the resolution for this peak pair is decreased, while there is decrease in the peak efficiency for all of the investigated analytes.

It is important to state that the developed three step on-line focusing technique tolerates a variation in the electric current strength at the start of the matrix removal process (related to a varied electric conductivity of the injected pre-treated sample) in the range of  $-1.4$  to  $-5.1 \mu\text{A}$  without having an impact on the quantitative result. This was confirmed by a separate experiment conducted with artificial samples (nucleosides in water), which were extracted with PBA column. We have observed an excellent linearity of the calibration function for all analytes investigated (as will be shown in detail later), although the recorded electric current strength at the start of the matrix removal was differing between  $-1.4$  and  $-5.1 \mu\text{A}$ .

Analytical performance characteristics of the developed method

#### Assessment of linearity

The developed method was validated according to the International Conference on Harmonisation (ICH) guidelines on the validation of analytical methods [31]. In order to determine the linearity of the developed method, five to nine calibration standards of the studied nucleosides (four replicates each) were taken to construct the calibration curves. Peak height, peak area or corrected peak area (peak area/migration time) are used as the response factors to obtain the calibration curves. As stated by the ICH guidelines [31], the correlation coefficient  $r$ , the  $y$ -intercept  $a$ , the slope of the regression line  $b$ , and the sum of squared errors SSE are required for the evaluation of linearity. The previously mentioned parameters in addition to the linearity range, the standard deviation of the intercept and the slope, the standard deviation of the residuals  $S_{yx}$ , the confidence interval of the slope and the intercept, and the method standard deviation  $S_{x0}$  are listed in Table 1 and Table S2 (Electronic Supplementary Material). The correlation coefficient  $r$  of the calibration curve is higher in all cases than 0.9944. Despite the widespread use of the correlation coefficient as a measurement of linearity, its use for the assessment of linearity may be misleading or even discouraged [46–48]. Therefore, beside the determination of correlation coefficients, the linearity was assessed by carrying

out Mandel's fitting test [49]. Mandel's test needs at least seven calibration levels to be applied [49]. By applying Mandel's test at  $P=0.99$ , all Mandel's test values are lower than the critical  $F$  values (Table 1 and Table S2 (Electronic Supplementary Material)), which indicates that the chosen linear regression model adequately fits the data. As recommended by the ICH guidelines [31], plots of the calibration data in addition to plots of the residuals are included in the Electronic Supplementary Material (Figs. S4 and S5).

The residuals were examined visually by inspection of their plot against  $x$  (independent variable) and by carrying out a David [49] and a Neumann test [49]. As shown in Figs. S4b and S5b (Electronic Supplementary Material), the residuals are randomly distributed within a horizontal band. All test values are inside the boundaries of the David table at  $P=0.99$  (residuals are normally distributed) and all test values are larger than the critical limits tabulated by Neumann (no trend). Suspicious outliers in the residual plot are subjected to an  $F$  test ( $P=0.99$ ) [49]. None of the test values exceeds the critical  $F$  value, so that all data points have to be included in the calibration data set.

As shown in Table 1 and Table S2 (Electronic Supplementary Material), the linearity range in most cases is wider (higher upper limit of the linearity range) when using the peak area or the corrected peak area compared to that when using the peak height. The reason is that the use of the peak height leads to nonlinear calibration functions (can be well approximated by a parabolic function) because of overload (electrophoretic dispersion) at higher sample concentration [48, 50]. It should also be mentioned that the use of the corrected peak area (to counteract the variation in observed velocity) is not providing a significant improvement with regard to the uncorrected peak area (decision based on a comparison of correlation coefficients, see Table 1 and Table S2 (Electronic Supplementary Material)). This result can be attributed to the high reproducibility of the migration times and the very good precision of the injection system.

#### Limits of detection and limits of quantitation

The signal-to-noise ratio is calculated (according to the European Pharmacopoeia [51]) using the following expression:

$$S/N = \frac{2H}{h_n} \quad (1)$$

where  $H$  is the height of the peak, related to the average base signal (base line) calculated from the distance between the maximum of the peak to the extrapolated base line of the signal observed over a distance equal to twenty times the width at half-height ( $w_{0.5}$ ).  $h_n$  is the maximum spread of the

base line signal observed over a distance equal to 20 times the width at half-height of the peak.

Limits of detection and limits of quantitation are then defined as the concentration, which guarantees a signal to noise ratio ( $S/N$ ) of 3 or 10, respectively. As listed in Table 2, the limits of detection and quantitation for the nucleoside standards injected directly (without SPE) are in the range from 0.017 to 0.255  $\mu\text{g mL}^{-1}$  and 0.050–1.020  $\mu\text{g mL}^{-1}$ , respectively. These values are further lowered after extraction of the nucleosides with the PBA column due to the ionic constituents of the sample matrix as explained before (LOD and LOQ are then in the range of 0.010–0.040  $\mu\text{g mL}^{-1}$  and 0.041–0.161  $\mu\text{g mL}^{-1}$ , respectively). Cyd has the highest LOD as for this compound the chosen wavelength is not at the optimum (selected wavelength is a compromise between the absorbance maxima of the analytes). A lower LOD could be obtained for Cyd, if the wavelength would be adjusted to 272 nm [38]. The achieved LODs of the developed method (including sample pretreatment by SPE) are up to more than two orders of magnitude lower than those obtained by previously published methods [6, 9, 13, 24–28] (see Table S3, Electronic Supplementary Material). Those values listed in Table 2 represent the lowest LODs and LOQs reported so far for the analysis of nucleosides using CE with UV detection. In Fig. 7, electropherograms are presented which are obtained from synthetic samples (solutes dissolved in water) with analyte concentrations near the LOD either (a) injected directly (instrumental LOD) or (b) after sample pretreatment by SPE (method LOD).

### Precision

The repeatability of migration times, peak heights and peak areas (intra-day variation) were measured for the developed optimized method with nine replicate injections of a sample containing 12.8, 12.2, 12.1, 8.3, 8.1, 6.2, 2.0  $\text{mg L}^{-1}$  of Ado, Cyd, 5MeUrd, Guo, Urd, Ino, and Xao, respectively. The inter-day variation was evaluated by analyzing the same sample over a period of 3 days. Precision was expressed as RSD (%).

As given in Table 3, the repeatability of the migration times for all nucleosides is  $\leq 0.73$  and 0.93 % for intra- and inter-day precision, respectively. The highest values for RSD (%) of the peak height and peak area (intra-day precision) are 2.1 and 2.8 %, respectively. For inter-day precision, all RSD (%) values are lower than 4.7 and 4.6 % for the peak height and the peak area, respectively, which indicates a good reproducibility of the proposed enrichment procedure. Rinsing the outer wall of the capillary (after BGE injection and before sample injection) by immersing the inlet-end into a vial containing water is an important step to maintain the reproducibility and the stacking efficiency (especially with extremely diluted samples). Without this step RSD values up to 14.9 % (Cyd), 15.2 % (Ado), and 1.4 % (Xao) for intra-day variation of peak height, peak area, and migration time, respectively were obtained. This effect can be explained by the observation that buffer adhering to the outer wall of the capillary might contaminate the sample solution during the injection step [52]. Moreover, to ensure reproducible results, the BGE should be replenished every two to four runs.

**Table 2** Limit of detection and limit of quantitation

	M. wt (g mol <sup>-1</sup> )	LOD <sup>a</sup> ( $\mu\text{g mL}^{-1}$ )	LOD <sup>a</sup> ( $\mu\text{mol L}^{-1}$ )	LOQ <sup>b</sup> ( $\mu\text{g mL}^{-1}$ )	LOQ <sup>b</sup> ( $\mu\text{mol L}^{-1}$ )	LOD <sup>c</sup> ( $\mu\text{g mL}^{-1}$ )	LOD <sup>c</sup> ( $\mu\text{mol L}^{-1}$ )	LOQ <sup>d</sup> ( $\mu\text{g mL}^{-1}$ )	LOQ <sup>d</sup> ( $\mu\text{mol L}^{-1}$ )	Improvement in concentration sensitivity based on PA ratio in Fig. 5 <sup>e</sup>
Ado	267.24	0.107	0.40	0.530	1.98	0.020	0.07	0.080	0.30	4.5
Cyd	243.22	0.255	1.05	1.020	4.19	0.040	0.16	0.161	0.66	4.6
5MeUrd	258.23	0.101	0.39	0.404	1.56	0.020	0.08	0.080	0.31	2.8
Guo	283.24	0.052	0.18	0.208	0.73	0.010	0.04	0.041	0.14	1.8
Urd	244.20	0.051	0.21	0.202	0.83	0.010	0.04	0.040	0.16	1.8
Ino	268.23	0.025	0.09	0.103	0.38	0.010	0.04	0.040	0.15	1.2
Xao	284.23	0.017	0.06	0.050	0.18	0.021	0.07	0.103	0.36	-1.1 <sup>f</sup>

<sup>a</sup> Limit of detection of the developed method without applying the calibration standards (dissolved in water) to the PBA column

<sup>b</sup> Limit of quantitation of the developed method without applying the calibration standards (dissolved in water) to the PBA column

<sup>c</sup> Limit of detection of the developed method after extracting the calibration standards with PBA column and reconstitution in water

<sup>d</sup> Limit of quantitation of the developed method after extracting the calibration standards with PBA column and reconstitution in water

<sup>e</sup> It was difficult to calculate the improvement in detection sensitivity based on LOD ratio due to the lamp exchange and different base line noises (see Fig. 7), therefore the peak area ratio in Fig. 5 was used for comparison

<sup>f</sup> The negative sign indicates no improvement in the LOD for Xao and it implies that the LOD is reduced by a factor equal to 1.1

## Application to human urine samples

The proposed extraction–enrichment procedure was applied to the analysis of nucleosides in urine from a healthy volunteer. If the urine sample is reconstituted after extraction in 2 mL water, the electric current strength at the start of the matrix removal is above  $-5 \mu\text{A}$ , which results in an incomplete resolution for Ado and Cyd. By reconstitution of the lyophilized eluate in a larger volume of water, the electric current strength at the start of matrix removal step can be reduced to a value between  $-1.4 \mu\text{A}$  and  $-5.1 \mu\text{A}$ . As demonstrated in Fig. 8a, the proposed enrichment strategy can then be applied successfully for the determination of nucleosides in urine. Here, the eluate (after extraction) was diluted two times relative to the original urine sample volume (sample was reconstituted in 4 mL water), so that the current at the start of the matrix removal step was  $-3.1 \mu\text{A}$ . Figure 8b shows an electropherogram with the same eluate which was off-line concentrated ten-fold to the original urine sample volume (sample was reconstituted in 0.2 mL water). Consequently, the nucleoside concentration in the injected sample in Fig. 8b is 20-fold higher than that in Fig. 8a. This comparison clearly demonstrates that the proposed on-line enrichment procedure surpasses the off-line pre-treatment procedure with regard to provided concentration efficiency even under the most unfavorable conditions. Based on a previous report [9], we assume that the peak marked with (?) can be ascribed to pseudouridine, which is the most predominant modified nucleoside in tRNA.

With the aim to show that the enrichment procedure developed is applicable to the analysis of real urine samples, three different blank unspiked urine samples were analyzed. These

**Table 3** Intra- and Inter-day precision of the developed method

	Intra-day precision ( $n=9$ ), RSD <sup>a</sup> (%)			Inter-day precision, 3 days ( $n=26$ ), RSD (%)		
	MT <sup>b</sup>	PH <sup>c</sup>	PA <sup>d</sup>	MT	PH	PA
Ado	0.63	2.1	1.6	0.86	2.7	2.5
Cyd	0.64	2.0	2.8	0.87	3.2	3.0
5MeUrd	0.68	1.4	0.97	0.89	4.3	3.6
Guo	0.70	0.76	0.95	0.90	2.6	2.4
Urd	0.73	0.52	0.93	0.92	4.7	4.5
Ino	0.70	0.58	1.1	0.89	4.4	4.6
Xao	0.63	1.5	2.0	0.82	3.9	3.0

<sup>a</sup> Relative standard deviation

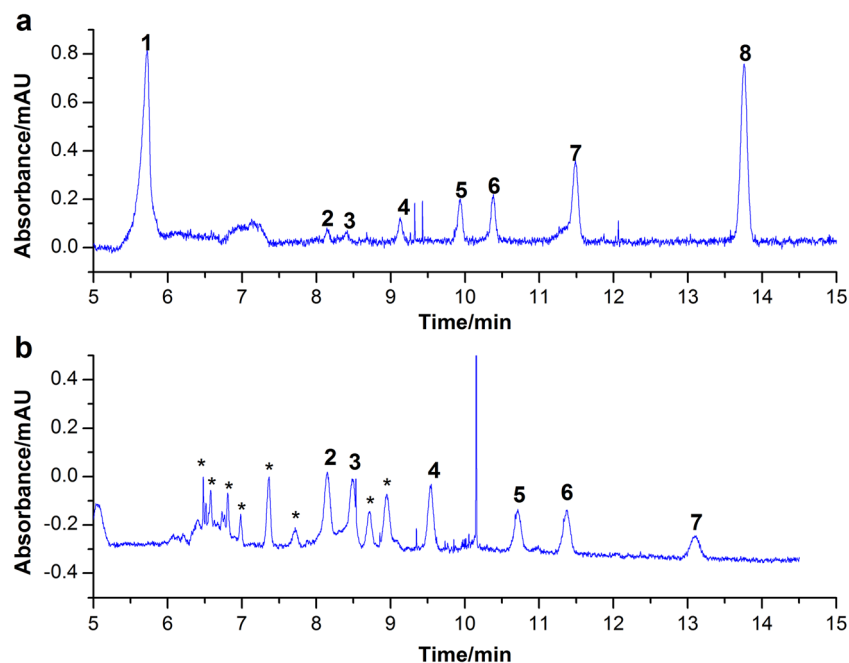
<sup>b</sup> Migration time

<sup>c</sup> Peak height

<sup>d</sup> Peak area

extracted samples were reconstituted in three different volumes of water (relative to the original urine sample volume) prior to their analysis by CE. The electropherograms given in Fig. 9 (absorbance scale is not identical) demonstrate that the proposed enrichment strategy can be successfully applied to the analysis of nucleosides in urine if the extracts from the PBA columns are diluted appropriately. In Fig. 9a, an electropherogram is shown for an extract that was reconstituted in 2 mL water (resulting in a concentration identical to that of the original urine sample). With this sample, the current at the start of the matrix removal step was  $-13.5 \mu\text{A}$ . These unfavorable conditions preclude a good resolution between Ado and Cyd. However, other analytes are focused and can be

**Fig. 7** Electropherograms obtained close to the LOQ/LOQ under dynamic pH junction/sweeping/LVSS conditions using (a) nucleosides dissolved in water and injected in CE directly or (b) nucleosides extracted on PBA column and reconstituted in water. Sample solution in (a) is  $0.20 \mu\text{g mL}^{-1}$  of all of the investigated nucleosides and in (b)  $0.16 \mu\text{g mL}^{-1}$  Ado and  $5 \text{ MeUrd}$ ,  $0.32 \mu\text{g mL}^{-1}$  Cyd,  $0.08 \mu\text{g mL}^{-1}$  Guo and Urd,  $0.04 \mu\text{g mL}^{-1}$  Ino. Xao conc. in (b) is below the LOD. Other CE conditions and peak designation as in Fig. 5. \*-unidentified peak





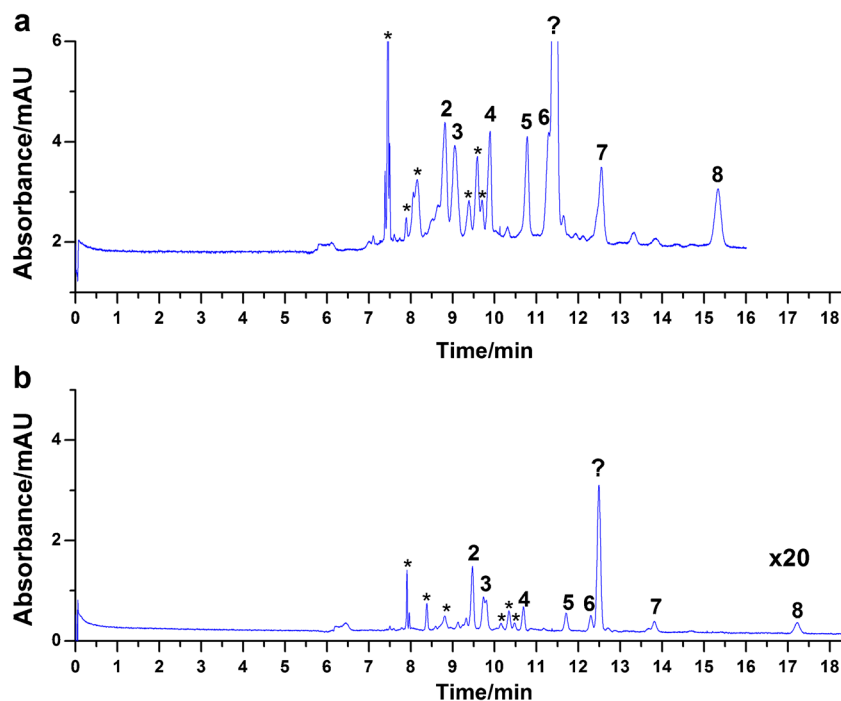


**Fig. 8** Electropherograms of a spiked urine sample obtained under **a** dynamic pH junction/sweeping/LVSS conditions or **b** conventional injection conditions. Concentration of nucleosides in the injected sample in **a** is 20-fold less than that in **b**. Nucleoside concentrations added are  $0.8 \mu\text{g mL}^{-1}$  Ado, Cyd and 5MeUrd,  $0.40 \mu\text{g mL}^{-1}$  Urd and Guo,  $0.20 \mu\text{g mL}^{-1}$  Ino and Xao  $\mu\text{g mL}^{-1}$ . CE conditions:  $42.0 \text{ mg L}^{-1}$  2-HP- $\beta$ -CD in

$40 \text{ mmol L}^{-1}$  sodium tetraborate, pH 9.25 as BGE, capillary 648(500) mm  $\times$   $50.2 \mu\text{m}$  I.D., separation voltage +20 kV, pressure injection 600 mbar for 1 min (**a**) or 30 mbar for 0.2 min (**b**), oven temperature  $35 \text{ }^\circ\text{C}$ . In case of **a** applied voltage during dynamic pH junction/sweeping/LVSS/sample matrix removal  $-20 \text{ kV}$ . Peak designation: see Fig. 2. \*unidentified peak, ?pseudouridine

determined with excellent sensitivity: Guo, pseudouridine, Ino, and Xao. The modified nucleoside 5MeUrd has a concentration below the detection limit. Its presence is associated

with an increasing RNA's turnover. The concentration of Xao is already in the overload region and its peak starts to split.

**Fig. 9** Analysis of blank unspiked urine samples using the developed enrichment procedure. Urine samples are reconstituted after extraction with the PBA column in **a** 2 mL, **b** 4 mL, **c** 8 mL water. For experimental details, CE conditions, and peak designation: see Fig. 8a. \*unidentified peak, ?pseudouridine

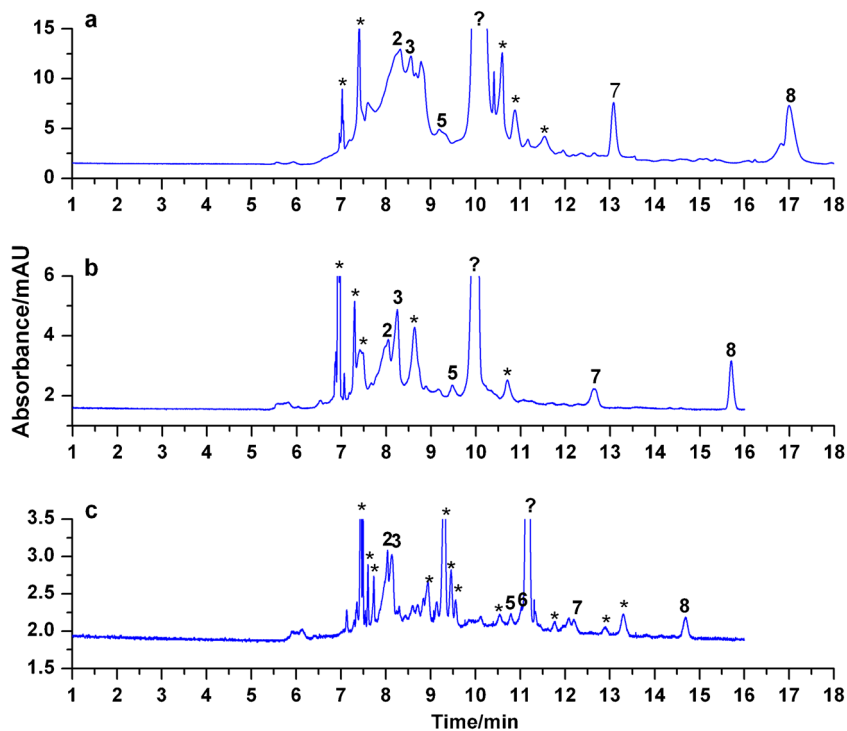


Figure 9b shows the electropherogram obtained for another urine sample. Here, after extraction with a PBA column, the extract was reconstituted in 4 mL water (two-fold dilution relative to the original concentration). The current at the start of the matrix removal step was  $-8.5 \mu\text{A}$ . The resolution between Ado and Cyd is improved and Xao can be easily quantified (without splitting). For Fig. 9c, the extract from the PBA column was reconstituted in 8 mL water (four-fold dilution relative to the original concentration). Here, the current at the start of the matrix removal step was  $-1.4 \mu\text{A}$ . This electropherogram shows the ability of the enrichment procedure to quantify selected nucleosides and to detect all of the studied nucleosides (including Urd). As expected, the sample does not contain a detectable quantity of 5MeUrd. For clinical studies, the resulting nucleoside concentration must be normalized on the creatinine concentration, which has to be determined simultaneously in the same urine sample.

#### Sensitivity enhancement factor

To allow a better understanding of the enrichment procedure, the following investigations were made with standards dissolved in water. In Fig. S6 (Electronic Supplementary Material) two electropherograms are compared: (a) obtained under dynamic pH junction-sweeping-LVSS conditions and (b) obtained with conventional injection conditions. However, the determination of the sensitivity enhancement factor by simply calculating the ratio of the peak height obtained under sample enrichment conditions to that obtained under conventional injection conditions multiplied with the dilution factor is inherently somewhat arbitrary [53], as it is difficult to define exactly “conventional injection conditions” [54].

Therefore, we employed the approach developed by El-Awady et al. [32]. According to this approach, the sweeping efficiency corresponds to the ratio of the peak heights (in the volume overload region) obtained under sweeping and under conventional injection conditions. In the subsequent discussion, we will use the term sensitivity enhancement factor (SEF) to express the enrichment efficiency as we have combined three different enrichment principles: dynamic pH junction, sweeping, and LVSS:

$$\text{SEF} = h_2/h_1 \quad (2)$$

where  $h_1$  is the limiting peak height in the plateau region under non-focusing conditions (analytes are dissolved in BGE), and  $h_2$  is the limiting peak height in the plateau region under focusing conditions (analytes are dissolved in low conductivity matrix void of borate). The value of either  $h_1$  or  $h_2$  was determined by plotting the peak height vs. the product of the injection pressure multiplied with the injection time. Via non-linear regression the parameters of the equation  $y = a(1 - e^{-bx})$

are determined, where the parameter  $a$  is the limiting peak height (height in the plateau region of the curve) [32].

However, with the developed enrichment method, it is impossible to reach the volume overload region. Therefore,  $h_2$  was considered as the peak height obtained for a given concentration of the nucleoside. On the other hand,  $h_1$  was calculated (using the same nucleoside concentration) by non-linear regression (see Fig. S7, Electronic Supplementary Material). The SEF values calculated via this procedure are given in Table 4. The corresponding electropherograms are shown in Fig. S8 (Electronic Supplementary Material). Therefore, the obtained SEF values shown in Table 4 are “worst case” values and higher values of SEF (1.5 times) would be obtained by dividing  $h_2$  by the peak height obtained under “conventional injection conditions”.

An approach (analogous to the equation derived by Quirino et al. [17] for the calculation of the length of the focused analyte zone after sweeping with a charged PSP) was adopted by the same authors [19] for calculating the length of the focused analyte zone  $l_{\text{sweep}}(\text{complex})$  after sweeping with borate:

$$l_{\text{sweep}}(\text{complex}) = l_{\text{inj}} \left( \frac{\mu_{\text{ep}}(b) - \mu_{\text{ep}}^*(a)}{\mu_{\text{ep}}(b)} \right) \quad (3)$$

where  $\mu_{\text{ep}}(b)$  and  $\mu_{\text{ep}}^*(a)$  are the electrophoretic mobility of the tetrahydroxyborate ion and the effective electrophoretic mobility of the neutral solute after complexation, respectively.  $\mu_{\text{ep}}^*(a)$  is given by:

$$\mu_{\text{ep}}^*(a) = \frac{1}{1 + K[b]} \mu_{\text{ep}}(a) + \frac{K[b]}{1 + K[b]} \mu_{\text{ep}}(ab) \quad (4)$$

**Table 4** Values of the sensitivity enhancement factors (SEF),  $h_1$ ,  $h_2$ , and  $h_3$

Nucleoside	$h_1^a$	$h_2^b$	SEF ( $h_2/h_1$ )	$h_3^c$	SEF ( $h_2/h_3$ )
Ado	0.993	6.474	7	0.762	9
Cyd	0.555	3.460	6	0.421	8
5MeUrd	0.511	6.516	13	0.367	18
Guo	0.205	4.972	24	0.143	35
Urd	0.164	4.151	25	0.108	38
Ino	0.236	8.817	37	0.162	54
Xao	0.180	15.074	84	0.119	127

<sup>a</sup>  $h_1$  equals the coefficient “a” obtained from non-linear regression fitting. For experimental details, see Fig. S8 (Electronic supplementary material)

<sup>b</sup>  $h_2$  is the peak height obtained (under dynamic pH junction-sweeping-LVSS) from the same concentration of nucleosides that was used in Fig. S8 (Electronic supplementary material)

<sup>c</sup>  $h_3$  is the peak height obtained using conventional injection parameter (30 mbar for 0.1 min)

where  $K$  is the formation constant,  $[b]$  is the molar concentration of tetrahydroxyborate ion, and  $\mu_{ep}(a)$  and  $\mu_{ep}(ab)$  are the electrophoretic mobility of the analyte and the analyte-borate complex, respectively. For neutral analytes,  $\mu_{ep}(a)=0$  and Eq. (4) can be further simplified [19].

Taking into consideration that the value of  $\mu_{ep}(b)$  is always larger than  $\mu_{ep}^*(a)$ , narrower zones can be obtained when  $\mu_{ep}^*(a)$  approaches  $\mu_{ep}(b)$ . As described by Eqs. (4–6), this can be achieved by: (i) a high complex formation constant  $K$  (between analyte and tetrahydroxyborate), (ii) a high concentration of tetrahydroxyborate, (iii) alkaline pH conditions with  $pH > 9.24$  ( $9.24 = pK_{a1}$  of boric acid), and (iv) an increased electrophoretic mobility of the analyte-tetrahydroxyborate complex. These four factors are the essential parameters to reduce the length of the swept analyte zone to a minimum.

The complex formation constant between the nucleosides and tetrahydroxyborate is given by:

$$K = \frac{[nb]}{[n][b]} \quad (5)$$

where  $[n]$  is the molar concentration of the nucleoside and  $[nb]$  is the molar concentration of the nucleoside-tetrahydroxyborate complex. In our previous work, we have confirmed that under alkaline pH conditions ( $pH > 9.24$ , tetrahydroxyborate is the dominant species), the degree of complexation between nucleoside and tetrahydroxyborate is very high and can be approximated by one even at a low tetrahydroxyborate concentration [14]. If tetrahydroxyborate is present in a high concentration, the fraction which is consumed by complexation can be neglected. By substituting  $K[b]$ ,  $\mu_{ep}(b)$  and  $\mu_{ep}^*(a)$  in Eq. (4) by  $[nb]/[n]$ ,  $\mu_{ep}(n)$  and  $\mu_{ep}(nb)$ , respectively, the following equation can be obtained:

$$\mu_{ep}^*(n) = \frac{1}{1 + \left(\frac{[nb]}{[n]}\right)} \mu_{ep}(n) + \frac{\left(\frac{[nb]}{[n]}\right)}{1 + \left(\frac{[nb]}{[n]}\right)} \mu_{ep}(nb) \quad (6)$$

At pH 9.25 and due to the high complex formation constant between the nucleosides and tetrahydroxyborate, we can assume that  $[n]$  becomes infinitesimally small and all the tested nucleosides are in their complexed form. Therefore, the first term in Eq. (6) can be deleted and  $\mu_{ep}^*(a)$  equals  $\mu_{ep}(nb)$ . Ado and Cyd acquire their charge only due to complexation with borate. Therefore, these two compounds are not focused due to dynamic pH junction, as their uncomplexed species are neutral.

In case of 5MeUrd, Guo, Urd, Ino and Xao, the analytes possess an additional charge due to the dissociation of the amidic group. In separation buffer their mobility increases in the order  $5MeUrd < Guo < Urd < Ino < Xao$ , corresponding to the  $pK_a$  of the nucleoside. When substituting  $\mu_{ep}^*(a)$  in

Eq. (3) by  $\mu_{ep}(nb)$ , it can be expected that the narrowest zone will be obtained for Xao. This highlights the importance of the additional negative charge acquired by the dissociated amidic group. Moreover, the value of  $\mu_{ep}(nb)$  is dependent on the charge to size ratio of the complex formed; therefore smaller molecules are more efficiently focused than larger ones. The comparison of the SEF obtained for Guo and Urd (see Table 4) clearly manifests this observation, because Urd and Guo, have equal  $pK_a$  values (equal charge) but Guo is larger than Urd.

It is noteworthy to mention that (shortly after the negative voltage is applied) Xao, in contrast to other nucleosides and before complexation with borate, migrates toward the anode. Xao is negatively charged in the water sample matrix ( $pK_a = 5.7$ ) causing an initial narrowing of its zone, followed by the steps described in Fig. 1. From the SEF data (see Table 4), it is clear that for this compound a higher SEF can be reached than for the other nucleosides, which cannot be explained solely with the complete dissociation of the amidic group at  $pH = 9.25$ . It must be attributed also to this initial focusing step that occurs before complexation with borate takes place.

As indicated in Table 4, we can conclude that the enrichment efficiency is highly dependent on the electrophoretic mobility of the nucleosides, i.e. the higher is the mobility, the higher is the SEF. Fig. 10 demonstrates the dependency of the SEF on  $\mu_{eff}$  of the nucleosides. Assuming an equal degree of focusing caused by both dynamic pH junction (with the exception of Ado and Cyd) and stacking, Eq. 3 predicts a linear relationship between the length of the swept zone and the electrophoretic mobility of the nucleoside-tetrahydroxyborate complex. The length of the swept zone is inversely proportional to the SEF. However, there is a nonlinear relationship between the SEF and the electrophoretic mobility of complexed nucleoside, because Xao encounters an additional (initial) focusing step (Fig. 10).

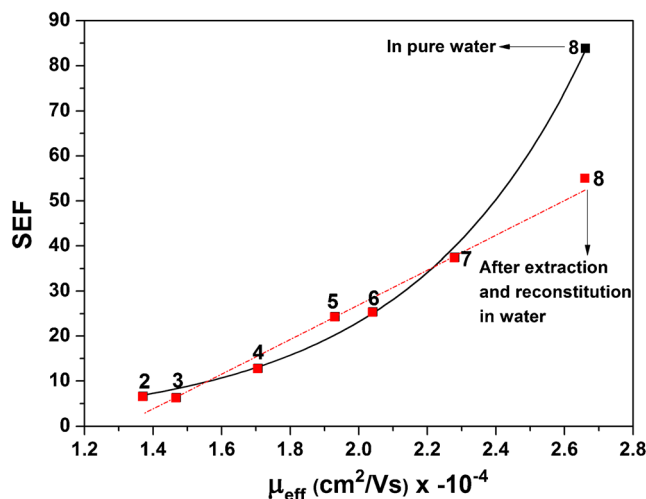


Fig. 10 SEF dependent on nucleoside mobility. For analyte numbering, refer to Fig. 2

When nucleosides are extracted using the PBA column (due to the higher ion concentration in the reconstituted sample relative to that of pure water), the initial focusing step for Xao is no longer present, as its electrophoretic velocity will be reduced (relative to that in pure water). Therefore, we observe a reduction in the peak area and peak height if the results for pre-treated real samples are compared with those obtained for pure standard solutions (see Figs. 5 and 6). If we use the ratio of the peak heights recorded for Xao in Figs. 5a, b as a quantitative measure for the associated reduction in the enrichment efficiency, we obtain a factor of 1.54. If the SEF of Xao (84) is divided by this factor (and the resulting value is plotted against the electrophoretic mobility, see Fig. 10), a linear dependency of the SEF on the electrophoretic mobility is obtained for all studied nucleosides ( $r=0.9892$ ). This dependency supports our hypothesis regarding the additional initial focusing step for Xao if pure water is the sample matrix.

Ado does not fit perfectly in this linear model as for this compound (although it was not focused by dynamic pH junction), there is some sweeping resulting from its specific interaction with 2-HP- $\beta$ -CD which causes an additional improvement in its SEF. Moreover, by selecting the charged analytes (5MeUrd, Urd, Guo, Ino, and Xao) and plotting the measured SEF against their electrophoretic mobility a regression line with very low residual standard deviation ( $r=0.9960$ ) is obtained, which gives an indication that these charged analytes behave different with regard to the neutral analytes (Ado and Cyd). This different behavior is expected due to the dissociation of their amidic functional group within the “titrated” sample plug at the start of the enrichment process. However, we cannot measure quantitatively the contribution of this dynamic pH junction step relative to the total enrichment factor as this process is of transient nature. It is active only at the start of the enrichment process when hydroxide ions migrate into the sample zone before borate complexation (with the slower tetrahydroxyborate ions) takes place.

## Conclusions

The developed three-step enrichment method based on dynamic pH junction-borate sweeping-LVSS can be applied successfully for the on-line focusing and separation of the seven urinary nucleosides, which have been selected for this study. The enrichment procedure is very simple and requires no additional equipment. Application of the proposed on-line enrichment procedure results in a considerable improvement of the sensitivity of the method. The charge of the nucleoside, the formation constant of the formed tetrahydroxyborate-nucleoside complex, and the electric conductivity and the pH of the sample matrix and the BGE are the key parameters determining the focusing efficiency. The positive impact of

the ionic constituents (remaining in the reconstituted sample after extraction) on the achieved focusing efficiency plays a significant role in a better understanding of the exact mechanisms of the developed enrichment procedure. Owing to the excellent extraction selectivity provided by commercially available phenylboronate affinity gels and because of the very low detection limits achieved in combination with the developed on-line focusing strategy, the proposed method is applicable to human urine samples and shows a great potential for the analysis of nucleosides in other types of biological fluids.

**Acknowledgments** A.H. Rageh thanks the Egyptian ministry of higher education and state for scientific research and the Deutscher Akademischer Austauschdienst (DAAD) for funding her PhD scholarship through German Egyptian Research Long-Term Scholarship program (GERLS). We thank Prof. M. Marahiel for providing the lyophilizer. We thank the workshops of the Department of Chemistry for the development of the data-recording unit.

## References

1. Markuszewski MJ, Waszczuk-Jankowska M, Struck W, Koslinski P (2013) In: Buszewski B, Dziubakiewicz E, Szumski M (eds) *Electromigration techniques: theory and practice*. Springer, Berlin, p 274
2. Xu G, Liebich HM, Lehmann R, Müller-Hagedorn S (2001) *Methods Mol Biol* 162:459–474
3. Cho SH, Choi MH, Lee WY, Chung BC (2009) *Clin Biochem* 42: 540–543
4. Rodriguez-Gonzalo E, Garcia-Gomez D, Carabias-Martinez R (2011) *J Chromatogr A* 1218:9055–9063
5. Sasco AJ, Rey F, Reynaud C, Bobin JY, Clavel M, Niveleau A (1996) *Cancer Lett* 108:157–162
6. Wang S, Zhao X, Mao Y, Cheng Y (2007) *J Chromatogr A* 1147: 254–260
7. Helboe T, Hansen SH (1999) *J Chromatogr A* 836:315–324
8. Zhang M, El-Rassi Z (1999) *Electrophoresis* 20:31–36
9. Szymanska E, Markuszewski MJ, Bodzioch K, Kaliszan R (2007) *J Pharm Biomed Anal* 44:1118–1126
10. Zheng YF, Kong HW, Xiong JH, Shen L, Xu GW (2005) *Clin Biochem* 38:24–30
11. Liebich HM, Müller-Hagedorn S, Klaus F, Meziane K, Kim KR, Frickenschmidt A, Kammerer B (2005) *J Chromatogr A* 1071:271–275
12. Liebich HM, Lehmann R, Xu G, Wahl HG, Häring HU (2000) *J Chromatogr B Biomed Sci Appl* 745:189–196
13. Zheng YF, Xu GW, Liu DY, Xiong JH, Zhang PD, Zhang C, Yang Q, Shen L (2002) *Electrophoresis* 23:4104–4109
14. Rageh AH, Pyell U (2013) *J Chromatogr A* 1316:135–146
15. Haunschmidt M, Buchberger W, Klampfl CW (2008) *J Chromatogr A* 1213:88–92
16. Terabe S (2010) *Procedia Chem* 2:2–8
17. Quirino JP, Terabe S (1998) *Science* 282:465–468
18. Breadmore MC, Dawod M, Quirino JP (2011) *Electrophoresis* 32: 127–148
19. Quirino JP, Terabe S (2001) *Chromatographia* 53:285–289
20. Liu J, Zhu F, Liu Z (2009) *Talanta* 80:544–550
21. Pyell U (2006) In: Pyell U (ed) *Electrokinetic chromatography: theory, instrumentation & applications*. Wiley, Chichester

22. Kazarian AA, Hilder EF, Breadmore MC (2011) *J Sep Sci* 34:2800–2821
23. Markuszewski MJ, Britz-McKibbin P, Terabe S, Matsuda K, Nishioka T (2003) *J Chromatogr A* 989:293–301
24. Liebich HM, Xu G, Di S, Lehmann R, Häring HU, Lu P, Zhang Y (1997) *Chromatographia* 45:396–401
25. Beckman Coulter (2003) *P/ACE Setter* 7:1–4
26. Jiang Y, Ma Y (2009) *Anal Chem* 81:6474–6480
27. Iqbal J, Müller CE (2011) *J Chromatogr A* 1218:4764–4771
28. Rodriguez-Gonzalo E, Hernandez-Prieto R, Garcia-Gomez D, Carabias-Martinez R (2014) *J Pharm Biomed Anal* 88:489–496
29. Britz-McKibbin P, Bebault GM, Chen DDY (2000) *Anal Chem* 72:1729–1735
30. Gehrke CW, Kuo KC, Davis GE, Suits RD, Waalkes TP, Borek E (1978) *J Chromatogr* 150:455–476
31. ICH Harmonised Tripartite Guidelines, Validation of analytical procedures: text and methodology Q2(R1) (1996) <http://www.ich.org/products/guidelines/quality/article/quality-guidelines.html>. (Accessed 16 Jun 2014)
32. El-Awady M, Huhn C, Pyell U (2012) *J Chromatogr A* 1264:124–136
33. Landers JP (2008) *Handbook of capillary and microchip electrophoresis and associated microtechniques*, 3rd edn. CRC, Taylor and Francis Group, Boca Raton
34. Riekkola ML, Joensuu JA, Smith RM (2004) *Pure Appl Chem* 76:443–451
35. van de Merbel NC (2008) *Trends Anal Chem* 27:924–933
36. Kuo KC, Phan DT, Williams N, Gehrke CW (1990) In: Gehrke CW, Kuo KC (eds) *Chromatography and modification of Nucleosides. Part c modified nucleosides in cancer and normal metabolism methods and applications*. Elsevier, Oxford, p C41
37. IUPAC-IUB (1974) *Pure Appl Chem* 40:277–290
38. Lundblad RL, MacDonald F (2010) *Handbook of biochemistry and molecular biology*, 4th edn. CRC, Taylor and Francis Group, Boca Raton
39. Wang P, Ren J (2004) *J Pharm Biomed Anal* 34:277–283
40. Xiang TX, Anderson BD (1990) *Int J Pharm* 59:45–55
41. Kawamura K (1998) *J Chromatogr A* 802:167–177
42. Tadey T, Purdy WC (1994) *J Chromatogr B Biomed Sci Appl* 657:365–372
43. Peng X, Bebault GM, Sacks SL, Chen DDY (1997) *Can J Chem* 75:507–517
44. Oestergaard J, Jensen H, Holm R (2009) *J Sep Sci* 32:1712–1721
45. Britz-McKibbin P, Chen DDY (2002) *Electrophoresis* 23:880–888
46. Van Loco J, Elskens M, Croux C, Beernaert H (2002) *Accred Qual Assur* 7:281–285
47. Sonnergaard JM (2006) *Int J Pharm* 321:12–17
48. Wätzig H, Degenhardt M, Kunkel A (1998) *Electrophoresis* 19:2695–2752
49. Reichenbaecher M, Einax JW (2011) *Challenges in analytical quality assurance*. Springer, Berlin
50. Wätzig H (1995) *J Chromatogr A* 700:1–7
51. *European Pharmacopoeia (7.8)*, 7th edn. (2013) Online Version, European directorate for the quality of medicines & healthcare (EDQM), Strasbourg
52. Chun MS, Chung DS (2003) *Anal Chim Acta* 491:173–179
53. Simpson SL, Quirino JP, Terabe S (2008) *J Chromatogr A* 1184:504–541
54. Pawel K, Edward B (2013) In: Boguslaw B, Ewelina D, Michal S (eds) *Electromigration techniques: theory and practice*. Springer, Berlin, p 217
55. Miller JC, Miller JN (2005) *Statistics and chemometrics for analytical chemistry*, 5th edn. Pearson, Prentice Hall



**Analytical and Bioanalytical Chemistry**

**Electronic Supplementary Material**

**Determination of urinary nucleosides via borate complexation capillary electrophoresis combined with dynamic pH junction-sweeping-large volume sample stacking as three sequential steps for their on-line enrichment**

Azza H. Rageh, Achim Kaltz, Ute Pyell

This supplementary material includes:

- Chemical structures and  $pK_a$  values of the investigated nucleosides
- Extraction of nucleosides using phenylboronate affinity gel
- Electropherograms illustrating the effect of borax concentration on the separation of the studied nucleosides
- Calculation of the injected sample volume and the sample plug length
- Electropherograms illustrating the effect of the injection parameter on the detection sensitivity.
- Calibration curves and residuals plots using peak height or corrected peak area as response factor
- Comparison between limits of detection achieved by the developed method and by other reported CE methods
- Electropherograms showing the enrichment efficiency achieved by the proposed enrichment strategy
- Assessment of  $h_1$  using non-linear regression fitting
- Electropherograms demonstrating the separation of nucleosides under non-focusing conditions



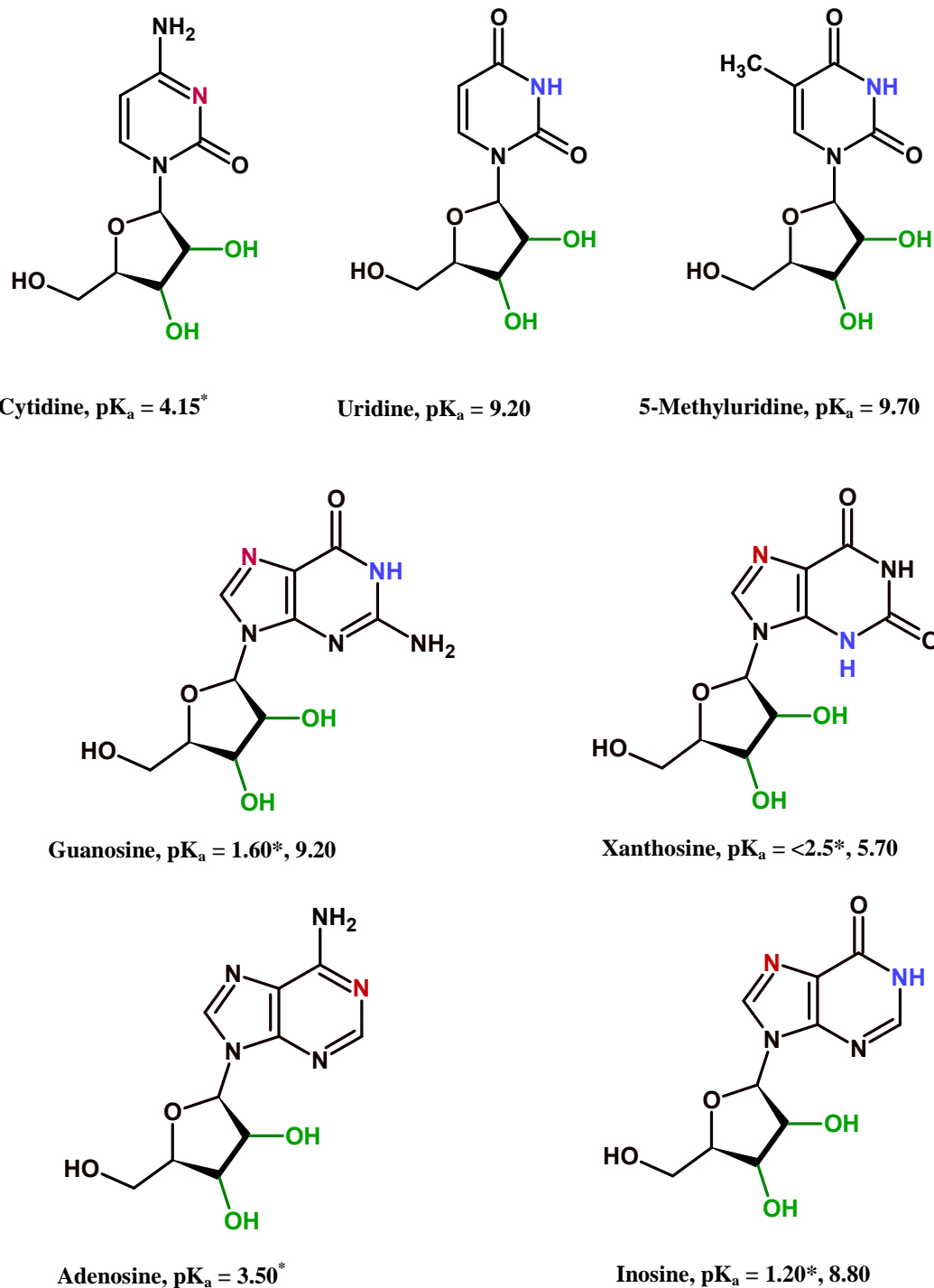


**Fig. S1** Structural formulas and  $pK_a$  values of the investigated nucleosides. \* Values of  $pK_a$  are those of the cationic protonated conjugate acid form. Red and blue colours are used to mark the protonation and dissociation sites, respectively.  $pK_a$  values of cis-diol moieties (marked with the green colour) are  $\sim 12.5$

**Extraction of nucleosides using phenylboronate affinity gel**

The extraction procedure was exactly followed as in [9] with minor modifications:

- 1- Urine samples (approximately 40 mL, pH 6.37) were treated with few drops of conc. ammonia 25% (3-4 drops) to adjust the pH between 8.6-8.8. The samples were mixed for 1 min using a vortex mixer and centrifuged at 12000 rpm for 5 min. Two millilitres from the supernatant were applied to the PBA column. For preparation of the calibration standards to be applied to the PBA column, 1 mL of 0.25 mol L<sup>-1</sup> ammonium acetate pH 8.8 (to maximize the extractability of these compounds on the PBA column) was added to make the final volume 2 mL using distilled water after adding different volumes of the working standard solution
- 2- The PBA column consisted of a polypropylene SPE tube, 3 mL (Sigma Aldrich, Steinheim, Germany) with polyethylene frit (20 µm porosity), packed with the stationary phase material (200.0 mg). Before the first use, the gel was allowed to swell in 3 mL water for 10 min. The gel was then alternatively washed with methanol and water for at least ten cycles, 0.5 mL each. After that, the gel was washed two times with 0.1 mol L<sup>-1</sup> NaCl (3 mL), 3 times with 0.1 mol L<sup>-1</sup> formic acid (3 mL), 3 times with 0.25 mol L<sup>-1</sup> ammonium acetate pH 8.8 (3 mL), 3 times with 0.1 mol L<sup>-1</sup> formic acid in 50% methanol (3 mL) and finally 3 times with 0.25 mol L<sup>-1</sup> ammonium acetate pH 8.8 (3 mL).
- 3- After transferring the standard or urine samples on the PBA column with a Pasteur pipet, a rinse of 0.5 mL 0.25 mol L<sup>-1</sup> ammonium acetate pH 8.8 was added to each sample and the rinse was transferred on the PBA column. The gel was washed with 0.5 mL 0.25 mol L<sup>-1</sup> ammonium acetate pH 8.8 and left to stand for 10 min. Then the column was washed with 0.25 mol L<sup>-1</sup> ammonium acetate pH 8.8 (4 mL) and two times with 0.3 mL 50% methanol (a 3 min interval was applied between each rinse). 0.5 mL 0.1 mol L<sup>-1</sup> formic acid in 50% methanol was added to replace 50% methanol and again 3 min interval was applied to prepare the column for elution of the nucleosides.
- 4- 2.5 mL 0.1 mol L<sup>-1</sup> formic acid in 50% methanol was used for the elution of the nucleosides (taken into account that the first 0.5 ml of 0.1 mol L<sup>-1</sup> formic acid in 50% methanol, used in Step 3, was also collected to make the volume of the final eluate 3 mL). Methanol from the eluate was evaporated under vacuum and the remaining volume of the eluate (~ 1.5 mL) was shell freezed in a slanted position using liquid nitrogen before it was lyophilized to dryness. The residue was dissolved in 2 mL distilled water, unless otherwise mentioned, and injected directly into the capillary.
- 5- The column was washed three times with 0.1 mol L<sup>-1</sup> formic acid in 50% methanol and it was stored in the same solution. Before the next use, the column was washed two times with 2 mL 50% methanol and three times with 3 mL 0.25 mol L<sup>-1</sup> ammonium acetate pH 8.8 before the previously described steps were repeated starting from Step 3. The PBA column was used up to 12 times and then it was disposed.

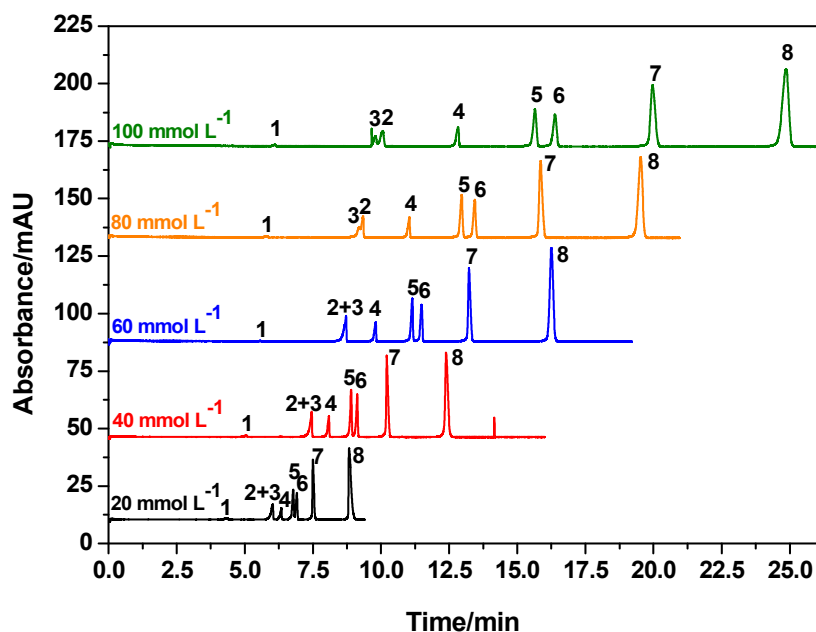


**Fig. S2** Electropherograms obtained with different concentration of sodium tetraborate in the BGE, pH 9.25. Sample solution is 20.0 mg L<sup>-1</sup> of each of the studied analytes and 25.0 mg L<sup>-1</sup> thiourea in water. CE conditions: capillary 648(500) mm × 50.2 μm I.D., applied voltage during dynamic pH junction/sweeping/LVSS/sample matrix removal -20 kV, separation voltage +20 kV, pressure injection 120 mbar for 5 min, oven temperature 35 °C. Peak designation: (1) thiourea, (2) adenosine, (3) cytidine, (4) 5-methyluridine, (5) guanosine, (6) uridine, (7) inosine, and (8) xanthosine

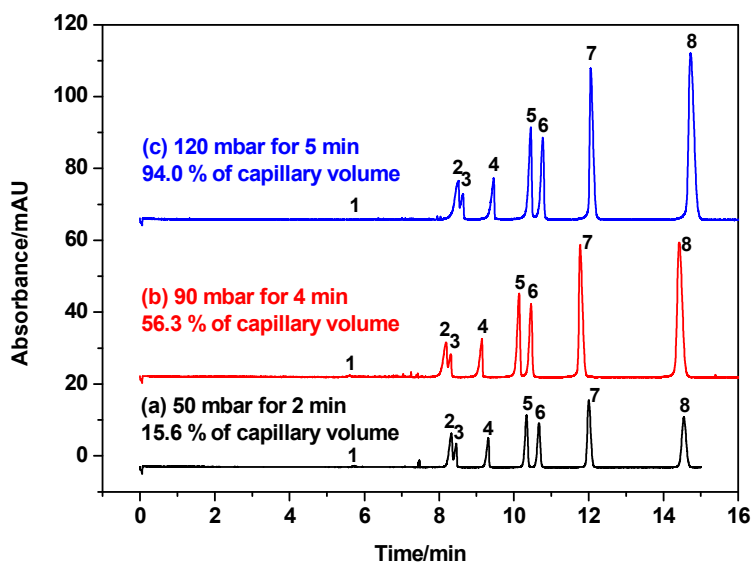


**Fig. S3** Electropherograms obtained using different injection volumes. Sample: 25.0 mg L<sup>-1</sup> of each of the investigated nucleosides and 25.0 mg L<sup>-1</sup> thiourea in water. CE conditions: 16.4 mg mL<sup>-1</sup> β-CD in 40 mmol L<sup>-1</sup> sodium tetraborate, pH 9.25 as BGE, other conditions and peak designation as in Fig. S2

**Calculation of the sample injection volume**

In order to calculate the volume of the sample injected into the capillary by hydrodynamic injection, Hagen-Poiseuille law is used:

$$Q_{inj} = \frac{\pi \Delta p r^4 t_{inj} c}{8 L \eta} \quad (\text{S-1})$$

where  $Q_{inj}$  is the amount of substance of analyte introduced into the capillary,  $\Delta p$  is the pressure difference,  $r$  is capillary inner radius,  $t_{inj}$  is the injection time,  $c$  is the molar concentration of the analyte in the sample,  $L$  is the length of the capillary,  $\eta$  is the viscosity of the liquid inside the capillary. To calculate the sample injection volume  $V$ , the following expression is used:

$$V = \frac{\pi \Delta p r^4 t_{inj}}{8 L \eta} \quad (\text{S-2})$$

The injected plug length is then calculated by dividing  $V$  by  $\pi r^2$ . The total volume of the capillary  $V_{tot}$  is calculated from known geometrical parameters:

$$V_{tot} = \pi r^2 L \quad (\text{S-3})$$

**Table S1** Calculation of sample injection volume and injection plug length

Injection parameter	Injection volume	% of the capillary volume	Injected plug length
1- 30 mbar/0.2 min	0.01 $\mu\text{L}$	0.80	0.5 cm
2- 50 mbar/2 min	0.20 $\mu\text{L}$	15.6	10.1 cm
3- 90 mbar/4 min	0.72 $\mu\text{L}$	56.3	36.4 cm
4- 120 mbar/5 min	1.20 $\mu\text{L}$	93.8	61.0 cm

Taking the second injection parameter as an example to show how the injection volume is calculated:

$$\Delta p = 50 \text{ mbar} = 50 \times 10^2 \text{ N m}^{-2}, r = 25.1 \text{ } \mu\text{m} = 25.1 \times 10^{-6} \text{ m}, t = 120 \text{ s}, L = 0.648 \text{ m}, \eta (\text{water}, 35^\circ \text{C}) = 0.00072 \text{ Ns. m}^{-2}, V_{tot} = 1.28 \text{ } \mu\text{L}.$$

**N.B.** We used the viscosity of the sample solution (water) and not that of the BGE to calculate the injection volume as under the employed condition, the sample plug represents a significant portion of the capillary length.

**Table S2** Linear regression parameters of the developed method for calibration standards reconstituted in water after SPE

	No. of calib. standards (n)	Linearity range ( $\mu\text{g mL}^{-1}$ )	Intercept (a) $\pm$ SD <sup>a</sup>	Slope (b) $\pm$ SD <sup>b</sup>	SSE <sup>c</sup>	S <sub>yx</sub> <sup>d</sup>	S <sub>x0</sub> <sup>e</sup>	Confidence interval of (a) <sup>f</sup>	Confidence interval of (b) <sup>f</sup>	r <sup>g</sup>	Mandel's test value <sup>h</sup>
Ado											
PH <sup>i</sup>	7	0.04-8.04	0.156 $\pm$ 0.111	1.466 $\pm$ 0.032	0.275	0.233	0.159	$\pm$ 0.448	$\pm$ 0.129	0.9988	20.75
PA <sup>j</sup>	7	0.04-16.08	0.094 $\pm$ 0.267	12.203 $\pm$ 0.039	1.706	0.584	0.048	$\pm$ 1.075	$\pm$ 0.157	0.9999	0.000
Corr. PA <sup>k</sup>	7	0.04-16.08	0.045 $\pm$ 0.132	1.305 $\pm$ 0.019	0.419	0.289	0.222	$\pm$ 0.503	$\pm$ 0.078	0.9995	12.46
Cyd											
PH	6	0.08-8.04	-0.055 $\pm$ 0.049	0.985 $\pm$ 0.014	0.035	0.093	0.095	$\pm$ 0.225	$\pm$ 0.062	0.9996	nd
PA	7	0.08-32.16	0.101 $\pm$ 0.967	6.007 $\pm$ 0.071	22.460	2.119	0.353	$\pm$ 3.902	$\pm$ 0.286	0.9997	6.24
Corr. PA	7	0.08-32.16	0.014 $\pm$ 0.108	0.609 $\pm$ 0.008	0.281	0.237	0.390	$\pm$ 0.437	$\pm$ 0.032	0.9996	4.90
5MeUrd											
PH	7	0.04-8.04	-0.045 $\pm$ 0.104	1.447 $\pm$ 0.030	0.238	0.218	0.151	$\pm$ 0.419	$\pm$ 0.121	0.9989	4.20
PA	9	0.04-32.16	-0.501 $\pm$ 0.777	9.700 $\pm$ 0.063	25.876	1.923	0.198	$\pm$ 2.721	$\pm$ 0.220	0.9999	0.94
Corr. PA	9	0.04-32.16	-0.142 $\pm$ 0.181	0.973 $\pm$ 0.015	1.407	0.448	0.461	$\pm$ 0.634	$\pm$ 0.052	0.9992	13.37
Guo											
PH	7	0.04-8.04	-0.157 $\pm$ 0.246	2.099 $\pm$ 0.069	1.285	0.507	0.241	$\pm$ 0.994	$\pm$ 0.280	0.9973	0.67
PA	8	0.04-16.32	0.386 $\pm$ 2.180	14.838 $\pm$ 0.328	146.094	4.934	0.333	$\pm$ 8.084	$\pm$ 1.214	0.9985	7.78
Corr. PA	8	0.04-16.32	-0.073 $\pm$ 0.062	1.388 $\pm$ 0.009	0.120	0.141	0.102	$\pm$ 0.232	$\pm$ 0.035	0.9999	0.98
Urd											
PH	7	0.04-8.00	-0.049 $\pm$ 0.207	1.924 $\pm$ 0.060	0.909	0.426	0.220	$\pm$ 0.834	$\pm$ 0.240	0.9977	0.86
PA	8	0.04-16.00	-0.084 $\pm$ 1.174	14.793 $\pm$ 0.180	42.349	2.658	0.180	$\pm$ 4.353	$\pm$ 0.667	0.9996	1.39
Corr. PA	8	0.04-16.00	-0.124 $\pm$ 0.094	1.327 $\pm$ 0.014	0.272	0.213	0.160	$\pm$ 0.349	$\pm$ 0.053	0.9996	15.72
Ino											
PH	6	0.04-4.04	-0.166 $\pm$ 0.109	2.402 $\pm$ 0.058	0.155	0.197	0.082	$\pm$ 0.503	$\pm$ 0.265	0.9989	nd
PA	7	0.04-8.08	0.175 $\pm$ 1.833	21.706 $\pm$ 0.520	69.396	3.725	0.172	$\pm$ 7.390	$\pm$ 2.098	0.9986	3.95
Corr. PA	7	0.04-8.08	-0.098 $\pm$ 0.043	1.759 $\pm$ 0.012	0.038	0.087	0.049	$\pm$ 0.173	$\pm$ 0.049	0.9999	1.28
Xao											
PH	5	0.10-2.06	-0.148 $\pm$ 0.065	1.695 $\pm$ 0.061	0.028	0.097	0.057	$\pm$ 0.377	$\pm$ 0.354	0.9981	nd
PA	6	0.10-4.12	0.415 $\pm$ 1.924	18.651 $\pm$ 0.991	46.533	3.411	0.183	$\pm$ 8.856	$\pm$ 4.564	0.9944	nd
Corr. PA	6	0.10-4.12	-0.040 $\pm$ 0.043	1.278 $\pm$ 0.022	0.023	0.076	0.060	$\pm$ 0.198	$\pm$ 0.102	0.9994	nd

<sup>a</sup> Standard deviation of the intercept, <sup>b</sup> Standard deviation of slope, <sup>c</sup> Sum of square errors, <sup>d</sup> Residual standard deviation (standard error of estimate (SEE)),

<sup>e</sup> Method standard deviation ( $= S_{yx}/b$ ), <sup>f</sup> Confidence interval calculated at P=0.99, <sup>g</sup> r is the correlation coefficient, <sup>h</sup> Tabulated f values at P = 0.99 are 13.74, 16.25, 21.19 at (df1 (1), df2 (n-3) = (1,6), (1,5), (1,4), respectively, <sup>i</sup> Peak height, <sup>j</sup> Peak area, <sup>k</sup> Corrected peak area. nd: not determined as n is below 7.

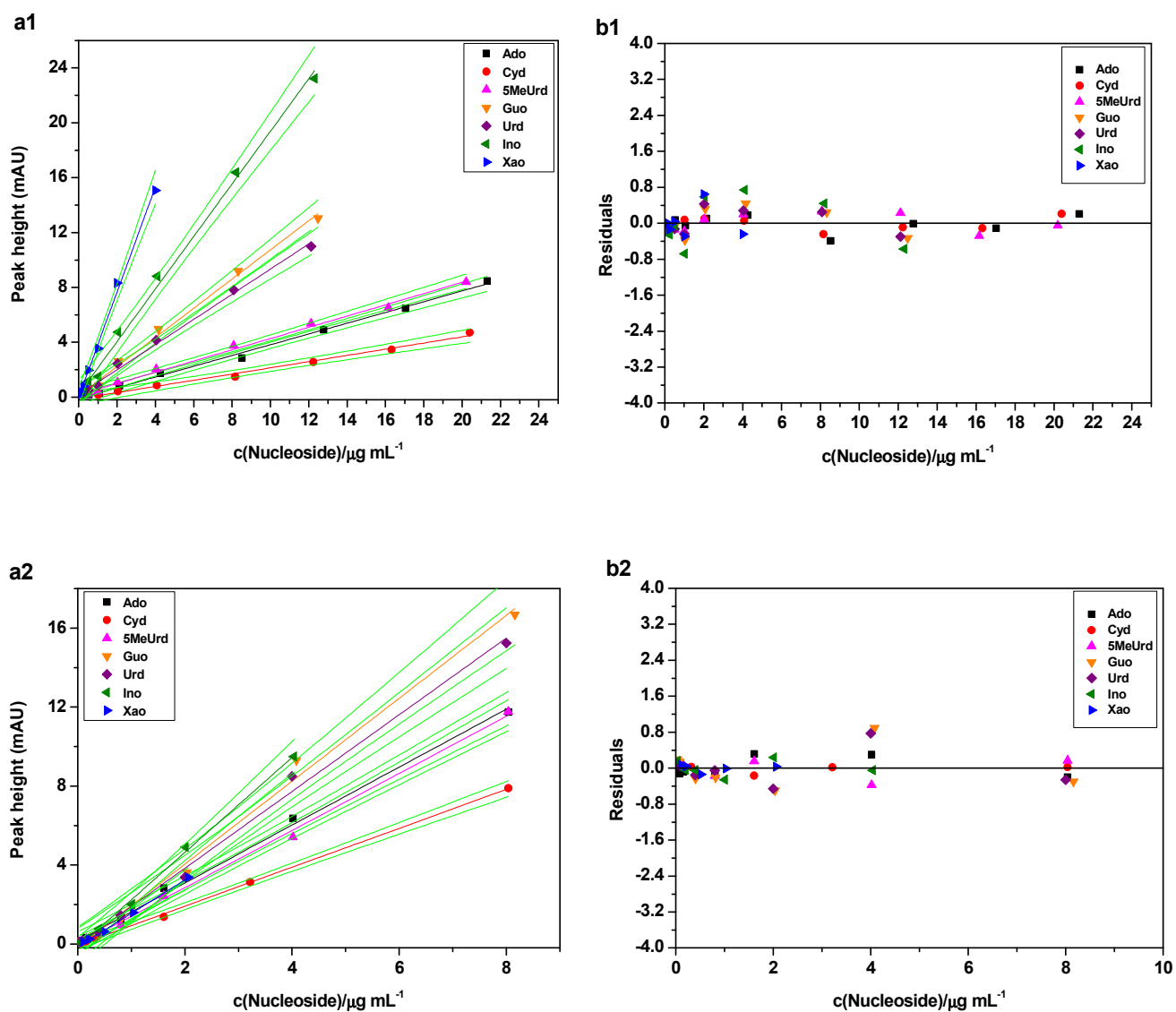


**Fig. S4** Calibration curve (a) and residuals plot (b) using peak height as the response factor. The green line in (a) indicates the confidence interval at 99% significance level. (a1) and (b1) represents the peak height and the residuals of the calibration standards dissolved in water and injected directly. (a2) and (b2) represents the peak height and the residuals of the calibration standards after their extraction using PBA column

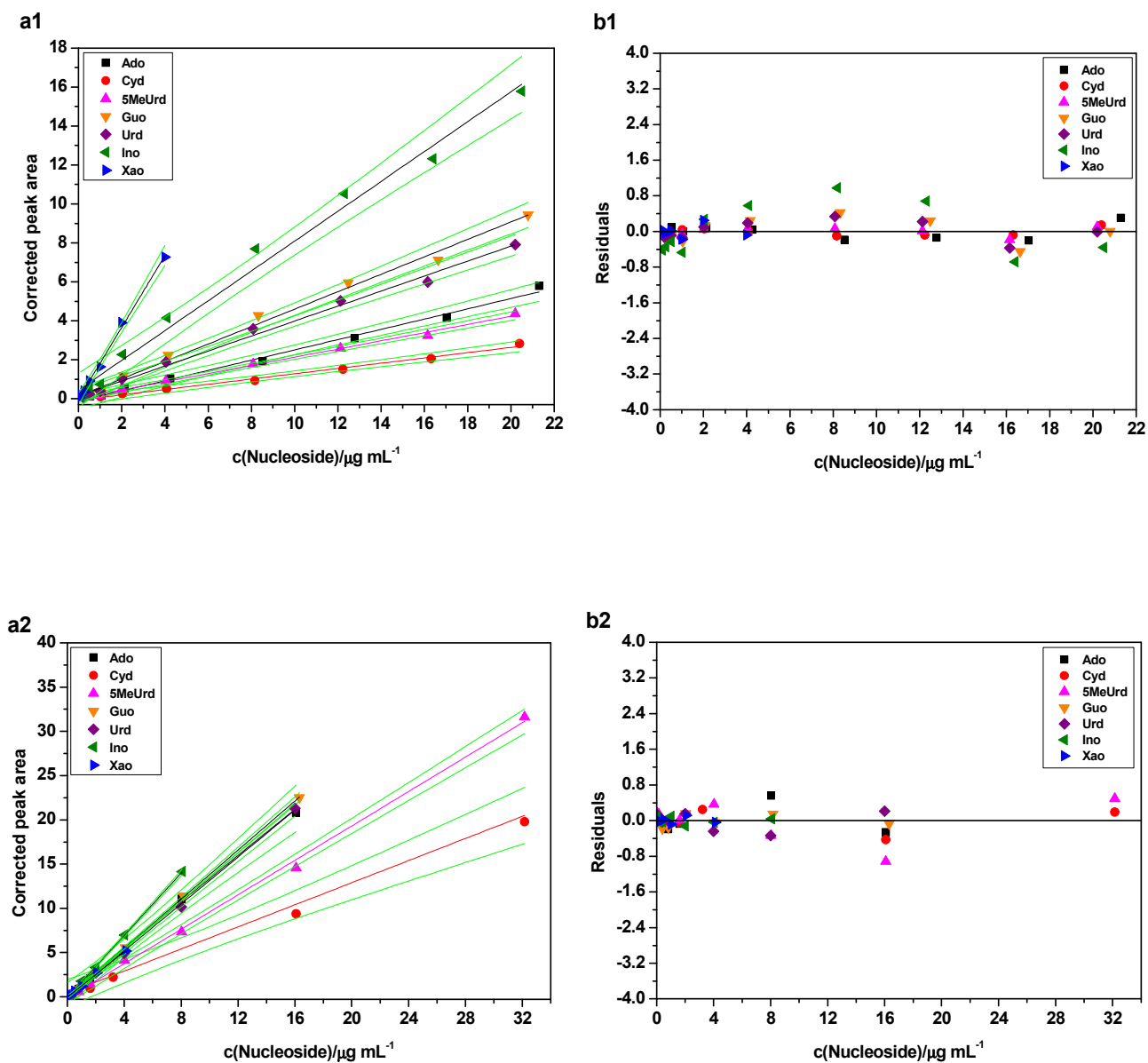


**Fig. S5** Calibration curve (a) and residuals plot (b) using corrected peak area as the response factor. The green line in (a) indicates the confidence interval at 99% significance level. (a1) and (b1) represents the corrected peak area and the residuals of the calibration standards dissolved in water and injected directly. (a2) and (b2) represents the corrected peak area and the residuals of the calibration standards after their extraction using PBA column

**Table S3** Comparison between the limits of detection achieved by the developed method and the other reported methods

Analyte	This work/UV	LOD <sup>a</sup> ( $\mu\text{mol L}^{-1}$ )									
		[9]/UV	[13]/UV	[24]/UV	[25]/UV	[26]/UV	[27]/UV	[28]/MS	[6]/MS		
Ado	0.07	0.78	6.40	2.00	7.00	1.09	0.09	0.30	0.02		
Cyd	0.16	0.50	4.00	3.10	10.00	1.67	----- <sup>b</sup>	0.16	0.02		
5MeUrd	0.08	0.98	3.50	----- <sup>b</sup>	6.00	----- <sup>b</sup>	----- <sup>b</sup>	----- <sup>b</sup>	0.96		
Guo	0.04	0.55	5.60	2.60	5.40	0.77	----- <sup>b</sup>	----- <sup>b</sup>	0.10		
Urd	0.04	0.17	5.00	3.50	12.50	1.06	----- <sup>b</sup>	----- <sup>b</sup>	2.04		
Ino	0.04	0.61	3.10	2.50	12.00	0.56	0.06	----- <sup>b</sup>	3.82		
Xao	0.07	0.41	10.00	9.20	14.60	0.78	----- <sup>b</sup>	----- <sup>b</sup>	----- <sup>b</sup>		

<sup>a</sup> Limit of detection, <sup>b</sup> not reported



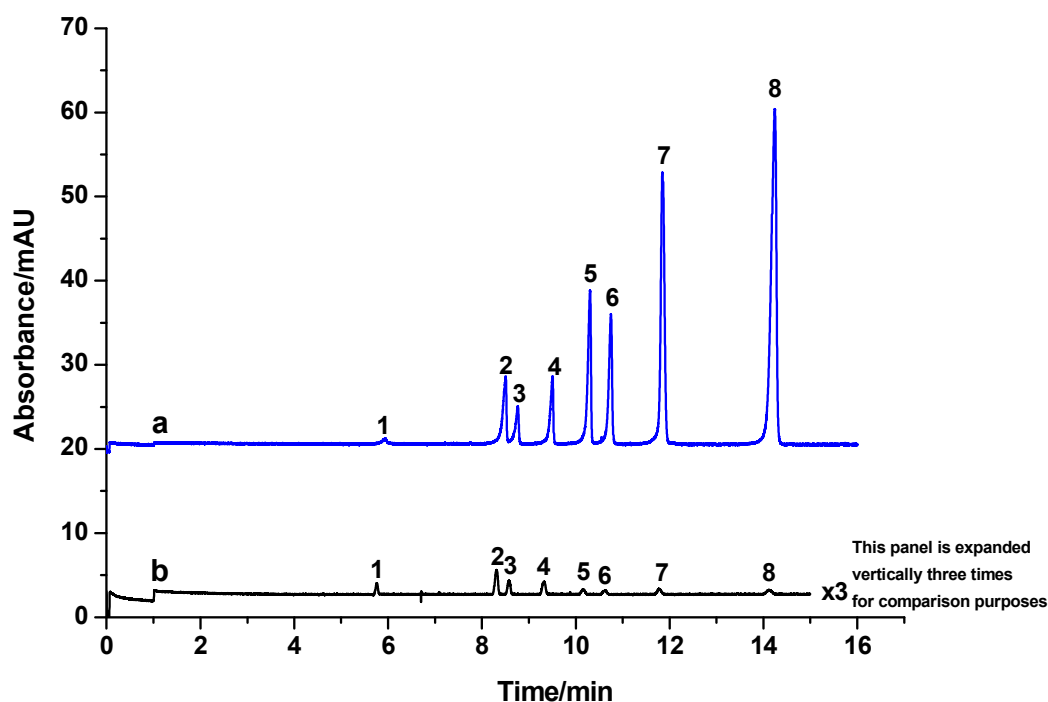


**Fig. S6** Electropherograms obtained under (a) dynamic pH junction/sweeping/LVSS conditions or (b) conventional injection condition. Sample solution in (a) is 20.0 mg L<sup>-1</sup> of each of the investigated nucleosides and 25.0 mg L<sup>-1</sup> thiourea in water. Sample solution in (b) is 4.0 mg L<sup>-1</sup> of Guo, Urd, Ino and Xao, 16.0 mg L<sup>-1</sup> of Ado, Cyd, 5MeUrd and 25.0 mg L<sup>-1</sup> thiourea in BGE. CE conditions: 42.0 mg L<sup>-1</sup> 2-HP- $\beta$ -CD in 40 mmol L<sup>-1</sup> sodium tetraborate, pH 9.25 as BGE, capillary 648(500) mm  $\times$  50.2  $\mu$ m I.D., separation voltage +20 kV, pressure injection 120 mbar for 5 min (a) or 30 mbar for 0.2 min (b), oven temperature 35  $^{\circ}$ C. In case of (a) applied voltage during dynamic pH junction/sweeping/LVSS/sample matrix removal -20 kV. Peak designation: see Fig. S2

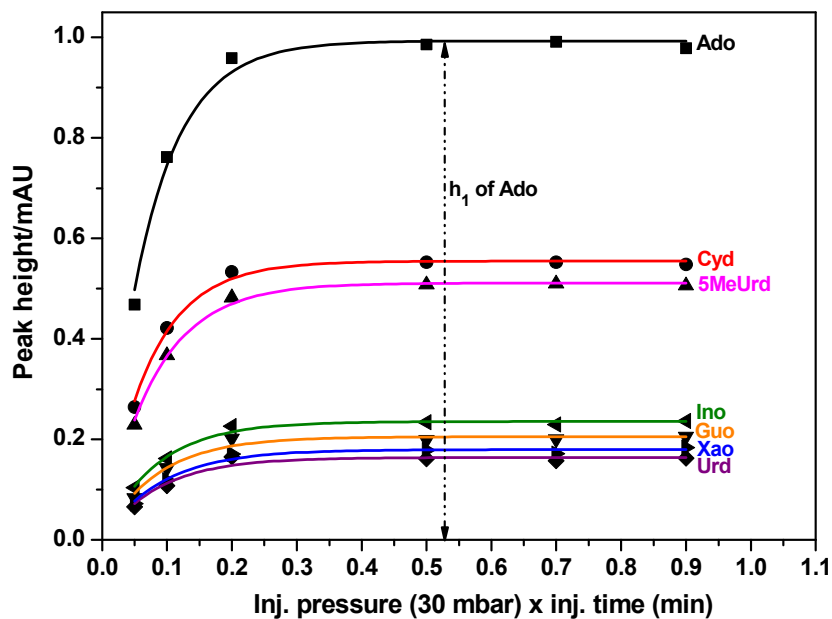


Fig. S7 Assessment of  $h_1$  using non-linear regression fitting. For experimental details, see Fig. S8

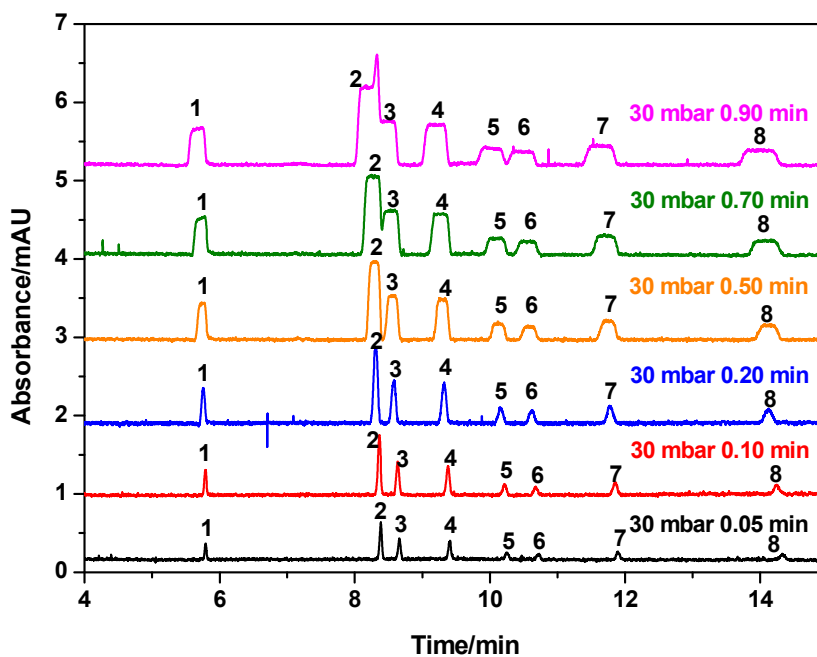


Fig. S8 Electropherograms obtained under non-focusing conditions with varied sample injection volume ( $4.0 \text{ mg L}^{-1}$  of Guo, Urd, Ino and Xao,  $16.0 \text{ mg L}^{-1}$  of Ado, Cyd, 5MeUrd and  $25.0 \text{ mg L}^{-1}$  thiourea in 90% BGE: 10%  $\text{H}_2\text{O}$ ). CE conditions:  $42.0 \text{ mg L}^{-1}$  2-HP- $\beta$ -CD in  $40 \text{ mmol L}^{-1}$  sodium tetraborate, pH 9.25 as BGE, capillary 648(500) mm  $\times$  50.2  $\mu\text{m}$  I.D., separation voltage +20 kV, oven temperature 35  $^\circ\text{C}$ . Peak designation: see Fig. S2

**SPRINGER LICENSE  
TERMS AND CONDITIONS**

Apr 08, 2015

---

This is a License Agreement between Azza Rageh ("You") and Springer ("Springer") provided by Copyright Clearance Center ("CCC"). The license consists of your order details, the terms and conditions provided by Springer, and the payment terms and conditions.

**All payments must be made in full to CCC. For payment instructions, please see information listed at the bottom of this form.**

License number	3604360465963
License date	Apr 08, 2015
Licensed content publisher	Springer
Licensed content publication	Analytical and Bioanalytical Chemistry
Licensed content title	Determination of urinary nucleosides via borate complexation capillary electrophoresis combined with dynamic pH junction sweeping-large volume sample stacking as three sequential steps for their on-line enrichment
Licensed content author	Azza H. Rageh, Achim Kaltz, Ute Pyell
Licensed content date	Jan 1, 2014
Volume number	406
Issue number	24
Type of Use	Thesis/Dissertation
Portion	Full text
Number of copies	15
Author of this Springer article	Yes and you are the sole author of the new work
Title of your thesis/dissertation	On-line and Off-line Enrichment Techniques Combined with Capillary Electromigration Separation Methods in the Analysis of Highly Hydrophilic Analytes in Biological and Environmental Samples
Expected completion date	May 2015



### **5.3. Publication III**

**Boronate affinity-assisted MEKC separation of highly hydrophilic urinary nucleosides using imidazolium-based ionic liquid-type surfactant as pseudostationary phase**

**Azza H. Rageh**, Ute Pyell

**Electrophoresis, 36 (2015) 784-795**

[doi: 10.1002/elps.201400357](https://doi.org/10.1002/elps.201400357)



### 5.3.1. Summary and discussion

In this publication, we investigate the combination of an alkyl or aryl boronate with the imidazolium-based IL-type surfactant ( $C_{14}\text{MImBr}$ ) as PSP for the MEKC separation of highly hydrophilic urinary nucleosides. The studied alkyl- and arylboronic acids are: 1-butylboronic acid; BBA, 1-hexylboronic acid; HBA, 1-dodecylboronic acid; DBA, and 3-nitrophenylboronic acid; 3-NPBA). We investigate the mechanism of interaction between the negatively charged nucleosides (the negative charge is acquired either due to deprotonation of the amidic group and/or complexation with boronate) and the positively charged PSP. It is shown that addition of alkyl- and arylboronic acids to the BGE introduces, beside electrostatic (Coulombic) interaction, an additional mode of interaction of the nucleosides with the PSP. Boronic acid (replacing borate as complexing agent) can bind selectively to the nucleosides via complex formation, while increasing their partitioning into the micelles formed by  $C_{14}\text{MImBr}$  via the attached hydrophobic alkyl/aryl group (Fig. 3). In this case, alkylboronates can act as a cosurfactant that increases the partitioning coefficient of the analytes into the micelles.

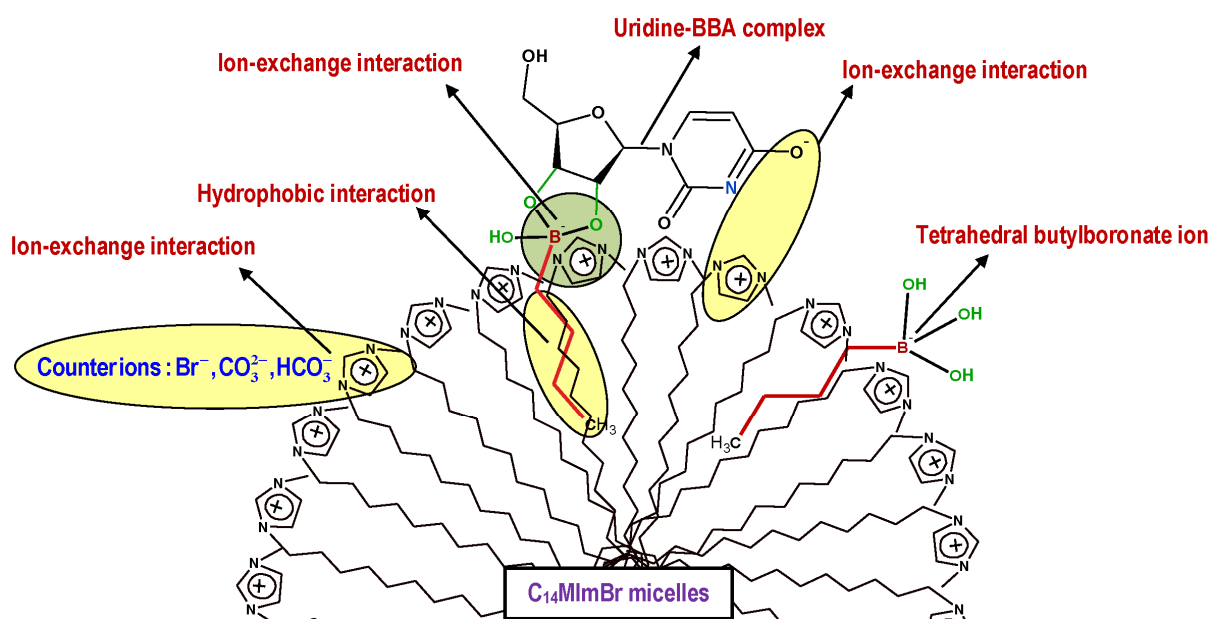


**Figure 3:** Schematic illustration of the mechanism of interaction of uridine–BBA complex with  $C_{14}\text{MImBr}$  assuming one-site mixed-mode retention.

We show that the migration and retention behavior of the studied analytes can be fully explained based on the concept of one-site hydrophobically assisted ion exchange (chromatography), whereas one-site mixed-mode retention denotes the situation that there is only one type of site and the only interaction that the charged analyte undergoes is a simultaneous interaction with both the hydrophobic core of the micelles and a charged surfactant head group (Fig. 3). The retention factors of all nucleosides under investigation are increased considerably in the presence an alkylboronate in the BGE when compared to

a BGE without this additive. This is very demandable in real sample application to avoid interference with matrix components. As an extension to previous studies with C<sub>14</sub>MImBr in borate buffer, the retention factors of the studied nucleosides are calculated either under variation of (i) the length of alkyl chain of boronic acid or (ii) the concentration of the competing ion in the BGE (in the presence of BBA). We demonstrate that with a BGE containing the combination of an alkyl/aryl boronate and C<sub>14</sub>MImBr, we can regulate the retention factors of the nucleosides by adjusting the competing ion concentration and we can further increase the retention factor by an increase in the length of the alkyl chain of the boronic acid added. Using a BGE composed of 5 mmol L<sup>-1</sup> BBA and 20 mmol L<sup>-1</sup> C<sub>14</sub>MImBr in 20 mmol L<sup>-1</sup> carbonate buffer, pH 9.71, the applicability of this approach is demonstrated for the separation and determination of nucleosides in a spiked urine sample after their extraction from urine using the commercially available phenylboronate affinity gel (PBA).



### **5.3.2. Author contribution**

The design of experiments and all the practical steps of this study were carried out by me. The draft of the manuscript was written by me and corrected by Prof. Dr. Ute Pyell. The final revision of the manuscript was conducted by me and Prof. Dr. Ute Pyell before submission to the journal. Prof. Dr. Ute Pyell was responsible for the supervision of this work.



**Azza H. Rageh**  
**Ute Pyell**

Department of Chemistry,  
University of Marburg, Marburg,  
Germany

Received July 22, 2014  
Revised September 5, 2014  
Accepted September 20, 2014

## Research Article

# Boronate affinity-assisted MEKC separation of highly hydrophilic urinary nucleosides using imidazolium-based ionic liquid type surfactant as pseudostationary phase

In this work, we extend our investigations regarding the separation of urinary nucleosides by MEKC with the ionic liquid type surfactant 1-tetradecyl-3-methylimidazolium bromide ( $C_{14}MImBr$ ). We study the impact of adding alkyl- and arylboronic acids (in the presence of  $C_{14}MImBr$  micelles) to the separation of these highly hydrophilic metabolites and investigate the mechanism of interaction between the negatively charged nucleosides (the negative charge is acquired either due to deprotonation of the amidic group and/or complexation with boronate) and the positively charged pseudostationary phase. This interaction is not only due to electrostatic (Coulombic) forces, but also due to hydrophobic interaction of the alkyl or aryl group of the boronate that forms a complex with the *cis*-diol group of the nucleoside. In this case, alkylboronates can act as a cosurfactant that increases the partitioning coefficient of the analytes into the micelles. In the presence of an alkylboronate in the BGE (employing only 20 mmol/L  $C_{14}MImBr$ ), the retention factors of the studied analytes are increased considerably when compared to a BGE without this additive. It is shown that the concept of one-site hydrophobically assisted ion exchange can be applied to describe the observed retention behavior. The high selectivity of boronates toward *cis*-diol-containing compounds can be used to adjust selectively the migration behavior of members of this compound class. By adding alkylboronic acid to the BGE, the separation selectivity is fine-tuned so that interferences from matrix components can be avoided in real sample analysis.

### Keywords:

Boronic acid / Ionic liquid type surfactant / MEKC / Phenylboronate affinity gel / Urinary nucleosides

DOI 10.1002/elps.201400357



Additional supporting information may be found in the online version of this article at the publisher's web-site

**Correspondence:** Professor Ute Pyell, Department of Chemistry, University of Marburg, Hans-Meerwein-Straße, D-35032 Marburg, Germany

**E-mail:** pyellu@staff.uni-marburg.de

**Fax:** +49-6421-2822124

**Abbreviations:** **Ado**, adenosine; **BBA**, 1-butylboronic acid;  **$C_{14}MImBr$** , 1-tetradecyl-3-methylimidazolium bromide; **CTAB**, cetyltrimethylammonium bromide; **Cyd**, cytidine; **DBA**, 1-dodecylboronic acid; **DC-CE**, dynamic complexation-capillary electrophoresis; **Guo**, guanosine; **HBA**, 1-hexylboronic acid; **IL**, ionic liquid; **Ino**, inosine; **5MeUrd**, 5-methyluridine; **3-NPBA**, 3-nitrophenylboronic acid;  **$pK_a^*$** , apparent acidity constant; **PSP**, pseudostationary phase; **TTAB**, tetradecyltrimethylammonium bromide; **Urd**, uridine; **Xao**, xanthosine

## 1 Introduction

Nucleosides are metabolites of either RNA turnover or oxidative damage of DNA. Abnormal urinary levels of these metabolites can occur under pathological conditions such as inflammation and cancer diseases. Their diagnostic value as potential markers for predicting cancer attracts the interest of many researchers for developing methods for the analysis of these compounds in both normal and cancer patients [1–8]. These methods employ either RP-HPLC, HILIC (due to their highly hydrophilic nature) or MEKC for the separation of similar compounds. Although separation by HILIC might be seen as the state of art for the determination of these highly hydrophilic nucleosides, we have demonstrated that our developed MEKC strategy provides a faster, more

**Colour Online:** See the article online to view Figs. 2 and 5–7 in colour.

efficient, highly reproducible and highly selective method for the analysis of these hydrophilic metabolites [9]. Most of the reported MEKC methods for the analysis of nucleosides are based on using SDS as pseudostationary phase (PSP) for the separation of these compounds as neutral species, however, due to their high hydrophilicity, a high concentration of the PSP (up to 300 mmol/L) is needed to obtain resolution. These conditions are typically associated with high electric current strength, excessive Joule heating, and a noisy baseline. Regarding the separation in alkaline buffer, we were able to show that the interaction between the nucleosides as negatively charged species and SDS is negligible due to electrostatic repulsion [9]. One approach to increase retention factors without the need to use an extremely high concentration of the PSP is using an oppositely charged (cationic) surfactant under conditions, where the analytes are present as anionic species.

Rageh and Pyell [9] and Orentaite et al. [10] were the first who studied the retention of (partially) charged solutes by oppositely charged micelles through the application of the classical theory of IEC (plotting  $\lg(k)$  against  $\lg(c(\text{competing ion}))$ ), which requires the ionic micelles to be regarded as pseudostationary ion exchangers that provide a fixed concentration of ion-exchange sites. In addition, the role of different contributions (hydrophobic and ion-exchange interactions) to the overall mixed-mode retention of neutral and (partially) charged solutes was studied [9, 10]. In [9], we have investigated the use of the ionic liquid (IL) type surfactant 1-tetradecyl-3-methylimidazolium bromide ( $C_{14}\text{MImBr}$ ) as PSP for the separation of seven urinary nucleosides, which are adenosine (Ado), cytidine (Cyd), 5-methyluridine (5MeUrd), uridine (Urd), guanosine (Guo), inosine (Ino), and xanthosine (Xao) [9].

We have studied the mechanism of interaction between the micelles formed by  $C_{14}\text{MImBr}$  and the negatively charged nucleosides. It was confirmed that electrostatic interaction is the main mode of interaction, and hydrophobic interaction can be considered to be negligible [9]. We have demonstrated that using only 20 mmol/L  $C_{14}\text{MImBr}$  in the BGE (5 mmol/L tetraborate, pH 9.38), a complete separation of all the studied analytes (existing as negatively charged complexes) is achieved. By calculating the retention factors at different tetraborate concentrations, we have found that highest retention factors are obtained at the lowest tetraborate concentration. Therefore, we regard the micelles formed by  $C_{14}\text{MImBr}$  as a pseudostationary ion exchanger that enables the regulation of the retention factor by variation of the competing ion concentration [9, 10]. However, even under optimized conditions (lowest tetraborate concentration), the retention factors of Ado and Cyd (the first-migrating nucleosides) are still extremely low. This necessitates the use of an alternative strategy in order to increase the partitioning coefficients and consequently the retention factors of these highly hydrophilic metabolites (especially, Ado and Cyd). This improvement is very demandable in real sample applications to avoid interference with matrix components. We will show that this objective can be accomplished by adding

boronic acid (replacing borate as complexing agent), which can bind selectively to the nucleosides via complex formation, while increasing their partitioning into the micelles formed by  $C_{14}\text{MImBr}$  via the hydrophobic alkyl/aryl group.

Boronate affinity interaction provides a unique means for the selective capture, isolation, and enrichment of *cis*-diol-containing biomolecules CDCBs [11]. These CDCBs include nucleosides, saccharides, and glycoproteins [12]. The principle of most of the applications of boronic acids is based on their ability to bind covalently to vicinal-diol moieties under alkaline pH conditions to form stable five- or six-membered cyclic esters, which can reversibly dissociate when the pH is changed to acidic conditions or another diol with higher affinity is added to the solution [11, 12]. This pH switch property allows boronic acids to be excellent ligands for saccharide sensing [11, 13]. In the recent years, boronate affinity has attracted great attention in separation science, particularly boronate affinity chromatography [11, 14–18]. Boronate affinity chromatography is nowadays involved in many -omics studies such as proteomics, metabolomics, and glycomics, especially, because CDCBs constitute a group of biomolecules that comprise several major classes of target molecules in -omics studies [14, 16–18].

Most of the boronate affinity chromatography applications are based on phenylboronate moieties [14–18] with very few reports concerning the applicability of alkylboronates [19]. It was recently reported that the association constant between 1-butylboronate and different nucleosides is in the range of 200–205  $\text{M}^{-1}$  at pH 10.0, and it was found that the six nucleosides studied exhibit only slight variations in their association constant with 1-butylboronate [12]. Based on these data, a method called "boronate affinity assisted MEKC" has been developed to improve the selectivity of the separation of nucleosides compared to MEKC methods without employing a boronate [12, 19]. In [19], the authors have reported that alkylboronates can be used in combination with the traditional cationic surfactant, cetyltrimethylammonium bromide (CTAB), in the separation of urinary nucleosides. They have found that the introduction of 1-butylboronic acid (BBA) at 25 mmol/L, urea (2 mol/L), and CTAB (25 mmol/L) to the BGE (200 mmol/L CHES) affords the best resolution between the studied analytes. The method was successfully applied to the analysis of urine samples. However, (i) they have not explained the quantitative effect (represented by the retention factor) of the addition of different boronic acids to the BGE, which is the main focus of our presented study. Moreover, (ii) we assume that the use of a high concentration of CHES in the BGE results in the displacement of the investigated nucleosides (especially, those containing an amidic functional group) from the ion-exchange sites present on the PSP. This will result in a low resolution for the first-migrating nucleosides investigated. To confirm this hypothesis, we study (for selected nucleosides), in addition to the impact of different alkylboronates, also the influence of the buffer ion concentration on the retention factor.

The imidazolium-based IL-type surfactant  $C_{14}\text{MImBr}$  will be used in this study as cationic surfactant PSP in

lieu of the conventional cationic surfactants such as tetradecyltrimethylammonium bromide (TTAB) and CTAB. In accordance with the previously reported results [9], we assume that  $C_{14}$ MImBr as PSP in MEKC provides generally a higher repeatability of migration times than either TTAB or CTAB and a modified selectivity. This improvement in repeatability and modification of selectivity is attributed by us to the efficiency by which  $C_{14}$ MImBr dynamically coats the inner capillary wall and to the versatility of the interaction sites provided by the imidazolium head group. Besides electrostatic interaction (that is also existing with TTAB or CTAB), the imidazolium head group offers additional types of intermolecular interactions ( $\pi$ – $\pi$ , ion-dipole, and hydrogen-bonding interactions) that modify the selectivity and provide a higher retention for hydrophilic analytes (via increase in  $\Delta G$ ) [9]. Additionally, in our previous study, we confirmed experimentally for selected nucleosides that the repeatability in migration times is significantly better with  $C_{14}$ MImBr as PSP than with TTAB [9].

In this paper, we investigate the combination of an alkyl or aryl boronate with the imidazolium-based IL-type surfactant ( $C_{14}$ MImBr) as PSP for the MEKC separation of highly hydrophilic urinary nucleosides. As an extension to previous studies with  $C_{14}$ MImBr in borate buffer, we demonstrate that with a BGE containing the combination of an alkyl/aryl boronate and  $C_{14}$ MImBr, (i) we can regulate the retention factors of the nucleosides by adjusting the competing ion concentration [9] and (ii) we can further increase the retention factor by an increase in the length of the alkyl chain of the boronic acid added. A comparison between the retention factors obtained in the presence and absence of alkylboronate is made with a special emphasis on the importance of the hydrophobic interaction introduced by the alkyl group of the boronate (shifting the retention factors to higher values). In accordance with the concept developed in [9], we investigate the impact of the buffer concentration on the retention factors in the presence of BBA. It is shown that the migration behavior of the studied analytes can be fully explained based on the concept of one-site hydrophobically assisted ion exchange (chromatography). In addition, we study whether also arylboronate (here, 3-nitrophenylboronate) can be employed as a retention modifier. The applicability of this approach is demonstrated taking the separation and determination of nucleosides in a spiked urine sample as an example.

## 2 Materials and methods

### 2.1 Chemicals and background electrolytes

Cyd, Ado, 5MeUrd, Urd, Guo, Ino, and Xao were purchased from Sigma-Aldrich (Steinheim, Germany; chemical structures,  $pK_a$  and  $\lg P_{ow}$ ; see Supporting Information Fig. 1). SDS, boric acid, trisodium phosphate dodecahydrate, and sodium hydroxide were purchased from Fluka (Buchs, Switzerland). Sodium dihydrogen phosphate monohydrate, disodium hydrogen phosphate dihydrate, sodium hydrogen carbonate, and disodium tetraborate decahydrate (borax) were

purchased from Merck (Darmstadt, Germany). Thiourea was purchased from Riedel-de Haën (Seelze, Germany). Sodium carbonate was purchased from Grüssing (Filsulm, Germany). Methanol (HPLC grade) was from VWR-BDH-Prolabo (Leuven, Belgium). BBA, 1-hexylboronic acid (HBA), 1-dodecylboronic acid (DBA), and 3-nitrophenylboronic acid (3-NPBA) were purchased from Alfa-Aesar (Karlsruhe, Germany; chemical structures and  $pK_a$  values; see Supporting Information Fig. 2). Decanophenone was purchased from Sigma-Aldrich. All analyte stock solutions (800 mg/L of Ado, Cyd, Urd, 5MeUrd, Ino, 400 mg/L of Xao, Guo) were prepared in water. Stock solutions of the nucleosides were stored in the refrigerator and used within 1 month. The working standard solutions were prepared daily (concentration of each of the studied nucleosides 20 mg/L, unless otherwise specified). A stock solution of thiourea (1000 mg/L) was prepared in water, while decanophenone (300 mg/L) was prepared in methanol. The Affi-gel 601, used as the stationary phase for the extraction of nucleosides from urine, was purchased from Bio-Rad (Hercules, CA, USA). The synthesis and characterization of  $C_{14}$ MImBr is described in detail in [9]. For the preparation of buffer stock solutions, refer to Supporting Information. Compositions of the micellar and nonmicellar BGEs are given in Table 1. All buffer solutions were filtered through a 0.45  $\mu$ m nylon membrane filter (WICOM, Heppenheim, Germany). BGEs were replaced after every two runs.

### 2.2 Instrumentation

All measurements were done using the ATI Unicam CE System, Crystal 300 Series, Model 310 equipped with UV/vis detector Spectra 100 (with deuterium lamp) from Thermo Separation Products (San Jose, USA), set to a wavelength of 257 nm (optimized wavelength). The oven temperature was kept at 35°C. Data acquisition was done using an AD converter (USB-1280FS, Measurement Computing, Middleborough, USA). Data were recorded using CE-Kapillarelektrophorese software (development of the electronic workshop of the Department of Chemistry, University of Marburg based on Delphi). Data analysis was performed with Origin 8.5 software (OriginLab, Northampton, USA). Fused-silica capillaries (50  $\mu$ m id, 360  $\mu$ m od) were obtained from Polymicro Technologies (Phoenix, AZ, USA), with a total length of 649 mm and a length to the detector of 501 mm (if not stated otherwise). SPEs were performed on a vacuum manifold column processor (J.T. Baker, Griesheim, Germany). The flow rate during sample loading and elution is 0.5 mL/min. The eluate obtained after the extraction procedure was lyophilized in a Christ Alpha 2–4 LSC Freeze Dryer (Martin Christ, Osterode am Harz, Germany).

New capillaries were conditioned by flushing them first with NaOH solution (1 mol/L) for 60 min, water for 30 min, and BGE for 5 min using an applied pressure of 800 mbar. Between runs, the capillaries were rinsed with NaOH solution (1 mol/L) for 2 min, water for 2 min, and finally with BGE for 2 min using an applied pressure of 800 mbar. To ensure a high repeatability of migration times,

**Table 1.** Compositions of the employed micellar and nonmicellar BGEs

<i>(A) Nonmicellar BGEs</i>	
1–20 mmol/L phosphate buffer, pH 11.05	
2–20 mmol/L phosphate buffer, pH 11.05 containing either 10 or 30 mmol/L BBA (adjusted with 1 mol/L NaOH)	
3–20 mmol/L carbonate buffer, pH 9.71, BGE 1	
4–20 mmol/L carbonate buffer, pH 9.71 containing 10 mmol/L boric acid (adjusted with 1 mol/L NaOH), BGE 3	
5–20 mmol/L carbonate buffer, pH 9.71 containing 10 mmol/L BBA (adjusted with 1 mol/L NaOH), BGE 5	
6–20 mmol/L carbonate buffer, pH 9.71 containing 10 mmol/L HBA (adjusted with 1 mol/L NaOH), BGE 7	
7–10 mmol/L BBA in either 5, 10, 15 or 20 mmol/L carbonate buffer, pH 9.71 (adjusted with 1 mol/L NaOH)	
<i>(B) Micellar BGEs</i>	
1–50 mmol/L SDS and 2 mmol/L DBA in 20 mmol/L phosphate buffer, pH 11.50 containing 20% methanol (adjusted with 1 mol/L NaOH)	
2–50 mmol/L SDS in 20 mmol/L phosphate buffer, pH 11.50 containing 20% methanol (adjusted with 1 mol/L NaOH)	
3–50 mmol/L SDS and 30 mmol/L BBA in 20 mmol/L phosphate buffer, pH 11.05 (adjusted with 1 mol/L NaOH)	
4–20 mmol/L C <sub>14</sub> MImBr in 20 mmol/L carbonate buffer, pH 9.71 (adjusted with 1 mol/L NaOH), BGE 2	
5–20 mmol/L C <sub>14</sub> MImBr and 10 mmol/L boric acid in 20 mmol/L carbonate buffer, pH 9.71 (adjusted with 1 mol/L NaOH), BGE 4	
6–20 mmol/L C <sub>14</sub> MImBr and 10 mmol/L BBA in 20 mmol/L carbonate buffer pH 9.71 (adjusted with 1 mol/L NaOH), BGE 6	
7–20 mmol/L C <sub>14</sub> MImBr and 10 mmol/L HBA in 20 mmol/L carbonate buffer pH 9.71 (adjusted with 1 mol/L NaOH), BGE 8	
8–20 mmol/L C <sub>14</sub> MImBr and 10 mmol/L BBA in either 5, 10, 15 or 20 mmol/L carbonate buffer, pH 9.71 (adjusted with 1 mol/L NaOH)	
9–20 mmol/L C <sub>14</sub> MImBr and 2 mmol/L 3-NPBA in 20 mmol/L phosphate buffer, pH 6.94	
10–50 mmol/L SDS and 2 mmol/L 3-NPBA in 20 mmol/L phosphate buffer, pH 7.02	
11–20 mmol/L C <sub>14</sub> MImBr in 2.5 mmol/L tetraborate, pH 9.71 (adjusted with 1 mol/L NaOH)	

The pH of the micellar BGEs containing C<sub>14</sub>MImBr is lower than that of the corresponding nonmicellar BGEs containing no C<sub>14</sub>MImBr due to the slight acidity of the imidazolium cation; therefore, the pH of the micellar BGEs containing C<sub>14</sub>MImBr must be adjusted to be exactly the same as the pH of the nonmicellar BGEs by using 1 mol/L NaOH.

the dynamic coating formed by C<sub>14</sub>MImBr should be completely removed between the runs. To accomplish this, the capillary, after using the BGE containing C<sub>14</sub>MImBr, was rinsed (every two runs) with the corresponding nonmicellar BGE containing no C<sub>14</sub>MImBr by application of a positive polarity (+15 kV) for 5 min. The separations were performed with the micellar and nonmicellar BGE under an applied voltage of –15 or +15 kV, respectively, unless otherwise specified. The samples were pressure-injected at 30 mbar for 12 s. The electroosmotic holdup time  $t_0$  [20] was determined using thiourea as neutral marker. Peak identities were confirmed by spiking.

### 2.3 Urine samples and extraction conditions

Samples of human urine were obtained from a 27-year-old healthy female volunteer and collected in 100 mL plastic bottles and frozen immediately until analysis. Before use, the samples were thawed at room temperature. For the study of spiked urine samples, samples were pre-treated with a PBA (phenylboronate affinity gel) column. The extraction conditions are based on what was previously reported [1, 4, 21, 22]. A brief description of the extraction procedure is given in [23].

## 3 Results and discussion

### 3.1 Mixed micelles of SDS with long-chain alkylboronates

BBA, HBA, DBA, and 3-NPBA are selective complexing agents that introduce both a negative charge and hydropho-

bic moiety to the complex formed with a nucleoside. BBA, HBA, DBA, 3-NPBA have  $pK_a$  values of 10.37, 10.47, 11.0, and 6.9, respectively (Supporting Information Fig. 2). For the first three boronic acids, the pH of the BGE must be higher than boric acid ( $pK_a = 9.24$ ) to provide a suitable solubility of the added modifier and to ensure the formation of the tetrahedral boronate ion. In the case of 3-NPBA, the pH of the BGE can be lower than boric acid (for details regarding the use of 3-NPBA, refer to the discussion in Supporting Information Fig. 3 and Table 1).

Our initial target was to form mixed micelles of SDS with the long-chain boronic acid DBA. DBA can act as a complex-forming cosurfactant that increases the partitioning of the highly hydrophilic nucleosides into the micelles formed by SDS. The limited solubility of DBA in aqueous buffers necessitates (i) working at high pH value and (ii) the presence of an organic solvent. BGEs are composed of (i) 20 mmol/L phosphate buffer containing 2 mmol/L DBA, 50 mmol/L SDS, and 20% methanol, pH 11.50 and (ii) the same BGE containing no DBA were tested. As shown in Fig. 1B, a shift of the migration times to longer values (in case of Ado and Cyd) is observed for the DBA containing BGE if compared to the electropherogram shown in Fig. 1A. In addition, the peaks of these two analytes are broadened (Fig. 1B). Ado and Cyd are neutral under these conditions. The increase in migration time can be ascribed exclusively to an increase in the retention factor, as DBA is completely incorporated into formed DBA-SDS mixed micelles. Band broadening of this extent must be ascribed to analyte–wall interaction, which can be explained by complex formation of the analyte with the highly hydrophobic DBA adsorbed on the capillary wall. For the other nucleosides: 5MeUrd, Urd, Guo, Ino, and Xao, only a very small

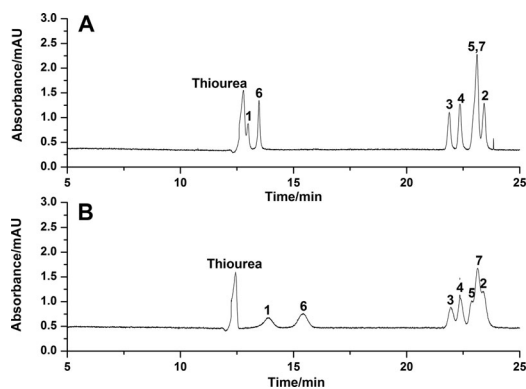


**Figure 1.** Electropherograms obtained from a standard solution mixture of 20 mg/L of each of the investigated nucleosides and 25 mg/L thiourea in water using BGE composed of 20 mmol/L phosphate buffer, pH 11.50 containing 50 mmol/L SDS and 20% methanol with (A) 0 mmol/L DBA or (B) 2 mmol/L DBA. Other CE conditions: capillary 649 (501) mm · 50  $\mu$ m I.D., applied voltage +15 kV, pressure injection 30 mbar for 12 s, oven temperature 35°C. Peak designation: 1 = cytidine, 2 = uridine, 3 = 5-methyluridine, 4 = guanosine, 5 = xanthosine, 6 = adenosine, 7 = inosine.

shift in migration times was observed (Fig. 1B). These nucleosides are negatively charged at the pH of the BGE due to the dissociation of their amidic group. Because of electrostatic repulsion (also the SDS micelles are negatively charged), complex formation with DBA is effectively suppressed. DBA is incorporated as a neutral species in the hydrophobic core of the SDS micelles so that it becomes inaccessible for the negatively charged nucleosides. The small band broadening observed for these analytes might be due to complex formation with DBA adsorbed on the inner capillary wall. Because of the excessive band broadening observed for those analytes interacting strongly with the added boronic acid, we selected shorter chain alkylboronic acids for further investigations.

### 3.2 Complexation with medium- to short-chain alkylboronates in the presence of SDS

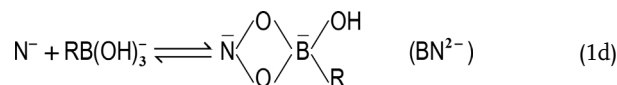
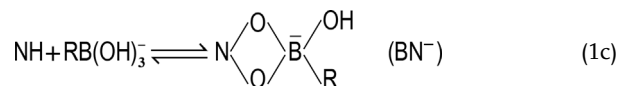
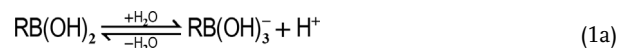
Recently, we have proved that the degree of complexation between tetrahydroxyborate and a nucleoside is very high even at a very low tetraborate concentration [9]. Taking BBA as a representative example, a BGE composed of 20 mmol/L phosphate buffer, pH 11.05 was investigated for the separation of the studied compounds in the absence and presence of BBA. In the absence of BBA (Supporting Information Fig. 4A), Ado and Cyd comigrate with the EOF marker (as they are neutral under the studied conditions), while Urd, 5MeUrd, Guo, Ino, and Xao are eluted after the EOF marker due to the negative charge acquired by the deprotonation of the amidic group. In the presence of BBA (Supporting Information Fig. 4B and C), all nucleosides acquire an additional negative charge due to complexation, and their migration times are shifted to longer values if compared to those observed using a BGE without BBA. The effective electrophoretic mobility  $\mu_{\text{eff}}$  of all the studied nucleosides was calculated at two different concentrations

of BBA (10 and 30 mmol/L) and compared to that obtained in the absence of the modifier. It was found that  $\mu_{\text{eff}}$  is constant for the two investigated BBA concentrations. This finding can be explained with a degree of complexation (between the nucleoside and alkylboronic acid) close to 1 (within the parameter range investigated). A concentration of 10 mmol/L alkylboronic acid is used for subsequent investigations.

Further addition of 50 mmol/L SDS to the BGE (containing 10 or 30 mmol/L BBA) does not improve the resolution of the investigated nucleosides (Supporting Information Fig. 4D). Based on these results, which are in agreement with what we have reported previously [9], we can conclude that SDS is not a suitable PSP because the MEKC separation of nucleosides as negatively charged compounds (electrostatic repulsion between negatively charged SDS micelles and negatively charged analytes). Consequently, a PSP with opposite charge (cationic surfactant, e.g.  $C_{14}\text{MImBr}$ ) must be employed. This oppositely charged PSP permits ion-exchange interaction (via Coulomb forces) with the negatively charged solutes that can be assisted by hydrophobic interaction of the hydrophobic moieties of the analytes with the hydrophobic core of the micelles.

### 3.3 Concept of one-site hydrophobically assisted ion exchange with $C_{14}\text{MImBr}$ micelles

Mixed-mode retention is retention due to both hydrophobic and ion-exchange (electrostatic) interactions. Under alkaline pH conditions, the tetrahedral boronate ion is capable of forming reversibly negatively charged complexes with nucleosides via their vicinal diol moieties. As shown in Fig. 2, the nucleosides can then interact with the positively charged PSP by (i) electrostatic interaction (due to the negative charge acquired by dissociation and/or complexation) and (ii) simultaneously by hydrophobic interaction due to the alkyl group of the boronic acid. In aqueous solution, the following dissociation (Eqs. 1a and b) and complexation (Eqs. 1c and d) equilibria have to be taken into consideration:



where NH is the neutral nucleoside,  $\text{N}^-$  is the deprotonated nucleoside,  $\text{RB(OH)}_2$  is the alkylboronic acid, and  $\text{RB(OH)}_3^-$  is the tetrahedral boronate ion. For Ado and Cyd, only the complexation equilibrium described in Eq. (1c) has to be considered and the monovalent negatively charged complex with boronic acid,  $\text{BN}^-$  is the only existing species. In case of Urd,

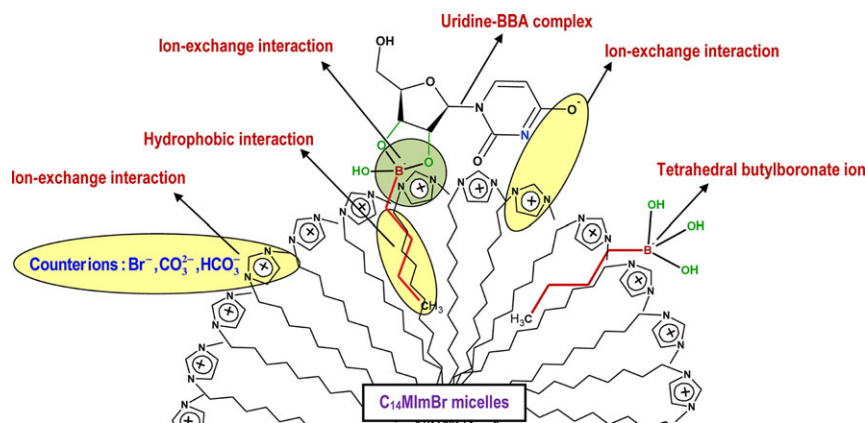


**Figure 2.** Schematic illustration of the mechanism of interaction of uridine-BBA complex with C<sub>14</sub>MImBr assuming one-site mixed-mode retention.

5MeUrd, Guo, Ino, and Xiao, all these equilibria (Eqs. 1b–1d) are involved as these compounds have a deprotonation site. However, due to the high complex formation constant, it can be concluded that the deprotonated complex with boronic acid (divalent,  $\text{BN}^{2-}$ ) will be the dominant species for these analytes, which will be taken into account in further considerations.

As shown in Fig. 2, the major modes of retention of the negatively charged complexed nucleosides with the positively charged PSP are both hydrophobic and ion-exchange interactions. The simultaneous presence of both hydrophobic and ion-exchange (electrostatic) interactions is defined as mixed-mode retention. Two models have been developed, which qualitatively and quantitatively describe a mixed-mode (ion-exchange and hydrophobic interaction) retention of analytes on an LC stationary phase: the one-site retention model and two-site retention model [24]. These models were also applied in CEC to describe both qualitatively and quantitatively the contribution of ion-exchange and hydrophobic interaction to the overall retention of cationic solutes on a mixed-mode (negatively charged) monolithic stationary phase [25]. Transferred to MEKC, one-site mixed-mode retention denotes the situation that there is only one type of site and the only interaction that the charged analyte undergoes is a simultaneous interaction with both the hydrophobic core of the micelles and a charged surfactant head group. Two-site mixed-mode retention refers to a situation in which there are pure ion-exchange sites and pure hydrophobic interaction sites, and the interaction of the analytes with the two sites takes place spatiotemporally independently. In MEKC such a situation would be given, if there were one type of micelles providing a hydrophobic interaction site and one type of micelles providing an ion-interaction site [26].

According to our retention model (see Fig. 2), we assume that both hydrophobic and ion-exchange interactions take place simultaneously at a single type of site (one-site model). In this case, the total molar free energy  $\Delta G_{\text{T}}^{\circ}$  of the phase transition is the sum of the partial molar free energies  $\Delta G_{\text{RP}}^{\circ}$  and  $\Delta G_{\text{IEX}}^{\circ}$  [27]:

$$\ln k = \ln \varphi + \left( \frac{\Delta G_{\text{RP}}^{\circ}}{RT} + \frac{\Delta G_{\text{IEX}}^{\circ}}{RT} \right), \quad (2)$$

where  $k$  is the overall retention factor,  $\varphi$  is the phase ratio (volume of the micellar phase divided by the volume of the surrounding aqueous phase), and  $\Delta G_{\text{RP}}^{\circ}$  and  $\Delta G_{\text{IEX}}^{\circ}$  are the free energy contributions from the RP (hydrophobic) and ion-exchange interaction, respectively [25]. It is important to note that according to this model, the overall retention factor  $k$  results from the product  $k_{\text{RP}} \cdot k_{\text{IEX}}$ .

In the ion-exchange mode, the retention factor for a deprotonated divalent ion  $\text{BN}^{2-}$  is not only determined by the ion-exchange capacity of the pseudostationary ion exchanger (micelles), but also by the molar concentration and type of the competing ion ( $\text{C}^{-}$ ) in the BGE. The following chemical equilibrium has to be regarded:



For this ion-exchange reaction, the ion-exchange equilibrium constant can be written as:

$$K_{\text{IEX}} = \frac{c(\text{PSP}^{2+}\text{BN}^{2-}) \cdot c(\text{C}^{-})^2}{c(\text{PSP}^{2+}2\text{C}^{-}) \cdot c(\text{BN}^{2-})}, \quad (4)$$

where  $c(\text{PSP}^{2+}2\text{C}^{-})$  is the amount of substance of accessible (available) imidazolium dicationic sites (formed by two imidazolium groups) normalized to the volume of the pseudostationary ion exchanger (ion-exchange capacity),  $c(\text{BN}^{2-})$  is the molar concentration of the deprotonated complexed nucleoside in the BGE,  $c(\text{PSP}^{2+}\text{BN}^{2-})$  is the molar concentration of the deprotonated complexed nucleoside in the PSP, and  $c(\text{C}^{-})$  is the molar concentration of the counterion in the BGE. The retention factor  $k_{\text{IEX}}$  due to the ion-exchange process is defined as:

$$k_{\text{IEX}} = \varphi \frac{c(\text{PSP}^{2+}\text{BN}^{2-})}{c(\text{BN}^{2-})} = \varphi K_{\text{IEX}} \frac{c(\text{PSP}^{2+}2\text{C}^{-})}{c(\text{C}^{-})^2}. \quad (5)$$

According to Eq. (5), increasing the concentration of the counterion will decrease the retention factor. Taking into account the dependence of  $k_{\text{IEX}}$  on the counterion concentration, the following equation for the overall retention factor  $k$  is obtained:

$$k = k_{\text{RP}} k_{\text{IEX}} = k_{\text{RP}} \frac{\varphi K_{\text{IEX}} c(\text{PSP}^{2+}2\text{C}^{-})}{c(\text{C}^{-})^2}. \quad (6)$$



According to this equation, the only interaction that a negatively charged solute undergoes is a simultaneous interaction with both the hydrophobic moiety and a pair of positively charged imidazolium cationic groups (see Fig. 2). According to Neue et al. [27], this site is called hydrophobically assisted ion-exchange site. Taking the logarithm of Eq. (6) results in:

$$\lg k = A' + \lg k_{\text{RP}} - 2 \lg(c(\text{C}^-)), \quad (7)$$

where  $A'$  is a constant equal to  $\lg(\varphi K_{\text{IEX}} c(\text{PSP}^{2+} 2 \text{C}^-))$ . Following the Martin equation [28]:

$$\lg k_{\text{RP}} = A + B n_{\text{CH}_2}, \quad (8)$$

where  $A$  and  $B$  are constants and  $n_{\text{CH}_2}$  is the methylene group number, a modified equation can be obtained [24]:

$$\lg k = A'' + B n_{\text{CH}_2} - 2 \lg(c(\text{C}^-)), \quad (9)$$

where  $A'' = A + A'$ . Based on Eq. (9), it can be predicted that the slope of plotting  $\lg k$  vs.  $\lg(c(\text{C}^-))$  for  $\text{BN}^{2-}$  and a competing ion of a charge  $-1$  in the BGE must be close to  $-2$ . Simultaneously, for a homologous series of alkylboronates, there will be a linear dependence of  $\lg k$  on  $n_{\text{CH}_2}$ .

The key assumption of the alternative two-site model of mixed-mode retention is that the two binding sites (the hydrophobic and the ion-exchange sites) are locally separated (e.g. two different PSPs) and independent. In this case, the solute molecules interact independently with the two types of sites and retention is the sum of two independent processes,  $k = k_{\text{RP}} + k_{\text{IEX}}$  [24, 25]. However, these presumptions are not fulfilled in our case.

### 3.4 Boronate affinity assisted retention

#### 3.4.1 Retention factor dependent on the length of the alkyl chain

In these studies, a carbonate buffer (pH 9.71) replaced the phosphate buffer (pH 11.05) that was used as BGE in previous experiments. This can be ascribed to the following reasons: (i) the low buffering capacity of phosphate buffer at high pH value, (ii) phosphate buffer with pH 11.05 is more likely for atmospheric  $\text{CO}_2$  absorption, (iii) the low resolution between the investigated nucleosides while using phosphate buffer, pH 11.05 as five of them (5MeUrd, Urd, Guo, Ino, and Xao) are completely deprotonated under these conditions. At pH 9.71, a molar fraction of 18 and 15% of BBA and HBA is present in its deprotonated form. It is important to note that the apparent acidity of the free boric acid is increased by complexation with *cis*-diols, i.e.  $\text{p}K_{\text{a}}^* < \text{p}K_{\text{a}}$  [29, 30], which in turn means that the molar fraction of the deprotonated species is higher for the boronate ester than for the free non-complexed boronate. A relatively high concentration carbonate buffer was selected (20 mmol/L, pH 9.71). This concentration was selected to minimize the electrostatic interaction of the investigated analytes with  $\text{C}_{14}\text{MImBr}$ , as carbonate and bicarbonate anions act as competing ions (see Fig. 2).

Eight cases were compared as given in Fig. 3. In the first case (Fig. 3A), 20 mmol/L carbonate buffer, pH 9.71 (BGE 1) was used as a BGE. There is no separation of Ado and Cyd, as these compounds are neutral under these conditions and they comigrate with the EOF marker. The other nucleosides—Urd, 5MeUrd, Ino, Guo, and Xao—are eluted after the neutral marker due to the dissociation of their amidic groups. In the second case (Fig. 3B), the separation of the same analytes was examined using 20 mmol/L  $\text{C}_{14}\text{MImBr}$  in 20 mmol/L carbonate buffer, pH 9.71 (BGE 2). As shown in Fig. 3B, their effective charge number is too low for separation via interaction between the investigated analytes and  $\text{C}_{14}\text{MImBr}$  micelles. In the third case (Fig. 3C), the presence of boric acid in the BGE 3 results in shifting the migration times of all of the investigated analytes to longer times if compared to Fig. 3A. This can be ascribed to the additional negative charge gained by complexation. However, under these conditions, Ado and Cyd are still comigrating. In Fig. 3D (using BGE 4, 20 mmol/L  $\text{C}_{14}\text{MImBr}$  in 20 mmol/L carbonate buffer in the presence of borate), a good separation between the studied analytes was achieved. However, four of them are eluted before the neutral marker, which indicates their weak interaction with the  $\text{C}_{14}\text{MImBr}$  micelles. At pH 9.71, all nucleoside–tetrahydroxyborate complexes will be present as tetrahedral (negatively charged) borate esters due to the lowering of the  $\text{p}K_{\text{a}}^*$  of boric acid after complexation.

In the fifth and seventh cases (Fig. 3E and G), using BGEs 5 and 7 containing BBA and HBA, respectively, the situation is similar to that in the case of Fig. 3C (when using boric acid in the BGE) with a difference in the resolution between Ado and Cyd, and Urd and Guo. In addition, the migration times of the nucleosides are shorter (compared to those of Fig. 3C) as the charge-to-size ratio of the complexed nucleosides is becoming lower with increased  $n_{\text{CH}_2}$ . In the sixth case (Fig. 3F) using BGE 6, which contains BBA and  $\text{C}_{14}\text{MImBr}$ , all studied nucleosides are eluted after the neutral marker. The increase in  $k$  with  $n_{\text{CH}_2}$  (see Table 2) indicates the significant role of hydrophobic interactions in the overall retention process. With a BGE containing BBA and  $\text{C}_{14}\text{MImBr}$ , a good resolution between all of the studied nucleosides was obtained. A further improvement in the resolution of Guo and Xao was achieved by lowering the concentration of BBA in the BGE to 5 mmol/L (Fig. 4). There is a slight band broadening (see Table 3) for most of the studied nucleosides in case of using BGE 6, while compared with the peak efficiencies obtained with BGE 4. In the latter case (BBA replaced by HBA, Fig. 3H), the situation is very similar to that depicted in Fig. 3F. However, the adsorption of the complexed analytes onto the capillary wall results in severe peak broadening (see Table 3). It is interesting that this severe peak broadening (with BGE 8) is observed only for the first four migrating nucleosides. This observation will be discussed in detail later. There is also an increase in the migration times relative to the peaks depicted in Fig. 3F, which is consistent with the increase in  $n_{\text{CH}_2}$  (Eq. (9)).

Details concerning the calculation of the retention factors are described in the Supporting Information. The

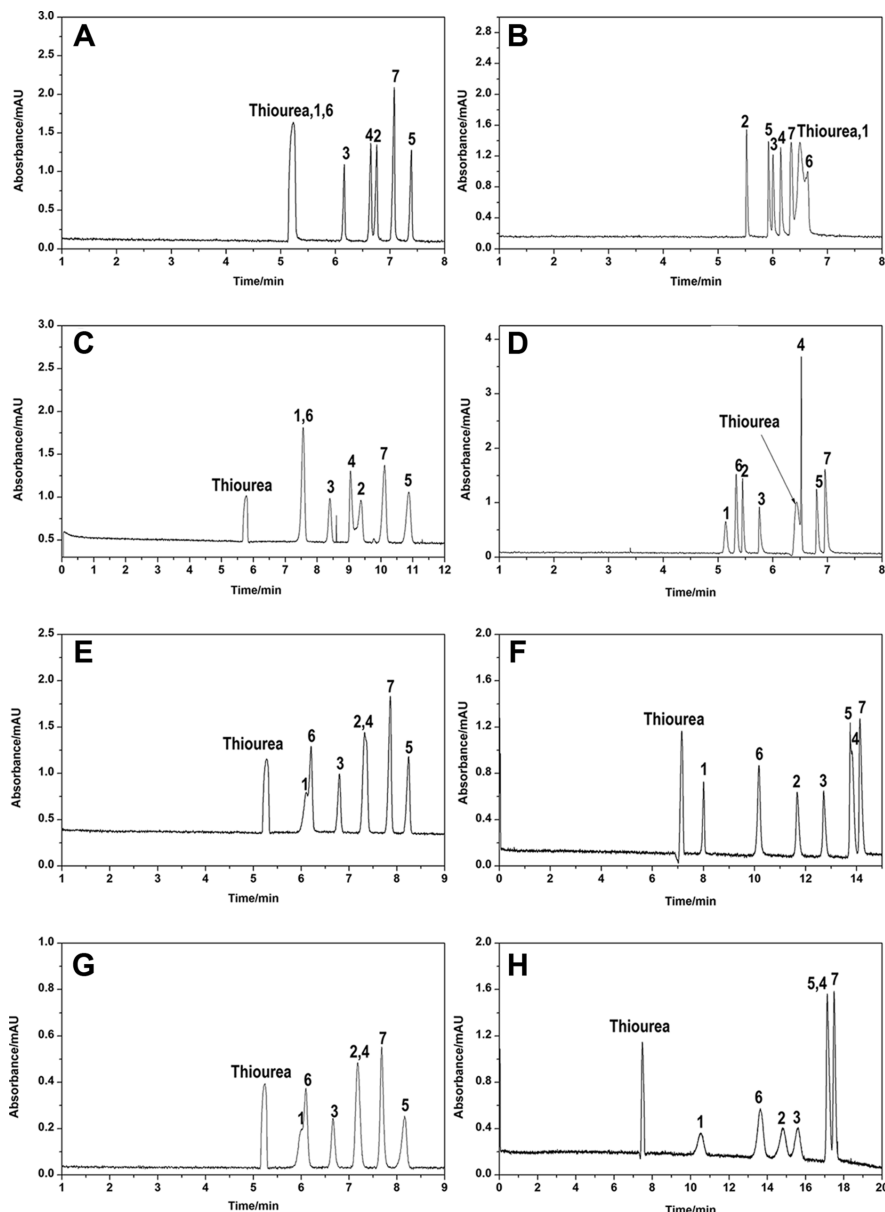


**Figure 3.** Electropherograms obtained from a standard solution mixture of 20 mg/L of each of the investigated nucleosides and 25 mg/L thiourea in water. The nonmicellar BGEs composed of (A) 20 mmol/L carbonate buffer, pH 9.71; (C) 10 mmol/L boric acid in 20 mmol/L carbonate buffer, pH 9.71; (E) 10 mmol/L BBA in 20 mmol/L carbonate buffer, pH 9.71 and (G) 10 mmol/L HBA in 20 mmol/L carbonate buffer, pH 9.71. The micellar BGEs composed of 20 mmol/L  $C_{14}$ MImBr in either (B) 20 mmol/L carbonate buffer, pH 9.71; (D) 10 mmol/L boric acid in 20 mmol/L carbonate buffer, pH 9.71; (F) 10 mmol/L BBA in 20 mmol/L carbonate buffer, pH 9.71 or (H) 10 mmol/L HBA in 20 mmol/L carbonate buffer, pH 9.71. Other CE conditions: capillary 649 (501 mm · 50  $\mu$ m I.D.), applied voltage +15 or –15 kV in case of nonmicellar and micellar BGEs, respectively, pressure injection 30 mbar for 12 s, oven temperature 35°C. Peak designation as in Fig. 1.

electrophoretic mobilities were calculated in the presence (MEKC mode) and absence (CZE mode) of  $C_{14}$ MImBr. The nonmicellar BGEs were used to calculate  $\mu_{\text{eff}}$  (the effective electrophoretic mobility of the analyte in micelle-free BGE) of each of the studied nucleosides. The micellar BGEs (containing 20 mmol/L  $C_{14}$ MImBr) were employed to calculate  $\mu$  (the pseudoeffective electrophoretic mobility of the analyte in the micellar BGE) and  $\mu_{\text{MC}}$  (the electrophoretic mobility of the micelles in micellar BGE) under exactly the same conditions as the experiment performed in the CZE mode. Decanophenone was employed as micelle marker in a sample matrix of micellar BGE/water/methanol (50:40:10, v/v/v) to solubilize this hydrophobic compound.

Figure 5 depicts the calculated effective and pseudoeffective electrophoretic mobilities for the nucleosides in different

BGEs (BGEs 1–8). Strong interaction of the nucleosides both with the boronic acids and  $C_{14}$ MImBr micelles is represented by the change of sign of the mobility. The retention factors calculated for the  $C_{14}$ MImBr containing BGEs are given in Table 2. The comparison of the data indicates the important role of hydrophobic interactions, as there is an increase in  $k$  with increasing alkyl group length of the boronic acid. For analytes having the same effective charge number (e.g. Ado and Cyd or Urd and Guo), the purine nucleosides (Ado and Guo) have higher retention factors than the corresponding pyrimidine nucleosides (Cyd and Urd) as they are more hydrophobic (Supporting Information Fig. 1). In addition, 5MeUrd has a higher retention factor than Urd as this compound is more hydrophobic due to the additional methyl group.

**Table 2.** Retention factors calculated in different BGEs

Analyte	$k/\text{BGE}^{\text{a}}$			
	BGE 2 <sup>b</sup>	BGE 4 <sup>b</sup>	BGE 6 <sup>b</sup>	BGE 8 <sup>b</sup>
	20 mmol/L C <sub>14</sub> MImBr in 20 mmol/L carbonate buffer, pH 9.71	10 mmol/L boric acid and 20 mmol/L C <sub>14</sub> MImBr in 20 mmol/L carbonate buffer, pH 9.71	10 mmol/L BBA and 20 mmol/L C <sub>14</sub> MImBr in 20 mmol/L carbonate buffer, pH 9.71	10 mmol/L HBA and 20 mmol/L C <sub>14</sub> MImBr in 20 mmol/L carbonate buffer, pH 9.71
Ado	0.0	0.1	1.8	4.3
Cyd	0.0	0.0	0.6	1.5
Urd	0.2	0.4	4.1	8.2
Guo	0.4	0.8	9.2	24.3
Ino	0.6	1.3	11.6	34.2
Xao	0.4	1.3	10.0	27.5
5MeUrd	0.2	0.4	5.4	10.0

a) Listed values are the average of at least three measurements. Retention factors in the case of a BGE containing 20 mmol/L C<sub>14</sub>MImBr in 2.5 mmol/L tetraborate, pH 9.70 are 0.3, 0.2, 2.2, 4.0, 6.0, 6.4, 2.0 for Ado, Cyd, Urd, Guo, Ino, Xao, and 5MeUrd, respectively [9].

b)  $\mu_{\text{MC}}$  in the case of BGEs 2 and 4:  $2.84 \times 10^{-4} \text{ cm}^2 \text{ V}^{-1} \text{ s}^{-1}$  and in the case of BGEs 6 and 8:  $2.92 \times 10^{-4} \text{ cm}^2 \text{ V}^{-1} \text{ s}^{-1}$ .

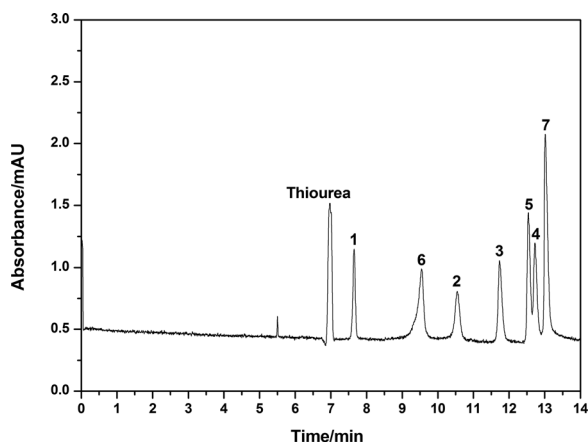


**Figure 4.** Electropherogram obtained from a standard solution mixture of 20 mg/L of each of the investigated nucleosides and 25 mg/L thiourea in water using 5 mmol/L BBA and 20 mmol/L C<sub>14</sub>MImBr in 20 mmol/L carbonate buffer, pH 9.71 as a BGE. Other CE conditions: applied voltage –15 kV, pressure injection 30 mbar for 12 s, oven temperature 35°C. Peak designation as in Fig. 1.

**Table 3.** Peak efficiencies calculated in different BGEs

Analyte	$N$ (peak efficiency)			
	BGE 2 <sup>a</sup>	BGE 4 <sup>a</sup>	BGE 6 <sup>a</sup>	BGE 8 <sup>a</sup>
Ado	n.d. <sup>b</sup>	100 000	41 000	10 000
Cyd	n.d. <sup>b</sup>	48 000	70 000	5000
Urd	270 000	240 000	52 000	10 000
Guo	220 000	(2 080 000) <sup>c</sup>	n.d. <sup>b</sup>	n.d. <sup>b</sup>
Ino	99 000	130 000	95 000	107 000
Xao	240 000	190 000	n.d. <sup>b</sup>	n.d. <sup>b</sup>
5MeUrd	210 000	170 000	74 000	14 000

a) Refer to Table 2 for the exact compositions of the employed BGEs.

b) n.d.: not determined.

c) The very high peak efficiency of Guo can be attributed to peak focusing by transient isotachphoretic stacking.

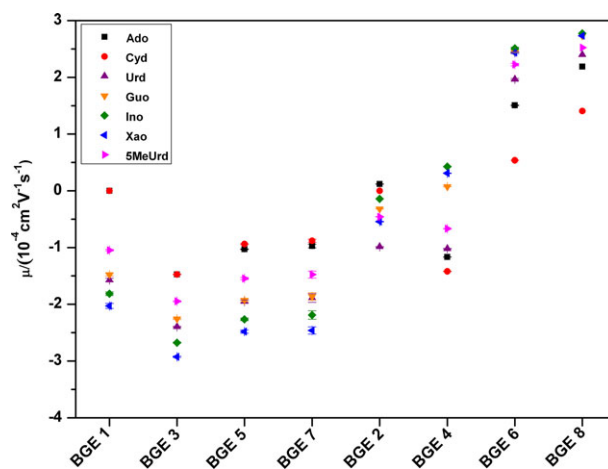


**Figure 5.** Effective mobilities of nucleosides obtained in different BGEs. Each data point is the average of at least five measurements, standard deviation represented as error bar. For experimental details, refer to Fig. 3.

By taking the logarithm of the retention factors obtained with BGEs 4, 6, and 8, a plot of  $\lg(k)$  against  $n_{\text{CH}_2}$  (number of methylene units) is constructed, which results in straight lines with regression coefficients  $r$  between 0.9878 and 0.9999 (Fig. 6A). As seen from Fig. 6A, there is a slight variation in the values of the slopes. A statistical significance test, however, indicates that these differences are not significant (see Supporting Information), confirming the presumptions in the derivation of Eq. (9).

### 3.4.2 Retention factor dependent on competing ion concentration

With the aim to show the impact of the competing ion concentration on the retention factors, eight cases were

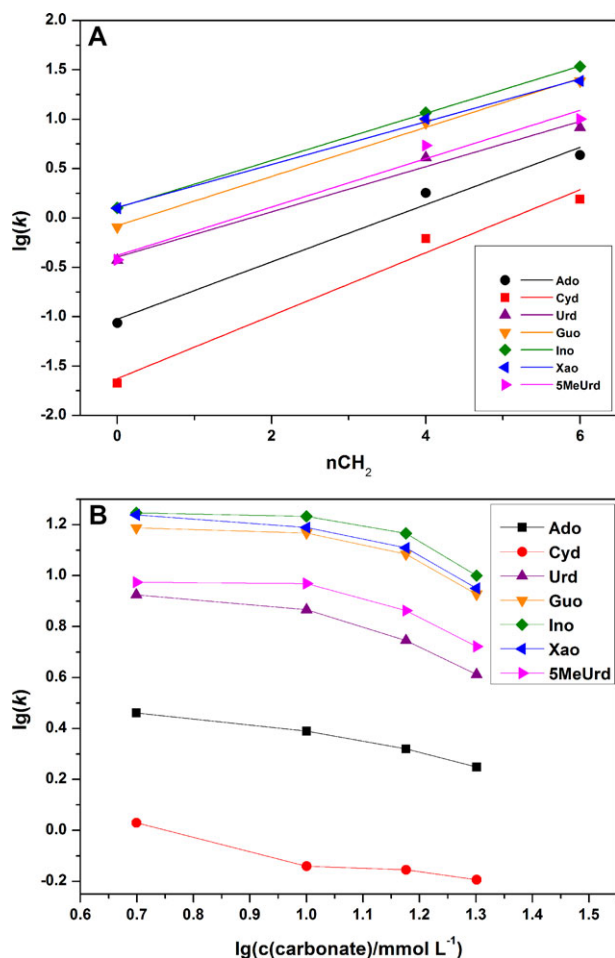


**Figure 6.** Plot of  $\lg(k)$  against (A)  $n\text{CH}_2$  of alkylboronic acid and (B)  $\lg(c(\text{carbonate}))$ .

compared (Supporting Information Fig. 5). In these eight cases, each micellar BGE is studied with its corresponding nonmicellar BGE, which has exactly the same composition but without  $\text{C}_{14}\text{MImBr}$ . Four different carbonate buffer concentrations, pH 9.71 were tested: 5, 10, 15 and 20 mmol/L. Each BGE contains either (1) 10 mmol/L BBA (Supporting Information Fig. 5A, C, E, and G) or (2) 10 mmol/L BBA and 20 mmol/L  $\text{C}_{14}\text{MImBr}$  (Supporting Information Fig. 5B, D, F, and H). Higher concentrations of carbonate buffer were not accessible due to a resulting increase in the baseline noise and electric current strength noise (Supporting Information Fig. 6).

It was reported that IL-based surfactants (this term was suggested by Pino et al. [31]) can change their self-assembly structures in the aqueous solution (when increasing their concentration) from spherical micelles to rod-like micelles and then to vesicles [32]. Moreover, the aggregation behavior of a single-chain imidazolium-based IL-type surfactant was studied on a surface-oxidized silicon wafer [33]. It was shown that this surfactant, by increasing its concentration, is capable of forming a multilayer structure adsorbed onto a silica surface. Although the concentration of the employed cationic surfac-

tant within this study is  $\leq 20$  mmol/L, the effect of the counterion concentration on the micelle aggregation behavior, CMC and, critical surface aggregation concentration cannot be neglected. The CMC of long-chain ILs is reduced by increasing the counterion concentration [34]. Additionally, the counterion concentration influences the self-assembly structure via changes in the aggregation number and molecular packing parameter  $P$ . Assuming a similar effect on the critical surface aggregation concentration and on the formed admicelles, we can conclude that the structure of the micellar coating on the inner capillary wall might be also changed by increasing the salt concentration (at a fixed concentration of  $\text{C}_{14}\text{MImBr}$  of 20 mmol/L). The observed increased noise at increased counterion concentration might be due to the formation of a multilayer structure.

As shown in Supporting Information Fig. 5, in case of micellar BGEs, the increase in buffer concentration does not result in a considerable increase in the migration times of the nucleosides as would be expected from the simultaneous decrease in the EOF velocity. This can be explained by the influence of the competing ion concentration (Fig. 2) on the retention factors of the analytes.

Retention factors were calculated as discussed before using the electrophoretic mobilities determined using the nonmicellar BGEs (Supporting Information Table 2) and micellar BGEs (Supporting Information Table 3). The calculated retention factors are listed in Supporting Information Table 4. The retention factors for all the nucleosides investigated are highly dependent on the competing ion concentration (represented by  $\text{CO}_3^{2-}$  and  $\text{HCO}_3^-$  ions) being the highest at the lowest carbonate buffer concentration. These results are corresponding to what is expected from the classical theory of IEC. In addition, these results support our previously reported results [9, 10] that micelles (in case of analytes of opposite charge) can be considered as a pseudostationary ion exchanger. As expected from Eq. (9), a plot of  $\lg(k)$  against  $\lg(c(\text{carbonate}))$  should result in a straight line with a slope equal to  $-x/y$  (where  $x$  is the effective charge of the analyte that is  $-2$  in case of charged nucleosides and  $y$  is the effective charge number of the competing ion). As shown in Fig. 6B, there is a clear deviation from linearity, which can be attributed to the presence of a third competing ion, the bromide ion (Fig. 2). The effect of the third competing ion manifests itself substantially at low carbonate concentration resulting in a constant plateau value at low  $c(\text{carbonate})$ , while a linear decrease in  $\lg(k)$  is obtained at higher  $c(\text{carbonate})$  (influence of bromide ion can be neglected). These observations are in agreement with former reports [9, 10]. Although the maximum slope of the curves does not match with the theoretical value of  $-1$  or  $-2$ , Fig. 6B shows clearly that there is a considerable influence of the concentration of the competing ion(s) on the retention factors. Ion-exchange interaction (beside hydrophobic interaction) dominates the retention of the analytes by the (mixed-mode) PSP. The plots shown in Fig. 6A and B confirm that the selected one-site hydrophobically assisted ion-exchange model describes adequately the observed retention of the investigated nucleosides.

### 3.5 Mechanism of band broadening

Adsorption onto the inner wall of the fused-silica capillary is a well-known phenomenon that can be attributed to hydrophobic and/or electrostatic interactions between the capillary wall and the analyte. Wall adsorption can occur in the BGE compartment [35,36] or can be constrained to the sample zone [37] (if the composition of the sample solution deviates strongly from that of the BGE). One of the consequences of analyte adsorption onto the capillary wall is deterioration of the peak efficiency (Table 3) [38].  $C_{14}$ MImBr dynamically coats the capillary wall by forming admicelles (bilayer arrangement) [9], whereas multilayer arrangements were also reported for the lower homologue 1-dodecyl-3-methylimidazolium bromide [33]. With a BGE containing  $C_{14}$ MImBr, the capillary wall is covered with a positively charged layer onto which BBA and HBA (free and/or complexed) can be adsorbed by electrostatic and/or hydrophobic forces. Being more hydrophobic than BBA, HBA is more strongly adsorbed than BBA. The comparison of the electropherograms shown in Fig. 3 clearly reveals that peak broadening is mostly pronounced with a BGE containing HBA. It is now very interesting to see that only the peaks of the analytes with lower retention factor are broadened, while there is no peak broadening for those analytes with higher retention factor (Table 3).

Two coupled equilibria are involved in the observed processes: adsorption (onto the wall from the aqueous phase) and distribution (between the aqueous and the micellar phase). The different retention factors influence the states of the equilibria involved, which can explain the observed peak broadening dependent on  $k$ . The molar fraction of analyte present in the aqueous phase is increased with decreased retention factor, which concomitantly increases the molar fraction of adsorbed analyte even if the adsorption constant is fixed and the adsorption equilibrium is reached instantaneously. Increasing peak broadening is expected with increasing molar fraction of adsorbed analyte. As depicted in Fig. 3H, the first four analytes (lower  $k$ ) have broadened peaks, while the efficiency is not decreased for the later eluted analytes (higher  $k$ , see Table 3).

### 3.6 Application to urine sample analysis

A solution of standards and spiked urine samples were pre-treated with a PBA column (see Section 2.3). After the lyophilization of the eluate, the dried extract was reconstituted in 2 mL water (CE sample). The BGE used for the subsequent separation of the nucleosides contained 5 mmol/L BBA and 20 mmol/L  $C_{14}$ MImBr in 20 mmol/L carbonate buffer, pH 9.71. Figure 7A shows the separation of the standard nucleosides after extraction with the PBA column, whereas Fig. 7B depicts an electropherogram obtained for a spiked urine sample. The presence of nucleosides as endogenous compounds in the investigated urine sample can be confirmed by the increase in the peak area (e.g. for Cyd and Xao) visible in the electropherogram shown in Fig. 7B when

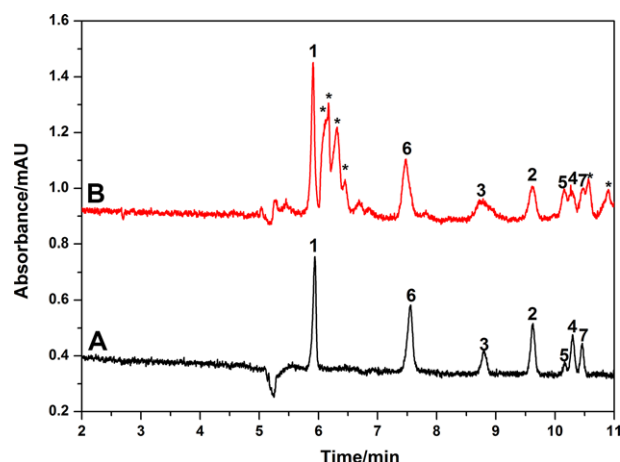


**Figure 7.** Electropherograms of standard nucleosides and spiked urine samples: (A) Nucleoside standards after extraction with PBA column and (B) spiked urine sample after extraction with PBA column. Concentration of standards or spiked nucleosides: 16.08 mg/L Ado and 5MeUrd, 32.16 mg/L Cyd, 8.16 mg/L Guo, 8.00 mg/L Urd, 4.00 mg/L Ino, 2.06 mg/L Xao. Extracts are reconstituted in 2 mL water and injected by pressure injection of 30 mbar for 12 s. BGE: 5 mmol/L BBA and 20 mmol/L  $C_{14}$ MImBr in 20 mmol/L carbonate buffer, pH 9.71. CE conditions: capillary 648 (500) mm  $\times$  50.2  $\mu$ m I.D., applied voltage  $-20$  kV, oven temperature  $35^{\circ}\text{C}$ . Peak designation: see Fig. 1. \*Unidentified peak.

compared to the corresponding peaks in Fig. 7A. As shown in Fig. 7B, Ado and Cyd are very well separated and clearly separated from possible matrix interferences. Because of the excellent extraction selectivity of PBA, there are only few peaks that have to be assigned to unknown compounds present in the urine matrix. There is a remarkable high resolution for Urd and 5MeUrd. For clinical studies, the determined nucleoside concentrations have to be normalized on the creatinine content. Band broadening is more visible for Urd in the case of the spiked urine sample that can be ascribed to matrix effects. The analysis of a spiked urine sample shows that the addition of the modifier BBA allows to fine-tune the selectivity of the separation system so that interferences from matrix constituents (which are often a problem when analysing a real sample) can be actively avoided.

## 4 Concluding remarks

The separation of seven highly hydrophilic urinary nucleosides can be successfully achieved using 5 mmol/L BBA and 20 mmol/L  $C_{14}$ MImBr in 20 mmol/L carbonate buffer, pH 9.71. The involved retention mechanism is hydrophobically assisted electrostatic interaction. Application of a one-site retention model can fully describe the retention behavior observed regarding the influence of the alkyl chain length of the alkylboronic acid and the influence of the competing ion concentration. Retention factors can be controlled by the type and concentration of the alkylboronic acid added, the type and concentration of the (cationic) surfactant, the pH, and the concentration of the competing ion. The ability

to fine-tune the retention factors over a very large range in addition to the high extraction selectivity of the commercially available phenylboronate affinity gels provides a promising approach for the routine analysis of urine samples.

A. H. Rageh thanks the Egyptian Ministry of Higher Education and Ministry of State for Scientific Research (MHESR) and the Deutscher Akademischer Austauschdienst (DAAD) for funding her PhD scholarship through German Egyptian Research Long-Term Scholarship program (GERLS). We thank Prof. M. Marahiel for providing the lyophilizer. We thank the workshops of the Department of Chemistry for the development of the data-recording unit.

The authors have declared no conflict of interest.

## 5 References

- [1] Xu, G., Liebich, H. M., Lehmann, R., Müller-Hagedorn, S., *Methods Mol. Biol.* 2001, 162, 459–474.
- [2] Cho, S. H., Choi, M. H., Lee, W. Y., Chung, B. C., *Clin. Biochem.* 2009, 42, 540–543.
- [3] Rodriguez-Gonzalo, E., Garcia-Gomez, D., Carabias-Martinez, R., *J. Chromatogr. A* 2011, 1218, 9055–9063.
- [4] Szymanska, E., Markuszewski, M. J., Bodzioch, K., Kaliszan, R., *J. Pharm. Biomed. Anal.* 2007, 44, 1118–1126.
- [5] Zheng, Y. F., Kong, H. W., Xiong, J. H., Shen, L., Xu, G. W., *Clin. Biochem.* 2005, 38, 24–30.
- [6] Liebich, H. M., Müller-Hagedorn, S., Klaus, F., Meziane, K., Kim, K. R., Frickenschmidt, A., Kammerer, B., *J. Chromatogr. A* 2005, 1071, 271–275.
- [7] Liebich, H. M., Lehmann, R., Xu, G., Wahl, H. G., Häring, H. U., *J. Chromatogr. B: Biomed. Sci. Appl.* 2000, 745, 189–196.
- [8] Zheng, Y. F., Xu, G. W., Liu, D. Y., Xiong, J. H., Zhang, P. D., Zhang, C., Yang, Q., Shen, L., *Electrophoresis* 2002, 23, 4104–4109.
- [9] Rageh, A. H., Pyell, U., *J. Chromatogr. A* 2013, 1316, 135–146.
- [10] Orentaite, I., Maruska, A., Pyell, U., *Electrophoresis* 2011, 32, 604–613.
- [11] Li, H., Wang, H., Liu, Y., Liu, Z., *Chem. Commun.* 2012, 48, 4115–4117.
- [12] Lu, C., Li, H., Wang, H., Liu, Z., *Anal. Chem.* 2013, 85, 2361–2369.
- [13] James, T. D., Sandanayake Samankumara, K. R. A., Shinkai, S., *Angew. Chem. Int. Ed. Engl.* 1996, 35, 1910–1922.
- [14] Ren, L., Liu, Z., Dong, M., Ye, M., Zou, H., *J. Chromatogr. A* 2009, 1216, 4768–4774.
- [15] Ren, L., Liu, Z., Liu, Y., Dou, P., Chen, H. Y., *Angew. Chem. Int. Ed.* 2009, 48, 6704–6707.
- [16] Li, H., Liu, Z., *Trends Anal. Chem.* 2012, 37, 148–161.
- [17] Li, Y., Pfüller, U., Linne Larsson, E., Jungvid, H., Galaev, I. Y., Mattiasson, B., *J. Chromatogr. A* 2001, 925, 115–121.
- [18] Li, Y., Larsson, E. L., Jungvid, H., Galaev, I. Y., Mattiasson, B., *J. Chromatogr. A* 2001, 909, 137–145.
- [19] Wang, H., Lü, C., Li, H., Chen, Y., Zhou, M., Ouyang, J., Liu, Z., *Anal. Bioanal. Chem.* 2013, 405, 8579–8586.
- [20] Riekkola, M. L., Joensuu, J. A., Smith, R. M., *Pure Appl. Chem.* 2004, 76, 443–451.
- [21] Kuo, K. C., Phan, D. T., Williams, N., Gehrke, C. W., in: Gehrke, C. W., Kuo, K. C. (Eds.), *Chromatography and Modification of Nucleosides. Part C Modified Nucleosides in Cancer and Normal Metabolism-Methods and Applications*, Elsevier, Oxford 1990, pp. C41–C113.
- [22] Gehrke, C. W., Kuo, K. C., Davis, G. E., Suits, R. D., Waalkes, T. P., Borek, E., *J. Chromatogr.* 1978, 150, 455–476.
- [23] Rageh A.H., Kaltz, A., Pyell, U., *Anal. Bioanal. Chem.* 2014, 406, 5877–5895.
- [24] Yang, X., Dai, J., Carr, P. W., *J. Chromatogr. A* 2003, 996, 13–31.
- [25] Al-Rimawi, F., Pyell, U., *J. Chromatogr. A* 2007, 1160, 326–335.
- [26] Zakaria, P., Macka, M., Haddad, P. R., *Anal. Chem.* 2002, 74, 1241–1248.
- [27] Neue, U. D., Phoebe, C. H., Tran, K., Cheng, Y. F., Lu, Z., *J. Chromatogr. A* 2001, 925, 49–67.
- [28] Vigh, G., Varga-Puchony, Z., *J. Chromatogr.* 1980, 196, 1–9.
- [29] Ni, W., Fang, H., Springsteen, G., Wang, B., *J. Org. Chem.* 2004, 69, 1999–2007.
- [30] Fei, F., Britz-McKibbin, P., *Anal. Bioanal. Chem.* 2010, 398, 1349–1356.
- [31] Pino, V., German-Hernandez, M., Martin-Perez, A., Anderson, J. L., *Sep. Sci. Technol.* 2012, 47, 264–276.
- [32] Wang, H., Zhang, L., Wang, J., Li, Z., Zhang, S., *Chem. Commun.* 2013, 49, 5222–5224.
- [33] Ao, M., Xu, G., Pang, J., Zhao, T., *Langmuir* 2009, 25, 9721–9727.
- [34] Wang, H., Feng, Q., Wang, J., Zhang, H., *J. Phys. Chem. B* 2010, 114, 1380–1387.
- [35] Graf, M., Garcia, R. G., Wätzig, H., *Electrophoresis* 2005, 26, 2409–2417.
- [36] Towns, J. K., Regnier, F. E., *Anal. Chem.* 1992, 64, 2473–2478.
- [37] El-Awady, M., Pyell, U., *Electrophoresis* 2014, 35, 605–616.
- [38] Beale, S. C., *Anal. Chem.* 1998, 70, 279R–300R.

**Boronate affinity-assisted MEKC separation of highly hydrophilic urinary nucleosides using imidazolium-based ionic liquid type surfactant as pseudostationary phase**

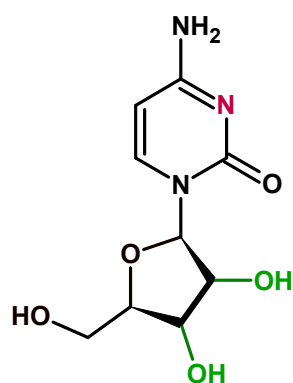
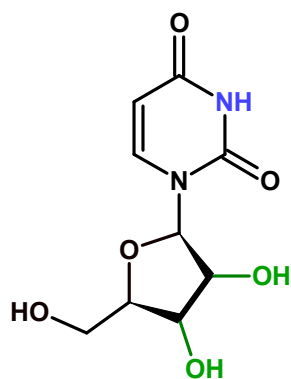
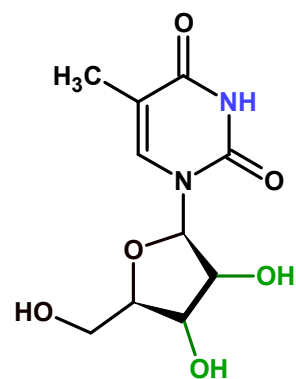
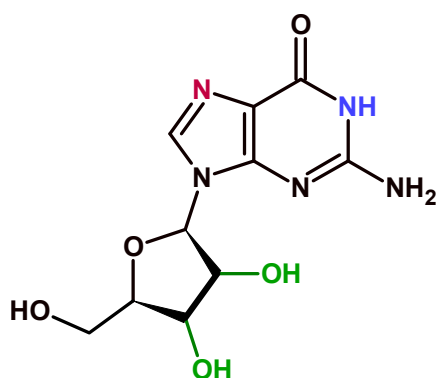
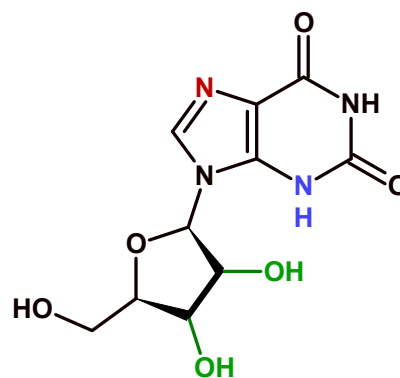
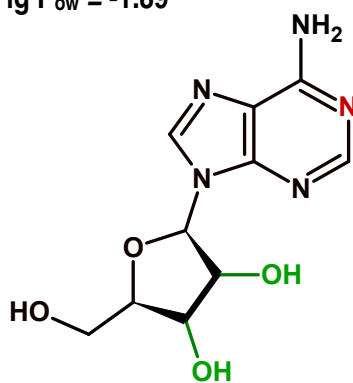
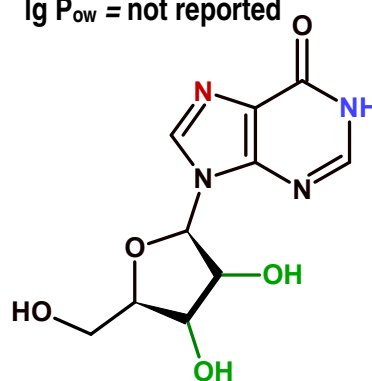
Azza H. Rageh, Ute Pyell\*

University of Marburg, Department of Chemistry, Hans-Meerwein-Straße, D-35032 Marburg, Germany

\* corresponding author

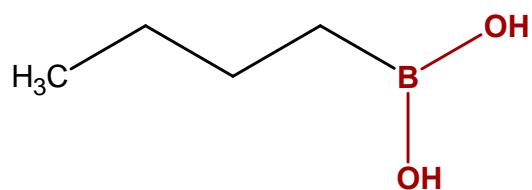
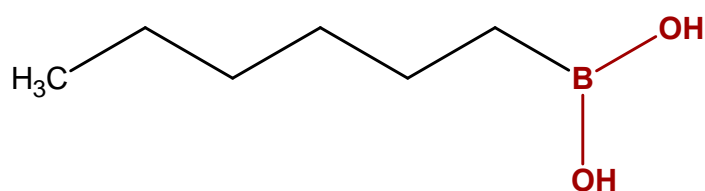
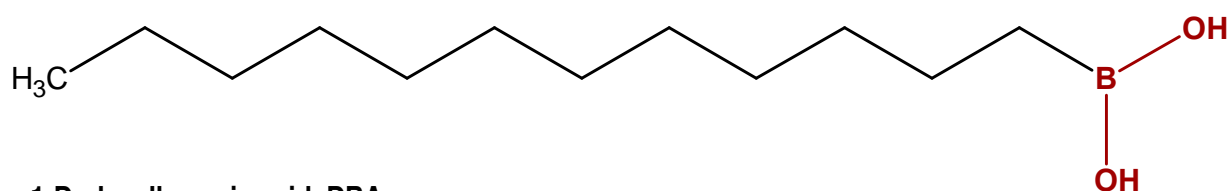
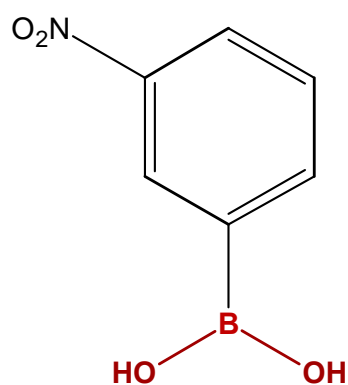
**Supporting information**

S-2

1. Cytidine,  $pK_a = 4.15^*$  $\lg P_{ow} = -2.51$ 2. Uridine,  $pK_a = 9.20$  $\lg P_{ow} = -1.98$ 3. 5-Methyluridine,  $pK_a = 9.70$  $\lg P_{ow} = \text{not reported}$ 4. Guanosine,  $pK_a = 1.60^*, 9.20$  $\lg P_{ow} = -1.89$ 5. Xanthosine,  $pK_a = <2.5^*, 5.70$  $\lg P_{ow} = \text{not reported}$ 6. Adenosine,  $pK_a = 3.50^*$  $\lg P_{ow} = -1.23$ 7. Inosine,  $pK_a = 1.20^*, 8.80$  $\lg P_{ow} = -2.1$ 

**Figure S1:** Structural formulas,  $pK_a$  [1] and  $\lg P_{ow}$  [2] of the investigated nucleosides. \* Values of  $pK_a$  are those of the cationic protonated conjugate acid form. Red and blue colours are used to mark the protonation and dissociation sites, respectively.  $pK_a$  values of cis-diol moieties (marked with the green colour) are  $\sim 12.5$  [1].



**1-Butylboronic acid, BBA****pK<sub>a</sub> = 10.35****1-Hexylboronic acid, HBA****pK<sub>a</sub> = 10.47****1-Dodecylboronic acid, DBA****pK<sub>a</sub> = 11.0****3-Nitrophenylboronic acid, 3-NPBA****pK<sub>a</sub> = 6.9****Figure S2:** Structural formulas and pK<sub>a</sub> values of the studied boronic acids.

**Preparation of the buffer stock solutions**

Stock solutions of phosphate buffer and carbonate buffer were prepared and further diluted for the preparation of the background electrolytes. Stock phosphate buffer (40 mmol/L, pH 11.05) was prepared by dissolving 0.2782 g (2.9 mmol/L) of trisodium phosphate dodecahydrate and 1.6550 g (37.1 mmol/L) of disodium hydrogen phosphate dihydrate in 200 mL water and diluting to 250 mL with water. Stock carbonate buffer solution (40 mmol/L, pH 9.71) was prepared by dissolving 0.6217 g (29.7 mmol/L) of sodium bicarbonate and 0.2702 g (10.3 mmol/L) of sodium carbonate in 200 mL water and diluting to 250 mL with water. Stock phosphate buffer (40 mmol/L, pH 7.00) was prepared by dissolving 0.5865 g (17 mmol/L) of sodium dihydrogen phosphate monohydrate and 1.0280 g (23.1 mmol/L) of disodium hydrogen phosphate dihydrate in 200 mL water and diluting to 250 mL with water.

### **Complexation with phenylboronates**

3-NPBA had been employed as an electrokinetic probe in dynamic complexation-capillary electrophoresis (DC-CE) for screening and direct analysis of polyols [3, 4]. We have combined the use of 3-NPBA (2 mmol/L) with either SDS (50 mmol/L) or C<sub>14</sub>MImBr (20 mmol/L) in 20 mmol/L phosphate buffer, pH 7.0 for the separation of nucleosides as negatively charged complexes without the dissociation of their amidic groups (except Xao with pK<sub>a</sub> = 5.7, that is negatively charged under these conditions). As indicated in Fig. S3, the introduction of 3-NPBA in the BGE creates two large negative system peaks. The first one is ascribed to the EOF and the second one is attributed to a zone void of 3-NPBA [4]. As observed in Fig. S3A, the complexation between the nucleosides and 3-NPBA enhances their interaction with C<sub>14</sub>MImBr micelles that in turn improves their resolution (if compared to SDS micelles as will be shown later). We can assume that all the investigated analytes have a charge number of -1 due to complexation with 3-NPBA (except Xao) based on the fact that pK<sub>a</sub><sup>\*</sup> of 3-NPBA/nucleoside complex < pK<sub>a</sub> of free 3-NPBA at the investigated pH value. Therefore, assuming equal interaction by the electrostatic forces, we can conclude that the order of migration will follow what would be expected based on their hydrophobicity (see Fig. S1), so that pyrimidine nucleosides migrate before purine nucleosides and within the same class of analytes, their migration order will be dependent on their lg P<sub>ow</sub>.

In order to highlight the importance of the electrostatic interaction besides the hydrophobic interaction with the PSP, a parallel experiment was performed using 2 mmol/L 3-NPBA and 50 mmol/L SDS as a BGE instead of using 20 mmol/L C<sub>14</sub>MImBr. As given in Fig. S3B, hydrophobic and electrostatic interactions with the SDS micelles are too low to provide sufficient resolution between these highly hydrophilic analytes (existing as negatively charged complexes). However, hydrophobic interaction with the phenyl moiety of 3-NPBA cannot be neglected especially if we compare Fig. S3B to the electropherogram obtained using BGE composed of only 50 mmol/L SDS in 20 mmol/L phosphate buffer, pH 7.0 with a low resolution between the studied nucleosides (see figure inset, Fig S3B). Table S1 demonstrates the calculated pseudoeffective electrophoretic mobilities ( $\mu$ ), which illustrate the strong interaction of the studied analytes with C<sub>14</sub>MImBr micelles. This can be reflected by the significant increase in the absolute values of  $\mu$  in case of using BGE (A) relative to those obtained using BGE (B) or (C).

We have reported before that a sufficient resolution between all the studied nucleosides can be obtained using 200 mmol/L SDS in 50 mmol/L phosphate buffer, pH 6.86 as a BGE but the use of high concentration of the PSP in the BGE results in low reproducibility, noisy baseline and Joule heating [5].

This can confirm that electrostatic interaction (that can be hydrophobically-assisted using the alkyl or the phenyl moiety boronic acids) is the main mode of interaction of the studied nucleosides with the oppositely charged PSP. Although 3-NPBA can be used for the analysis of CDCC that are labile to alkaline pH conditions, but due to the high background absorbance of the free 3-NPBA, it will not be considered further in the present study.

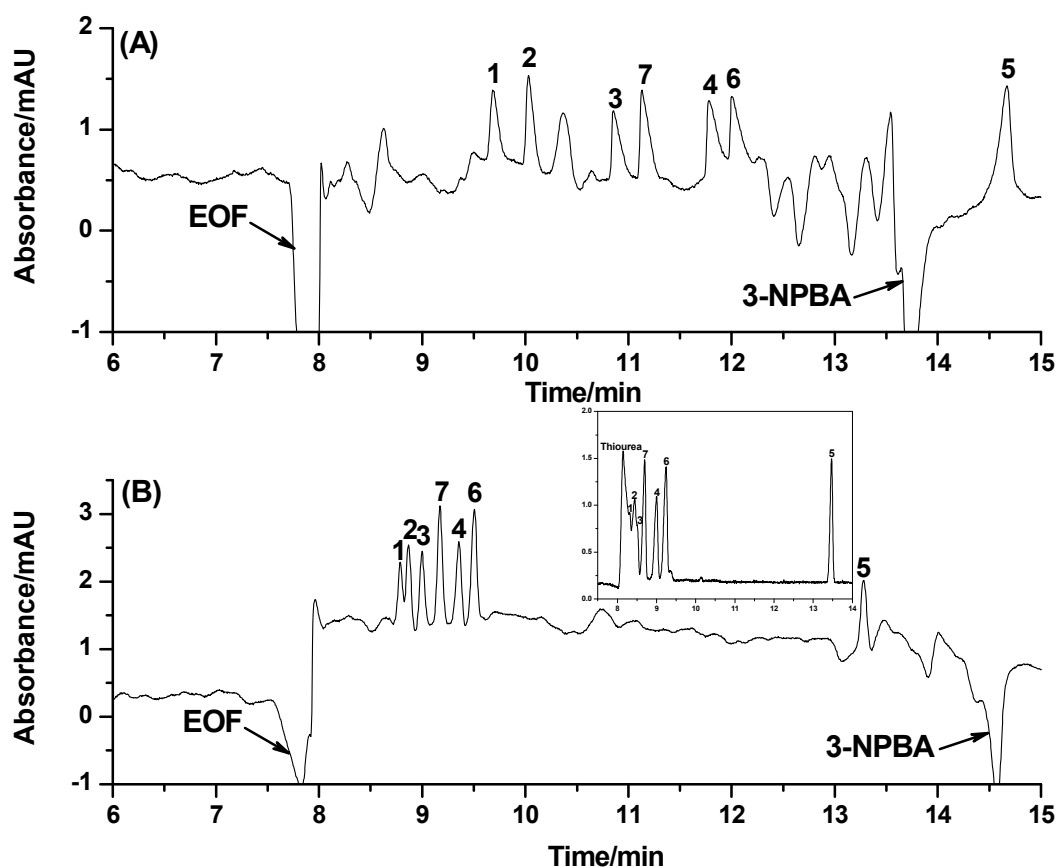


**Figure S3:** Electropherograms obtained from a standard solution mixture of 20 mg/L of each of the investigated nucleosides and 25 mg/L thiourea in water using (A) 2 mmol/L 3-NPBA and 20 mmol/L C<sub>14</sub>MImBr in 20 mmol/L phosphate buffer, pH 6.94 or (B) 2 mmol/L 3-NPBA and 50 mmol/L SDS in 20 mmol/L phosphate buffer, pH 7.0 as BGEs. Figure inset in B represents the electropherogram obtained using 50 mmol/L SDS in 20 mmol/L phosphate buffer, pH 7.0 as a BGE. Other CE conditions: capillary 645(508) mm × 50 μm I.D., applied voltage –15 kV or +15 kV in case of (A) and (B), respectively, pressure injection 30 mbar for 12 s, oven temperature 35 °C. Peak designation: 1 = cytidine, 2 = uridine, 3 = 5-methyluridine, 4 = guanosine, 5 = xanthosine, 6 = adenosine, 7 = inosine.

**Table S1.** Pseudoeffective electrophoretic mobilities (mean value  $\pm$  standard deviation, N = number of runs) determined using (A) 2 mmol/L 3-NPBA and 20 mmol/L C<sub>14</sub>MImBr in 20 mmol/L phosphate buffer, pH 6.94 or (B) 2 mmol/L 3-NPBA and 50 mmol/L SDS in 20 mmol/L phosphate buffer, pH 7.0 or (C) 50 mmol/L SDS in 20 mmol/L phosphate buffer, pH 7.0 as BGEs, capillary 645(508) mm x 50  $\mu$ m I.D., voltage +15 kV in case of BGE (B) and (C) and -15 kV in case of using BGE (A), pressure injection 30 mbar for 12 s, 1 = cytidine, 2 = uridine, 3 = 5-methyluridine, 4 = guanosine, 5 = xanthosine, 6 = adenosine, 7 = inosine.

BGE	$\mu_{eff}$ (1)/ cm <sup>2</sup> kV <sup>-1</sup> s <sup>-1</sup>	$\mu_{eff}$ (6)/ cm <sup>2</sup> kV <sup>-1</sup> s <sup>-1</sup>	$\mu_{eff}$ (2)/ cm <sup>2</sup> kV <sup>-1</sup> s <sup>-1</sup>	$\mu_{eff}$ (4)/ cm <sup>2</sup> kV <sup>-1</sup> s <sup>-1</sup>	$\mu_{eff}$ (7)/ cm <sup>2</sup> kV <sup>-1</sup> s <sup>-1</sup>	$\mu_{eff}$ (5)/ cm <sup>2</sup> kV <sup>-1</sup> s <sup>-1</sup>	$\mu_{eff}$ (3)/ cm <sup>2</sup> kV <sup>-1</sup> s <sup>-1</sup>
(A)	0.079 $\pm$ 0.00081 N = 3	0.151 $\pm$ 0.00079 N = 3	0.092 $\pm$ 0.00089 N = 3	0.146 $\pm$ 0.00080 N = 3	0.128 $\pm$ 0.00110 N = 3	0.206 $\pm$ 0.00063 N = 3	0.119 $\pm$ 0.00094 N = 3
(B)	-0.042 $\pm$ 0.00077 N = 3	-0.074 $\pm$ 0.00054 N = 3	-0.046 $\pm$ 0.00057 N = 3	-0.068 $\pm$ 0.00046 N = 3	-0.060 $\pm$ 0.00047 N = 3	-0.184 $\pm$ 0.00105 N = 3	-0.053 $\pm$ 0.00046 N = 3
(C)	-0.008 $\pm$ 0.00012 N = 2	-0.053 $\pm$ 0.00014 N = 2	-0.016 $\pm$ 0.00035 N = 3	-0.042 $\pm$ 0.00024 N = 2	-0.028 $\pm$ 0.00051 N = 2	-0.176 $\pm$ 0.00007 N = 2	-0.018 $\pm$ 0.00030 N = 2

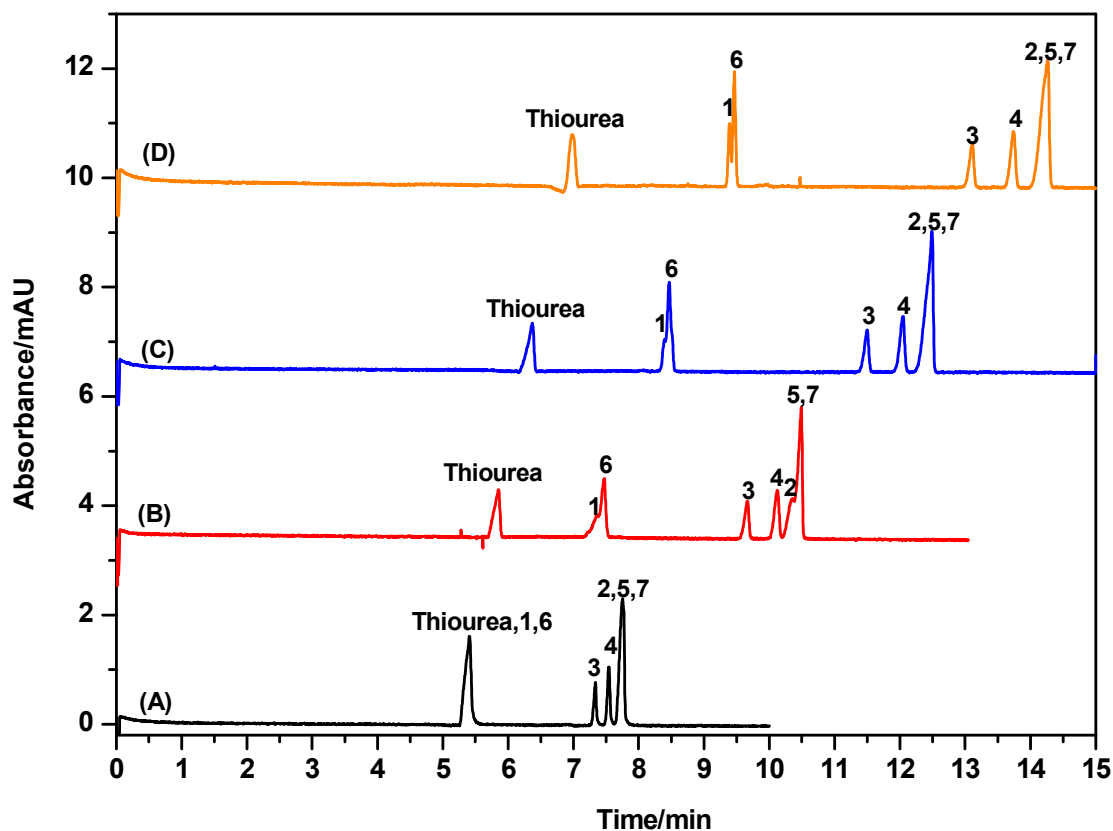


**Figure S4:** Electropherograms obtained from a standard solution mixture of 20 mg/L of each of the investigated nucleosides and 25 mg/L thiourea in water using a BGE composed of 20 mmol/L phosphate buffer, pH 11.05 containing (A) 0 mmol/L BBA, (B) 10 mmol/L BBA, (C) 30 mmol/L BBA and (D) 30 mmol/L BBA and 50 mmol/L SDS. Other CE conditions: capillary 649(501) mm  $\times$  50  $\mu$ m I.D., applied voltage +15 kV, pressure injection 30 mbar for 12 s, oven temperature 35  $^{\circ}$ C. Peak designation: as in Fig. S3.

**Calculation of the retention factors of the nucleosides as charged analytes**

To calculate the retention factor for a weak acid, the following equation can be employed [5-9]:

$$\mu = \frac{1}{k+1} \mu_{\text{eff}} + \frac{k}{1+k} \mu_{\text{MC}} \quad (\text{S-1})$$

where  $\mu$  is the pseudoeffective electrophoretic mobility of the analyte in micellar BGE,  $k$  is the overall retention factor of the analyte,  $\mu_{\text{eff}}$  is the effective electrophoretic mobility of the analyte in micelle-free BGE, and  $\mu_{\text{MC}}$  is the electrophoretic mobility of the micelles in micellar BGE. From Eq. (S-1) following expression can be derived, which allows to calculate the true retention factor  $k$  in MEKC from the mobilities  $\mu$ ,  $\mu_{\text{eff}}$ , and  $\mu_{\text{MC}}$  [7], which have to be determined in separate measurements with a separation electrolyte containing surfactant ( $\mu$  and  $\mu_{\text{MC}}$ ) and with a separation electrolyte containing no surfactant ( $\mu_{\text{eff}}$ ):

$$k = \frac{\mu - \mu_{\text{eff}}}{\mu_{\text{MC}} - \mu} \quad (\text{S-2})$$

Several assumptions have to be made: the influence of the pseudostationary phase on the ionic strength, viscosity, and dielectric constant of the BGE must be assumed to be very low, interaction of the analyte either with the capillary wall (solute-admicelle interaction) and with surfactant monomers is neglected. Regarding the last point, it was reported in a previous study [10] that  $\mu_{\text{eff}}$  in the presence of surfactant monomers is not significantly different from the values obtained in absence of such monomers i.e. ion pair formation can be neglected. It must be emphasized that analytes used in that study are hydrophilic, a situation which is quite similar to our case (highly hydrophilic nucleosides).

**Statistical significance of the slope b in Fig. 6a**

Regarding the statistical significance of the slope b, we applied t-test. We have selected the two lines with the maximum difference between their slope values. The t-value was calculated for Cyd with the highest slope  $b \pm \text{SD}$  ( $0.3187 \pm 0.0413$ ) and Xao with the lowest slope ( $0.2165 \pm 0.0085$ ). t-value was found to be 2.42 at  $df = 2$ , which is smaller than the tabulated t value (4.30 at  $df = 2$  and  $P = 0.05$ ). We can conclude that at the specified significance level, the slopes are not significantly different from each other. These findings support our assumption that hydrophobic interaction contributes considerably to the overall retention and cannot be neglected.

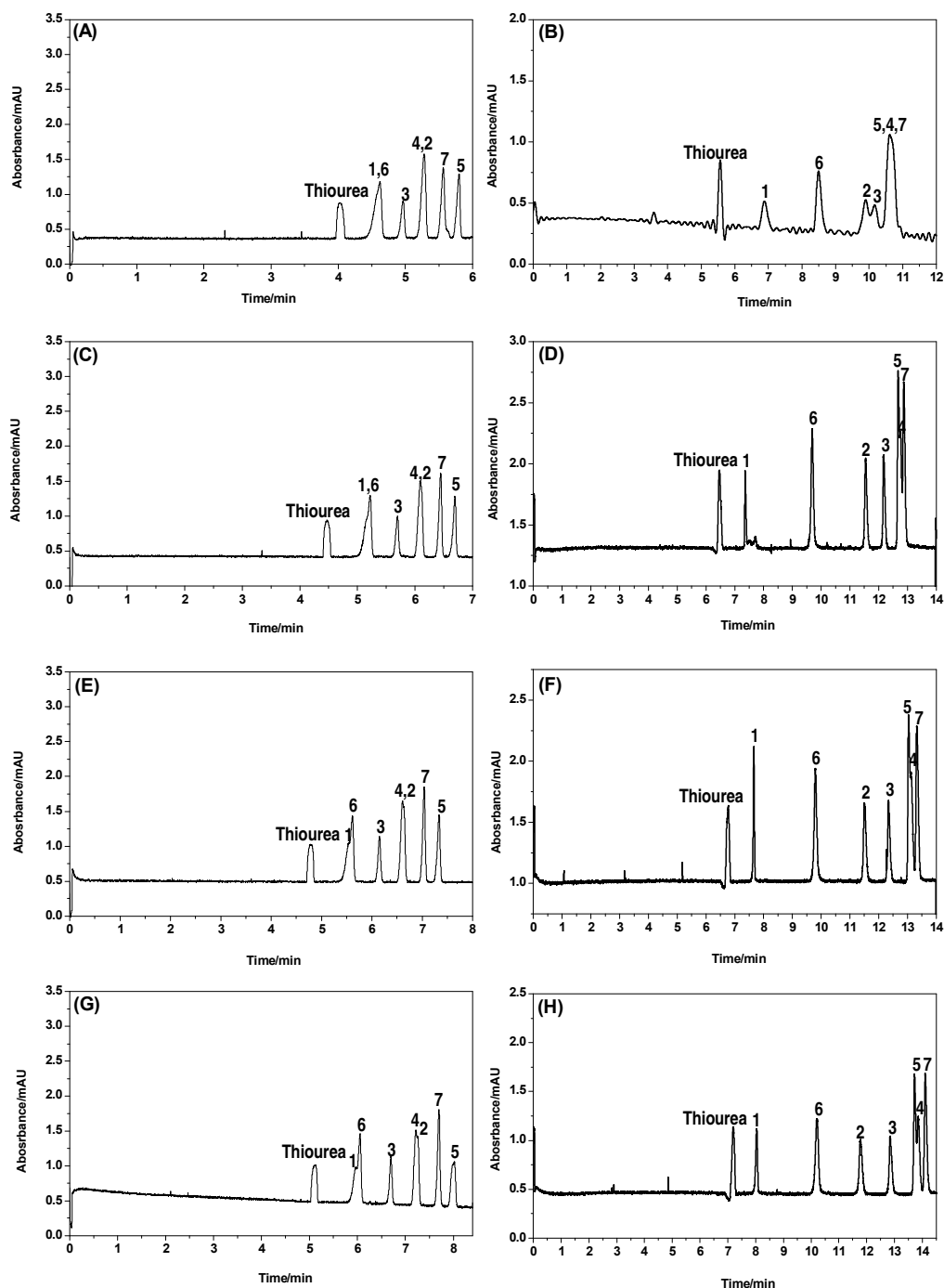


**Figure S5:** Electropherograms obtained from a standard solution mixture of 20 mg/L of each of the investigated nucleosides and 25 mg/L thiourea in water. The non-micellar BGEs composed of 10 mmol/L BBA in either (A) 5 mmol/L carbonate buffer, pH 9.71, or (C) 10 mmol/L carbonate buffer, pH 9.71, or (E) 15 mmol/L carbonate buffer, pH 9.71 or (G) 20 mmol/L carbonate buffer, pH 9.71. The micellar BGEs composed of 10 mmol/L BBA and 20 mmol/L  $C_{14}$ MImBr in either (B) 5 mmol/L carbonate buffer, pH 9.71, or (D) 10 mmol/L carbonate buffer, pH 9.71, or (F) 15 mmol/L carbonate buffer, pH 9.71 or (H) 20 mmol/L carbonate buffer, pH 9.71. Other CE conditions: capillary 646(501) mm  $\times$  50  $\mu$ m I.D., applied voltage +15 or -15 kV in case of non-micellar and micellar BGEs, respectively, pressure injection 30 mbar for 12 s, oven temperature 35  $^{\circ}$ C. Peak designation: 1 = cytidine, 2 = uridine, 3 = 5-methyluridine, 4 = guanosine, 5 = xanthosine, 6 = adenosine, 7 = inosine.



**Table S2.** Effective electrophoretic mobilities (mean value  $\pm$  standard deviation, N = number of runs) determined under variation of the concentration of carbonate buffer, pH = 9.71 with c(BBA) = 10 mmol/L, capillary 646(501) mm  $\times$  50  $\mu$ m I.D., voltage +15 kV, pressure injection 30 mbar for 12 s, 1 = cytidine, 2 = uridine, 3 = 5-methyluridine, 4 = guanosine, 5 = xanthosine, 6 = adenosine, 7 = inosine.

c(carbonate)/ mmol/L	$\mu_{eff}$ (1)/ cm <sup>2</sup> kV <sup>-1</sup> s <sup>-1</sup>	$\mu_{eff}$ (6)/ cm <sup>2</sup> kV <sup>-1</sup> s <sup>-1</sup>	$\mu_{eff}$ (2)/ cm <sup>2</sup> kV <sup>-1</sup> s <sup>-1</sup>	$\mu_{eff}$ (4)/ cm <sup>2</sup> kV <sup>-1</sup> s <sup>-1</sup>	$\mu_{eff}$ (7)/ cm <sup>2</sup> kV <sup>-1</sup> s <sup>-1</sup>	$\mu_{eff}$ (5)/ cm <sup>2</sup> kV <sup>-1</sup> s <sup>-1</sup>	$\mu_{eff}$ (3)/ cm <sup>2</sup> kV <sup>-1</sup> s <sup>-1</sup>
5	-0.103 $\pm 0.00000$ N = 2	-0.115 $\pm 0.00050$ N = 5	-0.213 $\pm 0.00194$ N = 5	-0.208 $\pm 0.00000$ N = 2	-0.247 $\pm 0.00067$ N = 5	-0.273 $\pm 0.00055$ N = 5	-0.169 $\pm 0.00051$ N = 3
10	-0.106 $\pm 0.00069$ N = 4	-0.115 $\pm 0.00050$ N = 4	-0.216 $\pm 0.00159$ N = 2	-0.113 $\pm 0.00048$ N = 4	-0.246 $\pm 0.00012$ N = 4	-0.267 $\pm 0.00057$ N = 4	-0.173 $\pm 0.00026$ N = 3
15	-0.102 $\pm 0.00145$ N = 4	-0.110 $\pm 0.00070$ N = 4	-0.209 $\pm 0.00133$ N = 4	-0.206 $\pm 0.00080$ N = 4	-0.240 $\pm 0.00058$ N = 4	-0.261 $\pm 0.00067$ N = 4	-0.166 $\pm 0.00058$ N = 3
20	-0.101 $\pm 0.00071$ N = 3	-0.109 $\pm 0.00040$ N = 3	-0.208 $\pm 0.00025$ N = 2	-0.206 $\pm 0.00032$ N = 2	-0.237 $\pm 0.00022$ N = 2	-0.255 $\pm 0.00041$ N = 2	-0.166 $\pm 0.00053$ N = 3

**Table S3.** Pseudoeffective electrophoretic mobilities (mean value  $\pm$  standard deviation, N = number of runs) determined under variation of the concentration of carbonate buffer, pH 9.71 with c(C<sub>14</sub>MImBr) = 20 mmol/L and c(BBA) = 10 mmol/L, capillary 646(501) mm x 50  $\mu$ m I.D., voltage -15 kV, pressure injection 30 mbar for 12 s, 1 = cytidine, 2 = uridine, 3 = 5-methyluridine, 4 = guanosine, 5 = xanthosine, 6 = adenosine, 7 = inosine, 8 = decanophenone.

c(carbonate)/ mmol/L	$\mu_{eff}^P$ (1) cm <sup>2</sup> kV <sup>-1</sup> s <sup>-1</sup>	$\mu_{eff}^P$ (6) cm <sup>2</sup> kV <sup>-1</sup> s <sup>-1</sup>	$\mu_{eff}^P$ (2) cm <sup>2</sup> kV <sup>-1</sup> s <sup>-1</sup>	$\mu_{eff}^P$ (4) cm <sup>2</sup> kV <sup>-1</sup> s <sup>-1</sup>	$\mu_{eff}^P$ (5) cm <sup>2</sup> kV <sup>-1</sup> s <sup>-1</sup>	$\mu_{eff}^P$ (7) cm <sup>2</sup> kV <sup>-1</sup> s <sup>-1</sup>	$\mu_{eff}^P$ (3) cm <sup>2</sup> kV <sup>-1</sup> s <sup>-1</sup>	$\mu_{eff}^P$ (8) cm <sup>2</sup> kV <sup>-1</sup> s <sup>-1</sup>
5	0.128 $\pm 0.00272$ N = 4	0.226 $\pm 0.00166$ N = 4	0.284 $\pm 0.00213$ N = 4	0.310 $\pm 0.00145$ N = 4	0.310 $\pm 0.00145$ N = 4	0.312 $\pm 0.00115$ N = 2	0.294 $\pm 0.00263$ N = 3	0.344 N = 1
10	0.068 $\pm 0.00064$ N = 2	0.186 $\pm 0.00079$ N = 2	0.246 $\pm 0.00104$ N = 2	0.275 $\pm 0.00132$ N = 2	0.274 $\pm 0.00124$ N = 2	0.278 $\pm 0.00125$ N = 2	0.262 $\pm 0.00131$ N = 2	0.309 N = 1
15	0.062 $\pm 0.00024$ N = 4	0.165 $\pm 0.00029$ N = 2	0.219 $\pm 0.00049$ N = 2	0.258 $\pm 0.00048$ N = 4	0.256 $\pm 0.00039$ N = 3	0.262 $\pm 0.00056$ N = 2	0.240 $\pm 0.00040$ N = 3	0.296 N = 1
20	0.052 $\pm 0.00044$ N = 2	0.147 $\pm 0.00078$ N = 2	0.194 $\pm 0.00118$ N = 2	0.239 $\pm 0.00139$ N = 2	0.237 $\pm 0.00126$ N = 2	0.244 $\pm 0.00134$ N = 2	0.219 $\pm 0.00155$ N = 2	0.292 extrapolated value

**Table S4.** Retention factors calculated at different carbonate concentrations

c(carbonate)/ mmol/L	Cyd	Ado	Urd	Guo	Ino	Xao	5MeUrd
5	1.07	2.89	8.41	15.40	17.64	17.33	9.43
10	0.72	2.45	7.35	14.70	17.10	15.44	9.32
15	0.70	2.09	5.56	12.14	14.67	12.85	7.29
20	0.64	1.77	4.09	8.45	10.01	8.92	5.27

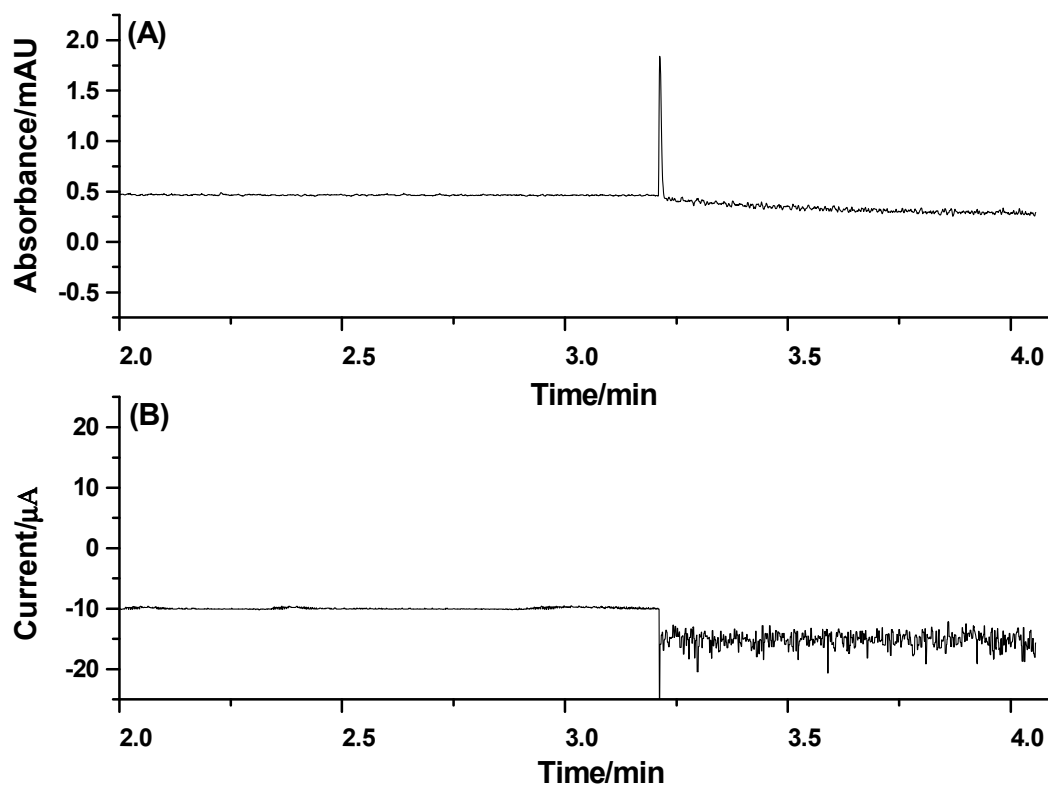


**Figure S6:** Absorbance and electric current strength profile for the first run after rinsing the capillary according to the procedure described in Section 2.2 when using a BGE composed of 10 mmol/L BBA and 20 mmol/L C14MImBr in 25 mmol/L carbonate buffer, pH 9.71. CE conditions: see Fig. S5.

## References

- [1] Lundblad, R. L., MacDonald, F., *Handbook of Biochemistry and Molecular Biology, 4th ed.*, CRC Press, Taylor and Francis Group, LLC, Boca Raton 2010.
- [2] Sangster, J., *Octanol-Water Partition Coefficients: Fundamentals and Physical Chemistry*, John Wiley & Sons, Ltd., Chichester 1997.
- [3] Fei, F., Britz-McKibbin, P., *Anal. Bioanal. Chem.* 2010, *398*, 1349-1356.
- [4] Kaiser, C., Segui-Lines, G., D'Amaral, J. C., Ptolemy, A. S., Britz-McKibbin, P., *Chem. Commun.* 2008, 338-340.
- [5] Rageh, A. H., Pyell, U., *J. Chromatogr. A* 2013, *1316*, 135-146.
- [6] Orentaite, I., Maruska, A., Pyell, U., *Electrophoresis* 2011, *32*, 604-613.
- [7] Ackermans, M. T., Everaerts, F. M., Beckers, J. L., *J. Chromatogr.* 1991, *585*, 123-131.
- [8] Khaledi, M. G., Smith, S. C., Strasters, J. K., *Anal. Chem.* 1991, *63*, 1820-1830.
- [9] Otsuka, K., Terabe, S., Ando, T., *J. Chromatogr.* 1985, *348*, 39-47.
- [10] Pyell, U., in: Pyell, U. (Ed.), *Electrokinetic Chromatography: Theory, Instrumentation & Applications*, John Wiley & Sons, Ltd., Chichester 2006.

**JOHN WILEY AND SONS LICENSE  
TERMS AND CONDITIONS**

Apr 08, 2015

This Agreement between Azza Rageh ("You") and John Wiley and Sons ("John Wiley and Sons") consists of your license details and the terms and conditions provided by John Wiley and Sons and Copyright Clearance Center.

**All payments must be made in full to CCC. For payment instructions, please see information listed at the bottom of this form.**

License number	3604351360166
License date	Apr 08, 2015
Licensed content publisher	John Wiley and Sons
Licensed content publication	Electrophoresis
Licensed content title	Boronate affinity-assisted MEKC separation of highly hydrophilic urinary nucleosides using imidazolium-based ionic liquid type surfactant as pseudostationary phase
Licensed content author	Azza H. Rageh, Ute Pyell
Licensed content date	Nov 7, 2014
Pages	12
Type of use	Dissertation/Thesis
Requester type	Author of this Wiley article
Format	Print and electronic
Portion	Full article
Will you be translating?	No
Title of your thesis/dissertation	On-line and Off-line Enrichment Techniques Combined with Capillary Electromigration Separation Methods in the Analysis of Highly Hydrophilic Analytes in Biological and Environmental Samples
Expected completion date	May 2015
Requester location	Azza Rageh Hans-Meerwein Str. 4, Chemie, Marburg, Germany 35032 Attn: University of Marburg



## **5.4. Publication IV**

**"Pseudostationary ion-exchanger" sweeping/dynamic pH junction/FASS  
on-line enrichment for the determination of nucleosides in urine via  
micellar electrokinetic chromatography after solid phase extraction with  
phenylboronate affinity gel**

**Azza H. Rageh, Ute Pyell**

**Submitted to: Journal of Chromatography A**





### 5.4.1. Summary and discussion

In this publication, two simple, fast, reproducible and sensitive MEKC methods combined with on-line enrichment techniques are developed and validated for the analysis of selected highly hydrophilic nucleosides in urine samples. In the first method,  $C_{14}$ MImBr is employed as PSP for the MEKC separation of the investigated nucleosides: Urd, 5MeUrd, Guo, Ino, and Xao using a BGE composed of 20 mmol L<sup>-1</sup>  $C_{14}$ MImBr in 5 mmol L<sup>-1</sup> disodium tetraborate buffer, pH 9.38. The separation of the studied nucleosides is achieved in less than 6 min. Retention factor gradient effect (RFGE)-“pseudostationary ion-exchanger” sweeping, FASS/dynamic pH junction are employed as on-line enrichment techniques (Fig. 4a). The high complex formation constant between the cis-diol moieties of the nucleosides and tetrahydroxyborate in addition to the strong electrostatic interaction of these negatively charged metabolites with the oppositely charged PSP (at low competing ion concentration and high pH) are the prerequisites for efficient sweeping using  $C_{14}$ MImBr micelles. We investigate the optimization of the sample matrix and the BGE with respect to maximum focusing efficiency while maintaining adequate resolution. It is shown that the maximum enrichment efficiency can be obtained by keeping the retention factors very high within the sample zone and very low within the BGE, while maintaining at the same time a sufficient resolution between the studied analytes.

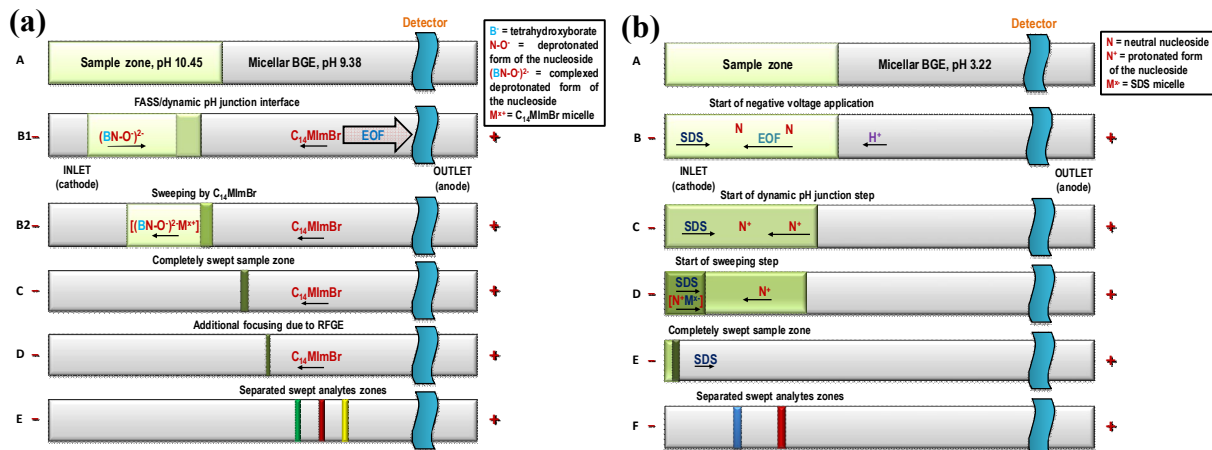


**Figure 4:** Schematic representation of the suggested enrichment mechanism using (a) Method 1 or (b) Method 2.

However, for the nucleosides Ado and Cyd (the first-migrating nucleosides), the  $k$  values are still extremely low even under optimized conditions (lowest tetraborate concentration and high pH). This will negatively affect their sweeping efficiency with  $C_{14}$ MImBr. Moreover, the matrix constituents in urine remaining after extraction of the nucleosides with phenylboronate affinity gel (PBA) interfere with the analysis of these two analytes, which indicates the unsuitability of Method 1 for the determination of Ado and Cyd in urine samples, therefore Method 1 has to be complemented with Method 2. Ado and

Cyd are positively charged under acidic pH conditions. As an alternative strategy, SDS is used for sweeping of these analytes (Method 2). Combined with dynamic pH junction/“pseudostationary ion-exchanger” sweeping (Fig. 4b), the MEKC separation of these two analytes is carried out using a BGE composed of 100 mmol L<sup>-1</sup> SDS in 25 mmol L<sup>-1</sup> aspartic acid, pH 3.22. The separation is achieved in less than 10 min. It is shown that the use of aspartic acid as a zwitterionic/isoelectric buffering component can minimize the dramatic effect of the co-ions (when using ordinary buffering constituents) on the *k* values and hence on the sweeping efficiency. For Methods 1 and 2 the sample injection volume is optimized by variation and selection of those parameters that give rise to the highest peak height and highest peak area, while maintaining at the same time, acceptable peak shapes and resolution. 50 mbar for 1 min is chosen as an optimum sample injection volume. The developed methods are validated according to the ICH guidelines. With several blank and spiked urine samples, the applicability of the developed and validated methods is demonstrated after the selective extraction of the target analytes with phenylboronate affinity gel (PBA).

### **5.4.2. Author contribution**

All the experimental part of this study was carried out by me. The draft of the manuscript was written by me and corrected by Prof. Dr. Ute Pyell. The final revision of the manuscript was conducted by me and Prof. Dr. Ute Pyell before submission to the journal. Prof. Dr. Ute Pyell was responsible for the supervision of this work.



**“Pseudostationary ion-exchanger” sweeping/dynamic pH junction/FASS on-line enrichment for the determination of nucleosides in urine via micellar electrokinetic chromatography after solid phase extraction with phenylboronate affinity gel**

Azza H. Rageh, Ute Pyell\*

University of Marburg, Department of Chemistry, Hans-Meerwein-Straße, D-35032 Marburg, Germany

\* Corresponding author

**Fax: ++49 6421 2822124**

**e-mail: [pyellu@staff.uni-marburg.de](mailto:pyellu@staff.uni-marburg.de)**

**Keywords**

Micellar electrokinetic chromatography, Ionic liquid-type surfactant, Urinary nucleosides, Borate complexation, “Pseudostationary ion-exchanger” sweeping, Dynamic pH junction, Field amplified sample stacking

## Abstract

The presented study shows the application of the ionic liquid (IL)-type surfactant 1-tetradecyl-3-methylimidazolium bromide ( $C_{14}MImBr$ ) to the analysis of the highly hydrophilic urinary nucleosides: uridine, 5-methyluridine, guanosine, inosine and xanthosine in urine samples under alkaline pH conditions. Taking the advantage of the high complex formation constant between borate and the cis-diol moieties of the nucleosides in addition to the strong interaction (at low competing ion concentration and high pH) between these negatively charged metabolites and the oppositely charged pseudostationary phase (represented by  $C_{14}MImBr$  micelles), field amplified sample stacking (FASS)/dynamic pH junction/retention factor gradient effect (RFGE)-"pseudostationary ion-exchanger" sweeping can be employed as on-line enrichment techniques for the determination of these polar analytes in urine samples (Method 1). We study the impact of the pH and the ionic strength of the sample matrix and the BGE on the enrichment efficiency. It is shown that the maximum enrichment efficiency can be obtained by keeping the retention factors very high within the sample zone and very low within the BGE, while maintaining at the same time a sufficient resolution between the studied analytes. The separation of the studied nucleosides is achieved in less than 6 min using a background electrolyte (BGE) composed of  $20 \text{ mmol L}^{-1}$   $C_{14}MImBr$  in  $5 \text{ mmol L}^{-1}$  disodium tetraborate buffer, pH 9.38. Due to the low retention factors encountered for the nucleosides adenosine and cytidine,  $C_{14}MImBr$  cannot be effectively employed for sweeping of these analytes. As an alternative, SDS was investigated for their analysis as positively charged compounds under acidic pH conditions. The positively charged nucleosides adenosine and cytidine can interact by electrostatic (Coulombic) forces with SDS which can be used for their sweeping and subsequent determination in urine samples (Method 2). The effect of a zwitterionic/isoelectric buffering compound on the enrichment efficiency is investigated. A BGE consisting of  $100 \text{ mmol L}^{-1}$  SDS in  $25 \text{ mmol L}^{-1}$  aspartic acid, pH 3.22 is used for the separation of adenosine and cytidine in less than 10 min. The applicability of Methods 1 and 2 to the analysis of the nucleosides under investigation is shown in blank and spiked human urine samples after their extraction using the commercially available phenylboronate affinity gel.

## 1. Introduction

The increasing interest in metabolomics and the diagnostic value of urinary nucleosides as cancer biomarkers have drawn the attention of many working groups to develop analytical methodologies [1-7] for their analysis in the urine of normal and cancer patients. Micellar electrokinetic chromatography (MEKC) is one of the capillary electromigration separation techniques that is widely involved in the analysis of these highly polar metabolites (as neutral compounds) using mostly sodium dodecyl sulphate (SDS) as surfactant [8-15]. Due to the low interaction between SDS and these analytes under neutral pH conditions, a high concentration of the pseudostationary phase is required for their separation, a problem that is typically associated with high electric current, Joule heating, noisy base line, irreproducible migration times and long analysis time [16]. With the need for new surfactants that are capable of interacting more strongly with these highly hydrophilic analytes, providing better resolution while maintaining reproducible migration times and short run time, we have reported an MEKC method for the analysis of nucleosides using the ionic liquid (IL)-type surfactant: 1-tetradecyl-3-methylimidazolium bromide ( $C_{14}MImBr$ ). It was shown that the separation of these polar analytes can be achieved (in less than 6 min) at low surfactant concentration using  $C_{14}MImBr$  as cationic surfactant under alkaline pH conditions, where the nucleosides are negatively charged [16]. The negative charge is acquired due to complexation between tetrahydroxyborate and the cis diol moieties of the nucleosides and/or dissociation of their amidic group.

$C_{14}MImBr$  as PSP in MEKC provides a higher repeatability in migration times than the conventional cationic surfactants (e.g. tetralkylammonium salts) and a modified selectivity, which are attributed by us to the efficiency by which  $C_{14}MImBr$  dynamically coats the inner capillary wall and to the versatility of the interaction sites provided by the imidazolium head group [16]. In MEKC, the interaction of charged analytes with the oppositely charged surfactant can be ascribed to both electrostatic interaction with the oppositely charged micellar outer shell and to hydrophobic interaction with the hydrophobic core of the micelle. We have confirmed that the main mode of interaction between the nucleosides and the  $C_{14}MImBr$  micelles is electrostatic interaction. Hydrophobic interaction can be considered to be negligible. By using only 20 mmol L<sup>-1</sup>  $C_{14}MImBr$  in the BGE (5 mmol L<sup>-1</sup> tetraborate, pH 9.38), a complete separation of all the studied analytes (existing as negatively charged complexes) is achieved.

The dependency of the retention factors  $k$  (calculated at different tetraborate concentrations) on borate concentration in the BGE was demonstrated [16]. We have found that the  $k$  values are the highest at the lowest borate concentration. Therefore and based on the classical theory of ion-exchange chromatography, the micelles formed by  $C_{14}MImBr$  can be regarded as a pseudostationary ion-exchanger that provides a fixed concentration of ion-exchange sites and enables the regulation of the

retention factor by variation of the competing ion concentration. Besides, the pH of the BGE strongly influences the  $k$  values of the nucleosides. The highest values of  $k$  are obtained at the pH that enables a full deprotonation of these analytes and hence permits the maximum interaction with the oppositely charged PSP.

Following the study of the fundamental aspects underlying the separation of the nucleosides using  $C_{14}MImBr$  [16], we want to integrate the outcome of our previous results, with emphasizing on the applicability of  $C_{14}MImBr$  as PSP in the analysis of the hydrophilic nucleosides in real urine samples. The involvement of on-line enrichment techniques for a further improvement of the detection limits will also be considered. "Pseudostationary ion-exchanger" sweeping (using  $C_{14}MImBr$ ) combined with dynamic pH junction/field amplified sample stacking (FASS) will be investigated as online enrichment technique for the focusing of the investigated nucleosides by employing a sample matrix void of PSP having a different pH and electric conductivity different from that of the background electrolyte (BGE).

Sweeping is one of the on-line enrichment techniques that is used to overcome the poor concentration sensitivity in CE. It is defined as the accumulation of analyte molecules by the pseudostationary phase (PSP) that penetrates the sample zone being void of PSP. Based on the concept presented by Terabe and co-workers [17,18], the length of the sample zone after sweeping  $l_{sweep}$  depends on the initial sample-plug length  $l_{inj}$  and on the retention factor in the sample zone  $k_s$  during sweeping. The enrichment factor ( $=l_{inj}/l_{sweep}$ ) is then directly proportional to  $k_s$ :

$$l_{sweep} = \frac{1}{1 + k_s} l_{inj} \quad (1)$$

According to Eq. (1) adjustment of the retention factors to be very high within the sample zone is the key factor in order to maximize the sweeping efficiency and hence the sensitivity of the developed methods.

Optimization of the ionic strength and the pH of the sample matrix with regard to its significant effect on the sweeping efficiency and the sensitivity of the developed method has not been considerably discussed in the literature [19]. This will be the main focus of the presented study. The pH and the ionic strength of the sample matrix affect strongly the retention factors of the charged analytes with respect to the oppositely charged micelles as they can increase/decrease the electrostatic interaction with the PSP. Additionally, a difference in pH and electric conductivity between the sample zone and the BGE compartment enables analyte focusing by dynamic pH junction [20,21] and FASS [22], respectively, if they are accompanied by an abrupt change in the analyte effective electrophoretic mobility  $\mu_{eff}$ . For charged analytes, differences in  $\mu_{eff}$  can be accomplished by variation in the degree of analyte ionization and/or the electric conductivity between the two compartments. Moreover, a difference in the pH and/or



ionic strength between the sample zone and the BGE compartment causes also a difference in the apparent distribution coefficient  $K_D$  and induces the retention factor gradient effect (RFGE) that can lead to additional focusing or defocusing of the swept analyte zone [19,23,24]. Focusing due to RFGE occurs when the swept analyte zone enters the BGE compartment of lower  $k$ , which results in a sudden reduction of its observed velocity and finally zone focusing. According to [24], Eq. (1) is expanded by introducing the additional focusing/defocusing factor  $f$ .  $l_{grad}$  is used to describe the length of the swept analyte zone after taking this effect into account [24]:

$$l_{grad} = \frac{1}{f} \frac{1}{1 + k_s} l_{inj} \quad (2)$$

This effect complements the sweeping process and occurs in the BGE compartment next to the sample zone. Reduction of the  $k$  values within the BGE relative to that in the sample zone, i.e.  $k_s > k_{BGE}$  leads to further improvement of the sweeping efficiency due to additional analyte focusing by RFGE [19,23,24].

It is noteworthy to mention that in [16] we have increased the  $k$  values of the studied nucleosides by increasing the pH of the BGE and reducing the co-ion concentration in the BGE. However, for the nucleosides Ado and Cyd (the first-migrating nucleosides), the  $k$  values are still extremely low even under optimized conditions (lowest tetraborate concentration and high pH). This will negatively affect their sweeping efficiency with  $C_{14}MImBr$ . As an alternative, we will show that the analysis of these compounds under acidic conditions permits their efficient sweeping when using the oppositely charged surfactant SDS and a BGE containing a zwitterionic/isoelectric buffering component (as defined by [25]) to minimize the dramatic effect of the co-ions (when using ordinary buffering constituents) on the  $k$  values and hence on the sweeping efficiency. To permit a better focusing efficiency, dynamic pH junction will be combined with “pseudostationary ion-exchanger” sweeping by employment of a BGE having a pH different from that of the sample matrix.

According to the best of our knowledge, dynamic pH junction/“pseudostationary ion-exchanger” sweeping using: (i)  $C_{14}MImBr$  under alkaline pH conditions with FASS as an additional focusing principle (Method 1) or (ii) SDS under acidic pH conditions (Method 2) for the analysis of the polar nucleosides as charged compounds in real urine samples has not been reported so far. In this work, we investigate the optimization of the sample matrix and the BGE with respect to maximum focusing efficiency while maintaining adequate resolution. Adjustment of the retention factors by variation of the pH, the BGE concentration or via the use of a zwitterionic/isoelectric buffering compound is studied. In addition, we optimize the sample injection volume by variation and selection of those parameters that give rise to the highest peak height and highest peak area, while maintaining at the same time,

acceptable peak shapes and resolution. Moreover, underlying focusing mechanisms are suggested. The developed methods are validated according to the ICH guidelines [26]. With several blank and spiked urine samples, the applicability of the developed and validated methods is demonstrated after the selective extraction of the target analytes with phenylboronate affinity gel (PBA).

## 2. Experimental

### 2.1. Chemicals and background electrolytes

Cytidine (Cyd), adenosine (Ado), 5-methyluridine (5MeUrd), uridine (Urd), guanosine (Guo), inosine (Ino), and xanthosine (Xao) were purchased from Sigma-Aldrich, Steinheim, Germany; chemical structures,  $pK_a$  [27] and  $\lg P_{ow}$  [28]: see Fig. S1, supplementary data). Abbreviations are given according to the IUPAC-IUB commission on biochemical nomenclature [29]. Sodium dodecyl sulphate (SDS), hydrochloric acid, orthophosphoric acid (85%), L-aspartic acid, and sodium hydroxide were from Fluka, Buchs, Switzerland. Disodium tetraborate decahydrate (borax) and sodium dihydrogen phosphate monohydrate were from Merck, Darmstadt, Germany. Methanol, HPLC grade was from VWR-BDH-Prolabo, Leuven, Belgium. Formic acid (98–100 %), sodium chloride and ammonium hydroxide (25 %) were from Sigma-Aldrich. The Affi-gel 601, used as solid phase for the extraction of nucleosides from urine, was purchased from Bio-Rad (Hercules, CA, USA). Ammonium acetate buffer (0.25 mol L<sup>-1</sup>, pH 8.80) was prepared by dissolving 9.6350 g of the salt in 400 mL water, adjusting with concentrated ammonium hydroxide (25 %) to pH 8.80 and then diluting to 500 mL with water. The synthesis and characterization of C<sub>14</sub>MImBr is described in detail in [16].

Stock solutions of tetraborate buffer, phosphate buffer and L-aspartic acid were prepared in water and further diluted for the preparation of the background electrolytes. Stock disodium tetraborate buffer (100 mmol L<sup>-1</sup>, pH 9.48) was prepared by dissolving 9.5342 g disodium tetraborate decahydrate in 250 mL water. Stock phosphate buffer (50 mmol L<sup>-1</sup>, pH 2.66) was prepared by dissolving 1.3799 g (40 mmol L<sup>-1</sup>) of sodium dihydrogen phosphate monohydrate in 200 mL water, adding of 0.17 mL of concentrated orthophosphoric acid (10 mmol L<sup>-1</sup>), and diluting to 250 mL with water. Stock L-aspartic acid (25 mmol L<sup>-1</sup>, pH 2.86) was prepared by dissolving 0.8319 g L-aspartic acid in 250 mL water.

BGEs were: (i) 20 mmol L<sup>-1</sup> C<sub>14</sub>MImBr in 5 mmol L<sup>-1</sup> sodium tetraborate, pH 9.38 (without any pH adjustment), (ii) 20 mmol L<sup>-1</sup> C<sub>14</sub>MImBr in 10 mmol L<sup>-1</sup> disodium tetraborate adjusted using 1 mol L<sup>-1</sup> HCl to pH 9.02, (iii) 100 mmol L<sup>-1</sup> SDS in 50 mmol L<sup>-1</sup> phosphate buffer, pH 2.82, and (iv) 100 mmol L<sup>-1</sup> SDS in 25 mmol L<sup>-1</sup> L-aspartic acid, pH 3.22 (without any pH adjustment). All buffer solutions were filtered prior to

use through a 0.45  $\mu\text{m}$  nylon membrane filter (WICOM, Heppenheim, Germany). BGEs were replaced after every four runs.

## 2.2. Instrumentation

All measurements were done using the ATI Unicam CE System, Crystal 300 Series, Model 310 equipped with UV/Vis detector Spectra 100 (with deuterium lamp) from Thermo Separation Products, San Jose, USA, set to a wavelength of 257 nm (optimized wavelength). Data acquisition was done using an AD-converter (USB-1280FS, Measurement Computing, Middleborough, USA). Data were recorded using CE-Kapillarelektrophorese software (development of the electronic workshop of the Department of Chemistry, University of Marburg based on Delphi). Data analysis was performed with Origin 8.5 software (OriginLab Corporation, Northampton, USA). Fused silica-capillaries (50  $\mu\text{m}$  I.D., 360  $\mu\text{m}$  O.D.) were obtained from Polymicro Technologies (Phoenix, AZ, USA), with a total length of 649 mm and a length to the detector of 501 mm (if not stated otherwise). InoLab pH 720 (WTW, Weilheim, Germany) was used for pH measurements. Solid phase extractions were performed on a vacuum manifold column processor (J.T. Baker, Griesheim, Germany). The flow rate during sample loading and elution is 0.5 mL/min. The eluate obtained after the extraction procedure was lyophilized in a Christ Alpha 2-4 LSC Freeze Dryer (Martin Christ, Osterode am Harz, Germany).

New capillaries were conditioned by flushing them first with NaOH solution (1 mol L<sup>-1</sup>) 60 min, water 60 min, and BGE 15 min using an applied pressure of 800 mbar. For Method 1, the capillaries were rinsed between runs with methanol 2 min, HCl (1 mol L<sup>-1</sup>) 2 min, water 2 min, NaOH solution (1 mol L<sup>-1</sup>) 2 min, water 2 min and finally with BGE for 2 min using an applied pressure of 800 mbar. For Method 2, the capillaries were rinsed between runs with BGE for 5 min. Peak identities were confirmed by spiking.

## 2.3 Urine samples and extraction conditions

Samples of human urine were obtained from a female 27-year old healthy volunteer and were collected in 100 mL plastic bottles and frozen immediately until analysis. Before use, the samples were thawed at room temperature. For the study of spiked urine samples, samples were pretreated with a PBA (phenylboronate affinity gel) column. The extraction conditions are based on what was previously reported [11,15,30,31]. The exact extraction procedure is given in [1]. In case of Method 1, the eluate after drying was redissolved 2 mL 2.5 mmol L<sup>-1</sup> disodium tetraborate, pH 10.45 whereas it was reconstituted in 2 mL water in case of Method 2.

## 2.4. Preparation of standard solutions and calibration curves

All single analyte stock solutions (800.0 mg L<sup>-1</sup> of Ado, Cyd, Urd, 5MeUrd, Ino, 400.0 mg L<sup>-1</sup> of Xao, Guo) were prepared in water and stored in the refrigerator (stock solutions of nucleoside standards are used within one month). The working standard solutions were prepared daily (concentration of each of the studied nucleosides in the sample solution mixture 20 mg L<sup>-1</sup>, unless otherwise specified).

It is unsuitable to prepare the reference samples in urine as the tested analytes are endogenously present in urine [32]. Distilled water was used as a surrogate or artificial matrix for the preparation of the standard solutions, as the studied analytes are highly polar [15]. The concentration ranges for the investigated analytes are listed in Table 1.

Following optimized method parameters were used: capillary 649(501) mm × 50.2 μm I.D., separation voltage -20 kV, injection pressure 50 mbar for 1 min, detection 257 nm. BGEs are 20.0 mmol L<sup>-1</sup> C<sub>14</sub>MImBr in 5 mmol L<sup>-1</sup> disodium tetraborate (Method 1, pH 9.38) and 100 mmol L<sup>-1</sup> SDS in 25 mmol L<sup>-1</sup> L-aspartic acid (Method 2, pH 3.22). Oven temperature is 35 °C (Method 1) or 25 °C (Method 2). Calibration curves are constructed by plotting either peak height, peak area, or corrected peak area against the corresponding concentration in μg mL<sup>-1</sup>.

## 3. Results and discussion

### 3.1. FASS/dynamic pH junction/RFGE-“pseudostationary ion-exchanger” sweeping using C<sub>14</sub>MImBr micelles (Method 1)

Nucleosides are glycosylamines consisting of a nucleobase linked to a D-ribose sugar unit via beta-glycosidic linkage. Five of the studied nucleosides: 5MeUrd, Urd, Guo, Ino and Xao are weak acids due to the presence of an amidic group. Under alkaline pH conditions, the nucleosides Ado and Cyd gain a negative charge only by borate complexation (via their cis-diol moieties), while the other nucleosides acquire negative charges due to complexation with borate (via their cis-diol moieties) and dissociation of the amidic group [1,16]. Therefore, MEKC separation of the negatively charged nucleosides with the oppositely charged IL-based surfactant C<sub>14</sub>MImBr is based on both electrophoretic and chromatographic phenomena [16]. A detailed description of the optimization of separation conditions was given in [16].

In the present study we will focus on the optimization of FASS/dynamic pH junction/RFGE-“pseudostationary ion-exchanger” sweeping conditions for on-line enrichment of the studied nucleosides. It should be taken into consideration that: (i) the degree of complex formation between tetrahydroxyborate and cis diol moieties of the nucleosides is close to one even at very low borate concentration (2.5 mmol L<sup>-1</sup> tetraborate), which gives an indication about the very high complex

formation constants of the formed complexes [16]. (ii) Higher concentrations of disodium tetraborate ( $>10 \text{ mmol L}^{-1}$ ) in the BGE can be used for the separation of the tested nucleosides with a suitable resolution. However, as the concentration of borate (buffering, complexing and competing ion) increases, it displaces the nucleosides (attracted to the PSP by electrostatic forces) from the ion-exchange sites of the pseudostationary ion exchanger, which ultimately results in a lowering of their retention factors and a reduction of their migration times [16]. These effects will have a negative impact on their analysis in urine samples as under these conditions there is a high possibility of coelution of the studied analytes with matrix components. Based on the previous discussion, we will therefore restrict our sweeping investigations to BGEs which contain a maximum of  $10 \text{ mmol L}^{-1}$  disodium tetraborate. (iii) The pH of the sample matrix and the BGE affects the degree of analyte ionization and degree of complexation with borate, which consequently affects the  $k$  values of the nucleosides and their sweeping by  $\text{C}_{14}\text{MImBr}$ . (iv) It should be also noted that in the case of a sample with an electric conductivity adapted to that of the BGE (sweeping under homogenous electric field conditions), the retention factor in the sample zone  $k_s$  (during sweeping) is the retention factor that is obtained in a buffer, which contains the PSP in a concentration identical to that of the BGE in a matrix which is identical to that of the injected sample solution [33]. (v) On the other side, in the case of a sample with an electric conductivity not adapted to that of the BGE (sweeping under inhomogeneous electric field conditions), the true retention factor in the sample zone (during sweeping), is not equal to the  $k_s$  values obtained under homogenous electric field, although in the first approximation the sweeping efficiency is not affected by the electric conductivity of the sample [33]. Actually, sweeping under inhomogeneous electric field conditions is a multistep enrichment process including: (1) stacking or destacking of the PSP when entering the sample zone, (2) sweeping of the neutral analytes by the stacked or destacked PSP, and (3) destacking or stacking of the swept analyte zone [33]. The true retention factor (which is dependent on the distribution coefficient and the phase ratio) might be higher (in case of  $E_s < E_{\text{BGE}}$ , where  $E$  is the electric field strength) or lower (in case of  $E_s > E_{\text{BGE}}$ ) than the  $k_s$  obtained under homogenous electric field conditions based on whether stacking or destacking of the PSP is taking place at the sample/BGE boundary [33]. In the following discussion, the given  $k_s$  values are taken from [16].

#### 3.1.1. Effect of sample matrix and BGE on the enrichment efficiency

The enrichment efficiency of the nucleosides can be improved by: (i) adjusting the retention factor in the sample zone  $k_s$  to be very high in order to increase the achievable sweeping efficiency (according to the concept presented by Quirino and Terabe [18]). Very high  $k_s$  values can be obtained by increasing the pH and decreasing the competing ion concentration in the sample zone [16]. It can be further improved

by (ii) keeping very low retention factors in the BGE  $k_{\text{BGE}}$  which permits analyte focusing by RFGE [24], (iii) inducing an analyte zone velocity difference between the sample zone and the BGE via a difference in the pH, which enables additional analyte focusing by dynamic pH junction, and (iv) using a low electric conductivity sample matrix to allow sample zone concentration by FASS. The pH of the BGE was preselected to be 9.02 [16] as it permits a good separation between the investigated nucleosides and ensures a low  $k_{\text{BGE}}$  [16] which is required for RFGE.

Our first trials were carried out by varying the pH and the composition of the sample matrix. In Fig. 1, four cases were studied (each at three different sample injection volumes, see figure caption) using Guo and Xao as representative analytes. In all cases the composition of the BGE is 20 mmol L<sup>-1</sup> C<sub>14</sub>MImBr in 10 mmol L<sup>-1</sup> disodium tetraborate, pH 9.02. We are varying the pH of the sample matrix (10.45 or 9.02) and the ionic concentration (electric conductivity) of the sample matrix (2.5 or 10 mmol L<sup>-1</sup> disodium tetraborate) either in the presence (non-sweeping conditions) or in the absence of C<sub>14</sub>MImBr micelles (sweeping conditions).

In Fig. 1A, 2.5 mmol L<sup>-1</sup> sodium tetraborate (adjusted to pH 10.45 using 1 mol L<sup>-1</sup> NaOH) is used as sample matrix (FASS + dynamic pH junction + RFGE-“pseudostationary ion-exchanger” sweeping with very high  $k_s$ ). From previous studies [16] we know that  $k_{\text{BGE}}$  with 20 mmol L<sup>-1</sup> C<sub>14</sub>MImBr in the BGE is higher with pH = 10.45 than with pH = 9.02:  $k_s$  at pH 10.45 is 5.1 for Guo and 6.2 for Xao. As seen in Fig. 1A, the peak height of Guo and Xao increases by increasing the sample injection volume (Figs. 1A1, A2 and A3). Sample injection volumes higher than that used in Fig. 1A3 can be applied without affecting peak shape and resolution between the two studied analytes. Hydrodynamic injection using a pressure of 80 mbar for 3.0 min is the maximum sample injection volume that can be applied without loss of resolution (Fig. S2, supplementary data).

In Fig. 1B the sample matrix is 2.5 mmol L<sup>-1</sup> sodium tetraborate adjusted to pH 9.02 using 1 mol L<sup>-1</sup> HCl (FASS + RFGE-“pseudostationary ion-exchanger” sweeping with high  $k_s$ ). Under these conditions, focusing due to dynamic pH junction is suppressed. However, focusing due to FASS and RFGE still exists due to different concentrations of sodium tetraborate in the sample matrix and the BGE. This difference causes a higher  $k$  value in the sample matrix than in the BGE, which is a precondition for focusing of the swept analyte zone by RFGE. Although in general the focusing factor  $f$  due to RFGE is expected to be in the range of 1 to 3 [33], its influence on the whole enrichment mechanism cannot be neglected. Deterioration of the peak shape of Guo was obtained at larger sample injection volume (70 mbar for 2 min, Fig. 1B3), because at pH 9.02 the degree of dissociation is decreased compared to that at 10.45 ( $k_s$  of Guo at pH 9.02 = 1.4 [16]) which is associated concomitantly by a lowering of the sweeping efficiency. On the other side, the peak height of Xao in Fig. 1B3 is only slightly lower than that

obtained with a BGE of higher pH ( $k_s$  of Xao at pH 9.02 = 5.2 [16]). This is because the amidic group of Xao is fully dissociated in both cases, and the slight differences in the peak height might be associated to small differences in the degree of nucleoside-tetrahydroxyborate-complex formation. Xao-tetrahydroxyborate does not have the full negative charge at pH 9.02 as the employed pH is lower than the  $pK_a$  value of boric acid [16]. This can be illustrated by comparing the  $\mu_{\text{eff}}$  of Xao-tetrahydroxyborate complex at pH 9.02 ( $-3.06 \times 10^{-4} \text{ cm}^2 \text{ V}^{-1} \text{ s}^{-1}$ ) and at pH 10.45 ( $-3.39 \times 10^{-4} \text{ cm}^2 \text{ V}^{-1} \text{ s}^{-1}$ ): values are taken from [16]. It is clear from Figs. 1A and 1B that the differences between the on-line-focusing efficiencies due to differences in the sample pH manifest themselves only at larger sample volumes showing that a sample matrix containing 2.5 mmol L<sup>-1</sup> sodium tetraborate, pH 10.45 has advantages over the conditions employed in Fig. 1B. This sample matrix will therefore be used for further investigations.

The sample matrices employed in Fig. 1C (FASS + dynamic pH junction + non-sweeping conditions) and 1D (no FASS+ no dynamic pH junction + non-sweeping conditions) are 20 mmol L<sup>-1</sup> C<sub>14</sub>MImBr in 2.5 mmol L<sup>-1</sup> sodium tetraborate, adjusted to pH 10.45 (using 1 mol L<sup>-1</sup> NaOH solution) and 20 mmol L<sup>-1</sup> C<sub>14</sub>MImBr in 10 mmol L<sup>-1</sup> sodium tetraborate, adjusted to pH 9.02 (using 1 mol L<sup>-1</sup> HCl), respectively. These matrices were studied to elucidate whether FASS + dynamic pH junction play a role in the combined focusing process and how much they can contribute to the overall enrichment mechanism. The peak height of Xao and Guo (in the volume overload region) is higher in Fig. 1C (FASS+ dynamic pH junction + non-sweeping conditions) than that obtained in Fig. 1D (no FASS + no dynamic pH junction + non-sweeping conditions), whereas Guo is much more focused than Xao. This is because the difference in the pseudoeffective electrophoretic mobility ( $\mu_{\text{eff}}^{\text{P}}$ ) of the Guo-tetrahydroxyborate-complex for pH 9.02 and for pH 10.45 is much higher than that of Xao (Table S1, supplementary data). Therefore, we can conclude that focusing by dynamic pH junction is more pronounced for nucleosides, whose degree of dissociation is affected by a variation of the pH between the sample zone and the BGE compartment. However, in general the contribution of FASS + dynamic pH junction to the overall enrichment process is relatively small when compared to sweeping conditions.

Applying the experimental conditions of Fig. 1A to all investigated nucleosides using 50 mbar for 1 min as sample injection conditions and 2.5 mmol L<sup>-1</sup> sodium tetraborate pH 10.45 as sample matrix, a deterioration of the peak efficiency of Ado and Cyd was observed (Fig. 2A). The  $k_s$  values of these two compounds are very low ( $k_s$  values at pH 10.45 are 0.33 and 0.17 for Ado and Cyd, respectively [16]) as these compounds gain their negative charge only by borate complexation (effective charge number = -1). Besides, the difference in  $\mu_{\text{eff}}$  [16] of these two compounds between the sample zone and the BGE is very low which is associated with insignificant focusing by FASS and dynamic pH junction. The effective electrophoretic mobilities  $\mu_{\text{eff}}$  of the Ado(Cyd)-tetrahydroxyborate-complexes are  $-1.46 \times 10^{-4} \text{ cm}^2 \text{ V}^{-1} \text{ s}^{-1}$  at

pH 9.02 and  $-1.76 \times 10^{-4} \text{ cm}^2 \text{ V}^{-1} \text{ s}^{-1}$  at pH 10.45 [16]. Lower sample injection volumes or using water as sample matrix (Fig. 1B, further discussion is given in the supplementary data) can be applied to improve their peak shapes. However, sweeping of Ado and Cyd by  $\text{C}_{14}\text{MImBr}$  micelles will not be considered further as the coelution of urine matrix constituents with these two compounds (as will be shown later) does not justify the use of lower injection volumes which will negatively affect the limits of detection for the other analytes.

As shown in Fig. 2A, the peaks of Urd and 5MeUrd coelute. Therefore, the next trial was to increase the pH of the BGE to be 9.38 and to reduce the concentration of tetraborate in the BGE to obtain a better resolution between the two compounds. Using  $20 \text{ mmol L}^{-1} \text{ C}_{14}\text{MImBr}$  in  $5 \text{ mmol L}^{-1}$  tetraborate, pH 9.38 improves the resolution between the two compounds when applying a pressure injection of 50 mbar for 1 min (Fig. 2C). Moreover, the peak heights of all the studied analytes are higher in Fig. 2C than in Fig. 2A, which can be ascribed to the negative influence of chloride ions (from HCl used for the pH adjustment of the BGE) entering the sample zone from the injection end on the retention factors of these analytes. Based on these investigations,  $20 \text{ mmol L}^{-1} \text{ C}_{14}\text{MImBr}$  in  $5 \text{ mmol L}^{-1}$  tetraborate, pH 9.38 was identified as optimum BGE composition. In addition, hydrodynamic injection using a pressure of 50 mbar for 1 min was employed in further studies as higher sample injection volumes are accompanied with a coelution of Urd and 5MeUrd.

#### **3.1.2. Mechanism of FASS/dynamic pH junction/RFGE-“pseudostationary ion-exchanger” sweeping with $\text{C}_{14}\text{MImBr}$ micelles**

Employing the final optimized enrichment conditions, the mechanism of FASS/dynamic pH junction/RFGE-“pseudostationary ion-exchanger” sweeping with  $\text{C}_{14}\text{MImBr}$  (using a nucleoside with a deprotonation site (e.g., Urd) as a representative example) can be summarized as follows: (i) after filling the capillary with the BGE ( $20 \text{ mmol L}^{-1} \text{ C}_{14}\text{MImBr}$  in  $5 \text{ mmol L}^{-1}$  sodium tetraborate, pH 9.38), the nucleoside containing sample (nucleosides are dissolved in  $2.5 \text{ mmol L}^{-1}$  sodium tetraborate, pH 10.45) is injected hydrodynamically by applying a pressure of 50 mbar for 1 min (Fig. 3A). A negative voltage is applied, whereas the complexed deprotonated nucleosides  $(\text{BN-O})^{2-}$  migrate with a high velocity towards the detection end. Focusing of the studied analytes by FASS/dynamic pH junction commences once the complexed deprotonated nucleosides  $(\text{BN-O})^{2-}$  reach the sample zone/BGE boundary, where they slow down due to the lower pH and higher electric conductivity in the BGE (Fig. 3B1). Simultaneously,  $\text{C}_{14}\text{MImBr}$  micelles start to sweep the analytes within the sample zone causing their migration towards the injection end  $[(\text{BN-O})^{2-}\text{M}^{\text{x}+}]$  (Fig. 3B2). The completely swept analytes are enriched at the rear of sample matrix/BGE boundary (Fig. 3C). Once the swept analytes pass the BGE/sample zone, their velocity is



reduced ( $k_{\text{BGE}} < k_{\text{S}}$ ) resulting in their additional focusing by RFGE (Fig. 3D) and then separation of the swept analyte zones starts (Fig. 3E).

### 3.2. Dynamic pH junction/“pseudostationary ion-exchanger” sweeping using SDS micelles (Method 2)

The low retention factor of Ado and Cyd with respect to  $\text{C}_{14}\text{MImBr}$  and the low sweeping efficiency obtained for these two compounds when using  $\text{C}_{14}\text{MImBr}$  in addition to the unsuitability of Method 1 for the determination of Ado and Cyd in urine samples (due to interfering matrix constituents) necessitate the development of an alternative strategy to enable their sensitive and selective analysis in urine samples. Recently, we have reported for selected nucleosides that the addition of a boronic acid (replacing borate as complexing agent) to the BGE can increase their partitioning coefficients regarding the distribution between the micelles formed by  $\text{C}_{14}\text{MImBr}$  and the surrounding aqueous phase via hydrophobic interaction between the alkyl/aryl group of the boronic acid added and the hydrophobic core of the cationic micelles [34]. Consequently, the retention factors of these highly hydrophilic metabolites with respect to  $\text{C}_{14}\text{MImBr}$  are increased. This method can be successfully applied to the analysis of all the investigated analytes in urine samples.

However, Ado and Cyd are weak bases. Under acidic pH conditions they are existing as positively charged species, which constitutes an ideal basis for their sweeping by the anionic surfactant SDS using electrostatic (Coulombic) forces between the positively charged species and the negatively charged PSP.

#### 3.2.1. Optimization of Method 2

We started our investigations by employing an acidic BGE (negligible electroosmotic flow (EOF)) for the separation of Ado and Cyd with a BGE consisting of 50 mmol  $\text{L}^{-1}$  SDS in 50 mmol  $\text{L}^{-1}$  phosphate buffer, pH 2.82. By application of a negative voltage and in the presence of SDS micelles (reversed elution mode), Ado migrates faster than Cyd, although the effective charge number of Ado is significantly lower than that of Cyd (see  $\text{pK}_{\text{a}}$  values in the supplementary data). Additional hydrophobic interaction of Ado (Ado is more hydrophobic than Cyd, see  $\log P_{\text{ow}}$ , supplementary data) with SDS explains the faster migration of Ado than Cyd due to the stronger interaction of the former with SDS (*i.e.*,  $k(\text{Ado}) > k(\text{Cyd})$ ). Optimum concentration of SDS in the BGE with regard to both peak shape and analyte resolution was found to be 100 mmol  $\text{L}^{-1}$  (Fig. 4A using two different sample injection volumes). Concentration of SDS  $>100$  mmol  $\text{L}^{-1}$  generates an excessive electric current strength as well as unfavourably increased analyte migration times.

The concentration of the co-ion influences the retention factors of charged species with respect to the oppositely charged PSP [16,24,35] and consequently the achievable sweeping efficiency [24]. However, the type of the co-ion also plays a role. El-Awady and Pyell [24] reported that the sweeping efficiency for some aromatic amines is higher when using glutamic acid, pH 3.35 as buffering sample constituent than when using phosphoric acid as sample matrix, pH 3.50. The authors have ascribed this result to the small difference in the degree of protonation of the analytes between the sample matrix and the BGE and accordingly slightly different  $k_s$  and slightly different sweeping efficiency. Based on this report [24], we studied the impact of L-aspartic acid as buffering sample constituent on the obtained sweeping efficiency of Ado and Cyd.

Buffering a solution with a zwitterionic/isoelectric buffering compound produces a buffered electrolyte (i) with low electrical conductivity, (ii) with satisfactory buffering capacity, and (ii) without the concomitant introduction of co-ions [25] that would be detrimental to the sweeping efficiency. Amino acids with two acidic groups and one basic group (or one acidic group and two basic groups) and with an isoelectric point ( $pI$ ) close to two of its  $pK_a$  values (within  $\sim\pm 1.5$  pH units) [25,36] can provide these advantages (e.g., aspartic acid, glutamic acid or lysine). The buffer is prepared simply by dissolving the amino acid in water and the pH is close to the  $pI$  of the amino acid [36].

L-aspartic acid is one of the non-essential amino acids that is normally synthesized in the body. It consists of two carboxylate groups with  $pK_{a1}$  and  $pK_{a2}$  of 1.95 and 3.71, and one amino group ( $pK_{a3}$  of 9.66). Its isoelectric point ( $pI$ ) equals 2.77 [27]. Based on these properties, L-aspartic acid can be used as a low conductivity buffer constituent providing a good buffering capacity at acidic pH values. In subsequent studies 100 mmol L<sup>-1</sup> SDS in 25 mmol L<sup>-1</sup> aspartic acid buffer, pH 3.22 (without any pH adjustment) was employed as BGE for the separation of Ado and Cyd using water or the BGE as sample matrix (see electropherograms in Fig. 4B). The figure inset in Fig. 2B1 demonstrates the separation of the two compounds under non-sweeping conditions. It is interesting to see that the peak heights, at two different samples injection volumes (Figs. 4B1 and 4B2), are significantly higher for both analytes in aspartic acid buffer than those obtained using phosphate buffer (Figs. 4A1 and 4A2). The peak height in aspartic acid buffer is higher than that in phosphate buffer, although the degree of protonation  $\alpha$  of Ado and Cyd in aspartic acid buffer (pH = 3.22) is lower ( $\alpha(\text{Ado}) = 0.656$  and  $\alpha(\text{Cyd}) = 0.895$ ) than that in phosphate buffer (here pH = 2.82,  $\alpha(\text{Ado}) = 0.827$ , and  $\alpha(\text{Cyd}) = 0.955$ ). The lower sweeping efficiency of Ado and Cyd in phosphate buffer results from the co-ions which migrate within the sample zone ( $\text{Na}^+$  and  $\text{H}^+$  ions) and compete with Ado and Cyd on the ion-exchange sites present on the pseudostationary ion-exchanger reducing  $k_s$  and lowering the sweeping efficiency. Trials to increase the degree of protonation of Ado and Cyd in aspartic acid buffer via addition of HCl resulted in

a dramatic decrease in the peak height due to the negative influence of the chloride ions on the retention factors and hence the sweeping efficiency (see figure inset in Fig. 4B2). Therefore, 100 mmol L<sup>-1</sup> SDS in 25 mmol L<sup>-1</sup> aspartic acid buffer, pH 3.22 was used as optimum BGE.

We have tested both water and 2.5 mmol L<sup>-1</sup> aspartic acid as sample matrix. The peak heights of Ado and Cyt are slightly higher when using water as sample matrix than those obtained when using 2.5 mmol L<sup>-1</sup> aspartic acid (Fig. S4, supplementary data). This difference can be attributed to the initial zone focusing by dynamic pH junction when using water as sample matrix that is not existing when using 2.5 mmol L<sup>-1</sup> aspartic acid, therefore the sample matrix water will be used for subsequent investigations. Field amplified sample stacking (FASS) as on-line focusing principle will not be considered here as the analytes are neutral in water.

The sample injection volume was varied by increasing both the pressure and the time of sample injection. Injection volumes higher than those produced by pressure injection of 50 mbar for 1 min, did not result in further increase in the peak height, which implies that this is the maximum injection volume which permits the movement of SDS micelles from the cathodic vial into the capillary (Fig. S4, supplementary data). At larger injection volume the absolute averaged bulk EOF velocity is larger than the absolute electrophoretic migration velocity of the micelles in the BGE compartment.

Hydrodynamic injection using a pressure of 50 mbar for 1 min will be considered for further studies. In addition, a voltage of -20 kV was applied as optimum providing an acceptable running time, resolution and electric current strength. The effect of the oven temperature on the separation was investigated in the range of 15–35°C. A capillary temperature of 25°C was selected as optimum.

#### **3.2.2. Mechanism of dynamic pH junction/“pseudostationary ion-exchanger” sweeping with SDS micelles**

Fig. 5 illustrates the suggested focusing mechanism of Ado and Cyt using SDS. (i) At the beginning (Fig. 5A), the capillary is filled with the BGE (100 mmol L<sup>-1</sup> SDS in 25 mmol L<sup>-1</sup> L-aspartic acid, pH 3.22), followed by hydrodynamic injection of the sample containing the nucleosides dissolved in water (Ado and Cyt are neutral in water). (ii) A negative voltage is applied, whereas the presence of a low conductivity sample matrix increases the averaged bulk electroosmotic flow (EOF) inside the capillary. This results in an initial loss of the neutral analytes from the injection end due to the high EOF velocity within the sample zone. Hydrogen ions migrate towards the injection end, whereas SDS migrates towards the detection end as its absolute electrophoretic velocity is higher than the bulk EOF velocity (Fig. 5B). (iii) Due to the migration of hydrogen ions within the sample zone, Ado and Cyt are protonated and migrate with a high velocity towards the injection end that results in their focusing by

dynamic pH junction (Fig. 5C). (iv) When the front of the protonated nucleosides reaches the front of the migrating micelles, SDS starts to sweep the protonated nucleosides leading to the reversal of their migration direction  $[N^+M^-]$  (Fig. 5D). Nucleosides continue to be accumulated by sweeping and concurrently the sample matrix is pumped out from the injection end. (v) As the sample matrix is removed, the bulk electroosmotic flow becomes very small and the focused analyte zones, which are concentrated at the interface between the sample and the BGE compartment (Fig. 5E), are separated and driven to the detection window (Fig. 5F).

### 3.3. Method performance and validation study

After applying the calibration standards to the phenylboronate affinity gel (PBA), drying of the eluate and reconstitution in the appropriate solvent (as described under Section 2.3), the calibration plots were constructed using the full optimized parameters (see Section 2.4) for Method 1 or Method 2. To determine the linearity of the developed methods, seven to nine calibration standards of the studied nucleosides (six replicates each) were used to construct the calibration curves. Peak height, peak area and corrected peak area (peak area/migration time) were used as the response factors. The results of the statistical analysis of the data are summarised in Table 1 showing the linearity range of the developed methods for each analyte.

As stated by the ICH guidelines [26], the correlation coefficient  $r$ , the y-intercept  $a$ , the slope of the regression line  $b$ , and the sum of squared errors SSE are required for the evaluation of linearity. The previously mentioned parameters in addition to the linearity range, the standard deviation of the intercept and the slope, the standard deviation of the residuals  $S_{yx}$ , the confidence interval of the slope and the intercept, the method standard deviation  $S_{x0}$  and the relative standard deviation of the method  $S_r$  are listed in Table 1. The correlation coefficient  $r$  of the calibration curve is higher in all cases than 0.9967, which indicates excellent linearity of the developed methods. In addition to the determination of correlation coefficients, the linearity was assessed by performing Mandel's fitting test [37]. At a significance level of  $P = 0.99$ , all Mandel's test values are lower than the critical F values (Table 1), which indicates that the chosen linear regression model is adequate.

As given in Table 1, the use of corrected peak area provides no significant improvement when compared to the uncorrected peak area (see  $r$  values in Table 1), which implies a high reproducibility of the migration times and a very good precision of the injection system. In addition, the linearity range in most cases is wider when using the peak area or the corrected peak area than when using the peak height for the construction of the calibration function. This is because the peak height is more affected

by peak broadening due to electrodispersion (concentration overload) at higher sample concentration (leading to non-linear calibration functions) than the peak area or the corrected peak area [1,38,39].

Limits of detection (LOD) and limits of quantitation (LOQ) were determined based on a signal to noise ratio (S/N) of 3 and 10, respectively. The S/N is calculated (according to the European Pharmacopoeia [40]) as given in our previously published work [1]. As shown in Table 1, the LOD and LOQ for the five studied nucleosides using Method 1 were found to be 0.1-0.2  $\mu\text{g mL}^{-1}$ . The LOD for Ado and Cyd using Method 2 was found to be 0.1 and 0.2  $\mu\text{g mL}^{-1}$ , and the LOQ to be 0.2 and 0.4  $\mu\text{g mL}^{-1}$ , respectively. The LOD of Cyd can be further reduced if the selected wavelength is changed to 272 nm, which is for Cyd the wavelength of maximum absorbance coefficient.

The repeatability of migration times, peak heights and peak areas (intra-day variation) was determined for the developed optimized methods with 12 replicate injections of a sample containing (i) 6.0  $\text{mg L}^{-1}$  of 5MeUrd, Guo, Urd, Ino, and Xao (Method 1) or (ii) 12  $\text{mg L}^{-1}$  Ado and Cyd, (Method 2). The inter-day variation was evaluated by analyzing the same sample over a period of 3 days. Precision was expressed as RSD (%).

As given in Table 2, the repeatability of the migration times of Method 1 is  $\leq 0.49$  and 1.91% for intra- and inter-day precision, respectively, whereas the repeatability of the migration times of Method 2 is  $\leq 0.48$  and 1.33% for intra- and inter-day precision, respectively. The highest values for RSD (%) of the peak height and peak area using Method 1 (intra-day precision) are 1.85 and 2.78%, respectively. With Method 2 highest values for RSD (%) of the peak height and peak area (intra-day precision) are 3.78 and 4.62%, respectively. For inter-day precision, all RSD (%) values using Method 1 are lower than 3.54 and 3.24% for the peak height and the peak area, respectively, which indicates in total a good repeatability of Method 1. In contrast to this result, the RSD (%) values for the peak height and the peak area with Method 2 (inter day precision) are  $\leq 10.42$  and 9.42%, respectively. These relatively high RSD (%) values for the peak height and the peak area can be attributed to the fluctuation of the EOF velocity under acidic pH conditions [41].

Although the obtained LODs are higher than those reported in [1], the developed methods provide a similar reproducibility and they are more simple and faster as the method presented in [1] as no polarity switching is needed.

### **3.4. Extraction using a PBA column and application to human urine samples**

The extraction procedure using a PBA column was used only for the clean-up of the urine sample and not for off-line sample concentration as the freeze-dried eluate was reconstituted in a volume which corresponds to the starting urine sample volume (see Section 2.3). However, the extraction process has

a positive influence on the focusing efficiency obtainable with Method 2. To clarify the last point, we have compared the electropherograms obtained with a standard solution containing Ado and Cyd dissolved in water without carrying out SPE with PBA (injected in CE directly, Fig. 6A) and the same standard solution but with carrying out the SPE step (Fig. 6B). This comparison was made for two different analyte concentrations. The peak heights and areas for Ado and Cyd are higher for those runs in which the nucleosides were first extracted on the PBA column although there is no off-line focusing. The ionic constituents which remain in the eluate after extraction (either the ions present in urine or brought in by the washing solutions) reduce the initial analyte loss at the beginning of the negative voltage application. This is due to a reduction of the averaged bulk EOF velocity caused by the increase of the ionic strength within the sample compartment. This result is in good agreement with what we have recently reported [1]. Moreover, the observed effect does not impede the quantitative analysis.

Figs. 7 and 8 show the application of the developed methods to the analysis of urinary nucleosides in blank or spiked urine samples. In each case a standard solution containing the nucleosides dissolved in water was also analyzed for comparison. The injected sample is the sample obtained after pre-treatment of the standard solution or the blank/spiked urine sample with a PBA column, freeze drying of the eluate and reconstitution in 2 mL in an aqueous solution of optimized matrix composition (See Section 2.3). Figs. 7A and 8A show the application of Methods 1 and 2, respectively, to blank urine samples. The presence of nucleosides as endogenous metabolites in the urine samples can be confirmed by (i) comparing the electropherograms in Figs. 7A and 8A by those obtained using standard solutions as sample (Figs. 7B and 8B) or (ii) by observing an appropriate increase in peak height or in peak area (*e.g.*, for Ino and Xao in Fig. 7C and Ado in Fig. 8C) when comparing the result obtained for the spiked sample with the result obtained for the unspiked sample (*cf.*, corresponding peaks in Figs. 7B and 8B). It is clear from Figs. 7 and 8 that there is an excellent extraction selectivity obtained with PBA as there are only few peaks that have to be assigned to unknown compounds present in the urine matrix. In addition these unknown constituents are in general well separated from the studied nucleosides. There is one important exception: As demonstrated in Figs. 7A and 7C, with Method 1 eluted matrix constituents coelute with Ado and Cyd. This method is therefore unsuitable for the determination of Ado and Cyd in human urine. Therefore Method 1 has to be complemented with Method 2. For clinical studies, the determined nucleoside concentrations have to be normalized on the creatinine content. Based on a previous report [15], we assume that the peak marked with (?) can be ascribed to pseudouridine, which is the most predominant modified nucleoside in tRNA.

#### **4. Conclusions**

Two simple, fast, reproducible and sensitive MEKC methods have been developed and validated for the analysis of urinary nucleosides. Combined with dynamic pH junction/“pseudostationary ion-exchanger” sweeping as online enrichment technique, the developed methods can be successfully applied for the analysis of nucleosides in real urine samples using either C<sub>14</sub>MImBr or SDS as PSP. For charged analytes separated with a charged PSP (acting as a pseudostationary ion-exchanger), adjustment of the retention factors both within the sample zone and within the BGE compartment, is the prerequisite for obtaining an adequate focusing efficiency in combination with RFGE-“pseudostationary ion-exchanger” sweeping especially if low limits of detections are needed. This adjustment of the retention factors can be realized by adjustment of the pH and the ionic strength within both the sample zone and the BGE compartment (while simultaneously providing an adequate resolution during the separation step). In this regard, isoelectric buffers due to zwitterionic buffer constituents (providing a very low co-ion concentration) are particularly favourable either in the optimization of the sample solution or in the optimization of the BGE composition.

#### **Acknowledgments**

A.H. Rageh thanks the Egyptian Ministry of Higher Education and the Ministry of State for Scientific Research and the Deutscher Akademischer Austauschdienst (DAAD) for funding her PhD scholarship through German Egyptian Research Long-Term Scholarship program (GERLS). We thank the workshops of the Department of Chemistry, University of Marburg for the development of the data recording unit.

## References

- [1] A.H. Rageh, A. Kaltz, U. Pyell, *Anal. Bioanal. Chem.* 406 (2014) 5877-5895.
- [2] E. Rodriguez-Gonzalo, R. Hernandez-Prieto, D. Garcia-Gomez, R. Carabias-Martinez, *J. Pharm. Biomed. Anal.* 88 (2014) 489-496.
- [3] E. Rodriguez-Gonzalo, D. Garcia-Gomez, R. Carabias-Martinez, *J. Chromatogr. A* 1218 (2011) 9055-9063.
- [4] S.H. Cho, M.H. Choi, W.Y. Lee, B.C. Chung, *Clin. Biochem.* 42 (2009) 540-543.
- [5] S. Wang, X. Zhao, Y. Mao, Y. Cheng, *J. Chromatogr. A* 1147 (2007) 254-260.
- [6] T. Helboe, S.H. Hansen, *J. Chromatogr. A* 836 (1999) 315-324.
- [7] A.J. Sasco, F. Rey, C. Reynaud, J.Y. Bobin, M. Clavel, A. Niveleau, *Cancer Lett.* 108 (1996) 157-162.
- [8] A.S. Cohen, S. Terabe, J.A. Smith, B.L. Karger, *Anal. Chem.* 59 (1987) 1021-1027.
- [9] H.M. Liebich, G. Xu, S. Di, R. Lehmann, H.U. Häring, P. Lu, Y. Zhang, *Chromatographia* 45 (1997) 396-401.
- [10] H.M. Liebich, R. Lehmann, G. Xu, H.G. Wahl, H.U. Häring, *J. Chromatogr. B: Biomed. Sci. Appl.* 745 (2000) 189-196.
- [11] G. Xu, H.M. Liebich, R. Lehmann, S. Müller-Hagedorn, *Methods Mol. Biol.* 162 (2001) 459-474.
- [12] Y.F. Zheng, G.W. Xu, D.Y. Liu, J.H. Xiong, P.D. Zhang, C. Zhang, Q. Yang, L. Shen, *Electrophoresis* 23 (2002) 4104-4109.
- [13] H.M. Liebich, S. Müller-Hagedorn, F. Klaus, K. Meziane, K.R. Kim, A. Frickenschmidt, B. Kammerer, *J. Chromatogr. A* 1071 (2005) 271-275.
- [14] Y.F. Zheng, H.W. Kong, J.H. Xiong, L. Shen, G.W. Xu, *Clin. Biochem.* 38 (2005) 24-30.
- [15] E. Szymanska, M.J. Markuszewski, K. Bodzioch, R. Kaliszan, *J. Pharm. Biomed. Anal.* 44 (2007) 1118-1126.
- [16] A.H. Rageh, U. Pyell, *J. Chromatogr. A* 1316 (2013) 135-146.
- [17] M.R. Monton, J.P. Quirino, K. Otsuka, S. Terabe, *J. Chromatogr. A* 939 (2001) 99-108.
- [18] J.P. Quirino, S. Terabe, *Science* 282 (1998) 465-468.
- [19] M. El-Awady, F. Belal, U. Pyell, *J. Chromatogr. A* 1309 (2013) 64-75.
- [20] P. Britz-McKibbin, G.M. Bebault, D.D.Y. Chen, *Anal. Chem.* 72 (2000) 1729-1735.
- [21] A.A. Kazarian, E.F. Hilder, M.C. Breadmore, *J. Sep. Sci.* 34 (2011) 2800-2821.
- [22] R.L. Chien, D.S. Burgi, *Anal. Chem.* 64 (1992) 489A-496A.



- [23] M. El-Awady, U. Pyell, *Electrophoresis* 35 (2014) 605-616.
- [24] M. El-Awady, U. Pyell, *J. Chromatogr. A* 1297 (2013) 213-225.
- [25] T. Rodemann, C. Johns, W.S. Yang, P.R. Haddad, M. Macka, *Anal. Chem.* 77 (2005) 120-125.
- [26] ICH Harmonised Tripartite Guidelines, Validation of analytical procedures: text and methodology Q2(R1). <http://www.ich.org/products/guidelines/quality/article/quality-guidelines.html> (accessed 10.03.2015).
- [27] R.L. Lundblad, F. MacDonald (Eds.), *Handbook of Biochemistry and Molecular Biology*, 4th edn., CRC Press, Taylor and Francis Group, LLC, Boca Raton, 2010.
- [28] G. Marrubini, B.E.C. Mendoza, G. Massolini, *J. Sep. Sci.* 33 (2010) 803-816.
- [29] IUPAC-IUB Commission on Biochemical Nomenclature (CBN), *Pure Appl. Chem.* 40 (1974) 277-290.
- [30] K.C. Kuo, D.T. Phan, N. Williams, C.W. Gehrke, in: C.W. Gehrke, K.C. Kuo (Eds.), *Chromatography and Modification of Nucleosides. Part C Modified Nucleosides in Cancer and Normal Metabolism Methods and Applications*, Elsevier, Oxford, 1990, p. C41-C113.
- [31] C.W. Gehrke, K.C. Kuo, G.E. Davis, R.D. Suits, T.P. Waalkes, E. Borek, *J. Chromatogr.* 150 (1978) 455-476.
- [32] N.C. van de Merbel, *Trends Anal. Chem.* 27 (2008) 924-933.
- [33] M. El-Awady, C. Huhn, U. Pyell, *J. Chromatogr. A* 1264 (2012) 124-136.
- [34] A.H. Rageh, U. Pyell, *Electrophoresis* (2014) In Press.
- [35] I. Orentaite, A. Maruska, U. Pyell, *Electrophoresis* 32 (2011) 604-613.
- [36] S. Hjerten, L. Valtcheva, K. Elenbring, J.L. Liao, *Electrophoresis* 16 (1995) 584-594.
- [37] M. Reichenbaecher, J.W. Einax (Eds.), *Challenges in Analytical Quality Assurance*, Springer-Verlag, Berlin Heidelberg, 2011.
- [38] H. Wätzig, *J. Chromatogr. A* 700 (1995) 1-7.
- [39] H. Wätzig, M. Degenhardt, A. Kunkel, *Electrophoresis* 19 (1998) 2695-2752.
- [40] *European Pharmacopoeia (7.8)*, Online Version, European directorate for the quality of medicines & healthcare (EDQM), Strasbourg, 2013.
- [41] J.P. Quirino, S. Terabe, *Anal. Chem.* 70 (1998) 149-157.

### Figure captions

**Figure 1:** Electropherograms obtained with samples containing Guo and Xao (each 20.0 mg L<sup>-1</sup>) dissolved in four different sample matrices including (A) 2.5 mmol L<sup>-1</sup> sodium tetraborate pH 10.45, (B) 2.5 mmol L<sup>-1</sup> sodium tetraborate pH 9.02, (C) 20 mmol L<sup>-1</sup> C<sub>14</sub>MImBr in 2.5 mmol L<sup>-1</sup> sodium tetraborate pH 10.45 and (D) BGE (no FASS + no dynamic pH junction + non-sweeping condition) employing three different injection parameters. CE conditions: 20 mmol L<sup>-1</sup> C<sub>14</sub>MImBr in 10 mmol L<sup>-1</sup> disodium tetraborate, pH 9.02 as BGE, hydrodynamic injection using pressure (A1, B1, C1, D1) 40 mbar for 0.4 min, (A2, B2, C2, D2) 50 mbar for 0.8 min, (A3, B3, C3, D3) 70 mbar for 2 min, capillary 649(501) mm × 50 μm I.D, applied voltage -20 kV, oven temperature 35 °C. Peak designation: 4 = Guo, 5 = Xao.

**Figure 2:** Electropherograms obtained with a standard solution containing 20.0 mg L<sup>-1</sup> of each of the studied analytes dissolved in different sample matrices including (A) and (C) 2.5 mmol L<sup>-1</sup> sodium tetraborate pH 10.45 and (B) water. CE conditions: BGEs are (A) and (B) 20 mmol L<sup>-1</sup> C<sub>14</sub>MImBr in 10 mmol L<sup>-1</sup> disodium tetraborate, pH 9.02 and (C) 20 mmol L<sup>-1</sup> C<sub>14</sub>MImBr in 5 mmol L<sup>-1</sup> disodium tetraborate, pH 9.38, capillary 649(501) mm × 50 μm I.D, hydrodynamic injection using pressure 50 mbar for 1 min, applied voltage -20 kV, oven temperature 35 °C. Peak designation: 1 = Cyd, 2 = Urd, 3 = 5MeUrd, 4 = Guo, 5 = Xao, 6 = Ado, 7 = Ino.

**Figure 3:** Schematic representation of the suggested enrichment mechanism using Method 1. (A) Capillary filled with BGE followed by hydrodynamic injection of the sample plug. (B1) Application of a negative voltage, where EOF is towards the anode. Focusing by FASS/dynamic pH junction start once the complexed deprotonated nucleosides reach the sample zone/BGE boundary. (B2) Simultaneously, C<sub>14</sub>MImBr commences to sweep the complexed deprotonated nucleosides within the sample zone. (C) Sweeping is completed and analytes are focused at the rear boundary of the sample zone/BGE compartment. (D) Additional focusing of the swept analyte zone by RFGE. (E) Separation of the focused analyte zones. The length of the arrow represents the magnitude of the velocity. It should be taken into consideration that step (B1) and (B2) are taking place concomitantly, however they are separated here for illustrative purpose.

**Figure 4:** Electropherogram obtained with a sample containing Ado and Cyd (20.0 mg L<sup>-1</sup> each) dissolved in water employing two different injection volumes using (A) 100 mmol L<sup>-1</sup> SDS in 25 mmol L<sup>-1</sup> phosphate buffer, pH 2.82 and (B) 100 mmol L<sup>-1</sup> SDS in 25 mmol L<sup>-1</sup> aspartic acid buffer, pH 3.22 as BGEs. Other CE conditions: hydrodynamic injection using pressure (A1, B1) 50 mbar for 0.5 min, (A2, B2) 50 mbar for 1 min, capillary 649(501) mm × 50 μm I.D, applied voltage -20 kV, oven temperature 25 °C. The Figure inset in Fig. 4B1 is the electropherogram which was obtained with the same conditions as that in Fig. 4B1 but with BGE as sample matrix. The Figure inset in Fig. 4B2 is the electropherogram

which was obtained with the same conditions as in Fig. 4B2 but after adjusting the pH of the BGE with HCl to pH 2.18. Peak designation: see Fig. 2.

**Figure 5:** Schematic representation of the suggested focusing mechanism using Method 2. (A) Capillary filled with BGE followed by hydrodynamic injection of the sample plug. (B) Application of a negative voltage, whereas hydrogen ions migrate towards the injection end and SDS migrates towards the detection end. (C) Hydrogen ions deprotonate the nucleosides within the sample zone starting their focusing by dynamic pH junction. (D) SDS commences sweeping of the positively charged nucleosides, while simultaneously the matrix is pumped out from the injection end. (E) After completion of the sweeping step and after pumping the largest part of the sample matrix plug out of the capillary, (F) separation of the swept analyte zones starts. The length of the arrow represents the magnitude of the velocity.

**Figure 6:** Electropherograms obtained using Method 2 for (A) nucleosides dissolved in water and injected in CE directly or (B) nucleosides extracted with a PBA column and reconstituted in the same volume of water. Sample solution is 4.0 mg L<sup>-1</sup> of Ado and 8.0 mg L<sup>-1</sup> Cyd in (A1, B1) or 8.0 mg L<sup>-1</sup> of Ado and 16.1 mg L<sup>-1</sup> Cyd in (A2, B2). CE conditions: 100 mmol L<sup>-1</sup> SDS in 25 mmol L<sup>-1</sup> aspartic acid buffer, pH 3.22 as BGE, hydrodynamic injection using pressure 50 mbar for 1 min, applied voltage -20 kV, current -30 μA, oven temperature 25 °C. Peak designation: see Fig. 2.

**Figure 7:** Electropherograms obtained using Method 1 for (A) a blank urine sample, (B) standard solution of nucleosides in water, and (C) a spiked urine sample after extraction on PBA column and reconstitution in 2 mL 2.5 mmol L<sup>-1</sup> sodium tetraborate pH 10.45. Nucleoside concentration in (B) and (C) is 4 mg L<sup>-1</sup> each. CE conditions: 20 mmol L<sup>-1</sup> C<sub>14</sub>MImBr in 5 mmol L<sup>-1</sup> disodium tetraborate, pH 9.38 as BGE, capillary 649(501) mm × 50 μm I.D, hydrodynamic injection using pressure 50 mbar for 1 min, applied voltage -20 kV, current -9.9 μA, oven temperature 35 °C. Peak designation: see Fig. 2. \*unidentified peak, ? = pseudouridine.

**Figure 8:** Electropherograms obtained using Method 2 for (A) a blank urine sample, (B) standard solution of nucleosides in water, and (C) a spiked urine sample after extraction on PBA column and reconstitution in 2 mL water. Nucleoside concentration in (B) and (C) is 8.0 mg L<sup>-1</sup> Ado and 16.1 mg L<sup>-1</sup> Cyd. CE conditions and peak designation: see Fig. 6.

**Table 1** Linear regression parameters of the developed methods for calibration standards after SPE

Studied analytes <sup>a</sup>	No. of calib. standards	Linearity range ( $\mu\text{g mL}^{-1}$ )	Intercept (a) $\pm$ SD <sup>b</sup>	Slope (b) $\pm$ SD <sup>c</sup>	SSE <sup>d</sup>	$S_{yx}$ <sup>e</sup>	$S_{x0}$ <sup>f</sup>	$S_r\%$ <sup>g</sup>	Confidence interval of (a) <sup>h</sup>	Confidence interval of (b) <sup>h</sup>	$r^i$	Mandel's test value <sup>i</sup>	LOD <sup>k</sup> ( $\mu\text{g mL}^{-1}$ ) S/N=3	LOQ <sup>l</sup> ( $\mu\text{g mL}^{-1}$ ) S/N=3
5MeUrd														
PH <sup>m</sup>	8	0.50-10.0	0.05 $\pm$ 0.03	0.30 $\pm$ 0.01	94.01	0.05	0.17	4.31	$\pm$ 0.10	$\pm$ 0.02	0.9991	6.31	0.10	0.20
PA <sup>n</sup>	9	0.50-12.0	0.03 $\pm$ 0.04	0.49 $\pm$ 0.01	151.07	0.08	0.17	3.46	$\pm$ 0.15	$\pm$ 0.02	0.9993	0.36		
Corr. PA <sup>o</sup>	9	0.50-12.0	0.01 $\pm$ 0.01	0.13 $\pm$ 0.00	151.07	0.02	0.18	3.71	$\pm$ 0.04	$\pm$ 0.01	0.9992	0.76		
Urd														
PH	7	0.50-8.00	0.08 $\pm$ 0.02	0.26 $\pm$ 0.01	52.68	0.04	0.16	4.98	$\pm$ 0.09	$\pm$ 0.02	0.9988	16.66	0.10	0.20
PA	9	0.50-12.0	0.00 $\pm$ 0.05	0.64 $\pm$ 0.01	151.02	0.09	0.14	2.87	$\pm$ 0.16	$\pm$ 0.03	0.9995	2.20		
Corr. PA	9	0.50-12.0	0.00 $\pm$ 0.01	0.16 $\pm$ 0.00	151.02	0.02	0.12	2.54	$\pm$ 0.04	$\pm$ 0.01	0.9996	1.49		
Guo														
PH	8	0.50-10.0	0.07 $\pm$ 0.04	0.30 $\pm$ 0.01	93.74	0.07	0.24	5.99	$\pm$ 0.15	$\pm$ 0.03	0.9982	11.25	0.10	0.20
PA	9	0.50-12.0	-0.07 $\pm$ 0.07	0.85 $\pm$ 0.01	150.73	0.13	0.15	3.07	$\pm$ 0.23	$\pm$ 0.04	0.9995	0.00		
Corr. PA	9	0.50-12.0	-0.01 $\pm$ 0.01	0.19 $\pm$ 0.00	150.73	0.03	0.14	2.91	$\pm$ 0.05	$\pm$ 0.01	0.9995	0.14		
Ino														
PH	7	0.50-8.00	0.09 $\pm$ 0.05	0.35 $\pm$ 0.01	52.59	0.08	0.22	7.09	$\pm$ 0.18	$\pm$ 0.04	0.9977	3.64	0.10	0.20
PA	9	0.50-12.0	0.03 $\pm$ 0.10	1.14 $\pm$ 0.02	150.88	0.19	0.17	3.48	$\pm$ 0.35	$\pm$ 0.06	0.9993	0.18		
Corr. PA	9	0.50-12.0	0.01 $\pm$ 0.02	0.23 $\pm$ 0.00	150.88	0.04	0.17	3.56	$\pm$ 0.07	$\pm$ 0.01	0.9993	0.48		
Xao														
PH	7	0.50-8.48	0.09 $\pm$ 0.02	0.24 $\pm$ 0.01	59.61	0.04	0.15	4.60	$\pm$ 0.08	$\pm$ 0.02	0.9990	9.09	0.10	0.20
PA	8	0.50-10.6	0.03 $\pm$ 0.08	1.00 $\pm$ 0.01	106.16	0.15	0.15	3.53	$\pm$ 0.30	$\pm$ 0.05	0.9994	7.78		
Corr. PA	8	0.50-10.6	0.01 $\pm$ 0.02	0.19 $\pm$ 0.00	106.16	0.03	0.14	3.34	$\pm$ 0.05	$\pm$ 0.01	0.9994	15.34		
Ado														
PH	9	0.20-16.0	0.05 $\pm$ 0.03	0.27 $\pm$ 0.00	263.82	0.06	0.23	3.74	$\pm$ 0.11	$\pm$ 0.01	0.9993	0.84	0.10	0.20
PA	9	0.20-16.0	-0.05 $\pm$ 0.09	0.88 $\pm$ 0.01	263.82	0.18	0.21	3.36	$\pm$ 0.32	$\pm$ 0.04	0.9994	0.65		
Corr. PA	9	0.20-16.0	0.00 $\pm$ 0.01	0.11 $\pm$ 0.00	263.82	0.02	0.20	3.25	$\pm$ 0.04	$\pm$ 0.01	0.9995	0.39		
Cyd														
PH	7	0.40-16.0	0.03 $\pm$ 0.01	0.04 $\pm$ 0.00	181.39	0.02	0.49	6.29	$\pm$ 0.05	$\pm$ 0.01	0.9967	0.14	0.20	0.40
PA	7	0.40-16.0	0.07 $\pm$ 0.04	0.13 $\pm$ 0.00	181.39	0.05	0.40	5.14	$\pm$ 0.14	$\pm$ 0.02	0.9978	0.22		
Corr. PA	7	0.40-16.0	0.01 $\pm$ 0.00	0.02 $\pm$ 0.00	181.39	0.01	0.37	4.76	$\pm$ 0.02	$\pm$ 0.00	0.9981	0.14		

<sup>a</sup> The linear regression parameters for 5MeUrd, Urd, Guo, Ino, and Xao are obtained using method 1, whereas the linear regression parameters for Ado and Cyd are obtained using method 2, <sup>b</sup> standard deviation of the intercept, <sup>c</sup> standard deviation of slope, <sup>d</sup> sum of square errors, <sup>e</sup> residual standard deviation (standard error of estimate (SEE)), <sup>f</sup> method standard deviation ( $= S_{yx}/b$ ), <sup>g</sup> relative standard deviation of the method ( $= S_{x0}/\bar{X}$ ), <sup>h</sup> confidence interval calculated at  $P=0.99$ , <sup>i</sup>  $r$  is the correlation coefficient, <sup>j</sup> tabulated  $f$  values at  $P = 0.99$  are 13.74, 16.25, 21.19 at (df1 (1), df2 (n-3) = (1,6), (1,5), (1,4), respectively, <sup>k</sup> limit of detection, <sup>l</sup> limit of quantitation, <sup>m</sup> peak height, <sup>n</sup> peak area, <sup>o</sup> corrected peak area

**Table 2** Intra- and Inter-day precision of the developed methods

Method		Intra-day precision (n = 12), RSD <sup>a</sup> (%)			Inter-day precision, 3 days (n = 37), RSD (%)		
		MT <sup>b</sup>	PH <sup>c</sup>	PA <sup>d</sup>	MT	PH	PA
5MeUrd	1	0.45	1.84	1.83	1.42	3.14	2.75
Urd	1	0.46	1.27	2.78	1.48	2.76	2.67
Guo	1	0.48	0.52	1.78	1.62	3.44	2.94
Ino	1	0.45	0.83	1.48	1.81	3.54	3.10
Xao	1	0.49	1.85	2.39	1.91	2.78	3.24
Ado	2	0.48	1.91	2.35	1.21	5.29	9.10
Cyd	2	0.46	3.78	4.62	1.33	10.42	5.81

<sup>a</sup>Relative standard deviation, <sup>b</sup> Migration time, <sup>c</sup> Peak height, <sup>d</sup> Peak area

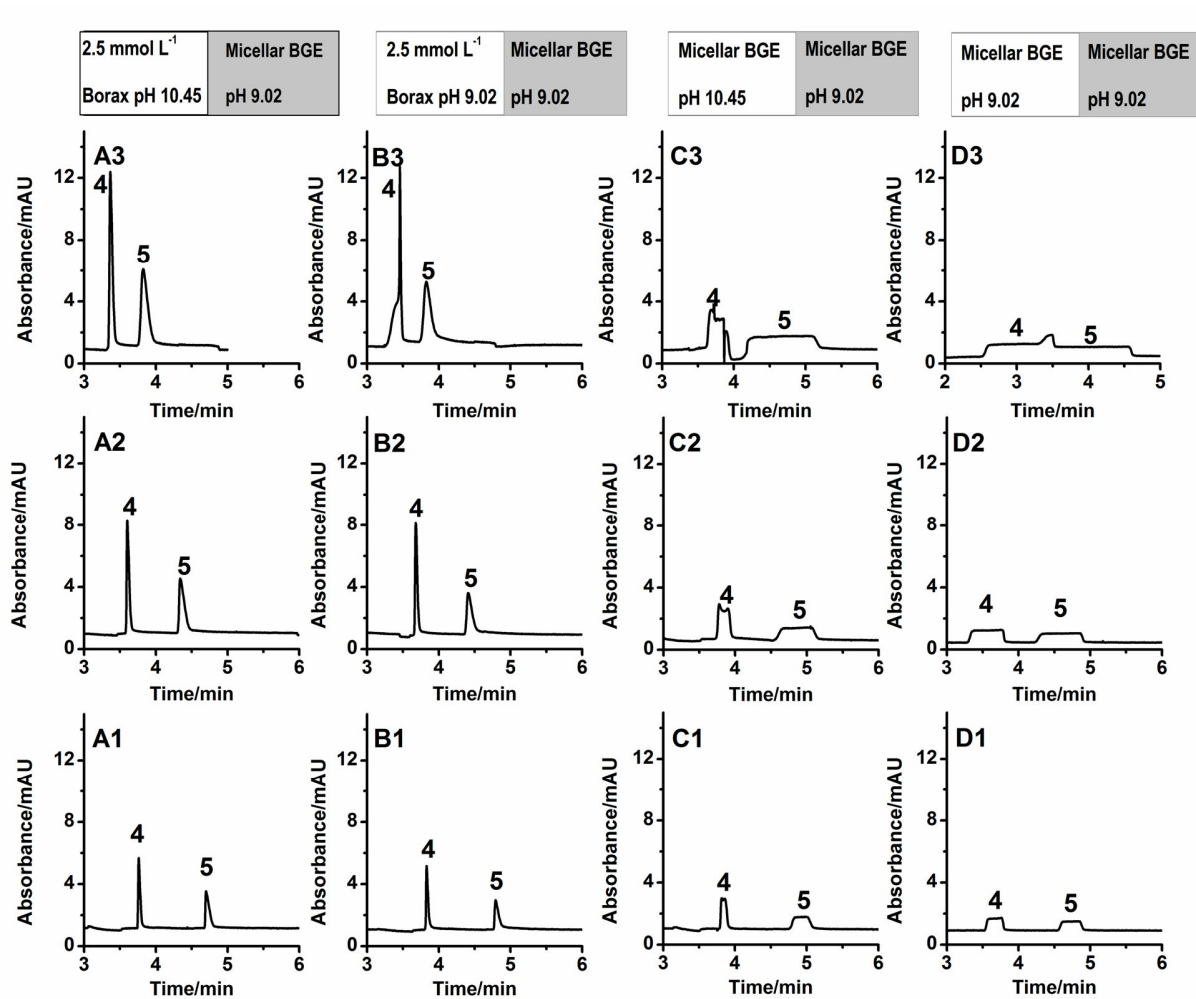
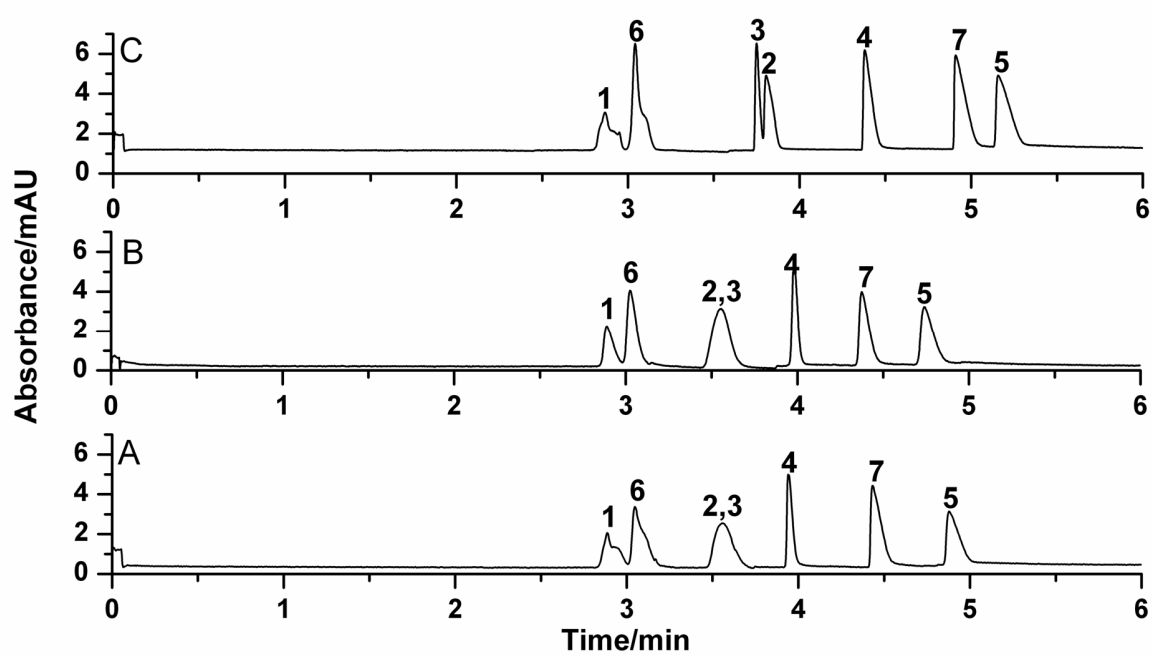


Figure 1



**Figure 2**

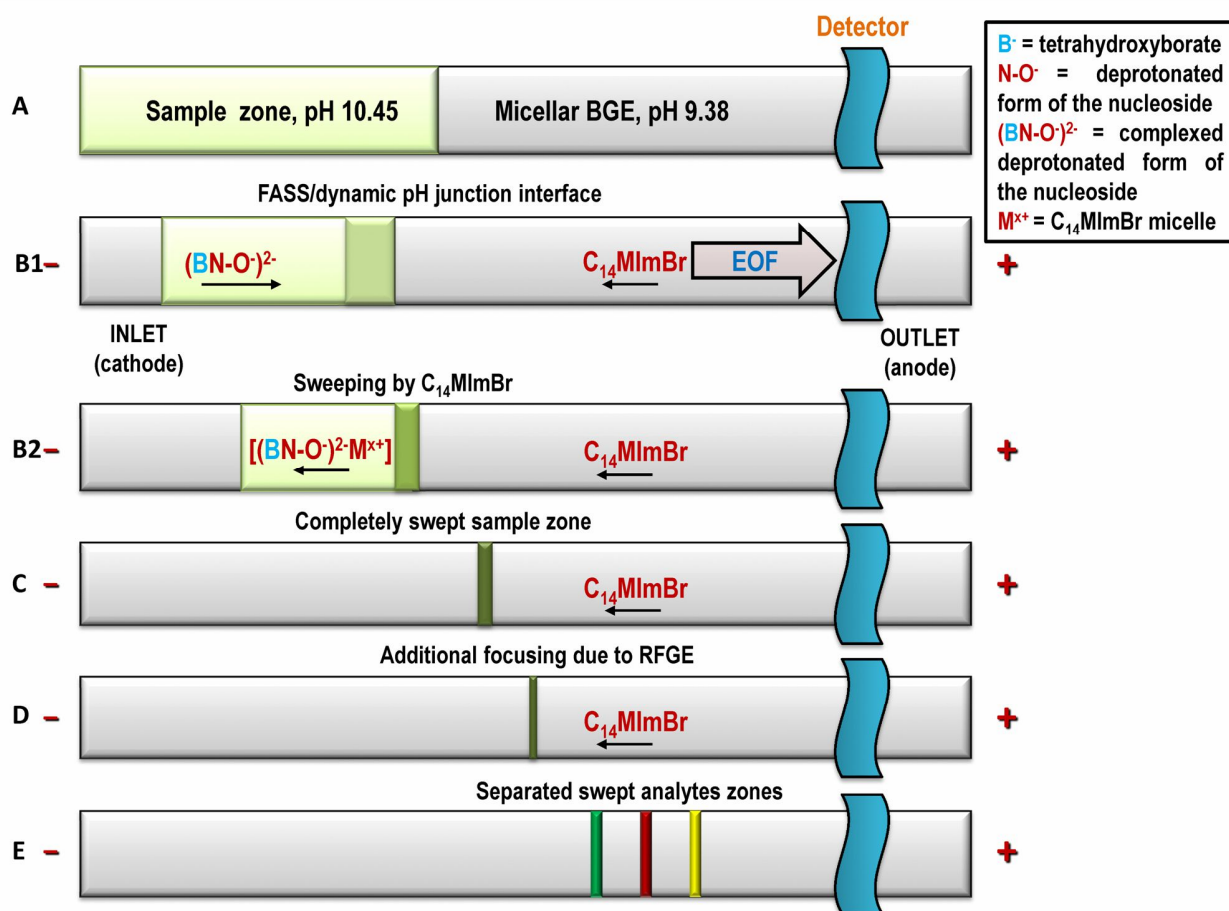
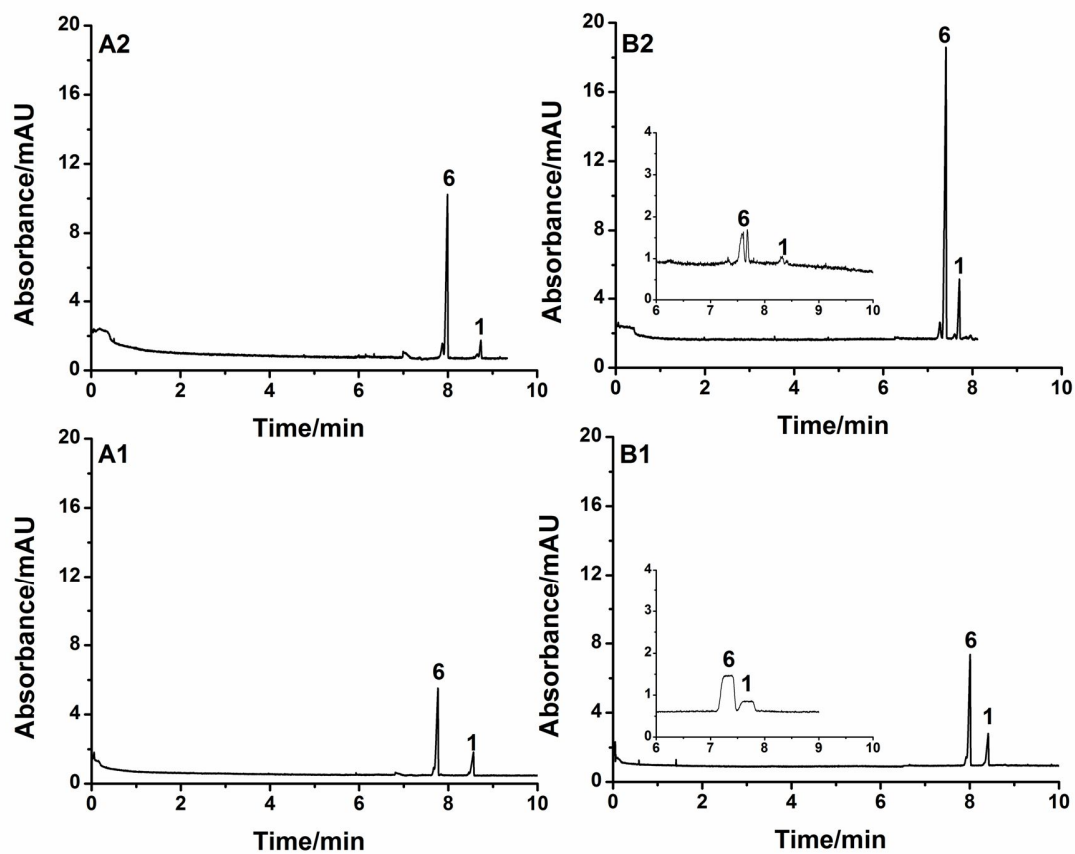


Figure 3





**Figure 4**

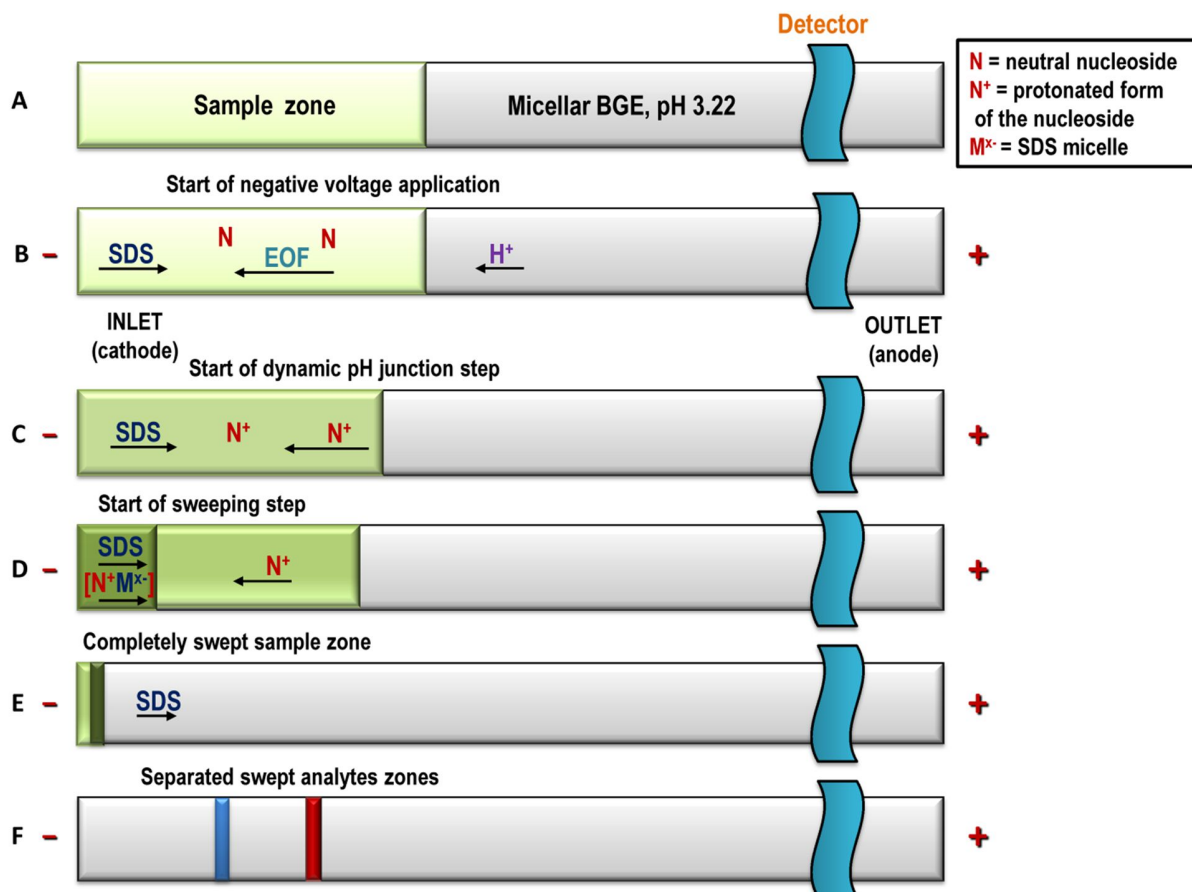
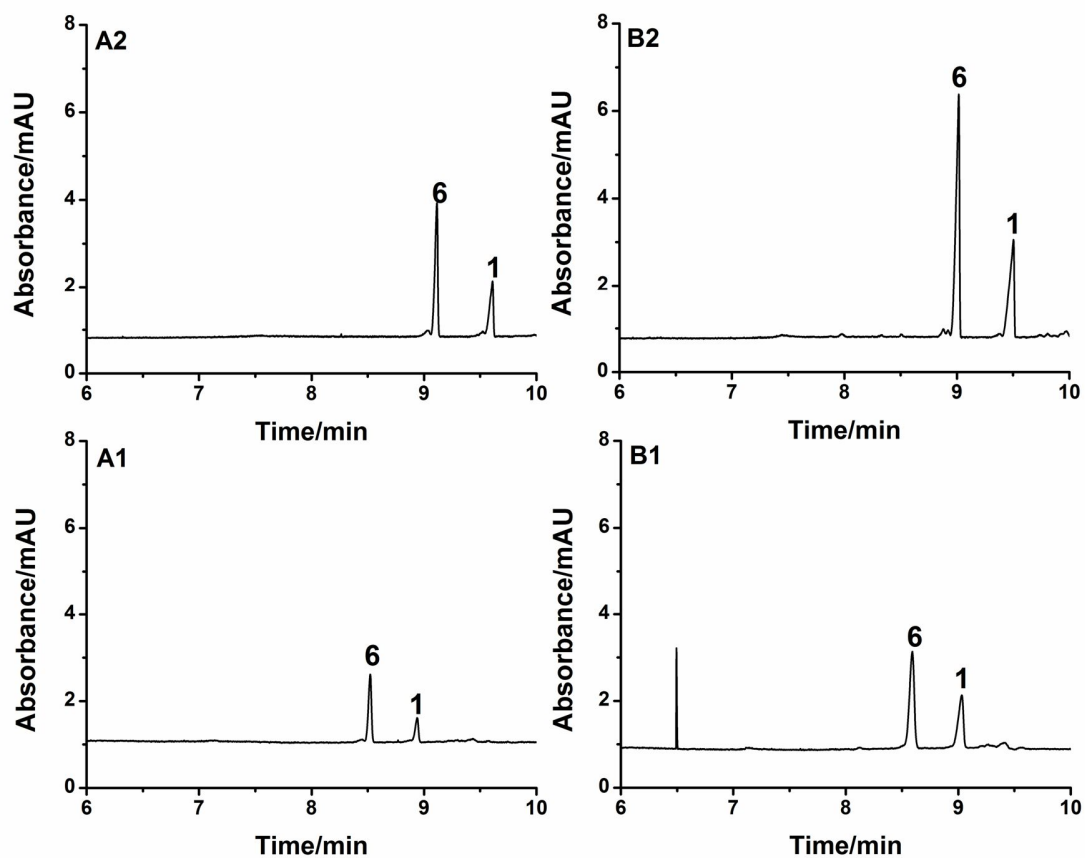
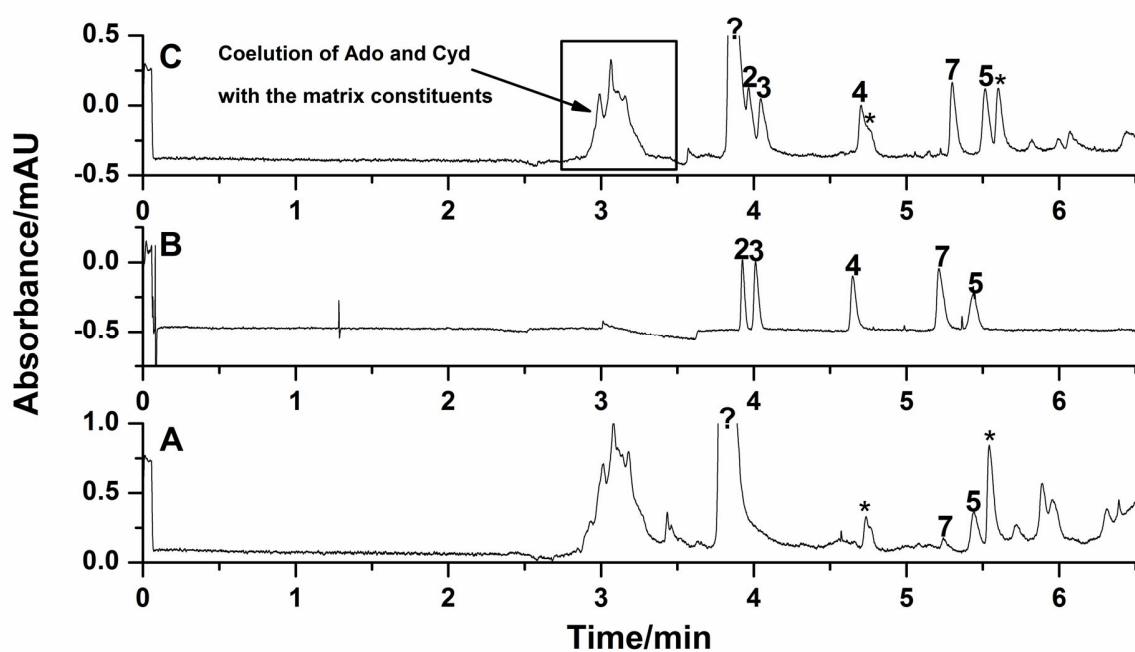


Figure 5



**Figure 6**



**Figure 7**

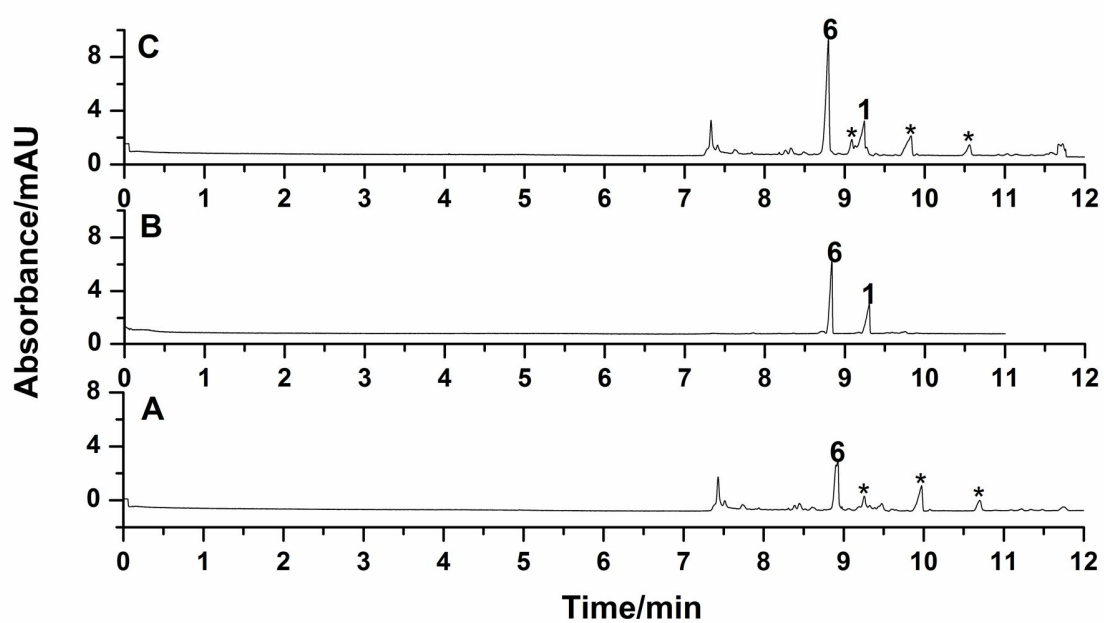


**Figure 8**



**“Pseudostationary ion-exchanger” sweeping/dynamic pH junction/FASS on-line enrichment for the determination of nucleosides in urine via micellar electrokinetic chromatography after solid phase extraction with phenylboronate affinity gel**

Azza H. Rageh, Ute Pyell\*

University of Marburg, Department of Chemistry, Hans-Meerwein-Straße, D-35032 Marburg, Germany

\* Corresponding author

**Supplementary data**

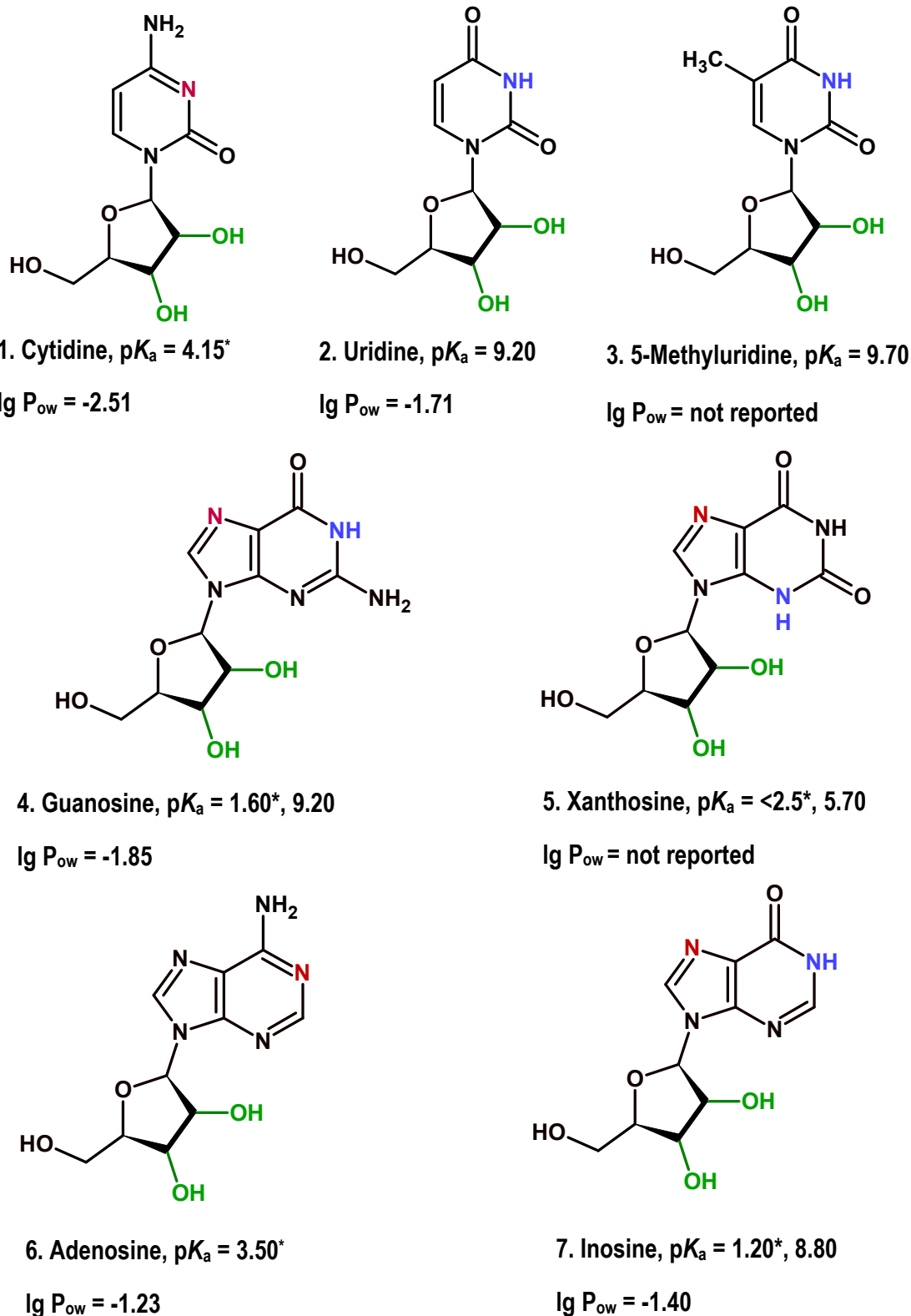


**Figure S1:** Structural formulas,  $pK_a$  and  $\lg P_{ow}$  of the investigated nucleosides. \* Values of  $pK_a$  are those of the cationic protonated conjugate acid form. Red and blue colours are used to mark the protonation and dissociation sites, respectively.  $pK_a$  values of cis-diol moieties (marked with the green colour) are  $\sim 12.5$ .



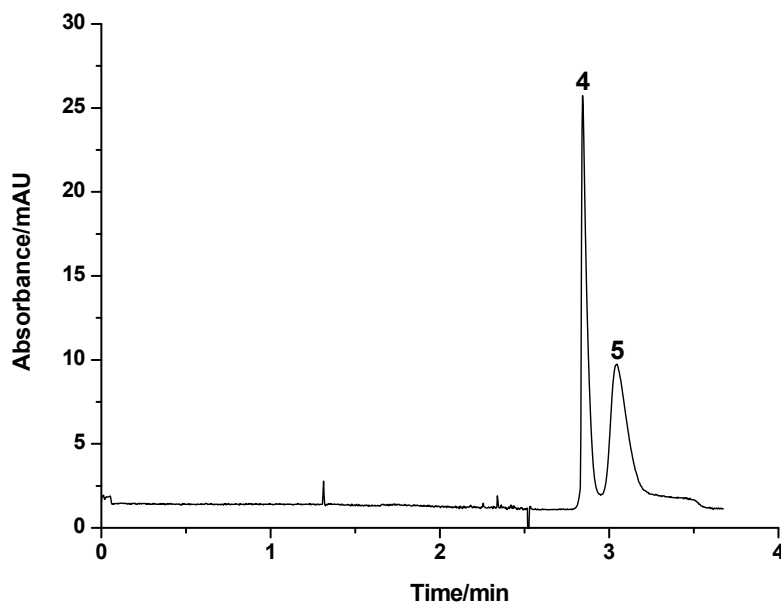


**Figure S2:** Electropherogram obtained with a sample containing Guo and Xao (each 20.0 mg L<sup>-1</sup>) dissolved in 2.5 mmol L<sup>-1</sup> sodium tetraborate pH 10.45. CE conditions: 20 mmol L<sup>-1</sup> C<sub>14</sub>MImBr in 10 mmol L<sup>-1</sup> disodium tetraborate, pH 9.02 as BGE, hydrodynamic injection using pressure 80 mbar for 3 min, capillary 649(501) mm × 50 μm I.D., applied voltage -20 kV, oven temperature 35 °C. Peak designation: 4 = Guo, 5 = Xao.

**Table S1.** Pseudoeffective electrophoretic mobilities determined for Guo and Xao (20 mg L<sup>-1</sup> each, dissolved in water) under variation of pH and concentration of borax with c(C<sub>14</sub>MImBr) = 20 mmol L<sup>-1</sup>, capillary 650(501) mm × 50 μm I.D., voltage -20 kV, pressure injection 30 mbar for 12 s, 4 = guanosine, 5 = xanthosine.

BGE	pH	$\mu_{\text{eff}}^{\text{P}}(4) \times 10^{-4} / \text{cm}^2 \text{V}^{-1} \text{s}^{-1}$	$\mu_{\text{eff}}^{\text{P}}(5) \times 10^{-4} / \text{cm}^2 \text{V}^{-1} \text{s}^{-1}$
20 mmol L <sup>-1</sup> C <sub>14</sub> MImBr in 10.0 mmol L <sup>-1</sup> borax	9.02	0.92	2.39
20 mmol L <sup>-1</sup> C <sub>14</sub> MImBr in 2.5 mmol L <sup>-1</sup> borax <sup>a</sup>	10.45	3.11	3.23

<sup>a</sup> Values of  $\mu_{\text{eff}}^{\text{P}}$  are taken from [16].

### **Water as sample matrix (Method 1)**

Employing water as sample matrix has improved the peak shape of Ado and Cyd (Fig. 2B). These two analytes are neutral in water. Sweeping of these two analytes by borate that enters the sample zone from the injection end and their final stacking on the front boundary of the sample matrix is possible due to their very low interaction with the C<sub>14</sub>MImBr micelles [1,16]. Therefore larger sample volumes can be used without loss of peak efficiency (Fig. 2B). For the other analytes: upon application of the negative voltage, hydroxide ions followed by borate ions migrate (toward the detection end) within the sample zone resulting in deprotonation of the amidic group-containing nucleosides and subsequent complexation with borate causing their migration towards the anode. Simultaneously, sweeping of the complexed deprotonated nucleosides takes place by the C<sub>14</sub>MImBr micelles (entering the sample zone from the detection end) resulting in zone narrowing on the rear boundary of the sample matrix/BGE compartment. The higher retention factors of amidic-group containing nucleosides (if compared to those of Ado and Cyd) with respect to the oppositely charged PSP is the reason for the higher sweeping efficiency of these compounds. It should be taken into account that the migration direction of the electroosmotic flow (EOF) is the same as that of hydroxide and borate, therefore, the contribution of dynamic pH junction/sweeping by borate in the focusing of the deprotonated nucleosides is lower under these conditions than that reported previously using CZE [1]. Although water as sample matrix has improved the peak shapes of Ado and Cyd and provides similar sweeping efficiencies to the matrix used in Fig. 1A, the latter will be used as optimum sample matrix because at larger sample injection volumes it gives a better sweeping efficiency for the amidic group-containing nucleosides (compare Figs. S3 and Fig. 1A3).

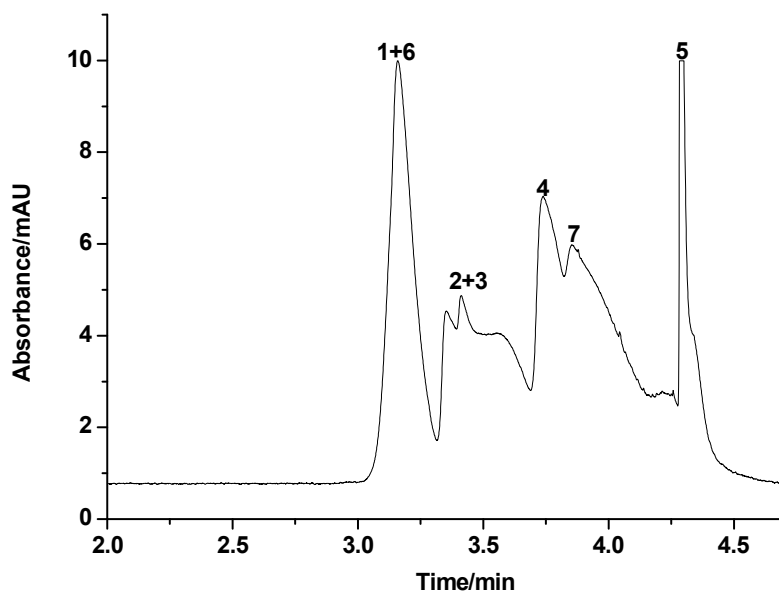


**Figure S3:** Electropherograms obtained with a standard solution containing  $20.0 \text{ mg L}^{-1}$  of each of the studied analytes dissolved in water. CE conditions: BGE is  $20 \text{ mmol L}^{-1} \text{ C}_{14}\text{MImBr}$  in  $10 \text{ mmol L}^{-1}$  disodium tetraborate, pH 9.02, capillary  $649(501) \text{ mm} \times 50 \text{ }\mu\text{m}$  I.D, hydrodynamic injection using pressure  $70 \text{ mbar}$  for  $2 \text{ min}$ , applied voltage  $-20 \text{ kV}$ , oven temperature  $35 \text{ }^\circ\text{C}$ . Peak designation: 1 = Cyd, 2 = Urd, 3 = 5MeUrd, 4 = Guo, 5 = Xao, 6 = Ado, 7 = Ino.

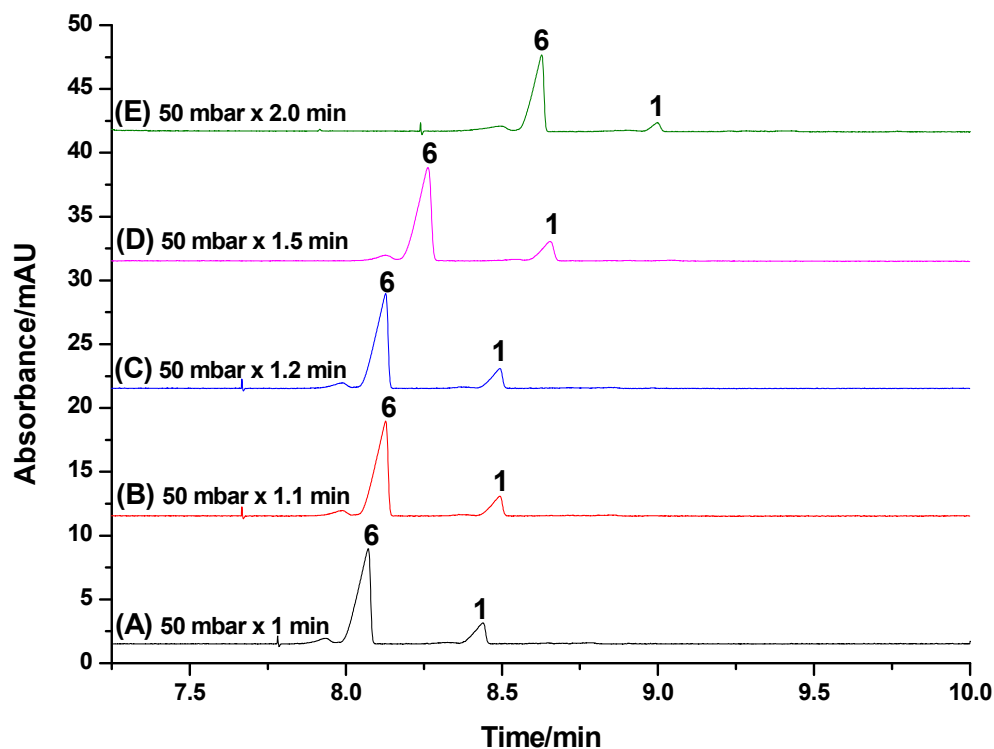


**Figure S4:** Electropherograms obtained using Method 2 at different injection volumes. CE conditions:  $100 \text{ mmol L}^{-1} \text{ SDS}$  in  $25 \text{ mmol L}^{-1}$  aspartic acid buffer, pH 3.22 as BGE, applied voltage  $-20 \text{ kV}$ , current  $-30 \text{ }\mu\text{A}$ , oven temperature  $25 \text{ }^\circ\text{C}$ . Peak designation: 1 = Cyd, 6 = Ado.



## **5.5. Publication V**

**Off-line and on-line enrichment of  $\alpha$ -aminocephalosporins for their analysis in surface water samples using CZE coupled to LIF**

**Azza H. Rageh, Karl-Friedrich Klein, Ute Pyell**

**Submitted to: Talanta**



### 5.5.1. Summary and discussion

In this publication, a highly sensitive method using capillary zone electrophoresis (CZE) coupled to laser induced fluorescence (LIF) detection is developed and validated for the analysis of  $\alpha$ -aminocephalosporins in surface water samples. The investigated analytes cefalexin (Cefx) and cefadroxil (Cefd) are non-fluorescent, but they are capable of forming a highly fluorescent derivative via the reaction of their  $\alpha$ -amino group with fluorescamine under alkaline pH conditions. The formed fluorescent derivative (Fig. 5) has a wavelength of maximum excitation ( $\lambda_{\text{exc}}$ ) of 372 and 370 nm for Cefx and Cefd, respectively which overlaps well with the output of a low-noise diode laser emitting at a wavelength of 375 nm ( $P_{\text{cw}} = 5.6$  mW). In order to connect the laser head to the capillary, we employ a fiber-optic coupled detection cell as an interface (Fig. 5).

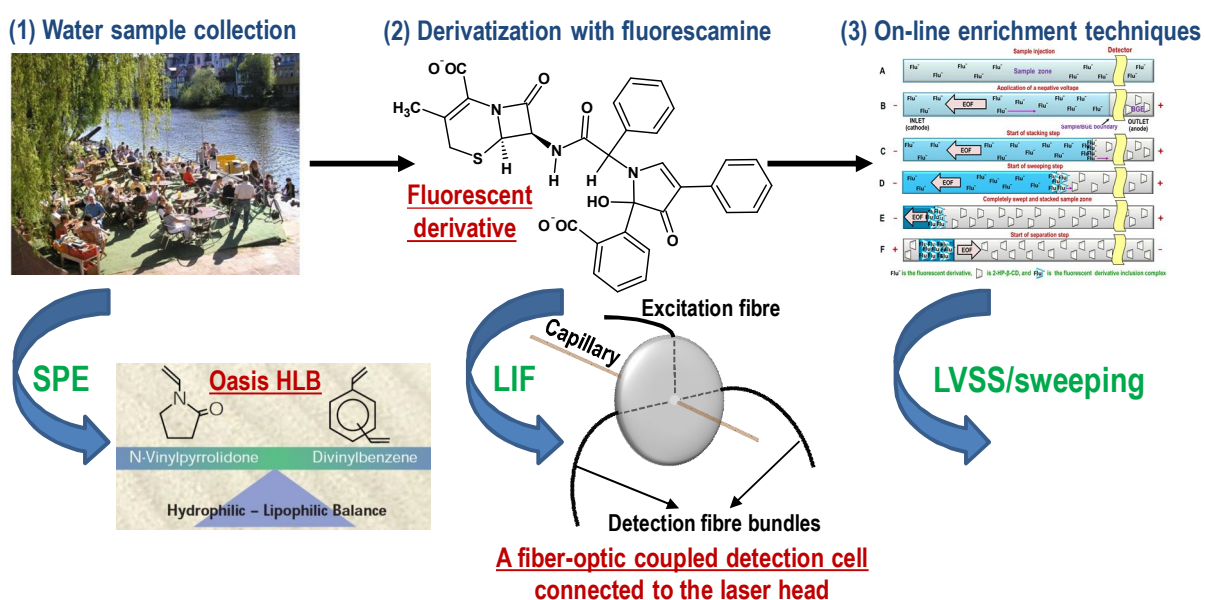


**Figure 5:** Schematic illustration showing the steps involved in the CZE/LIF analysis of  $\alpha$ -aminocephalosporins in surface water samples

We optimize the derivatization reaction for the two analytes investigated with regard to fluorescamine concentration, buffer pH, buffer concentration, concentration of organic solvent in the reaction mixture, reaction time, and stability of the formed derivative. Moreover, the separation of the two compounds after their derivatization is optimized by variation of the BGE pH, the BGE concentration, 2-HP- $\beta$ -CD concentration, the applied voltage, and the oven temperature. The optimum BGE is composed of 20 mg mL<sup>-1</sup> 2-HP- $\beta$ -CD in 30 mmol L<sup>-1</sup> sodium tetraborate, pH 9.25. It is shown also that the presence of 2-hydroxypropyl- $\beta$ -cyclodextrin (2-HP- $\beta$ -CD) in the BGE improves the fluorescence quantum yield.

The combination of on-line and off-line preconcentration techniques is studied for a further improvement of the Limits of detection (LODs). Different types of polymer-based SPE cartridges are studied and the extraction recovery of both antibiotics is maximized through the interplay of different factors like cartridge type, sample pH, sample volume, sample elution and washing steps in addition to the stability of the investigated analytes in the elution solvent. Highest recovery (Cefx:  $109.4 \pm 3.9\%$  and Cefd:  $92.6 \pm 4.0\%$ ) is reached with a polymer-based solid phase (Oasis HLB cartridge), with which we obtain a ten-fold off-line enrichment. Furthermore, the high complex formation constant between the formed derivative and 2-hydroxypropyl- $\beta$ -cyclodextrin (2-HP- $\beta$ -CD) and the low electric conductivity of the extract after the off-line enrichment constitute an ideal basis for additional analyte enrichment by sweeping and large volume sample stacking (LVSS), see Fig. 5. The on-line enrichment procedure provides a 25-fold improvement in the detection limits if compared to field amplified sample stacking (FASS). The validation criteria of the developed method are studied adopting ICH guidelines. With optimized derivatization, separation, detection, and extraction conditions, detection limits as low as 4.9 and 7.5 ng L<sup>-1</sup> are obtained for Cefx and Cefd, respectively, with a starting sample volume as low as 50 mL. The sensitivity of the proposed method is equivalent to other methods using more expensive equipment like HPLC-MS/MS. The applicability of the developed method to the analysis of the studied antibiotics is demonstrated with spiked Lahn river water samples. The very low LODs afforded by the proposed strategy provide a promising approach for the monitoring of these compounds in other types of water samples. Moreover, the application of this method can be extended to the analysis of other primary amino group-containing compounds in other types of environmental compartments.



### **5.5.2. Author contribution**

The majority of the experimental part of this study was carried out by me. Kathrin Geiger and Wolf Fronius assisted in water samples collection and data evaluation. The draft of the manuscript was written by me and corrected by Prof. Dr. Karl-Friedrich Klein and Prof. Dr. Ute Pyell. The final revision of the manuscript was conducted by me and Prof. Dr. Ute Pyell before submission to the journal. Prof. Dr. Ute Pyell was responsible for the supervision of this work.



**Off-line and on-line enrichment of  $\alpha$ -aminocephalosporins for their analysis in surface water samples using CZE coupled to LIF**

Azza H. Rageh<sup>a</sup>, Karl-Friedrich Klein<sup>b</sup>, Ute Pyell<sup>a\*</sup>

<sup>a</sup>University of Marburg, Department of Chemistry, Hans-Meerwein-Straße, D-35032 Marburg, Germany

<sup>b</sup>Technische Hochschule Mittelhessen, Wilhelm-Leuschner-Straße 13, D-61169 Friedberg, Germany

\* Corresponding author

**Fax: ++49 6421 2822124**

**e-mail: [pyellu@staff.uni-marburg.de](mailto:pyellu@staff.uni-marburg.de)**

**Keywords**

$\alpha$ -Aminocephalosporins, Capillary zone electrophoresis, Laser induced fluorescence detection, Surface water, Large volume sample stacking/sweeping, Solid phase extraction

## Abstract

This study examines the potential of application of capillary zone electrophoresis (CZE) coupled to laser induced fluorescence (LIF) detection involving derivatization with fluorescamine for the separation and determination of  $\alpha$ -aminocephalosporins in surface water samples. Via their  $\alpha$ -amino group, the non-fluorescent cefadroxil and cefalexin are capable of forming a highly fluorescent derivative via their reaction with fluorescamine. This reaction permits the selective and sensitive detection of aliphatic primary amines when combined with CE/LIF, which we realized with a low-noise diode laser emitting at a wavelength of 375 nm ( $P_{\text{cw}} = 5.6$  mW) in combination with a fiber-optic coupled detection cell. Different types of SPE cartridges were investigated to select the optimum solid phase providing maximum recovery for the studied antibiotics, which were extracted from spiked Lahn river water samples. Highest recovery (cefalexin:  $109.4 \pm 3.9\%$  and cefadroxil:  $92.6 \pm 4.0\%$ ) was reached with a polymer-based solid phase (Oasis HLB cartridge), with which we obtained a ten-fold off-line enrichment. On-line enrichment was achieved by sweeping and large volume sample stacking (LVSS). The high complex formation constant between the formed derivative and 2-hydroxypropyl- $\beta$ -cyclodextrin (2-HP- $\beta$ -CD) and the low electric conductivity of the extract after the off-line enrichment constitute an ideal basis for additional analyte enrichment by sweeping and LVSS. The enrichment efficiency obtainable with this on-line enrichment step (after having filled the complete capillary with the sample solution) in comparison to field amplified sample stacking (FASS) reaches approximately an additional 25-fold improvement. With the developed method, combining off-line and on-line enrichment with optimized fluorescence detection, detection limits as low as 4.9 and 7.5 ng L<sup>-1</sup> are obtained for cefalexin and cefadroxil, respectively, with a starting sample volume as low as 50 mL. The high repeatability and accuracy of the proposed strategy permits its application to the analysis of  $\alpha$ -aminocephalosporins in surface water samples. Its applicability can be extended to other environmental compartments and other types of primary amino group containing compounds. In addition, it provides equivalent sensitivity to other methods using more expensive equipment like HPLC-MS/MS.

## 1. Introduction

Antibiotic contamination has become an issue of a global environmental concern. Antibiotics have been classified as emerging pseudo-persistent organic pollutants due to their continual environmental input and permanent presence [1,2]. They have been detected in various compartments of the aquatic environment such as waste, surface, ground and drinking waters [3]. Antibiotics and/or their metabolites can be released from different pathways in the aquatic environment including hospital wastewater, municipal sewage, extensive use in farming and aquaculture, partial removal in waste water treatment plants (WWTPs), and sewage treatment plants (STPs) [4,5]. The increasing interest about the occurrence, the fate, and the persistence of the antibiotics in the environment stems from the fact that low levels of antibiotics can induce adverse effect in terrestrial or aquatic organisms and can favour the appearance of bacterial strains that are resistant to important classes of antibiotics, which can negatively affect the human health [4,6]. There are still knowledge gaps existing in assessing the risks associated with the long-term exposure to low concentrations of pharmaceuticals. Furthermore, the continual environmental input of the antibiotics and their metabolites can lead to high long-term concentrations, thus increasing the possibility for unobserved adverse effects that remain undetected until the effects become irreversible [7].

Cephalosporins are a class of  $\beta$ -lactam antibiotics, which belong to the most popular, the most widely prescribed and well recognized groups of antibiotics that are in use today. The consumption of  $\beta$ -lactam antibiotics accounts for 50-70% of the total amount of antibiotics applied in human medicine in most countries [6]. This can be ascribed to their high therapeutic index, their favourable safety profile, and the wide spectrum of activity against different types of bacterial infections. Although this group of compounds can be considered as one of the most important and most frequently used group of antibiotics, the literature available for the determination of cephalosporins (in contrast to other types of antibiotics) in environmental water samples is limited. Only some research papers described the detection of these antibiotics in different kinds of environmental waters [8,9]. E.g. the detection frequency of cefalexin in hospital discharge, WWTP influents, WWTP effluents and in surface waters is 100%, 100%, 30%, 22% respectively [9]. It was reported that cefalexin was detected at  $\text{ng L}^{-1}$  level ( $182 \text{ ng L}^{-1}$ ) in surface waters collected from Victoria Harbor, Hong Kong [10] and up to  $31433 \text{ ng L}^{-1}$  in the water samples investigated in [8]. Besides, cefalexin was detected at a concentration of  $64000 \text{ ng L}^{-1}$  in the influent and  $5070 \text{ ng L}^{-1}$  in the effluent of WWTPs [2]. According to what was stated in [2], the value of  $64000 \text{ ng L}^{-1}$  is the highest among the concentrations of any antibiotic detected in WWTPs.

It is noteworthy to mention that according to a very recent report, photodegradation may be the most important elimination process for cephalosporin antibiotics in surface water [11]. The by-products were

found to be even less photolabile and more toxic than the parent compounds. In surface waters,  $\beta$ -lactam antibiotics are not frequently detected [12], most likely due to their high removal efficiency during waste water treatment and relatively high method reporting limits [13]. In addition, intact  $\beta$ -lactams are not present frequently in the environment [14,15] due to the instability of the  $\beta$ -lactam ring [16], which is highly sensitive to pH, heat, and  $\beta$ -lactamase enzymes. However, it is not possible to exclude the presence of these compounds in the environment due to the large amount of daily consumption [17]. The previously mentioned difficulties in the analysis of this important class of antibiotics necessitates the setup of fast, sensitive and reliable analytical techniques that are capable of detecting these antibiotics at environmentally relevant concentrations (low ng L<sup>-1</sup> range) in different kinds of water samples.

As stated clearly in many reviews, HPLC or UHPLC, mainly in combination with MS, are widely used for the analysis of antibiotics and/or pharmaceuticals in water samples [3,7,18-22], however the involvement of capillary electrophoresis is increasing considerably [23]. In a similar way to HPLC, CE can be combined with several detection modes, suitable for automation with a high sample throughput, in addition to its high efficiency, flexibility, low consumption of samples and reagents [23]. Despite of its major drawback of suffering from low concentration sensitivity using UV detection due to the small loaded sample volume (nL) and the narrow optical path length (as defined by the diameter of the capillary), different strategies and approaches were reported to overcome this drawback. These approaches are mainly based on using: (i) physical methods such as the use of a bubble cell, (ii) on-line enrichment techniques via conversion of a long injected analyte zone into a narrow band inside the capillary utilizing either electrophoretic phenomena and/or chromatographic effects [24]. Techniques that can achieve this include different modes of on-line enrichment procedures such as field-amplified sample stacking (FASS) [25], large volume sample stacking (LVSS) [26] and sweeping [27]. Other approaches to decrease the detection limits in CE are to combine its use with (iii) off-line enrichment techniques such as solid phase extraction (SPE), and/or (iv) highly sensitive detection techniques such as LIF or MS.

One of the aforementioned approaches or a combination of these approaches has been utilized for the analysis of cephalosporin antibiotics in different kinds of water samples. A CZE/UV method was developed and applied for the analysis of four cephalosporin antibiotics (cefoperazone, ceftiofur, cefazolin and cefacetrile) in environmental waters preceded by off-line enrichment step using SPE. The reported limits of detection (LODs) were in the range of 3000-5000 ng L<sup>-1</sup> [28], which are far away from the demand of analysis of pharmaceuticals in environmental waters. Off-line SPE followed by either (i) LVSS or (ii) in-line SPE for the analysis of ceftiofur in environmental water samples using UV detection has resulted in LODs of 100 and 10 ng L<sup>-1</sup>, respectively [29]. As stated by the authors in [29]:

to reach such low values of the LODs, more time is needed to load a large sample volume (500 mL) during the off-line SPE step and more time is needed to load the sample in the SPE microcartridge that results ultimately in a long analysis time. Recently, [30] a CZE/DAD method was proposed for the simultaneous determination of five cephalosporins in environmental waters using both off-line and on-line concentration strategies in addition to a bubble cell capillary with an optical path length of 200  $\mu\text{m}$  [30]. Although three of the previously discussed approaches for a further gain in sensitivity were utilized within that study [30], the LODs achieved were in the range of 100-300  $\text{ng L}^{-1}$ . A highly sensitive MEKC/LIF [31] method was reported for the analysis of four  $\beta$ -lactam antibiotics in environmental water samples including both a derivatization step with sulfoindocyanine succinimidyl ester (Cy5) and an off-line SPE step for improvement of the detection limits. LODs from 30-45  $\text{ng L}^{-1}$  were obtained [31].

The aim of the presented study is to develop a fast, reproducible, and highly sensitive method for the analysis of cephalosporin antibiotics in surface water samples. According to the best of our knowledge and with the exception of the MEKC/LIF method reported previously for the analysis of  $\beta$ -lactam antibiotics [31], the combination of on-line and off-line preconcentration techniques besides the use of LIF detection has not been reported so far for the analysis of this class of compounds. For an additional lowering of the method detection limits (compared to those previously reported), we propose CZE/LIF for the analysis of two  $\alpha$ -aminocephalosporin antibiotics (cefalexin and cefadroxil) in surface water samples after their reaction with fluorescamine. The derivatization reaction with the two analytes investigated is optimized with regard to fluorescamine concentration, buffer pH, buffer concentration, concentration of organic solvent in the reaction mixture, reaction time, and the stability of the formed derivative. Moreover, the separation of the two compounds after their derivatization is investigated by variation of the BGE pH, the BGE concentration, 2-HP- $\beta$ -CD concentration, the applied voltage, and the oven temperature. Parameters affecting the detection sensitivity such as fluorescence enhancing agents, laser output power and injection volume are studied. The on-line enrichment methodology is accomplished using both LVSS and sweeping, which is optimized and combined with SPE for preconcentration of the analytes and sample cleanup. Furthermore, different types of polymer-based SPE cartridges were studied and the extraction recovery of both antibiotics were maximized through the interplay of different factors like cartridge type, sample pH, sample volume, sample elution and washing steps in addition to the stability of the investigated analytes in the elution solvent. The applicability of the proposed approach to the analysis of the studied antibiotics is demonstrated in spiked Lahn river water samples.

## 2. Experimental

### 2.1. Chemicals and background electrolytes

Cefalexin (Cefx) was generously provided by Prof. Fathala Belal, Faculty of Pharmacy, Mansoura University, Egypt. Cefadroxil (Cefd) was purchased from Sigma-Aldrich, Steinheim, Germany; their chemical structures are presented in Fig. S1 (supplementary data). Fluorescamine (99%) was from Applichem, Darmstadt, Germany. Disodium tetraborate decahydrate (borax), orthophosphoric acid, and  $\alpha$ -cyclodextrin ( $\alpha$ -CD) were from Merck, Darmstadt, Germany. Methanol and acetonitrile HPLC grade were from VWR-BDH-Prolabo, Leuven, Belgium. Sodium hydroxide and boric acid were from Fluka, Buchs, Switzerland. 2-Hydroxypropyl- $\beta$ -cyclodextrin, 2-HP- $\beta$ -CD (97%) was from Acros Organics, Geel, Belgium.  $\beta$ -Cyclodextrin hydrate,  $\beta$ -CD (99%), methyl- $\beta$ -cyclodextrin (Me- $\beta$ -CD), sulphated- $\beta$ -cyclodextrin, sodium salt, 2-hydroxypropyl- $\gamma$ -cyclodextrin (2-HP- $\gamma$ -CD), and Na<sub>2</sub>EDTA.2H<sub>2</sub>O (99%) were from Sigma-Aldrich. Molecular sieve 3Å was from Carl Roth, Karlsruhe, Germany. HPLC-grade water was obtained using a Milli-Q ultrapure water purification system (Millipore, USA). Fluorescamine stock solution (0.02% w/v) was prepared in dried acetonitrile (dried over molecular sieve 3Å). All buffer solutions were prepared in Milli-Q water. In addition, all buffer solutions were filtered prior to use through a 0.45  $\mu$ m nylon membrane filter (WICOM, Heppenheim, Germany). To avoid buffer depletion, the BGEs in the inlet and the outlet vials were replaced after every four runs [32]. For the preparation of buffer solutions, refer to the supplementary data.

### 2.2. Instrumentation

All measurements were done using the ATI Unicam System, Crystal 300 Series, Model 310 (Cambridge, UK). Oven temperature was kept at 25 °C, unless otherwise specified. Data analysis was performed with Origin 8.5 software (OriginLab Corporation, Northhampton, USA).

LIF detection was carried out employing a fiber-optic coupled detection cell/capillary holder (see drawing, Fig. 1) from J&M Analytik, Essingen, Germany. The detection cell is described in detail in [33]. The low noise diode laser head ( $375\pm 5$  nm,  $P_{cw} = 5.6$  mW, beam power stability/h < 0.4%) and the laser controller were from Omicron, Rodgau-Dudenhofen, Germany (Fig. 2A). The excitation fibre is a mono fibre of 200  $\mu$ m core diameter without cladding (Fig. 2B). The excitation fibre connects the excitation source and the detection cell (Fig. 2A). There are two detection fibre bundles at right angle position to the excitation fibre (Fig. 2B). The detection fibre bundles are composed of six fibres, each of 200  $\mu$ m core diameter. The two detection fibre bundles collect the fluorescence/the emitted radiations and are combined and directed to the optical filter (Fig. 2A) and the photomultiplier tube (PMT) (Fig. 2C). The optical filter is a 450 nm high performance long pass filter (diameter 12.5 mm, average transmission  $\geq$



91%, and optical density  $\geq 4.0$ ) and was purchased from Edmund Optics, Karlsruhe, Germany (Fig. 2A). The long pass filter was placed between the detection cell and the photomultiplier tube to: (i) absorb/reflect scattered excitation radiation and (ii) absorb radiation due to the Raman scattering of water. A photomultiplier detector (J&M Analytik) was used for measuring the fluorescence intensity (Fig. 2C). Data for LIF detection was recorded employing a software developed by J&M Analytik using a data sampling rate of 5 Hz.

As shown in Fig. 2A, this instrumental arrangement allows both LIF and UV detection to be carried out simultaneously within the same separation capillary. UV detection was accomplished with a Spectra 100 (with deuterium lamp) from Thermo Separation Products, San Jose, USA using a wavelength of 254 nm and a data sampling rate of 10 Hz. Data for UV detection were recorded using CE-Kapillarelektrophorese software (development of the electronic workshop of the Department of Chemistry, University of Marburg based on Delphi).

Fused-silica capillaries (50.2  $\mu\text{m}$  I.D., 362  $\mu\text{m}$  O.D.) were obtained from Polymicro Technologies LLC (Phoenix, AZ, USA). The length was set to 350/500/654 mm (effective length for LIF, UV detection, and total length, respectively). Data acquisition was done using an AD-converter (USB-1280FS, Measurement Computing, Middleborough, USA). Blue Ribbon 589/3 ashless quantitative filter paper (Schleicher & Schuell, Dassel, Germany) with a diameter of 125 mm and 2  $\mu\text{m}$  retention was used for the filtration of the Lahn river water samples. InoLab pH720 (WTW, Weilheim, Germany) was used for pH measurements. Solid phase extractions were performed on a vacuum manifold column processor (J.T. Baker, Griesheim, Germany).

New capillaries were conditioned by flushing them first with NaOH solution (1 mol L<sup>-1</sup>) for 60 min, water for 30 min, and BGE for 5 min using an applied pressure of 800 mbar. Between runs, the capillaries were rinsed with BGE for 2 min. After having filled the capillary with the BGE by application of pressure (800 mbar) and before sample injection, the capillary is dipped into a vial containing water (10 mbar for 0.05 min). This procedure ensures the reproducibility of the migration times and maintains the stacking efficiency as it reduces the contamination of the sample solution during the injection step by the buffer adhering to the outer wall of the capillary. The samples were pressure-injected at 30 mbar for 12 s, unless otherwise specified. After sample introduction, the capillary is dipped into the BGE vial (10 mbar for 0.1 min).

The electroosmotic hold-up time  $t_0$  [34] was determined using acetonitrile as neutral marker. Electrophoretic mobilities were determined from electropherograms containing a peak of the hold-up time marker. Peak identities were confirmed by spiking.

### 2.3. Water samples collection and sample pre-treatment prior to analysis

Surface water samples were gathered from the river Lahn in the region of Marburg/Germany over a period of three months (with average pH:  $7.8 \pm 0.2$ , and average conductivity:  $275 \pm 50 \mu\text{S cm}^{-1}$ ) and were collected in plastic bottles pre-rinsed with Milli-Q water and with the water sample before collection. Water samples were filtered using a quantitative filter paper and then through a  $0.45 \mu\text{m}$  nylon membrane filter to remove any particulate or suspended matter prior to the extraction. All of the glassware used was washed under ultrasonication. Then, it was rinsed with distilled water, Milli-Q water, 5% w/v  $\text{Na}_2\text{EDTA} \cdot 2\text{H}_2\text{O}$  solution and then Milli-Q water three times, respectively for each rinsing step.  $\text{Na}_2\text{EDTA} \cdot 2\text{H}_2\text{O}$  was employed for cleaning of the glassware and was added to all the water samples. This is the recommended protocol in the analysis of antibiotics residues in environmental samples [3,7] to chelate metal cations or other multivalent cations that are soluble in water or adsorbed on the surface of the sorbent and glassware [35]. It was also reported [36] that metal cations influence the rate of inactivation or can catalyse the hydrolytic opening of cephalosporin antibiotics. Therefore, the addition of  $\text{Na}_2\text{EDTA} \cdot 2\text{H}_2\text{O}$  to the sample is mandatory. All samples were stored at  $4^\circ\text{C}$  prior to SPE and used within 48 h after collection [17].

### 2.4. Solid phase extraction (SPE)

Different types of polymer-based SPE cartridges were investigated for maximizing the extraction recovery of the investigated antibiotics from spiked river water samples. Oasis HLB cartridge (60 mg/3 mL), which is a copolymer made from a balanced ratio of hydrophilic (*N*-vinylpyrrolidone) and lipophilic (divinylbenzene) monomers and Oasis MCX cartridge (60 mg/3 mL), which is a mixed-mode reversed phase/cation exchange sorbent containing a strong cation exchanger (sulphonic acid) were from Waters, Eschborn, Germany. Supelco Supel-Select HLB cartridge (60 mg/3 mL), which is a hydrophilic modified styrene-based polymer, was from Sigma-Aldrich.

Under optimized conditions, 50 mL of the filtered blank or spiked water sample was treated with 5%  $\text{Na}_2\text{EDTA} \cdot 2\text{H}_2\text{O}$  solution to achieve a final concentration of 0.1% (pH after EDTA treatment is  $4.80 \pm 0.2$ ). The sample was then acidified to  $\text{pH } 2.9 \pm 0.1$  by using  $1 \text{ mmol L}^{-1}$  phosphoric acid. It should be emphasized that working under highly acidic conditions results in degradation of  $\beta$ -lactam antibiotics [7,36]; therefore the extraction was carried out within 1 min after spiking the acidified water samples (pH 2.9) with the standards [35] to avoid any degradation. The acidified sample was loaded (at a flow rate of 1 to  $2 \text{ mL min}^{-1}$ ) on an Oasis HLB cartridge that was previously conditioned with 5 mL methanol and 5 mL Milli-Q water (acidified to pH 2.9 with  $1 \text{ mmol L}^{-1}$  phosphoric acid). Without carrying out any washing steps, the analytes were eluted with 3 mL methanol at a flow rate of  $0.5 \text{ mL min}^{-1}$ . The eluate was

evaporated to dryness under vacuum. Then the derivatization procedure described under Section 2.5 was conducted.

#### 2.5. Derivatization procedure

For method optimization (without carrying out SPE) the derivatization reaction was carried out as follows: in the dark, 50  $\mu\text{L}$  of a solution containing  $\alpha$ -aminocephalosporin were mixed with 500  $\mu\text{L}$  of 20  $\text{mmol L}^{-1}$  borate buffer pH 8.2 for 30 sec in a 10 mL volumetric flask. 500  $\mu\text{L}$  of fluorescamine (0.02% w/v in acetonitrile) were added gradually while mixing by shaking for 1 min. The reaction solution was then diluted to 10 mL with Milli-Q water and kept in the dark prior to the analysis. The analyte concentration in the final solution is 0.36  $\text{mg L}^{-1}$ , unless otherwise specified.

After carrying out SPE, the optimized derivatization procedure was performed as follows: after drying the eluate under vacuum, 2 mL of 20  $\text{mmol L}^{-1}$  borate buffer pH 8.2 were added under mixing for 30 sec. 500  $\mu\text{L}$  of fluorescamine (0.02% w/v in acetonitrile) were added gradually while mixing the solution thoroughly for 1 min. Subsequently, the solution was diluted to 5 mL with Milli-Q water and kept in the dark prior to the analysis.

#### 2.6. Preparation of standard solutions and calibration curves

Stock solutions containing 60  $\text{mg L}^{-1}$  of each antibiotic were prepared by dissolving the required amount in Milli-Q water and were stored in a refrigerator at 4  $^{\circ}\text{C}$  [17,37] for one week protected from light (covered by alumina foil) to prevent photodegradation [10]. Lahn river water samples were employed as sample matrix for the preparation of the standard solutions. The concentration range for the investigated analytes that were spiked into the water samples is between 15 and 720  $\text{ng L}^{-1}$ . Following optimized method procedures were employed: (1) derivatization reaction was performed as described under Section 2.5, (2) SPE cartridges were conditioned as described under Section 2.4, and (3) CE conditions: BGE 20.0  $\text{mg L}^{-1}$  2-HP- $\beta$ -CD in 30  $\text{mmol L}^{-1}$  borax buffer, pH 9.25, capillary 654(350)mm x 50.2  $\mu\text{m}$  I.D., applied voltage during LVSS/sweeping/matrix removal  $-20$  kV, separation voltage  $+20$  kV, capillary temperature 25  $^{\circ}\text{C}$ , pressure injection 1 bar for 1 min, laser  $P_{\text{cw}} = 5.6$  mW, PMT voltage = 600 V. Calibration curves were constructed by plotting either the peak height or the corrected peak area against the analyte concentration in ng per L.

### 3. Results and discussion

#### 3.1. Optimization of the derivatization reaction

The investigated  $\alpha$ -aminocephalosporin antibiotics cefalexin and cefadroxil are non-fluorescent but they contain a primary aliphatic amino group that makes them ideal candidates for the reaction with the fluorescence-derivatizing reagent fluorescamine [38]. This reagent is selective for compounds containing a primary amino group [39]. Fluorescamine itself is a non-fluorescent heterocyclic spiro compound. It reacts selectively with compounds containing primary amino groups in fractions of seconds under alkaline pH conditions at room temperature to form a blue-green highly fluorescent pyrrolinone derivative, while the remaining reagent hydrolyzes in water ( $t_{1/2} = 5-10$  s) to give non-fluorescent products (Fig. S1, supplementary data) [39]. We have to emphasize that based on previous reports [39-42] the fluorescence reaction does not go to completion due to the side reaction of fluorescamine with water, i.e. the reaction yield cannot reach 100%. Fluorescamine was utilized previously for the spectrofluorimetric determination of  $\alpha$ -aminocephalosporin antibiotics in pharmaceutical formulations and biological fluids [38].

In general, a precondition for the derivatization reaction is the presence of the amino group in its deprotonated form to allow its nucleophilic addition to the double bond of the reagent. Therefore, the reaction must be performed under alkaline conditions. However, if the pH is too high, hydrolysis of the reagent predominates [40]. The fluorescent derivative has a wavelength of maximum excitation ( $\lambda_{exc}$ ) of 372 and 370 nm for cefalexin and cefadroxil, respectively [38], which overlaps well with the output of the diode laser emitting at a wavelength of 375 nm. The wavelength of maximum emission ( $\lambda_{em}$ ) is 478 and 472 nm for cefalexin and cefadroxil, respectively [38].

Different parameters were investigated to maximize the derivatization reaction yield, which was evaluated by employing CE experiments. In these experiments the peak height of the formed derivative was used as response factor (optimization criterion). The studied parameters are (i) the concentration of fluorescamine, (ii) the pH (adjusted via borate buffer), (iii) the concentration of borate buffer, and (iv) the concentration of acetonitrile (each in the reaction mixture) in addition to (v) reaction time and (vi) stability of the formed derivative. Table 1 provides an overview about the optimization of these parameters. Each parameter was varied while keeping the other parameters at fixed values.

The influence of the concentration of fluorescamine in the reaction mixture on the peak height (using cefadroxil as a representative example) was studied with the procedure described in Section 2.5 using different volumes of 0.02% w/v fluorescamine in acetonitrile at pH 8.2 (Fig. S2, supplementary data). Increasing the concentration of the reagent causes a directly proportional increase of the peak height up

to an added volume of 400  $\mu\text{L}$ . A further increase in the added volume (up to 1000  $\mu\text{L}$ ) has no positive impact on the resulting peak height. 500  $\mu\text{L}$  of 0.02% w/v fluorescamine was chosen as the optimum concentration of the reagent. The buffer pH was varied from pH 8.0 up to pH 9.25. The highest peak height was obtained at pH 8.2 (Fig. S3, supplementary data). Under the optimum fluorescamine concentration and borate buffer pH, it was found that adding either 500  $\mu\text{L}$  or 1000  $\mu\text{L}$  of 20  $\text{mmol L}^{-1}$  borate buffer pH 8.2 results in the optimum peak height. A higher concentration of borate buffer (adding > 1000  $\mu\text{L}$  of 20  $\text{mmol L}^{-1}$  borate buffer pH 8.2) resulted in a lowering of the peak height due to the impairment of the stacking efficiency. Moreover, it was found that using either 5 or 10% (v/v) acetonitrile in the final derivatization reaction mixture has no impact on the peak height. Different time intervals were selected to define the time after which the solution attains maximum reaction yield. However, it was found that the reaction takes place quasi-instantaneously after mixing the solutions containing analyte or reagent, respectively. The determined peak height due the formed derivative reaches its maximum immediately after mixing and remains constant for one day as long as the solution is kept in the dark.

### 3.2. Optimization of separation

To optimize the separation of the two compounds investigated, following parameters were investigated (Table 1): (i) BGE ionic strength, (ii) BGE pH, (iii) c(2-HP- $\beta$ -CD) in the BGE, (iv) applied voltage and (v) oven temperature. The pH of the BGE is one of the critical factors in the resolution as the separation is based on the difference in the effective charge number of the two analytes, i.e. differences in their charge to size ratios. At lower pH the formed derivatives of both analytes have an effective charge number of -2 due to the dissociation of the two carboxylic acid moieties (see Fig. S1, supplementary data). At a pH higher than 9.2, the dissociation of the phenolic -OH group of cefadroxil contributes to an effective charge number > -2. Therefore, a pH lower than 9 results in a comigration of these compounds as the phenolic-OH group of cefadroxil is protonated under these conditions (Fig. S4, supplementary data), while a pH higher than 9.25 results in very long migration times (in addition to higher electric current strength, results not shown). Therefore, a buffer pH of 9.25 was selected as optimum. The tetraborate concentration was set to 30  $\text{mmol L}^{-1}$  producing an adequate electric current strength (Fig. S5, supplementary data). The concentration of 2-HP- $\beta$ -CD in the BGE was fixed to 20  $\text{mg mL}^{-1}$ , which will be discussed later (Fig. S6, supplementary data). A voltage of 20 kV was applied as optimum separation voltage providing an acceptable running time, sufficient resolution and adequate electric current strength. The effect of the oven temperature on the separation was investigated in the range of 15–35°C. Within this range the temperature of 25°C was selected as optimum.

In summary, following parameters were selected as optimum with regard to the separation of the two analytes investigated: BGE 20 mg mL<sup>-1</sup> 2-HP- $\beta$ -CD in 30 mmol L<sup>-1</sup> sodium tetraborate, pH 9.25, separation voltage +20 kV, and oven temperature 25 °C.

### 3.3. Optimization of detection sensitivity

#### 3.3.1. Fluorescence-enhancing agents

In an attempt to enhance the emission signal, we investigated the effect of different types of surfactants and cyclodextrins on the fluorescence quantum yield of the formed derivatives. Different surfactant solutions (20 mmol L<sup>-1</sup>) including anionic, cationic and non-ionic surfactants such as sodium dodecyl sulphate (SDS), 1-tetradecyl-3-methylimidazolium bromide (C<sub>14</sub>MImBr) and polyoxyethylene sorbitan monolaurate (Tween 20) were added to a BGE composed of 40 mmol L<sup>-1</sup> borax. These micellar BGEs investigated have resulted invariably in a reduction of the peak height. In addition, the surfactant solutions themselves are fluorescent which results in an unfavourably high background signal.

As a second step, we have investigated the effect of different types of cyclodextrins:  $\alpha$ -CD, 2-HP- $\gamma$ -CD, sulphated- $\beta$ -CD, Me- $\beta$ -CD, hydrated- $\beta$ -CD and 2-HP- $\beta$ -CD (abbreviations see Section 2.1). These investigations were performed with the objective of selecting the additive that provides the highest complex formation constant with the formed fluorescent derivative. This in turn can have a positive impact on the obtained LODs either via (i) an improved on-line enrichment of the investigated analytes by sweeping via complexation [24,43,44] and/or (ii) an increase in the fluorescence quantum yield via inhibition of the non-radiative deactivation of the excited state which is associated to restriction of molecular rotation in the rigid environment of the cavity [45].

In order to identify the additive that provides the highest complex formation constant, the effective electrophoretic mobility  $\mu_{\text{eff}}$  of the formed derivative was calculated using a BGE containing no cyclodextrin (40 mmol L<sup>-1</sup> borax) and a BGE containing 40 mmol L<sup>-1</sup> borax and 10 mg mL<sup>-1</sup> cyclodextrin. Then, the shift in the effective electrophoretic mobility  $\Delta\mu_{\text{eff}}$  ( $\mu_{\text{eff(without CD)}} - \mu_{\text{eff(with CD)}}$ ) was employed to quantify the CD-analyte-interaction. Indirectly,  $\Delta\mu_{\text{eff}}$  quantifies the CD-analyte complex formation constant, i.e. the larger is the shift, the higher is the complex formation constant.

As shown in Fig. 3, with the exception of sulphated- $\beta$ -CD, a shift of  $\mu_{\text{eff}}$  to more positive values compared to the values calculated in a BGE free from cyclodextrin was obtained. A shift of  $\mu_{\text{eff}}$  to a more negative value using sulphated- $\beta$ -CD is attributed to the negative charge of this additive.  $\Delta\mu_{\text{eff}}$  was small in the case of using sulphated- $\beta$ -CD due to the electrostatic repulsion between the negatively-charged additive and the negatively-charged derivative. Moreover,  $\Delta\mu_{\text{eff}}$  was small in the case of  $\alpha$ -CD and 2-HP- $\gamma$ -CD, which implies that the cavity size of either  $\alpha$ -CD or 2-HP- $\gamma$ -CD do not match well with the size

of the derivative. Concerning the neutral  $\beta$ -CDs (native  $\beta$ -CD or one of its derivatives), it is obvious that in this case  $\Delta\mu_{\text{eff}}$  is higher than those of the other types of CD investigated. Within the class of  $\beta$ -CDs, Me- $\beta$ -CD shows the largest  $\Delta\mu_{\text{eff}}$  and accordingly it is the additive that provides the highest complex formation constant. In addition, it was reported that Me- $\beta$ -CD gives the largest enhancement of the fluorescence of pencillamine-fluorescamine among the other  $\beta$ -CDs investigated [46]. However, as the aqueous solubility of 2-HP- $\beta$ -CD is 10 times higher than that of Me- $\beta$ -CD, the former was selected for subsequent investigations. By increasing two-fold the concentration of 2-HP- $\beta$ -CD in the BGE,  $\Delta\mu_{\text{eff}}$  is further increased to be even higher than that obtained by using Me- $\beta$ -CD, which indicates a high complex formation constant between 2-HP- $\beta$ -CD and the fluorescent derivative, a property that is important for analyte enrichment by sweeping as will be discussed later.

In order to define, which moiety of the derivative (the pyrrolinone and/or the phenyl moiety due to the derivative or another moiety due to the parent antibiotic) is involved in the formation of the inclusion complex with 2-HP- $\beta$ -CD,  $\mu_{\text{eff}}$  was calculated for the derivatized and for the non-derivatized antibiotic at different 2-HP- $\beta$ -CD concentrations. The viscosity change of the BGEs induced by adding 2-HP- $\beta$ -CD to the BGE was taken into account by multiplying each data point by what is called the viscosity correction factor (for more details regarding the calculation of the viscosity correction factor, *cf.* [47]). It was found that there is a negligible change in  $\mu_{\text{eff}}$  of the studied un-derivatized cephalosporins by varying the concentration of 2-HP- $\beta$ -CD (Fig. 4A), which indicates negligible interaction with this additive. This result is in agreement with a previous report [48]. On the other hand,  $\mu_{\text{eff}}$  changes significantly to more positive values by plotting the corrected effective electrophoretic mobility of the derivatized antibiotic against the increasing concentration of 2-HP- $\beta$ -CD (Fig. 4B). This increase must be attributed to the inclusion of either the pyrrolinone or the phenyl moiety of the derivative inside the CD cavity. Complexation of the antibiotics with 2-HP- $\beta$ -CD permits an approximately two-fold enhancement of the fluorescence intensity (via increase in the fluorescence quantum yield) compared to that obtained with a BGE containing no-CD (Fig. S6, supplementary data). The improvement in the fluorescence quantum yield was confirmed by calculating the corrected peak area in a BGE containing no 2-HP- $\beta$ -CD (30 mmol L<sup>-1</sup> borax, pH 9.25) and the same BGE containing different concentrations of 2-HP- $\beta$ -CD (Fig. S6, supplementary data). At all investigated 2-HP- $\beta$ -CD concentrations, the calculated corrected peak areas (for both analytes) are two-fold higher than those obtained with a BGE containing no 2-HP- $\beta$ -CD, which implies the significant role of this additive in optimizing the fluorescence quantum yield (beside its influence of the sweeping efficiency as will be discussed later). Based on these results, a BGE with 20 mg mL<sup>-1</sup> of 2-HP- $\beta$ -CD was employed in all subsequent investigations.

### 3.3.2. On-Line enrichment techniques

#### 3.3.2.1. Field amplified sample stacking (FASS)

The sample solution after derivatization with fluorescamine is of low conductivity, which enables on-line enrichment by field-amplified sample stacking (FASS) [25]. FASS is based on the difference in the electric conductivity between the sample solution and the BGE. This difference induces a change in the electric field strength and hence the analyte electrophoretic mobility between the sample and the BGE compartment that results in focusing of the analyte in a sharp zone at the sample/BGE boundary. Focusing by FASS permits higher sample volumes (before the volume overload region is reached) than those accessible with optimized injection parameters under non-focusing conditions, e.g. with a sample dissolved in BGE.

Under the conditions of FASS, the sample injection volume and the laser output power were optimized. The optimum injection parameters corresponding to the highest peak height were achieved using hydrodynamic injection with 30 mbar for 0.6 min (Fig. S7A, supplementary data).

The wavelength of the laser line is very close to the excitation maximum of the fluorescent derivative. Specific attention has to be paid to the optimization of the incident laser power. The optimum laser output power will depend (i) on the photodegradation rate of the compound, (ii) on the capillary diameter (which determines the flux of photons), (iii) on the velocity of the analyte in the capillary (influencing the transit time of the analyte molecules in the laser beam) [49], (iv) on spectroscopic rate constants which determine whether ground state depletion will be reached. Photodegradation/photodestruction means photoinduced reaction of the fluorescent molecule in the incident laser beam and its conversion into a non-fluorescent molecule [49]. Ground-state depletion (= photobleaching) means that at high laser intensities, a significant fraction of the molecules will be pumped into the excited state (or a metastable excited state via intersystem crossing) causing concomitantly a depletion (= significant reduction of the population) of the ground state [50]. While photodegradation and photobleaching cause a "saturation" of the fluorescence intensity, the fluorescence background and scattering processes are not influenced by these effects and increase proportionally with increasing laser output power, which implies that at high laser beam intensity a decrease in the S/N ratio can be obtained.

In the presented study the laser output power was varied from 1 mW to 5.6 mW. As given in Fig. S7B (supplementary data) the peak height increases continuously with increasing laser output power. There is also an increase in the base line noise (noise is defined as one-half the average value of the distance between a maximum peak and a minimum peak taken for a period of 1 min). However, the signal to noise ratio is also increasing continuously with increasing laser output power up to the maximum



possible laser output power. Therefore, when using the maximum laser output power, we can consider photodegradation and ground state depletion [49,50] to be negligible under these conditions. Accordingly, a 5.6 mW laser output power was employed for further studies. The voltage of the PMT was fixed at 600 V as this gives the highest electric output signal.

With optimized derivatization, separation and detection conditions, an LOD of 1400 ng L<sup>-1</sup> was obtained (Fig. 5A). The LOD is calculated at a signal to noise ratio (S/N) = 3 and S/N is calculated according to the European Pharmacopoeia [51]. The achieved LOD is still above the requirement for the analysis of pharmaceuticals in environmental waters.

#### 3.3.2.2. Large volume sample stacking (LVSS)/sweeping

The maximum enrichment efficiency that can be obtained applying FASS conditions is not exceeding a factor of 10 [52]. Therefore, our next attempt was to include another stacking technique such as large volume sample stacking (LVSS) [26] for a further reduction of the detection limits. Taking into account the high complex formation constant between the formed derivative and 2-HP- $\beta$ -CD, complex formation sweeping will also contribute to achieve a further improvement in the enrichment efficiency (besides that obtained from LVSS). We have to point out that complex formation sweeping will be also involved in the enrichment of the analytes in the case of applying FASS conditions, however, due to the very large sample volume injected in case of LVSS, we can assume that the role of sweeping is more important when combined with LVSS.

The exact mechanism of the analyte enrichment achieved by LVSS/sweeping is illustrated in Fig. 6. At the beginning of the enrichment process, the whole volume of the capillary is filled with the low conductivity sample solution (after derivatization with fluorescamine) using hydrodynamic injection at 1 bar for 1 min (Fig. 6A). Lower injection volumes were also employed (data not shown), however, the highest peak heights (without deterioration of peak efficiency) were obtained by filling the whole volume of the capillary with the sample solution. The inlet vial is then replaced with by a vial containing the BGE (30 mmol L<sup>-1</sup> sodium tetraborate, pH 9.25 containing 20 mg mL<sup>-1</sup> 2-HP- $\beta$ -CD) and a negative voltage (-20 kV) is applied, whereas the electric current strength is very low due to the high resistivity of the sample matrix. The direction of the EOF is toward the inlet, whereas the negatively-charged fluorescent derivative migrate with a very high velocity due to the high electric field strength toward the detection end (Fig. 6B). The stacking process commences once the deprotonated analyte reaches the sample/BGE boundary because of the reduced electric field strength in the BGE zone (Fig. 6C). After passing the stacking boundary, the derivatized analytes form inclusion complexes with 2-HP- $\beta$ -CD (Fig. 6D) resulting in an additional reduction of their velocity (sweeping). The stacking and the sweeping

processes continue until the sample matrix is almost completely pumped out from the injection end of the capillary (Fig. 6E). At this moment, the polarity of the applied voltage is reversed. This can be done by monitoring the electric current strength during the matrix removal step. The separation starts in the normal polarity mode with an applied voltage of +20 kV, when the electric current strength reaches 95% of its "original value" (Fig. 6F). The "original value" of the electric current strength is obtained by measuring the electric current strength with a capillary filled completely with BGE. Experimentally, the polarity is switched when the absolute electric current strength reaches  $23 \pm 0.5 \mu\text{A}$ , which represents 95% of the original electric current strength at 20 kV. The time elapsed between the application of the negative voltage (-20 kV) and the application of the positive voltage (+20 kV) is approximately  $3 \pm 0.05$  min.

To show the impact of LVSS/sweeping on the improvement of the detection limits, 1 mL of a Lahn river water sample was spiked with the antibiotics and derivatized as described under Section 2.5 before being injected. The electropherograms obtained under FASS (Fig. 5A) and under LVSS/sweeping (Fig. 5B) conditions were recorded using the same antibiotic concentration (in both cases  $c(\text{antibiotic})$  in the final derivatization reaction mixture is  $1400 \text{ ng L}^{-1}$ ). It is evident from Fig. 5 that there is a significant increase in S/N achieved when employing LVSS/sweeping conditions. The instrumental LOD obtained when employing the fully optimized procedure is  $1400 \text{ ng L}^{-1}$  in case of FASS, whereas it is  $60 \text{ ng L}^{-1}$  when using LVSS/sweeping conditions (see figure inset in Fig. 5B). This represents an approximately 25-fold improvement of the sensitivity.

### 3.4. Optimization of solid phase extraction (SPE)

In addition to sample-clean up from interfering substances and matrix constituents, additional improvement of the detection limits can be achieved by carrying out off-line enrichment by SPE. The water samples were spiked with an appropriate volume of a standard mixture of the analytes ( $600 \text{ ng L}^{-1}$ ). The investigated analytes are highly hydrophilic (see  $\lg P_{\text{ow}}$  and  $\lg D$  (at pH 3) values in the supplementary data), with low  $\text{pK}_a$  due to the presence of carboxylic groups. They are present in their anionic form under neutral conditions with a very high solubility in aqueous solution, which results in a poor extraction recovery [53]. Based on these properties, SPE based on HLB cartridges (HLB stands for hydrophilic-lipophilic balance) were investigated for their extraction from surface waters. The recovery is calculated by dividing the corrected peak areas (peak area/migration time) obtained after carrying out SPE, the derivatization reaction and the on-line enrichment technique by that obtained using a standard solution of the analyte without carrying out SPE. It should be taken into account that the recovery for cefadroxil is always lower than that for cefalexin as the former is more hydrophilic. Parameters influencing the recovery such as (i) type of sorbent, (ii) sample loading volume, (iii) sample pH, and (iv)

the type and performing of washing and elution steps were studied. Moreover, we investigated the stability of the antibiotics in the elution solvent.

At the beginning, Oasis MCX cartridge was tested as this cartridge can provide both hydrophobic/hydrophilic and cation exchange interactions with the analytes. Extractions using this cartridge were carried out at pH 2.75 and pH 2.56 to ensure that higher fractions of the analytes exist in their protonated form. However, the recovery was lower than 5% either with or without carrying the washing step (Table 2). This low recovery can either be ascribed to the instability of the investigated analytes in the eluent or to an insufficient eluent ionic strength, which is not adequate to elute the analytes from the cartridge. However, higher eluent concentrations cannot be tested, as they will have a negative impact on the efficiency of the on-line enrichment procedure, especially with LVSS.

As a next step, Oasis HLB and Supelco Supel-Select HLB were tested at slightly acidic pH conditions using a low sample volume (10 mL). As illustrated in Table 2, working under these conditions gives rise to a very low recovery for both antibiotics when employing Supelco HLB and a low recovery for cefadroxil using Oasis HLB. Working under highly acidic pH conditions (pH 2.78) increases the recovery for both compounds with both cartridge types which can be ascribed to the partial protonation of the carboxylic acid moieties. However, the recovery from Supelco HLB is significantly lower. Therefore Oasis HLB from Waters was selected. The high extraction efficiency of Oasis HLB can be attributed to its high specific surface area ( $800 \text{ m}^2 \text{ g}^{-1}$ ), its stability over a wide pH range of 0–14 and its wetting properties due to the hydrophilic N-vinylpyrrolidone monomer [3,5,54,55]. Therefore, this sorbent was selected also by other working groups for the extraction of pharmaceuticals from environmental waters [17,35,56,57]. Increasing the pH to 2.9 improved the recovery significantly for both compounds. Similarly, other authors found satisfactory recoveries for  $\beta$ -lactam antibiotics when the sample pH is around 2 and 3 [12,17,28,30,35,55]. With carrying out a washing step with 5 mL Milli-Q water, the recovery was reduced (due to the loss of the analytes in the washing solution). In addition, employing larger sample volume (50 mL) with Oasis HLB and with carrying out the washing step, the recovery was low. By increasing the sample volume to 100 mL, the recovery is reduced for cefadroxil as obviously the breakthrough volume for this compound is exceeded. Therefore, the sample volume was kept at 50 mL. Optimum extractions conditions were obtained with Oasis HLB using 50 mL water sample at pH 2.9.

To investigate the stability of the analytes in methanol as eluent, standards were spiked directly in 3 mL methanol and after drying the solution under vacuum, the derivatization procedure was performed as described under Section 2.5. Subsequently the derivatized sample solution was injected. The recovery was 100% for both analytes, which implies that within the time span for drying the eluate, the investigated analytes, are stable when dissolved in methanol.

Due to the slight acidity of the sample matrix after reconstitution in aqueous solution (especially when using larger sample volumes), a higher concentration of borate buffer was required to increase the pH of the sample solution for the subsequent derivatization reaction. As shown in Fig 7, four cases were compared using different concentrations and pH's of borate buffer in the final derivatization reaction mixture. 8 mmol L<sup>-1</sup> Borate buffer of pH 8.2 (Fig. 7B) in the final sample solution after derivatization was found to be the optimum concentration regarding simultaneously peak efficiency, peak resolution, and peak height. Therefore this concentration was selected as optimum for the subsequent derivatization reaction in the case SPE as first sample pretreatment step when analyzing surface water samples (see Section 2.5). Higher buffer concentration and higher pH value result in a deterioration of the stacking efficiency as seen in Figs. 7C and 7D.

Employing optimized SPE and optimized derivatization reaction results in an off-line enrichment efficiency factor of 10 (the starting sample volume is 50 mL and the final sample volume is 5 mL). Possibly, better off-line enrichment factors can be reached by increasing the mass of the sorbent employed.

### 3.5. Method performance and validation study

Preliminary tests revealed the absence of detectable antibiotics in Lahn river water. To assess possible matrix effects, concentrations of antibiotics between 15 ng L<sup>-1</sup> and 720 ng L<sup>-1</sup> were spiked to river water samples. Applying the fully optimized procedure (Section 2.6), the corresponding calibration plots were constructed. The method was validated according to the international Conference on Harmonisation (ICH) guidelines [58] on the validation of analytical methods. The performance of the method was evaluated through the estimation of the linearity, linearity range, sensitivity (method detection and quantitation limits), repeatability, recovery, and selectivity.

In order to determine the linearity of the developed method, 7 to 9 calibration standards of the studied antibiotics were taken to construct the calibration curves (5 replicates each). Peak height and corrected peak area (peak area/migration time) were used as the response factors. The results of the statistical analysis of the data are summarised in Table 3 showing the linearity range of the developed method for each analyte (corresponding calibration graphs and residual plots are shown in Fig. S8, supplementary data). As stated by the ICH guidelines [58], the correlation coefficient  $r$ , the y-intercept  $a$ , the slope of the regression line  $b$ , and the sum of squared errors SSE are required for the evaluation of linearity. The previously mentioned parameters in addition to the linearity range, the standard deviation of the intercept and the slope, the standard deviation of the residuals  $S_{yx}$ , the confidence interval of the slope and the intercept, the method standard deviation  $S_{x0}$ , and the relative standard deviation of the method

$S_r$  are also listed in Table 3. The correlation coefficient  $r$  of the calibration curve is higher in all cases than 0.9981, which indicates an excellent linearity of the developed method. Beside the determination of correlation coefficients, the linearity was assessed by carrying out Mandel's fitting test [59]. By applying Mandel's test at  $P=0.95$ , all Mandel's test values are lower than the critical  $F$  values (Table 3), which indicates that the chosen linear regression model is adequate.

LOD and LOQ were determined based on an  $S/N$  of 3 and 10, respectively. The  $S/N$  is calculated (according to the European Pharmacopoeia [51]) as given in our previously published work [47]. As shown in Table 3, the LOD was found to be 4.86 and 7.50 ng L<sup>-1</sup> for cefalexin and cefadroxil, respectively and the LOQ was found to be 15 and 30 ng L<sup>-1</sup>.

Intra-day and inter-day precisions were assessed using three concentrations and five replicates of each concentration. For each set of results, the RSD (%) was calculated for the peak area, peak height, and migration time. As given in Table 4, the repeatability of the migration times is  $\leq 0.9$  and 1.4% for intra- and inter-day precision, respectively. The highest values for RSD (%) of the peak height and peak area (intra-day precision) are 2.1 and 3.8%, respectively. For inter-day precision, all RSD (%) values are lower than 8.2 and 6.5% for the peak height and the peak area, respectively, which indicates a good repeatability of the developed method.

Recoveries were obtained by spiking Lahn river water samples with three different concentrations of the studied antibiotics covering the lower, the medium, and the upper range of the calibration curve. The average recoveries obtained are in the range of 94.0-99.8% for cefalexin and 95.5-98.7% for cefadroxil, which demonstrates a good accuracy and selectivity of the developed method. Fig. 8 shows electropherograms obtained from unspiked river water and water spiked with 600 ng L<sup>-1</sup> of each antibiotic. No matrix peaks comigrating with the analytes are observed.

### 3.6. The developed method compared to other approaches

The LODs and LOQs achieved by the combination of the LIF detection and on-line and off-line the pre-concentration procedures are lower than those reported for other CE methods employing off-line and/or on-line enrichment in combination with DAD detection for the analysis of cephalosporin antibiotics in environmental water samples [28-30,60]. In the presented study, the LOD obtained for cefalexin is one order of magnitude lower than that reported for a similar approach employing SPE, derivatization with Cy5 and MEKC-LIF with a diode laser emitting at 635 nm as excitation source [31].

It is noteworthy to mention that that our developed method provides comparable or better LODs than those obtained for the analysis of cephalosporins in environmental samples by: (i) off-line SPE followed by HPLC-UV [17], HPLC-MS [37], HPLC-MS/MS [9,10,61,62], HPLC-ESI(+)-MS [55], UHPLC-QTOF-

MS [56], or (ii) ion-pair extraction followed by HPLC-UV [53]. It should be taken into account that most of these approaches utilize larger starting sample volumes than our proposed method for carrying out the off-line enrichment technique. However, this in turn can affect negatively the total analysis time and subsequently the number of samples that can be processed per day.

The best LODs that were reported for the determination of cefalexin in river water are 0.77 ng L<sup>-1</sup> [35] and 1 ng L<sup>-1</sup> [8]. These values are lower than that achieved in the presented study by using UHPLC coupled to quadrupole-linear ion trap tandem mass spectrometry (UHPLC–QqLIT) and HPLC–MS/MS, respectively. However, this slight increase in sensitivity is gained with the application of much more expensive equipment. While the proposed method can confirm the absence of the studied antibiotics in surface water at adequate concentration level, it might result in a false positive identification due to its limited selectivity. Therefore, the use of the MS detection is mandatory [31], when the confirmation of the structure of the antibiotic detected is required.

#### 4. Conclusions

The developed and validated CZE/LIF approach provides a highly sensitive method for the successful determination of selected  $\alpha$ -aminocephalosporin antibiotics in surface water samples in the very low ng L<sup>-1</sup> range. The separation takes place in less than 7 min. Our proposed strategy is facilitated by its simplicity, robustness, high sensitivity, the rate of the labelling reaction in addition to the excellent overlapping between the fluorescence excitation maximum and the output of the diode laser emitting at 375 nm. The on-line enrichment procedure is very fast and requires no additional equipment. The high extraction efficiency provided by the Oasis HLB allows both analyte preconcentration and sample clean up together with a very low starting sample volume (50 mL). The very low LODs afforded by the proposed strategy provide a promising approach for the monitoring of these compounds in other types of water samples and permits the extension of this methodology to other potential pollutants containing primary amino groups.

### **Acknowledgments**

A.H. Rageh thanks the Egyptian ministry of higher education and the ministry of state for scientific research and the Deutscher Akademischer Austauschdienst (DAAD) for funding her PhD scholarship through German Egyptian Research Long-Term Scholarship program (GERLS). A.H. Rageh thanks Marburg University Research Academy (MARA) for the financial support. We also thank Prof. H.P. Aung for her valuable instructions regarding the solid phase extraction experiments. We thank Kathrin Geiger and Wolf Fronius for their assistance in taking water samples and in data evaluation. We thank the workshops of the Department of Chemistry, University of Marburg for the development of the data recording unit and J&M Analytik, Essingen for the loan of the PMT unit.

## References

- [1] M.D. Hernando, M. Mezcua, A.R. Fernandez-Alba, D. Barcelo, Environmental risk assessment of pharmaceutical residues in wastewater effluents, surface waters and sediments, *Talanta*, 69 (2006) 334-342.
- [2] T. Zhang, B. Li, Occurrence, Transformation, and Fate of Antibiotics in Municipal Wastewater Treatment Plants, *Crit. Rev. Environ. Sci. Technol.*, 41 (2011) 951-998.
- [3] M. Seifrtova, L. Novakova, C. Lino, A. Pena, P. Solich, An overview of analytical methodologies for the determination of antibiotics in environmental waters, *Anal. Chim. Acta*, 649 (2009) 158-179.
- [4] K. Kuemmerer, A. Henninger, Promoting resistance by the emission of antibiotics from hospitals and households into effluent, *Clin. Microbiol. Infect.*, 9 (2003) 1203-1214.
- [5] M.J. Gomez, M. Petrovic, A.R. Fernandez-Alba, D. Barcelo, Determination of pharmaceuticals of various therapeutic classes by solid-phase extraction and liquid chromatography-tandem mass spectrometry analysis in hospital effluent wastewaters, *J. Chromatogr. A*, 1114 (2006) 224-233.
- [6] K. Kuemmerer, Antibiotics in the aquatic environment - A review - Part I, *Chemosphere*, 75 (2009) 417-434.
- [7] M.S. Diaz-Cruz, D. Barcelo, Determination of antimicrobial residues and metabolites in the aquatic environment by liquid chromatography tandem mass spectrometry, *Anal. Bioanal. Chem.*, 386 (2006) 973-985.
- [8] A.Y.C. Lin, T.H. Yu, C.F. Lin, Pharmaceutical contamination in residential, industrial, and agricultural waste streams: Risk to aqueous environments in Taiwan, *Chemosphere*, 74 (2008) 131-141.
- [9] A.J. Watkinson, E.J. Murby, D.W. Kolpin, S.D. Costanzo, The occurrence of antibiotics in an urban watershed: From wastewater to drinking water, *Sci. Total Environ.*, 407 (2009) 2711-2723.
- [10] A. Gulkowska, Y. He, M.K. So, L.W.Y. Yeung, H.W. Leung, J.P. Giesy, P.K.S. Lam, M. Martin, B.J. Richardson, The occurrence of selected antibiotics in Hong Kong coastal waters, *Mar. Pollut. Bull.*, 54 (2007) 1287-1293.
- [11] X.H. Wang, A.Y.C. Lin, Phototransformation of cephalosporin antibiotics in an aqueous environment results in higher toxicity, *Environ. Sci. Technol.*, 46 (2012) 12417-12426.
- [12] R. Nageswara Rao, N. Venkateswarlu, R. Narsimha, Determination of antibiotics in aquatic environment by solid-phase extraction followed by liquid chromatography-electrospray ionization mass spectrometry, *J. Chromatogr. A*, 1187 (2008) 151-164.
- [13] S.M. Mitchell, J.L. Ullman, A.L. Teel, R.J. Watts, pH and temperature effects on the hydrolysis of three  $\beta$ -lactam antibiotics. Ampicillin, cefalotin and cefoxitin, *Sci. Total Environ.*, 466-467 (2014) 547-555.



- [14] F.J. Lara, M. del Olmo-Iruela, C. Cruces-Blanco, C. Quesada-Molina, A.M. Garcia-Campana, Advances in the determination of  $\beta$ -lactam antibiotics by liquid chromatography, *Trends Anal. Chem.*, 38 (2012) 52-66.
- [15] J.M. Cha, S. Yang, K.H. Carlson, Trace determination of  $\beta$ -lactam antibiotics in surface water and urban wastewater using liquid chromatography combined with electrospray tandem mass spectrometry, *J. Chromatogr. A*, 1115 (2006) 46-57.
- [16] R. Hirsch, T. Ternes, K. Haberer, K.L. Kratz, Occurrence of antibiotics in the aquatic environment, *Sci. Total Environ.*, 225 (1999) 109-118.
- [17] P. Wang, T. Yuan, J. Hu, Y. Tan, Determination of cephalosporin antibiotics in water samples by optimised solid phase extraction and high performance liquid chromatography with ultraviolet detector, *Int. J. Environ. Anal. Chem.*, 91 (2011) 1267-1281.
- [18] F. Hernandez, M. Ibanez, R. Bade, L. Bijlsma, J.V. Sancho, Investigation of pharmaceuticals and illicit drugs in waters by liquid chromatography-high-resolution mass spectrometry, *Trends Anal. Chem.*, 63 (2014) 140-157.
- [19] D. Fatta, A. Nikolaou, A. Achilleos, S. Meric, Analytical methods for tracing pharmaceutical residues in water and wastewater, *Trends Anal. Chem.*, 26 (2007) 515-533.
- [20] F. Hernandez, J.V. Sancho, M. Ibanez, C. Guerrero, Antibiotic residue determination in environmental waters by LC-MS, *Trends Anal. Chem.*, 26 (2007) 466-485.
- [21] A.A.M. Stolker, T. Zuidema, M.W.F. Nielen, M.W.F. Nielen, Residue analysis of veterinary drugs and growth-promoting agents, *Trends Anal. Chem.*, 26 (2007) 967-979.
- [22] M. Petrovic, M.D. Hernando, M.S. Diaz-Cruz, D. Barcelo, Liquid chromatography-tandem mass spectrometry for the analysis of pharmaceutical residues in environmental samples: a review, *J. Chromatogr. A*, 1067 (2005) 1-14.
- [23] A.M. Garcia-Campana, L. Gamiz-Gracia, F.J. Lara, M. del Olmo-Iruela, C. Cruces-Blanco, Applications of capillary electrophoresis to the determination of antibiotics in food and environmental samples, *Anal. Bioanal. Chem.*, 395 (2009) 967-986.
- [24] M. Urbanek, L. Krivankova, P. Bocek, Stacking phenomena in electromigration: From basic principles to practical procedures, *Electrophoresis*, 24 (2003) 466-485.
- [25] R.L. Chien, D.S. Burgi, On-column sample concentration using field amplification in CZE, *Anal. Chem.*, 64 (1992) 489A-496A.
- [26] R.L. Chien, D.S. Burgi, Sample stacking of an extremely large injection volume in high-performance capillary electrophoresis, *Anal. Chem.*, 64 (1992) 1046-1050.
- [27] J.P. Quirino, S. Terabe, Exceeding 5000-fold concentration of dilute analytes in micellar electrokinetic chromatography, *Science*, 282 (1998) 465-468.
- [28] P. Puig, F. Borrull, C. Aguilar, M. Calull, CE analysis of cephalosporins in environmental waters, *Chromatographia*, 65 (2007) 501-504.
- [29] P. Puig, F. Borrull, M. Calull, F. Benavente, V. Sanz-Nebot, J. Barbosa, C. Aguilar, Improving the sensitivity of the determination of ceftiofur by capillary electrophoresis in environmental

water samples: In-line solid phase extraction and sample stacking techniques, *Anal. Chim. Acta*, 587 (2007) 208-215.

- [30] C. Quesada-Molina, M. del Olmo Iruela, A.M. Garcia-Campana, Analysis of cephalosporin residues in environmental waters by capillary zone electrophoresis with off-line and on-line preconcentration, *Anal. Methods*, 4 (2012) 2341-2347.
- [31] J.M. Serrano, M. Silva, Use of SDS micelles for improving sensitivity, resolution, and speed in the analysis of  $\beta$ -lactam antibiotics in environmental waters by SPE and CE, *Electrophoresis*, 28 (2007) 3242-3249.
- [32] J.P. Landers, *Handbook of Capillary and Microchip Electrophoresis and Associated Microtechniques*, 3rd Edn, CRC Press, Taylor and Francis Group, LLC, Boca Raton, 2008.
- [33] C. Huhn, L.R. Ruhaak, J. Mannhardt, M. Wuhrer, C. Neusuess, A.M. Deelder, H. Meyer, Alignment of laser-induced fluorescence and mass spectrometric detection traces using electrophoretic mobility scaling in CE-LIF-MS of labeled N-glycans, *Electrophoresis*, 33 (2012) 563-566.
- [34] M.L. Riekkola, J.A. Joensson, R.M. Smith, Terminology for analytical capillary electromigration techniques, *Pure Appl. Chem.*, 76 (2004) 443-451.
- [35] M. Gros, S. Rodriguez-Mozaz, D. Barcelo, Rapid analysis of multiclass antibiotic residues and some of their metabolites in hospital, urban wastewater and river water by ultra-high-performance liquid chromatography coupled to quadrupole-linear ion trap tandem mass spectrometry, *J. Chromatogr. A*, 1292 (2013) 173-188.
- [36] A.D. Deshpande, K.G. Baheti, N.R. Chatterjee, Degradation of  $\beta$ -lactam antibiotics, *Curr. Sci.*, 87 (2004) 1684-1695.
- [37] R. Lindberg, P.A. Jarnheimer, B. Olsen, M. Johansson, M. Tysklind, Determination of antibiotic substances in hospital sewage water using solid phase extraction and liquid chromatography/mass spectrometry and group analogue internal standards, *Chemosphere*, 57 (2004) 1479-1488.
- [38] M. Hefnawy, Y. El-Shabrawy, F. Belal, Spectrofluorometric determination of alpha-aminocephalosporins in biological fluids and pharmaceutical preparations, *J. Pharm. Biomed. Anal.*, 21 (1999) 703-707.
- [39] S. Udenfriend, S. Stein, P. Boehlen, W. Dairman, W. Leimgruber, M. Weigele, Fluorescamine. Reagent for assay of amino acids, peptides, proteins, and primary amines in the picomole range, *Science*, 178 (1972) 871-872.
- [40] S. De Bernardo, M. Weigele, V. Toome, K. Manhart, W. Leimgruber, P. Boehlen, S. Stein, S. Udenfriend, Studies on the reaction of fluorescamine with primary amines, *Arch. Biochem. Biophys.*, 163 (1974) 390-399.
- [41] S. Stein, P. Boehlen, S. Udenfriend, Kinetics of reaction and hydrolysis of fluorescamine, *Arch. Biochem. Biophys.*, 163 (1974) 400-403.
- [42] R.F. Chen, P.D. Smith, M. Maly, The fluorescence of fluorescamine-amino acids, *Arch. Biochem. Biophys.*, 189 (1978) 241-250.

- [43] J.P. Quirino, S. Terabe, K. Otsuka, J.B. Vincent, G. Vigh, Sample concentration by sample stacking and sweeping using a microemulsion and a single-isomer sulfated  $\beta$ -cyclodextrin as pseudostationary phases in electrokinetic chromatography, *J. Chromatogr. A*, 838 (1999) 3-10.
- [44] A.T. Aranas, A.M. Guidote Jr., J.P. Quirino, Sweeping and new on-line sample preconcentration techniques in capillary electrophoresis, *Anal. Bioanal. Chem.*, 394 (2009) 175-185.
- [45] C. Huhn, M. Puetz, N. Martin, R. Dahlenburg, U. Pyell, Determination of tryptamine derivatives in illicit synthetic drugs by capillary electrophoresis and ultraviolet laser-induced fluorescence detection, *Electrophoresis*, 26 (2005) 2391-2401.
- [46] F.E.O. Suliman, Z.H. Al-Lawati, S.M.Z. Al-Kindy, A spectrofluorimetric sequential injection method for the determination of penicillamine using fluorescamine in the presence of  $\beta$ -cyclodextrins, *J. Fluoresc.*, 18 (2008) 1131-1138.
- [47] A.H. Rageh, A. Kaltz, U. Pyell, Determination of urinary nucleosides via borate complexation capillary electrophoresis combined with dynamic pH junction-sweeping-large volume sample stacking as three sequential steps for their on-line enrichment, *Anal. Bioanal. Chem.*, 406 (2014) 5877-5895.
- [48] D. Maffeo, L. Leondiadis, I.M. Mavridis, K. Yannakopoulou, Positive effect of natural and negatively charged cyclodextrins on the stabilization of penicillins towards beta-lactamase degradation due to inclusion and external guest-host association. An NMR and MS study, *Org Biomol Chem*, 4 (2006) 1297-1304.
- [49] C. Bayle, V. Poinot, C. Fournier-Noel, F. Couderc, Laser-induced Fluorescence Detection: A Summary, in: U. Pyell (Ed.), *Electrokinetic Chromatography: Theory, Instrumentation & Applications*, John Wiley & Sons, Ltd., Chichester, 2006.
- [50] R.A. Mathies, K. Peck, L. Stryer, Optimization of high-sensitivity fluorescence detection, *Anal. Chem.*, 62 (1990) 1786-1791.
- [51] European Pharmacopoeia (7.8), Online Version, European directorate for the quality of medicines & healthcare (EDQM), Strasbourg, 2013.
- [52] C. Huhn, U. Pyell, Diffusion as major source of band broadening in field-amplified sample stacking under negligible electroosmotic flow velocity conditions, *J. Chromatogr. A*, 1217 (2010) 4476-4486.
- [53] C. Quesada-Molina, A.M. Garcia-Campana, M. del Olmo-Iruela, Ion-paired extraction of cephalosporins in acetone prior to their analysis by capillary liquid chromatography in environmental water and meat samples, *Talanta*, 115 (2013) 943-949.
- [54] S. Weigel, R. Kallenborn, H. Huhnerfuss, Simultaneous solid-phase extraction of acidic, neutral and basic pharmaceuticals from aqueous samples at ambient (neutral) pH and their determination by gas chromatography-mass spectrometry, *J. Chromatogr. A*, 1023 (2004) 183-195.
- [55] O. Opris, M.L. Soran, V. Coman, F. Copaciu, D. Ristoiu, Determination of some frequently used antibiotics in waste waters using solid phase extraction followed by high performance liquid chromatography with diode array and mass spectrometry detection, *Cent. Eur. J. Chem.*, 11 (2013) 1343-1351.

- [56] M. Ibanez, C. Guerrero, J.V. Sancho, F. Hernandez, Screening of antibiotics in surface and wastewater samples by ultra-high-pressure liquid chromatography coupled to hybrid quadrupole time-of-flight mass spectrometry, *J. Chromatogr. A*, 1216 (2009) 2529-2539.
- [57] M.I. Bailon-Perez, A.M. Garcia-Campana, M. del Olmo-Iruela, L. Gamiz-Gracia, C. Cruces-Blanco, Trace determination of 10  $\beta$ -lactam antibiotics in environmental and food samples by capillary liquid chromatography, *J. Chromatogr. A*, 1216 (2009) 8355-8361.
- [58] ICH Harmonised Tripartite Guidelines, Validation of analytical procedures: text and methodology Q2(R1). <http://www.ich.org/products/guidelines/quality/article/quality-guidelines.html> (accessed 10.03.2015).
- [59] M. Reichenbaecher, J.W. Einax, *Challenges in Analytical Quality Assurance*, Springer-Verlag, Berlin Heidelberg, 2011.
- [60] P. Puig, F.W.A. Tempels, G.W. Somsen, J. de, F. Borrull, C. Aguilar, M. Calull, Use of large-volume sample stacking in on-line solid-phase extraction-capillary electrophoresis for improved sensitivity, *Electrophoresis*, 29 (2008) 1339-1346.
- [61] R.H. Lindberg, P. Wennberg, M.I. Johansson, M. Tysklind, B.A.V. Andersson, Screening of human antibiotic substances and determination of weekly mass flows in five sewage treatment plants in Sweden, *Environ. Sci. Technol.*, 39 (2005) 3421-3429.
- [62] A. Gulkowska, H.W. Leung, M.K. So, S. Taniyasu, N. Yamashita, L.W.Y. Yeung, B.J. Richardson, A.P. Lei, J.P. Giesy, P.K.S. Lam, Removal of antibiotics from wastewater by sewage treatment facilities in Hong Kong and Shenzhen, China, *Water Res.*, 42 (2008) 395-403.

### Figure captions

**Figure 1:** Schematic presentation of the fiber-optic coupled detection cell/capillary holder with arrangement of one excitation fibre and two detection fibre bundles.

**Figure 2:** Pictures of (A) the complete instrumental setup including the CE instrument, the detection cell, the UV detector, the optical fibres, the laser head, the laser controller and the optical filter, (B) the metallic part used to fix the detection cell plus the arrangement of the optical fibres, (C) the PMT, and (D) the arrangement of the separation capillary inside the detection cell plus another capillary showing the positioning of the detection window when placed inside the capillary holder.

**Figure 3:** Effect of different types of cyclodextrins on the effective electrophoretic mobility. Each data point is the average of at least two measurements (standard error represented as error bar).  $c(\text{Antibiotic})$  in the final derivatization reaction mixture is  $0.36 \text{ mg L}^{-1}$ . The BGE composed of  $40 \text{ mmol L}^{-1}$  sodium tetraborate, pH 9.25.  $c(\text{cyclodextrin})$  in the BGE is  $10 \text{ mg mL}^{-1}$ . CE conditions: capillary  $654(350) \text{ mm} \times 50.2 \text{ } \mu\text{m I.D.}$ , separation voltage  $+20 \text{ kV}$ , pressure injection  $40 \text{ mbar}$  for  $0.4 \text{ min}$ , oven temperature  $25 \text{ }^\circ\text{C}$ , laser  $P_{\text{cw}} 2 \text{ mW}$ , PMT voltage  $500 \text{ V}$ .

**Figure 4:** Effect of the concentration of 2-HP- $\beta$ -CD on the effective electrophoretic mobility taking into account the viscosity correction factor using (A) the non-derivatized antibiotics and (B) the antibiotics after derivatization.  $c(\text{Antibiotic})$  in (A) is  $14 \text{ mg L}^{-1}$  in water and in (B) is  $0.28 \text{ mg L}^{-1}$ . CE conditions: capillary  $654(350) \text{ mm} \times 50.2 \text{ } \mu\text{m I.D.}$ , separation voltage  $+20 \text{ kV}$ , pressure injection  $40 \text{ mbar}$  for  $0.4 \text{ min}$ , oven temperature  $25 \text{ }^\circ\text{C}$ , Laser  $P_{\text{cw}} 2 \text{ mW}$ , PMT voltage  $500 \text{ V}$ .

**Figure 5:** Electropherograms obtained from  $1 \text{ mL}$  Lahn river water sample after spiking with the studied antibiotics (without carrying out SPE) and treated as described under Section 2.5 either under FASS (A) or LVSS/sweeping conditions (B).  $c(\text{Antibiotic})$  in (A) and (B) in the final derivatization reaction mixture is  $1400 \text{ ng L}^{-1}$ . The figure inset in (B) is an electropherogram obtained under LVSS/sweeping conditions from  $1 \text{ mL}$  Lahn river water sample spiked with  $600 \text{ ng L}^{-1}$  of both antibiotics and treated as described under Section 2.5. The BGE composed of  $30 \text{ mmol L}^{-1}$  sodium tetraborate, pH 9.25 containing  $20 \text{ mg mL}^{-1}$  2-HP- $\beta$ -CD. CE conditions: capillary  $654(350) \text{ mm} \times 50.2 \text{ } \mu\text{m I.D.}$ , applied voltage during LVSS/sweeping/matrix removal  $-20 \text{ kV}$ , separation voltage  $+20 \text{ kV}$ , Laser  $P_{\text{cw}} 5.6 \text{ mW}$ , pressure injection  $30 \text{ mbar}$  for  $0.6 \text{ min}$  in (A) and  $1 \text{ bar}$  for  $1 \text{ min}$  in (B), oven temperature  $25 \text{ }^\circ\text{C}$ , PMT voltage  $600 \text{ V}$ . Peak designation: (1) cefalexin and (2) cefadroxil.

**Figure 6:** Schematic presentation of the suggested focusing mechanism (LVSS/sweeping). (A) Capillary filled with the BGE followed by hydrodynamic injection of the whole capillary with the sample solution after derivatization with fluorescamine. (B) Application of a negative voltage. (C) Stacking of the

deprotonated derivatized analytes at the sample matrix/BGE boundary. (D) 2-HP- $\beta$ -CD commences to sweep the derivatized analytes via complexation. (E) Analytes continue to be accumulated by stacking and sweeping, while simultaneously the matrix is pumped out from the injection end. (F) After the completion of the stacking and the sweeping steps and after pumping the largest part of the sample matrix plug, the polarity is switched and the separation starts. The length of the arrow represents the magnitude of the velocity.

**Figure 7:** Electropherograms showing the effect of borate buffer concentrations and borate buffer pH in the final derivatization reaction mixture on the peak resolution, peak height and peak efficiency.  $c(\text{Antibiotic})$  in the spiked water sample is  $600 \text{ ng L}^{-1}$ . The BGE composed of  $30 \text{ mmol L}^{-1}$  sodium tetraborate, pH 9.25 containing  $20 \text{ mg mL}^{-1}$  2-HP- $\beta$ -CD. CE conditions: capillary  $654(350) \text{ mm} \times 50.2 \text{ }\mu\text{m}$  I.D., applied voltage during LVSS/sweeping/matrix removal  $-20 \text{ kV}$ , separation voltage  $+20 \text{ kV}$ , pressure injection  $1 \text{ bar}$  for  $1 \text{ min}$ , oven temperature  $25 \text{ }^\circ\text{C}$ , Laser  $P_{\text{cw}}$   $5.6 \text{ mW}$ , PMT voltage  $600 \text{ V}$ . Peak designation: (1) cefalexin and (2) cefadroxil.

**Figure 8:** Electropherograms obtained from unspiked (A) and spiked (B) Lahn river water sample.  $c(\text{antibiotic})$  in the spiked water sample is  $600 \text{ ng L}^{-1}$ . Other conditions: see Fig. 7.

**Table 1**  
Parameters investigated for optimizing the fluorescence reaction yield and for optimizing the separation

<b>A- Optimization of the fluorescence reaction yield<sup>a</sup></b>						
Volume/ $\mu$ L of 0.02% w/v fluorescamine in acetonitrile	Borate buffer pH (20 mmol L <sup>-1</sup> )	Volume/ $\mu$ L of 20 mmol L <sup>-1</sup> borate buffer	% Acetonitrile in the reaction mixture	Reaction time/min	Stability of the formed derivative	BGE employed
<b>100-1000</b>	8.2	1000	10	One min	-----	b
1000	<b>8.0-9.25</b>	1000	10	One min	-----	c
1000	8.2	<b>500-5000</b>	10	One min	-----	b
1000	8.2	1000	<b>5 or 10</b>	One min	-----	b
1000	8.2	1000	10	<b>1 to 30 min</b>	-----	b
1000	8.2	1000	10	One min	<b>5 min to 24 hours</b>	b

<b>B- Optimization of separation</b>				
BGE pH	c(borax)/mmol L <sup>-1</sup>	c(2-HP- $\beta$ -CD)/mg mL <sup>-1</sup>	Applied voltage/kV	Oven temperature/ $^{\circ}$ C
<b>8.0-9.6</b>	20 <sup>d</sup>	0	20	25
9.25	<b>20-40</b>	10	20	25
9.25	30	<b>0-30</b>	20	25
9.25	30	20	<b>15-30</b>	25
9.25	30	20	20	<b>15-35</b>

<sup>a</sup> All the studied parameters were optimized on the basis of a final sample solution mixture of 10 mL.

<sup>b</sup> Employed BGE is 20 mmol L<sup>-1</sup> borate buffer pH 8.2.

<sup>c</sup> In order to counteract any improvement in the peak height due to the on-line enrichment, i.e. the pH difference between the sample compartment and the BGE compartment, the BGEs used in these experiments are composed exactly of the corresponding borate buffers used for adjusting the pH of the derivatization reaction. E.g. for studying the effect of borate buffer pH 8.0 on the peak height, the BGE employed is composed of 20 mmol L<sup>-1</sup> borate buffer pH 8.0 and so on....

<sup>d</sup> In case of studying the effect of BGE pH on the separation, borate buffers prepared as described in the supplementary data were used.

**Table 2**  
Extraction recoveries  $\pm$  SD (%) of the studied antibiotics by SPE employing different parameters (cartridge type, sample volume, sample pH, and washing step)

Cartridge type <sup>a</sup>	Oasis MCX		Supelco HLB		Oasis HLB		Supelco HLB		Oasis HLB		Oasis HLB <sup>b</sup>		Oasis HLB	
	25	50	10	10	10	10	10	10	10	10	50	50	50	100
Sample volume (Lahn water)/mL	2.75	2.56	5.00	4.85	2.78	2.78	2.90	2.90	2.90	2.75	2.89	2.89	2.84	
Sample pH														
Washing step <sup>c</sup>	yes	no	no	no	no	no	no	no	no	yes	yes	yes	no	no
<b>Cefx</b>														
Recovery, mean $\pm$ SD (%) (n=3)	< 5	< 5	13.8 $\pm$ 3.2	89.4 $\pm$ 3.3	53.8 $\pm$ 3.3	94.5 $\pm$ 6.8	107.3 $\pm$ 3.4	84.9 $\pm$ 5.5	72.2 $\pm$ 4.9	109.4 $\pm$ 3.9	108.6 $\pm$ 4.9			
<b>Cefd</b>														
Recovery, mean $\pm$ SD (%) (n=3)	< 5	< 5	< 5	45.5 $\pm$ 3.2	20.2 $\pm$ 3.6	90.8 $\pm$ 5.4	107.6 $\pm$ 5.2	68.8 $\pm$ 5.1	45.3 $\pm$ 5.9	92.6 $\pm$ 4.0	66.8 $\pm$ 3.4			

<sup>a</sup> Elution was done using 2 mL of 20 mmol L<sup>-1</sup> borate buffer, pH 8.2 in case of Oasis MCX and was carried out using 3 mL methanol using Oasis HLB and Supelco HLB then the derivatization procedure was followed as described under Section 2.5.

<sup>b</sup> Optimum SPE conditions

<sup>c</sup> Washing step was performed using 5 mL Milli-Q water.



**Table 3**  
Linear regression parameters of the developed method

	No. of calib. standards (n)	Linearity range (ng L <sup>-1</sup> )	Intercept (a) ± SD <sup>a</sup>	Slope (b) ± SD <sup>b</sup>	SSE <sup>c</sup>	S <sub>yx</sub> <sup>d</sup>	S <sub>x0</sub> <sup>e</sup>	Sr% <sup>f</sup>	Confidence interval of (a) <sup>g</sup>	Confidence interval of (b) <sup>g</sup>	r <sup>h</sup>	Mandel's test value <sup>i</sup>	LOD <sup>j</sup> (ng L <sup>-1</sup> ) S/N=3	LOQ <sup>k</sup> (ng L <sup>-1</sup> ) S/N=10
<b>Cefx</b>														
PH <sup>l</sup>	8	15-600	218.9±74.5	32463.1±235.9	0.343	138.2	0.004	1.68	±182.2	±577.3	0.9998	0.54	4.86	15
Corr PA <sup>m</sup>	9	15-720	5.7±2.1	323.1±5.4	0.550	4.0	0.012	4.11	±4.9	±12.8	0.9990	0.45		
<b>Cefid</b>														
PH	7	30-600	-172.4±167.4	25367.5±496.2	0.286	265.5	0.010	3.70	±430.3	±1275.6	0.9990	0.45	7.50	30
Corr PA	7	30-600	-0.115±2.0	212.7±5.8	0.286	3.1	0.015	5.60	±5.0	±14.9	0.9981	1.97		

<sup>a</sup> Standard deviation of the intercept

<sup>b</sup> Standard deviation of slope

<sup>c</sup> Sum of square errors

<sup>d</sup> Residual standard deviation (standard error of estimate (SEE))

<sup>e</sup> Method standard deviation (= S<sub>yx</sub>/b)

<sup>f</sup> Relative standard deviation of the method (= S<sub>x0</sub>/x̄)

<sup>g</sup> Confidence interval calculated at P=0.95

<sup>h</sup> r is the correlation coefficient

<sup>i</sup> Tabulated f values at P = 0.95 are 6.6, 5.98, 7.7 at (df1 (1), df2 (n-3)) = (1,6), (1,5), (1,4), respectively

<sup>j</sup> Limit of detection

<sup>k</sup> Limit of quantitation

<sup>l</sup> Peak height

<sup>m</sup> Corrected peak area

**Table 4**

Intra-day and inter-day precision data for the determination of cefalexin and cefadroxil in spiked Lahn river water in addition to the recovery of both antibiotics employing the developed method

	Intra-day precision (n=5), RSD <sup>a</sup> (%)			Inter-day precision, 3 days (n=15), RSD (%)			Recovery, mean $\pm$ SD (%) (n=5)
	PA <sup>b</sup>	PH <sup>c</sup>	MT <sup>d</sup>	PA	PH	MT	
<b>Cefx</b>							
120 ng L <sup>-1</sup>	2.82	1.04	0.26	5.34	6.67	0.82	99.8 $\pm$ 4.8
480 ng L <sup>-1</sup>	2.67	3.82	0.81	6.10	4.61	0.61	94.0 $\pm$ 5.3
600 ng L <sup>-1</sup>	2.23	2.52	0.44	4.82	5.55	1.33	98.9 $\pm$ 3.7
<b>Cefd</b>	PA	PH	MT	PA	PH	MT	
120 ng L <sup>-1</sup>	1.78	2.09	0.37	6.49	7.63	0.82	95.5 $\pm$ 6.1
480 ng L <sup>-1</sup>	1.44	3.58	0.89	5.73	8.15	0.73	98.7 $\pm$ 1.4
600 ng L <sup>-1</sup>	3.83	3.82	0.57	4.29	7.43	1.35	95.9 $\pm$ 4.0

<sup>a</sup> Relative standard deviation

<sup>b</sup> Peak area

<sup>c</sup> Peak Height

<sup>d</sup> Migration time

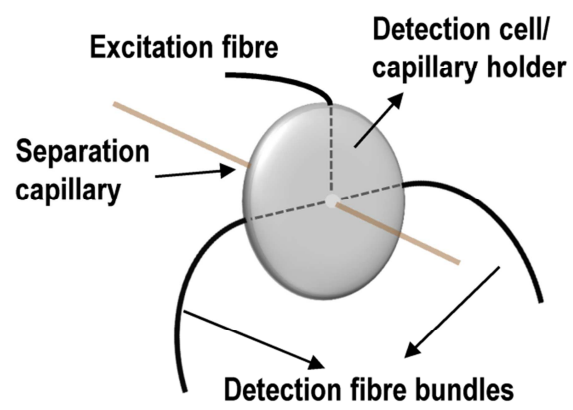


**Figure 1**

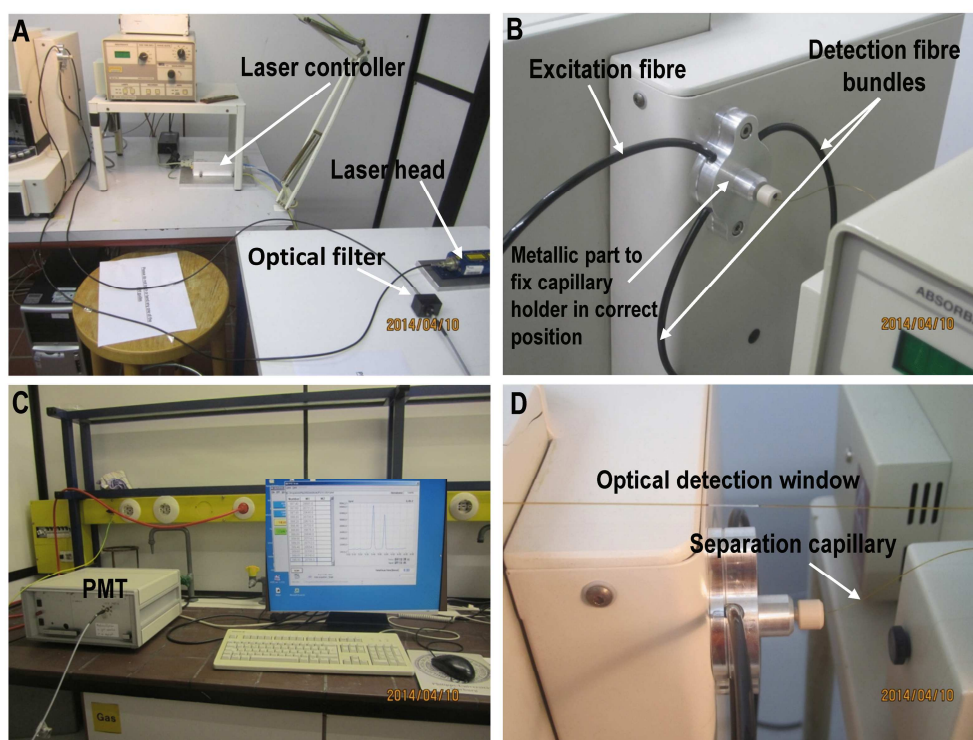


**Figure 2**

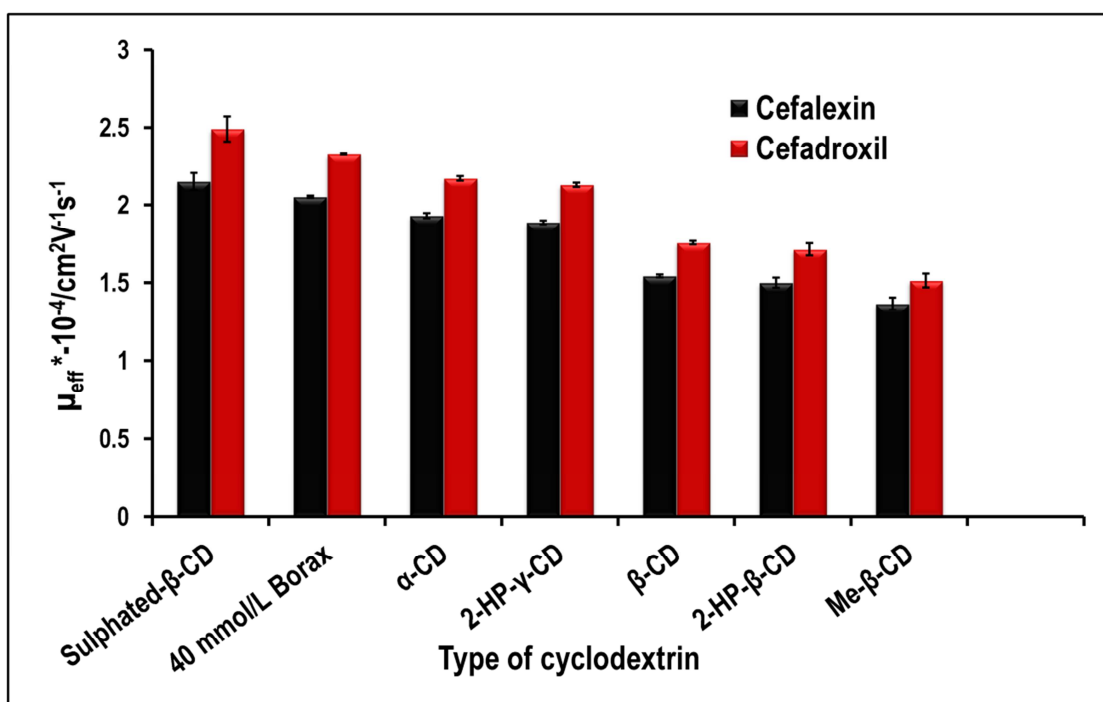


**Figure 3**

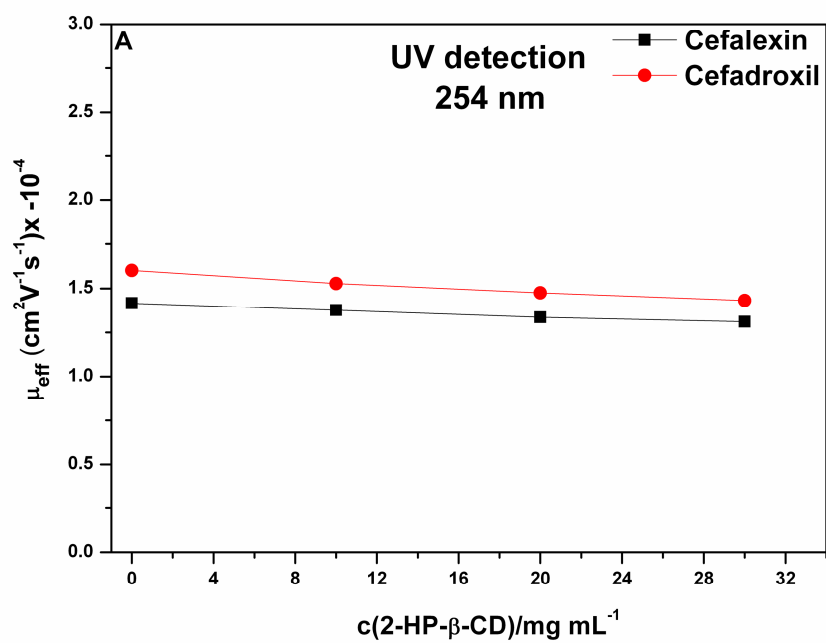


**Figure 4A**

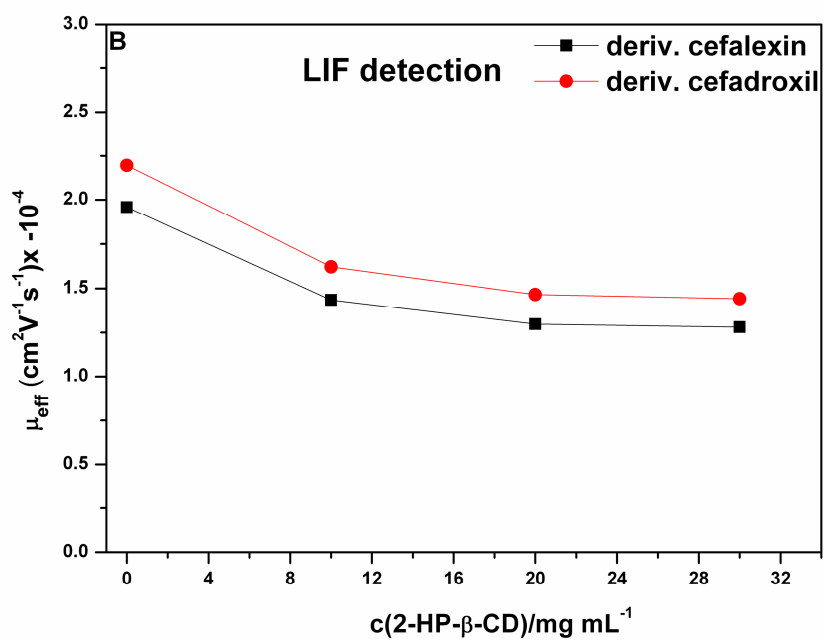


**Figure 4B**

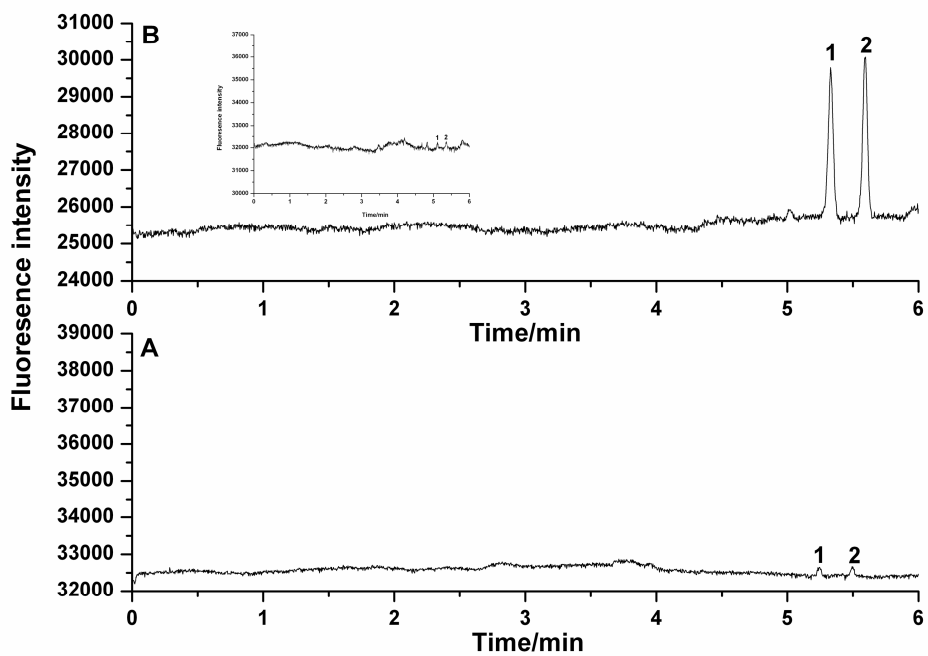


**Figure 5**





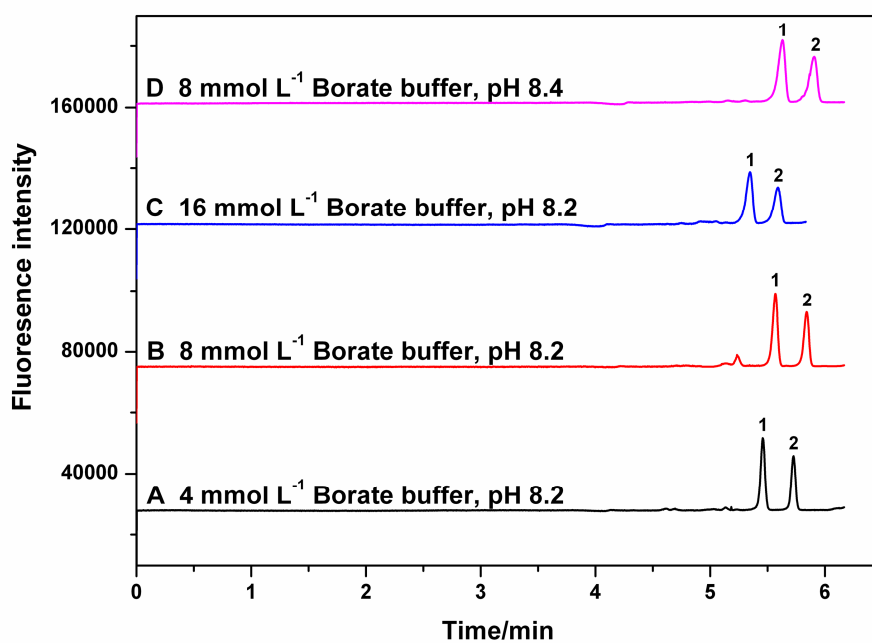


**Figure 7**

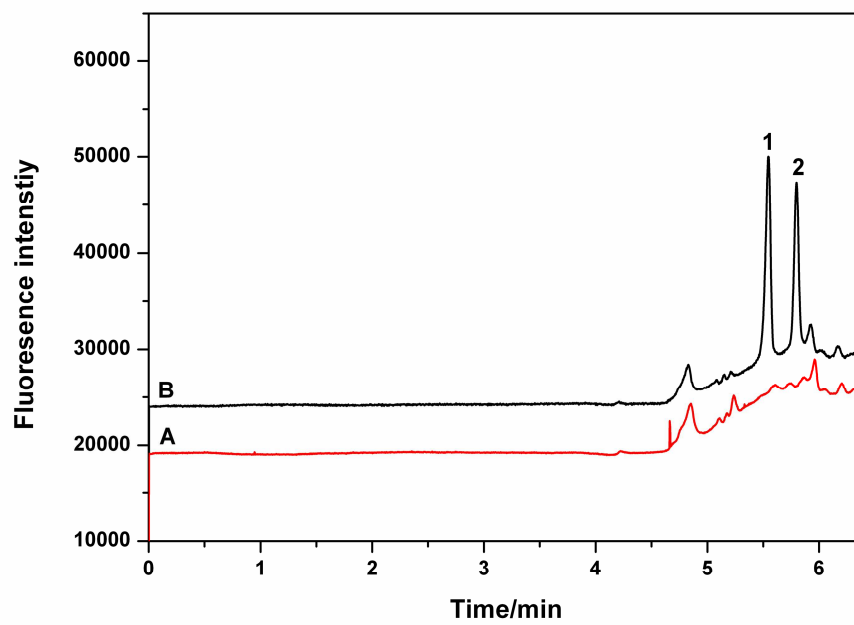


**Figure 8**



**Off-line and on-line enrichment of  $\alpha$ -aminocephalosporins for their analysis in surface water samples using CZE coupled to LIF**

Azza H. Rageh<sup>a</sup>, Karl-Friedrich Klein<sup>b</sup>, Ute Pyell<sup>a\*</sup>

<sup>a</sup>University of Marburg, Department of Chemistry, Hans-Meerwein-Straße, D-35032 Marburg, Germany

<sup>b</sup>Technische Hochschule Mittelhessen, Wilhelm-Leuschner-Straße 13, D-61169 Friedberg, Germany

\* Corresponding author

**Supplementary data**

### **Preparation of buffer solutions**

Stock disodium tetraborate (borax) buffer (100 mmol L<sup>-1</sup>, pH 9.30) was prepared by dissolving 9.5342 g disodium tetraborate decahydrate in 200 mL Milli-Q water and diluting to 250 mL with Milli-Q water. Lower concentrations of borax buffer were prepared by further dilution with Milli-Q water. Borate buffers, 20 mmol L<sup>-1</sup> (of different pH's) for carrying out the derivatization reaction and for studying the influence of BGE pH on separation were prepared by dissolving different amounts of boric acid and tetraborate in 200 mL Milli-Q water and diluting to 250 mL with Milli-Q water as follows: pH 8.02 (0.3005 g boric acid and 0.0533 g borax), pH 8.18 (0.2962 g boric acid and 0.0797 g borax), pH 8.43 (0.2837 g boric acid and 0.1573 g borax), pH 8.68 (0.2616 g boric acid and 0.2936 g borax), pH 8.95 (0.2059 g boric acid and 0.6365 g borax), pH 8.99 (0.1962 g boric acid and 0.6965 g borax), and pH 9.25 (0.7626 g borax). 20 mmol L<sup>-1</sup> Borax buffer of pH 9.4 and 9.6 were prepared by adjusting the pH using 1 mol L<sup>-1</sup> NaOH solution.

Different concentrations of 2-hydroxypropyl- $\beta$ -cyclodextrin (2-HP- $\beta$ -CD) solutions; 10.0, 20.0, 30.0 mg mL<sup>-1</sup> of 2-HP- $\beta$ -CD in 30 mmol L<sup>-1</sup> borax buffer, pH 9.25 were prepared by dissolving 0.500, 1.000 and 1.500 g, respectively in 30 mL of 30 mmol L<sup>-1</sup> borax buffer and diluting with the same buffer to 50 mL.

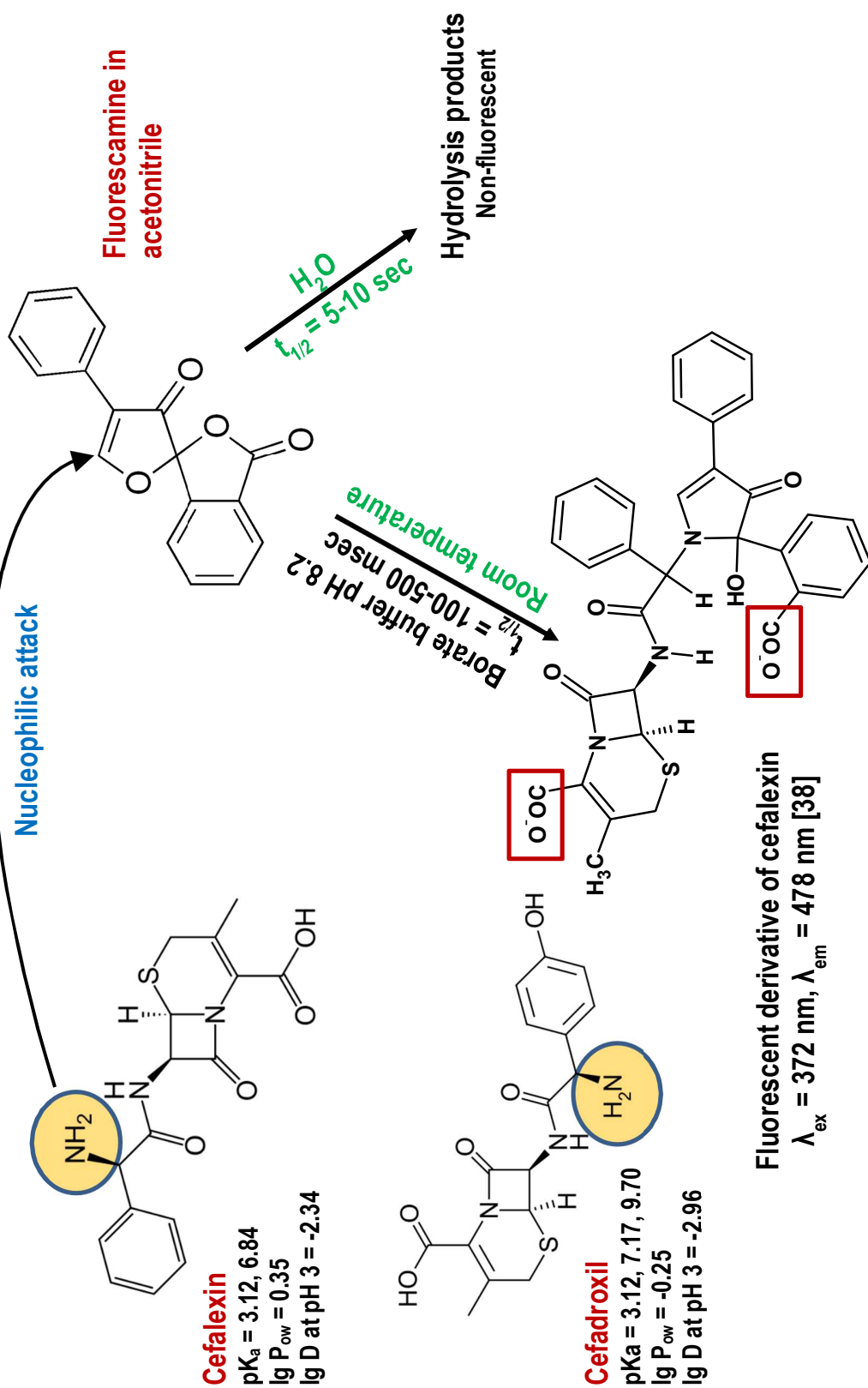


**Figure S1:** Reaction mechanism between the investigated  $\alpha$ -aminocephalosporins and fluorescamine.  $pK_a$ ,  $\lg P_{ow}$  and  $\lg D$  values are based on Science finder.  $t_{1/2}$  values were taken from [39], values determined for different classes of primary amines.

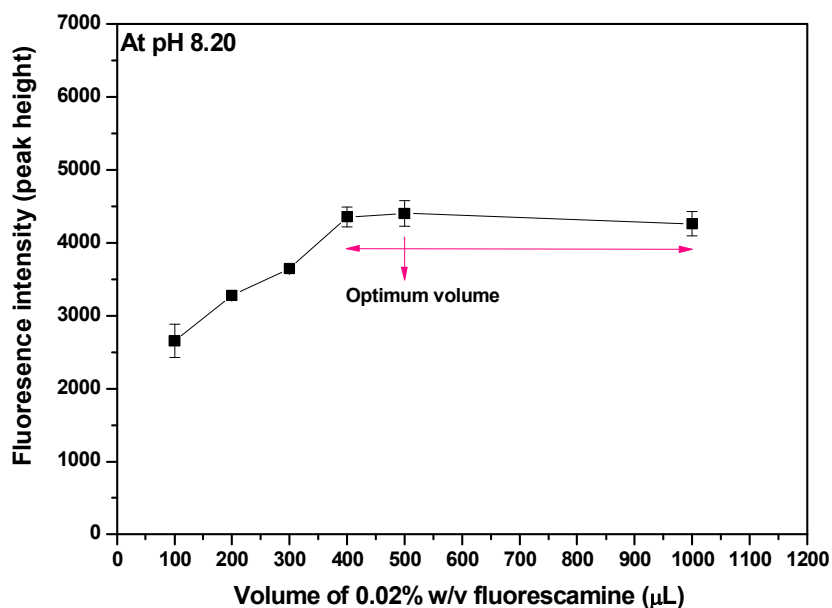


**Figure S2:** Effect of volume of 0.02% w/v fluorescamine on the fluorescence intensity of the reaction product of cefadroxil ( $0.36 \text{ mg L}^{-1}$ ) using  $20 \text{ mmol L}^{-1}$  borate buffer, pH 8.2 as a BGE. The derivatization procedure was conducted as described under Section 2.5. CE conditions: capillary 654(350) mm  $\times$  50.2  $\mu\text{m}$  I.D., separation voltage +20 kV, pressure injection 40 mbar for 0.4 min, oven temperature 25  $^{\circ}\text{C}$ , Laser  $P_{\text{cw}}$  2 mW, PMT voltage 500 V.

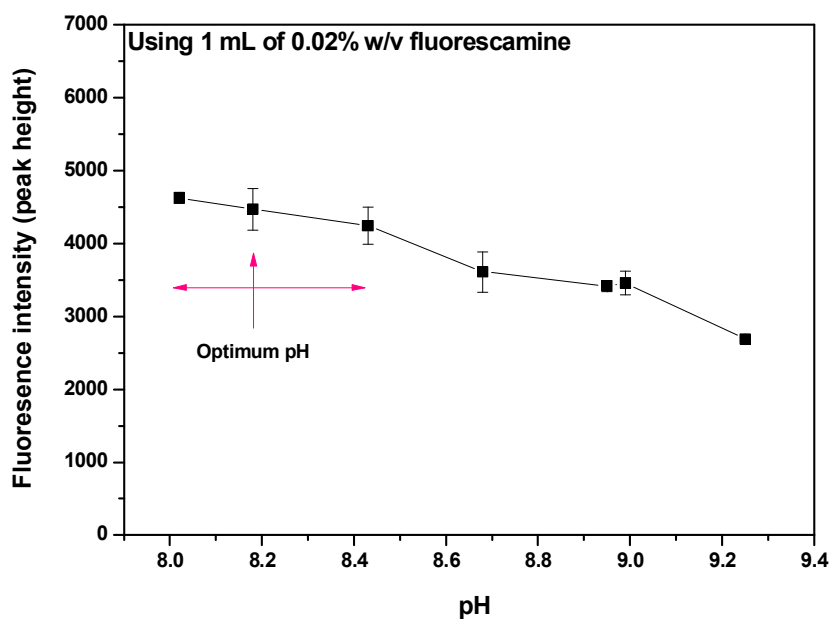


**Figure S3:** Effect of pH of the derivatization reaction (using 1 mL of  $20 \text{ mmol L}^{-1}$  borate buffer of different pH's and the derivatization procedure was conducted thereafter as described under Section 2.5) on the fluorescence intensity of the reaction product of cefadroxil ( $0.36 \text{ mg L}^{-1}$ ) with fluorescamine. The BGEs are composed of  $20 \text{ mmol L}^{-1}$  borate buffer of the same pH value as the one used in the derivatization reaction. Other CE conditions: as in Fig. S2.



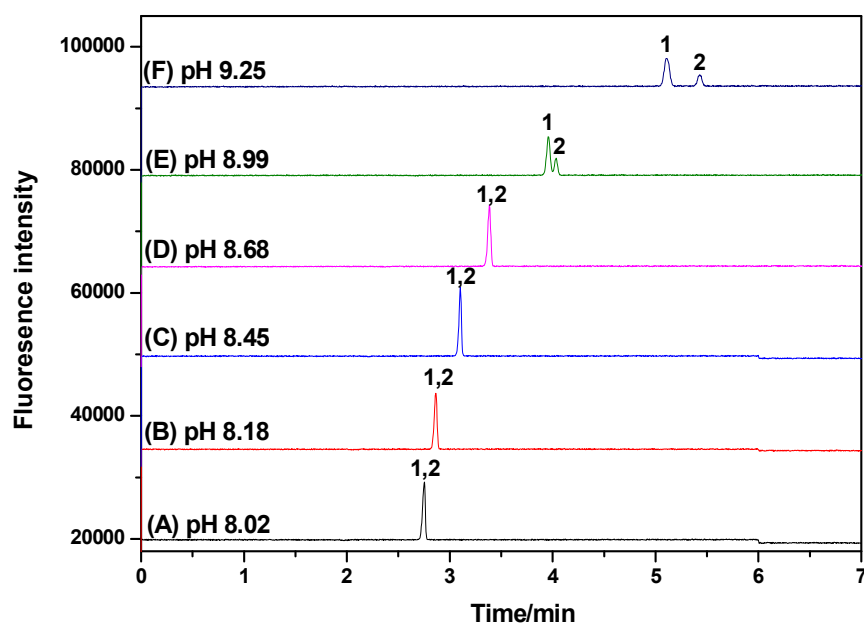


**Figure S4:** Electropherograms obtained with different pH's of the BGE. The BGEs employed as in Fig. S3.  $c(\text{cefalexin})$  and  $c(\text{cefadroxil})$  in the final derivatization reaction mixture are  $0.72$  and  $0.36 \text{ mg L}^{-1}$ , respectively. Other CE conditions: as in Fig. S2. Peak designation: (1) cefalexin and (2) cefadroxil.

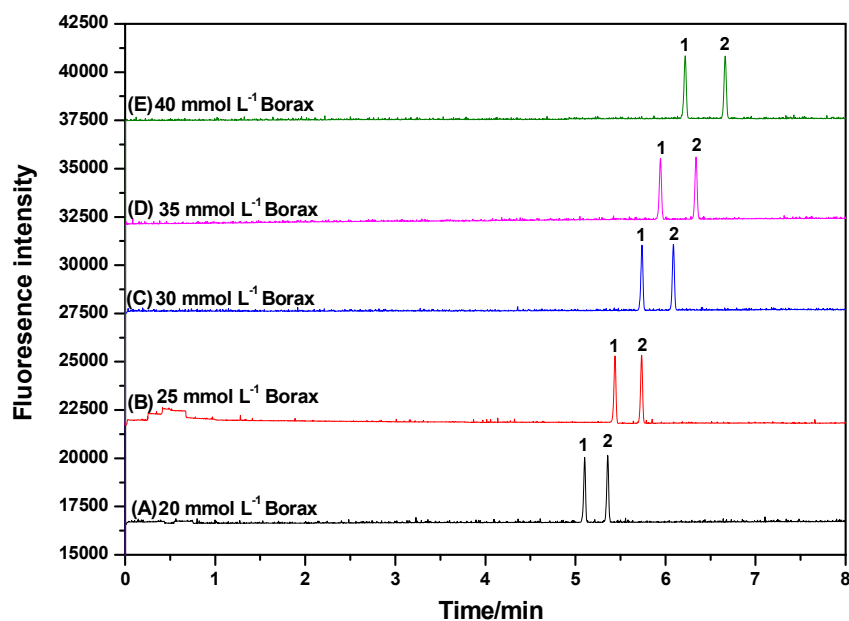


**Figure S5:** Electropherograms obtained with different concentration of sodium tetraborate in the BGE, pH 9.25 containing  $10 \text{ mg mL}^{-1}$  2-HP- $\beta$ -CD.  $c(\text{Antibiotic})$  in final derivatization reaction mixture is  $0.36 \text{ mg L}^{-1}$ . Sample was introduced hydrodynamically using an applied pressure of 30 mbar for 0.2 min. Other CE conditions: as in Fig. S2. Peak designation: (1) cefalexin and (2) cefadroxil.

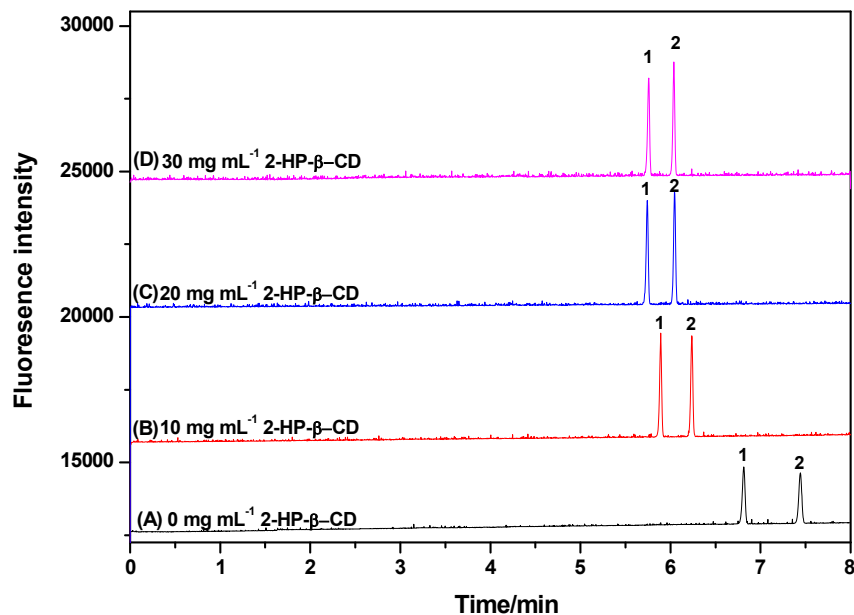


**Figure S6:** Electropherograms obtained with different concentration of 2-HP- $\beta$ -CD in the BGE. The BGE composed of  $30 \text{ mmol L}^{-1}$  sodium tetraborate, pH 9.25.  $c(\text{Antibiotic})$ , CE conditions and peak designations: as in Fig. S5.

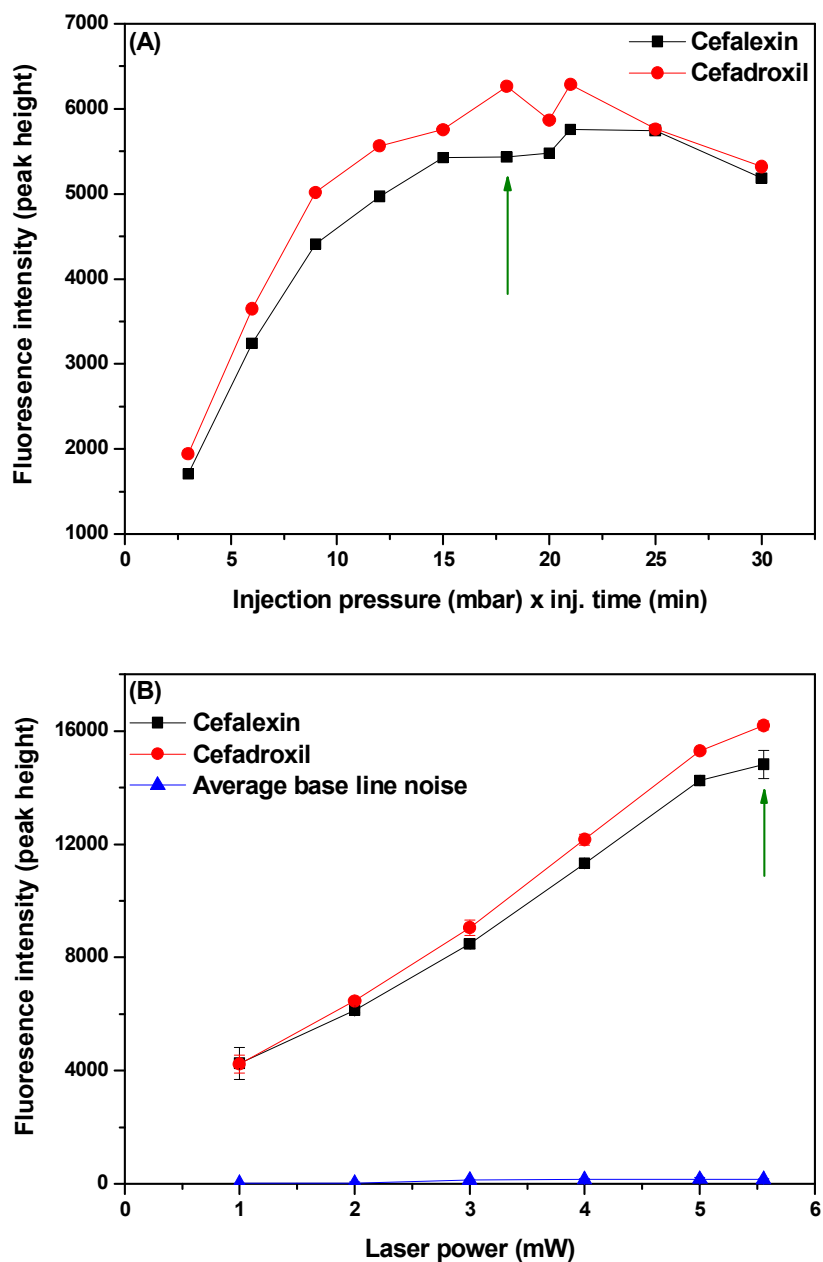


**Figure S7:** Peak height plotted against (A) injected sample volume or (B) laser output power under FASS conditions. Each data point is the average of at least three measurements (standard error represented as error bar).  $c(\text{Antibiotic})$  in the final derivatization reaction mixture is  $0.36 \text{ mg L}^{-1}$ . The BGE composed of  $30 \text{ mmol L}^{-1}$  sodium tetraborate, pH 9.25 containing  $20 \text{ mg mL}^{-1}$  2-HP- $\beta$ -CD. CE conditions: capillary 654(350) mm  $\times$  50.2  $\mu\text{m}$  I.D., separation voltage +20 kV, Laser  $P_{\text{cw}}$  2 mW in (A), pressure injection 30 mbar for 0.6 min in (B), oven temperature 25  $^{\circ}\text{C}$ , PMT voltage 500 V.

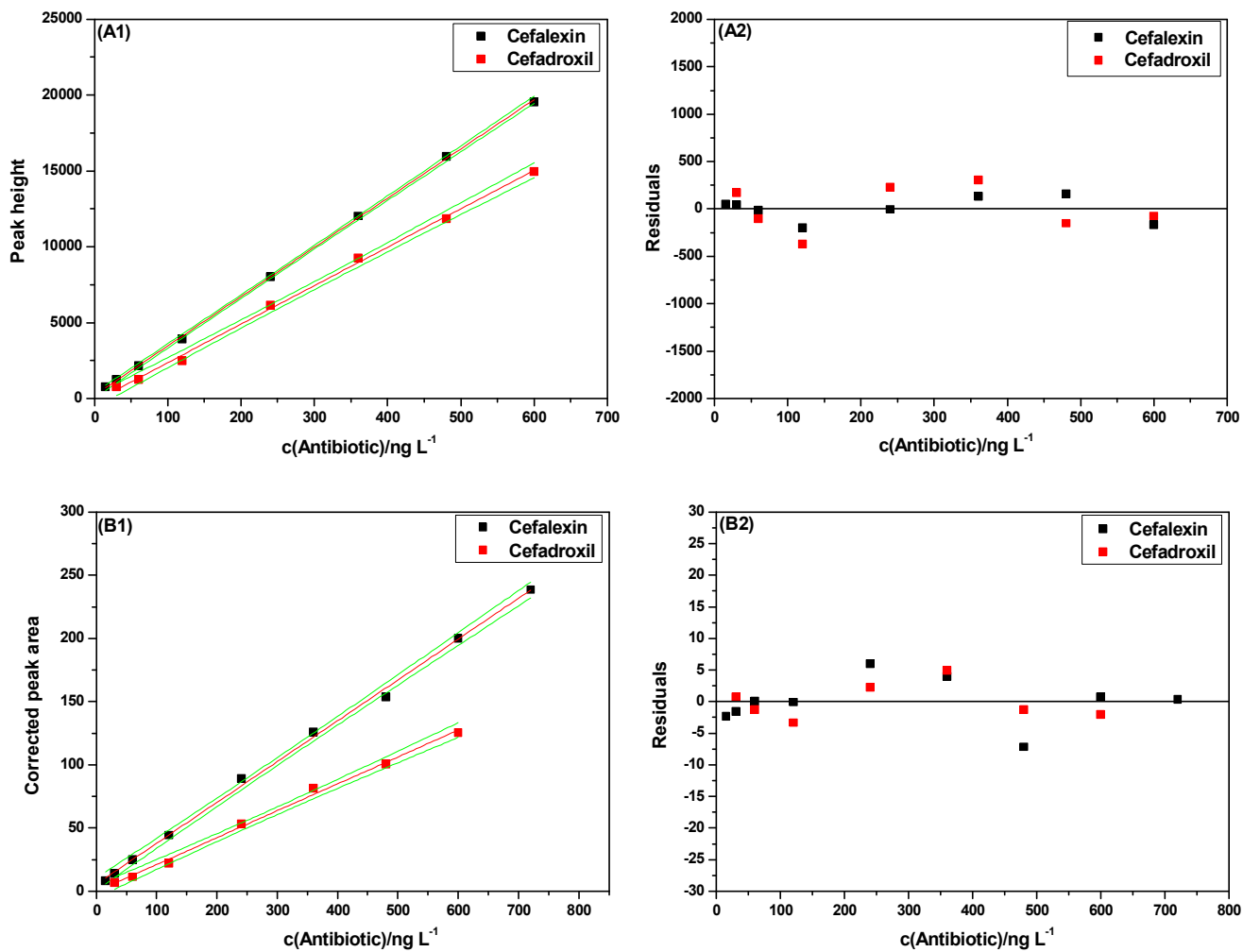


**Figure S8:** Calibration curve (A1) and residuals plot (A2) using peak height as the response factor. Calibration curve (B1) and residuals plot (B2) using corrected peak area as the response factor. The green line in (A1) and (B1) indicates the confidence interval at 95% significance level.

## 6. Curriculum Vitae

### M.Sc. Azza H. Rageh

University of Marburg, Department of Chemistry  
Hans-Meerwein-Straße 4, 35032 Marburg, Germany  
E-mail: [azhesham@yahoo.com](mailto:azhesham@yahoo.com), [rageh@staff.uni-marburg.de](mailto:rageh@staff.uni-marburg.de)

- **EDUCATION**

- **FORMAL EDUCATION**

- **1988-1993** Primary School.
    - **1994-1996** Preparatory School.
    - **1997-1999** Secondary School.

- **GRADUATION**

- **May 2004** Bachelor of Pharmaceutical Sciences, Faculty of Pharmacy, Assiut University, Assiut, Egypt; Excellent (Honor)

- **POST-GRADUATE STUDIES**

- **MASTER THESIS**

- **August 2006** Register a master thesis entitled: "*Analysis of certain cephalosporins via spectroscopic and densitometric methods*"
      - **June 2008** Master degree in Pharmaceutical Analytical Chemistry, Faculty of Pharmacy, Assiut University, Egypt

- **SOCIETIES and BOARDS**

- **1999-2004** High board member of the "Scientific Association of Assiut Pharmacy Students, SAAPS"
    - **2004** Member of the Assiut and Egyptian Pharmaceutical Syndicate
    - **2005** Active member of Pharmaceutical Society of Egypt
    - **2007** Member of "Performance Evaluation and Development Unit" in Assiut University
    - **2007** High board member of "Establishment of Internal Quality Assurance System Program" in Faculty of Pharmacy
    - **2011** Member in the German Chemical Society (GDCh)
    - **2012** Member in Marburg University Research Academy (MARA)

- **PREVIOUS AND CURRENT POSITIONS**

- **2005-2008:** Demonstrator of Pharmaceutical Analytical Chemistry, Faculty of Pharmacy, Assiut University, Assiut, Egypt and teaching assistant for undergraduate students.
- **2008-2010:** Assistant lecturer at the Department of Pharmaceutical Analytical Chemistry, Faculty of Pharmacy, Assiut University, Assiut, Egypt and teaching & Evaluation of the practical part of the pharmaceutical analytical Chemistry courses.
- **2011–to date:** PhD student at Marburg University, department of Chemistry (Analytical Chemistry), Marburg, Germany.

- **LIST of PUBLICATIONS**

- **M. Sc PUBLICATIONS**

- 1- S.R. El-Shaboury, G.A. Saleh, F.A. Mohamed, **A.H. Rageh**, "Analysis of cephalosporin antibiotics", *J. Pharm. Biomed. Anal.* 45 (2007) 1-19.
- 2- F.A. Mohamed, G.A. Saleh, S.R. El-Shaboury, **A.H. Rageh**, "Selective densitometric analysis of cephalosporins using Dragendorff's reagent", *Chromatographia* 68 (2008) 365-374.
- 3- G.A. Saleh, S.R. El-Shaboury, F.A. Mohamed, **A.H. Rageh**, "Kinetic spectrophotometric determination of certain cephalosporins using oxidized quercetin reagent", *Spectrochimica Acta part A* 73 (2009) 946-954.
- 4- G.A. Saleh, F.A. Mohamed, S.R. El-Shaboury, **A.H. Rageh**, "Selective densitometric determination of four  $\alpha$ -aminocephalosporins using ninhydrin reagent", *J. Chromatogr. Sci.* 48 (2010) 68-75.
- 5- S.R. El-Shaboury, F.A. Mohamed, G.A. Saleh, **A.H. Rageh**, "Kinetic spectrophotometric determination of certain cephalosporins using iodate/iodide mixture", *Natural Science* 2 (5) (2010) 432-443.
- 6- **A.H. Rageh**, S.R. El-Shaboury, G.A. Saleh, F.A. Mohamed, "Spectrophotometric method for determination of certain cephalosporins using 4-chloro-7-nitrobenzo-2-oxa-1,3-diazole (NBD-Cl)", *Natural Science* 2 (8) (2010) 828-840.

- **PhD PUBLICATIONS**

- 1- **A.H. Rageh**, U. Pyell, "Imidazolium-based ionic liquid-type surfactant as pseudostationary phase in micellar electrokinetic chromatography of highly hydrophilic urinary nucleosides", *J. Chromatogr. A* 1316 (2013) 135-146.
- 2- **A.H. Rageh**, A. Kaltz, U. Pyell, "Determination of urinary nucleosides via borate complexation capillary electrophoresis combined with dynamic pH junction-sweeping-large volume sample stacking as three sequential steps for their on-line enrichment", *Anal. Bioanal. Chem.* 406 (2014) 5877-5895.
- 3- **A.H. Rageh**, U. Pyell, "Boronate affinity-assisted MEKC separation of highly hydrophilic urinary nucleosides using imidazolium-based ionic liquid-type surfactant as pseudostationary phase", *Electrophoresis* 36 (2015) 784-795.

- 4- **A.H. Rageh**, U. Pyell, ""Pseudostationary ion-exchanger" sweeping/dynamic pH junction/FASS on-line enrichment for the determination of nucleosides in urine via micellar electrokinetic chromatography after solid phase extraction with phenylboronate affinity gel", *J. Chromatogr. A*, *Submitted*.
- 5- **A.H. Rageh**, K.F. Klein, U. Pyell, "Off-line and on-line enrichment of  $\alpha$ -aminocephalosporins for their analysis in surface water samples using CZE coupled to LIF", *Talanta*, *Submitted*.

- **AWARDS**

- **1999** Qena State Medal for Top Ten Secondary School Graduates; ranked as the 1<sup>st</sup>
- **2004** Assiut State Medal for Top Ten University Graduates; ranked as the 1<sup>st</sup>
- **2004** T3A Prize for Top Ten Pharmacy Graduates; ranked as the 1<sup>st</sup>
- **2005** Certificate of honour from the "Egyptian Pharmaceutical Syndicate" for scientific excellence
- **2008** Certificate of honour from the "Faculty of Pharmacy, Assiut University" for scientific effort and excellence in the Master Thesis
- **2010** Award of the best scientific master thesis in Medicinal and Pharmaceutical Sciences on Assiut University level
- **2013** Nominated for Agilent best poster award in HPLC 2013 Amsterdam

- **GRANTS**

- PhD scholarship through German Egyptian Research Long-Term Scholarship program GERLS/DAAD October 2010-June 2015
- German Chemical Society (GDCh) scholarship for the CE Forum organized in Hochschule Aalen, September 24-25, 2012, Aalen, Germany
- German Chemical Society (GDCh) scholarship for HPLC 2013 organized in Amsterdam, June 16-20, Netherlands
- German Chemical Society (GDCh) scholarship for active participation in '24. Doktorandenseminar des Arbeitskreises Separation Science der GDCh-Fachgruppe Analytische Chemie 2014' in Hohenroda
- Marburg University Research Academy (MARA) scholarship for supporting young woman scientists with children